UNIVERSITY OF
LIVERPOOL

Efforts Toward the Directed Evolution of a Bacterial Molybdenum-dependent Aldehyde Oxidase for Use in Synthesis

Thesis submitted in accordance with the requirements of the University of Liverpool for the degree of Doctor in Philosophy by:

Christopher Riley

March 2018

Dedication

For Robert, William and Philip…

Acknowledgements

First and foremost I would like to extend my deepest thanks to Dr. Andrew Carnell for allowing me to join his research group for the duration of my PhD.

Your patience, encouragement and enthusiasm have been a driving force in my development in both fields of chemistry and biology. Our meetings were full of ideas and optimistic discussion, which ultimately was instrumental in the late achievements of the project.

I would like to extend thanks to Dr. Abhishek Srivastava. You arrived at the end of my PhD but helped me so much during the last months in the lab. Your advice on mutagenesis and biological techniques played a significant role in the results I achieved.

I would also like to thank our collaborators Prof. Nick Turner and Prof. Silke Leimkühler for providing enzymes in addition to Prof. Rick Cosstick for general discussion. I'd like to thank Dr. Konstantin Luzyanin for his friendship and assistance with NMR and Dr. Adham Ahmed for invaluable help with all things HPLC.

I would like to thank past colleagues: Dr. Shane McKenna, Dr. Stephanie Yip, Dr. Teresa Almeida, Dr. Victoria Pedder and Dr. Katie Alexander who all helped me in some capacity get used to working on the 1st floor. I gained much experience especially from Shane who was also acting as a gym buddy in addition to mentoring me. The stark contrast between your social and professional attitude was always something I found particularly intriguing.

Thanks to my brothers in arms Paul McGillan and Matthew Pye. We've been through all eight years together and throughout you both took my mind off work when times were stressful.

Thanks to current members of lab 1.84/1.85 Neil, Kathryn and Harry. I'll miss going for meals and quiz of the week!

I would like to thank my Mum, Jen and John for their unwavering support, love and encouragement. Especially my mum, thank you for pushing me to reach my goals. All the times you forced me to get to school when I was young paid off! Talking about my work with everyone also helped me focus and reevaluate.

Finally I would like to thank the three men this body of work is dedicated to. My Father, Grandfather and Mentor. The three of you combined are the reason that I have become the person I am today. I can never repay your kindness and encouragement. I only hope I can continue to make you proud.

Abstract

Molybdenum-dependent xanthine oxidoreducatases (XOR) are a well-known family of enzymes, which oxidise purines, imines and aldehydes in cellular metabolism. Despite many studies relating to drug metabolism, application to chemical synthesis has only recently begun to be explored.

Herein we report the first use of XORs in the cascade synthesis of lactams from cyclic amines by the combination of the mutant monoamine oxidase (MAO) MAO-N D9 and XOR (*E.coli* XDH & *R. capsulatus* XDH E232V). A number of single step imine oxidations were also performed in excellent conversions with the methodology comparing well to current chemical oxidation methods. The reactions were performed in water at ambient temperature and pH using oxygen as the terminal oxidant with the only by-product being H_2O_2.

A solid-phase colorimetric assay has been developed to detect aldehyde oxidase activity from membrane-bound bacterial colonies of TP1000 x PaoABC using a coupled peroxidase system. The screen was used to assay a library of mutants generated at the Moco-containing sub unit of PaoABC with phenylacetaldehyde used as a model substrate. This resulted in the discovery of an improved mutant L443Q, which exhibited improved solid-phase activity in addition to improved kinetics.

A saturation mutagenesis approach has also been employed on *Ec* PaoABC at analogous positions responsible for substrate binding in *Rc* XDH to search for a novel "imine oxidase". An interesting variant L246G was isolated with a switch in substrate specificity toward 3,4-dihydroisoquinoline.

Abbreviations

4-CN	4-chloronapthol
AaP	*Agroybe aegerita* peroxidase
AADH	Amino acid dehydrogenase
AAOx	Amino acid oxidase
AlcOX	Alcohol oxidase
aldDH	Aldehyde dehydrogenase
ABTS	2,2'-Azino-bis(3-ethylbenzothiazoline-6-sulphonic acid)
ADH	Alcohol dehydrognenase
AldDH	Aldehyde dehydrogenase
AO	Aldehyde oxidase
AOX	Alcohol oxidases
AOX1	Mammalian AO
mAOX1	Mouse AO
API	Active pharmaceutical ingredient
APR	Aqueous phase reforming
BTX	Benzene toluene xylene isomers
$CDCl_3$	Chloroform-d
CPO	*Caldariomyces fumago* peroxidase
$_D$-AAO	$_D$-amino acid oxidase
DAB	3,3'-diaminobenzidine
DCM	Dichloromethane
DCPIP	2,6-dichlorophenolindophenol
DERA	2-deoxyribo-5-phosphate aldolase
DFF	Diformyl furan
dH_2O	Distilled water
DHIQ	Dihydroisoquinoline
DKR	Dynamic kinetic resolution
DMF	Dimethylformamide
DMSO	Dimethyl sulfoxide
DNA	Deoxyribonucleic acid
dNTP	Deoxy nucleotide triphosphate
epPCR	Error-prone PCR
EDTA	Ethylenediaminetetraacetic acid
FAD	Flavin adenine dinucleotide
FCC	Flash column chromatography
FDCA	Furan-2,5-dicarboxylic acid
FFCA	5-formylfuran-2-carboxylic acid
GDH	Glycerol dehydrogenase
GluOX	Glucose oxidase
GluDH	Glutamate dehydrogenase
GOase	Galactose oxidase
HBT	*N,N'*-Bis-(1*H*-tetrazol-5-yl)-hydrazine
HCl	Hydrochloric acid
HCN	Hydrogen cyanide
Hex	n-hexane
HHDH	Halohydrin dehalogenase
HLDH	Horse liver alcohol dehydrogenase
HMF	Hydroxymethyl furfural

HMFCA	Hydroxymethyl furan carboxylic acid
HPLC	High pressure liquid chromatography
HRP	Horseradish peroxidase
IPA	Isopropyl alcohol
IPTG	Isopropyl thio-β-$_D$-galactoside
$K_3Fe(CN)_6$	Potassium hexacyanoferrate
KDG	2-keto-3-deoxy-galactonate
KDPG	2-keto-3-deoxy-6-phosphogluconate
$KMnO_4$	Potassium permangante
KPi	Potassium phosphate
KRED	Ketoreductase
$_L$-AA	$_L$-Ascorbic acid
$_L$-AAO	$_L$-amino acid oxidase
LB	Lysogeny broth
LDH	Lactate dehydrogenase
LMS	Laccase mediator system
MAO-N	Monoamine oxidase
MCD	Molybdopterin-cytosine-dinucleotide
mCPBA	*meta*-Chloroperoxybenzoic acid
MeCN	Acetonitirile
MeOH	Methanol
MFE	Molybdo-flavoenzyme
MGD	Molybdopterin-guanine-dinucleotide
N_2	Nitrogen
$NaBH_4$	Sodium borohydride
NaCN	Sodium cyanide
NAD	Nicotinamide adenine dinucleotide
NADP	Nicotinamide adenine dinucleotide phosphate
$NaMoO_6$	Sodium molybdate
NaOH	Sodium hydroxide
NH_3-BH_3	Ammonia-borane complex
NMR	Nuclear magnetic resonance
P2O	Pyranose-2-oxidase
PAA	Phenylacetaldehyde
PaoABC	Periplasmic aldehyde oxidase
PCR	Polymerase chain reaction
PEF	Polyethylene furanoate
PET	Polyethylene terephthalate
RP-HPLC	Reverse phase high pressure liquid chromatography
RT-PCR	Reverse transcriptase-coupled PCR
TA	Transaminase
Taq	*Thermus aquatacus*
TEMPO	(2,2,6,6-Tetramethylpiperidin-1-yl)oxyl
TFA	Trifluoroacetic acid
THBC	Tetrahydro-β-carboline
THF	Tertahydrofuran
THIQ	Tetrahydroisoquinoline
TLC	Thin layer chromatography
UMP	Uridine monophosphate
UV	Ultra-violet

XDH	Xanthine dehydrogenase
XO	Xanthine oxidase
XOR	Xanthine oxidoreductase

Table of Contents

Chapter 1

1. Introduction

1.1. Green chemistry

Green chemistry is a broadly reaching discipline encompassing synthesis, chemocatalysis, biocatalysis and chemical engineering.[1-5] Reducing the impact of non-renewable and hazardous materials on human health and the environment emerged as an independent branch of chemistry over two decades ago.[6] In 1990 the US pollution prevention act was passed, which encouraged companies to reduce the level of pollutants produced through cost-effective modifications to chemical processes and handling of raw materials.[7] The journal *Green Chemistry* first published in 1999 by the Royal Society of Chemistry has become a hub for all aspects of sustainable chemistry and new methods in chemical engineering. Green chemistry's aim was more clearly defined following the publication "12 principles of green chemistry" first developed by Anastas and Warner.[8]

1.1.1. The twelve principles of green chemistry

The principles are intended as a guide in reducing the environmental impact of chemical production and are summarised as follows.

1) Prevention of waste preferred over treatment of waste

2) Methods of synthesis should be atom efficient

3) Synthetic products should not possess human/environmental toxicity

4) Products should retain efficacy while reducing toxicity

5) Solvents and other auxiliaries should be unnecessary where possible

6) Reduction of energy requirements and use of ambient conditions

7) Use of renewable feedstocks

8) Reducing derivatives (i.e. protection/deprotection)

9) Moving toward catalytic reagents from stoichiometric

10) Design of biodegradable products

11) Analytical methods for real time hazard/pollutant prevention

12) Use of safer reagents, which are benign in the event of an accidental spill

E factor (mass waste/mass product) and atom economy (atoms of product/atoms of all reagents) are two concepts devised by Roger Sheldon in the early 1990's and give a measurement of the environmental footprint for a given chemical process.[2] A decade prior, Sheldon had been alerted to the problem of waste after observing the closure of a plant producing phloroglucinol. The process that made the fine chemical on a moderate scale was producing 40 kg of waste for every 1 kg of product, the cost of disposal of which was negating any profit. After surveying other processes, it was clear that large amounts of waste were abundant in the fine chemical and pharmaceutical industries. In order to reduce the amount of waste being produced a paradigm shift from yield optimisation to also including environmental considerations in process design would be necessary.

1.1.2. Alternative energy & solvent

In addition to reducing the use of unsustainable and hazardous materials, an emphasis in reducing energy and solvent requirements is a key factor in greening synthesis. This has resulted in several approaches of using benign media/solvent free systems with alternative energy sources to drive reactions forward.

Mechanochemical mixing methods have been used to facilitate several solvent free reaction types including Biginelli,[9] Reformatsky,[10] Luche[10] and Sonogashira.[11]

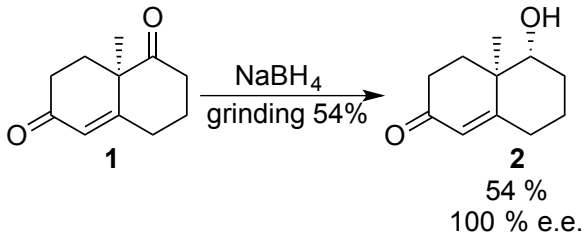

Scheme 1 Stereoselective reduction of a chiral diketone[12]

For example a diastereoselective reduction by grinding the reaction using a pestle and mortar furnished the chiral alcohol **2** in excellent optical purity, albeit in modest yield (**Scheme 1**).[12] This example of a solvent free approach is remarkable in that it is fully regio and diastereoselective, while not using harsh conditions.

Ultrasound has been utilised as an alternative form of energy input in reactions and has seen use in organic synthesis due to its selectivity in reactions, which offer results from use under ambient conditions.

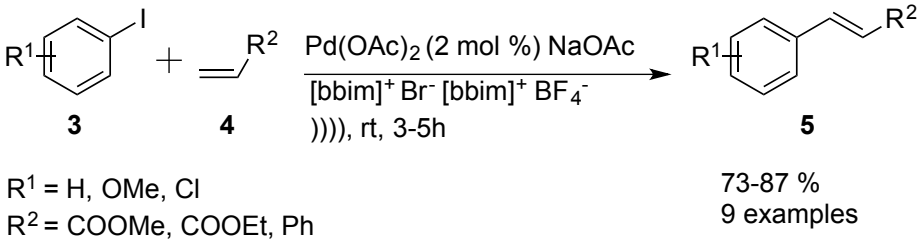

Scheme 2 Ultrasonic Heck coupling in ionic liquids[13]

Srinivasan *et al*. were able to use ultrasonication with ionic liquids to perform Heck couplings on a range aryl iodides to give exclusively *E* products in good to excellent yields (**Scheme 2**).[13] Heck reactions usually require long reaction times under reflux in polar solvents such as DMF. Ionic liquids themselves can also be generated using ultrasonication. Varma *et al*. synthesised 1,3-dialkylimidazolium compounds at room temperature using neat reagents and sonication, ordinarily these compounds require an excess of alkyl halide and an organic solvent.[14]

Microwaves as an alternate source of energy input have the advantages of uniform heat transfer, rapid initial heating and increased reaction kinetics. This has resulted in a solvent free alternative method of heating that is comparable or better than conventional heating. For example polyamides were prepared through microwave irradiation for 30 seconds whereas conventional heating took 1 minute.[15,16] Microwave irradiation

delivered diazepines and pyrazoles in a facile manner through condensation of hydrazines/diamines with 1,3-diketones in the absence of both solvent and catalyst (**Scheme 3**).[17]

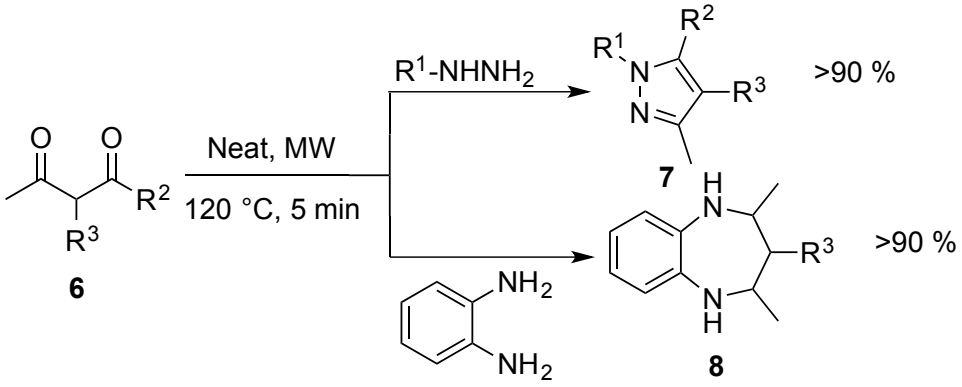

Scheme 3 Solvent and catalyst free synthesis of pyroles and diazepines[17]

Other notable transformations in solvent free conditions include synthesis of hydrazones,[18] 1,3-thiazoles[19] and ionic liquids.[20] Using basic water as solvent, efficient synthesis of *N*-heterocycles was carried out by microwave-facilitated double alkylation of primary amines[21] and hydrazines (**Scheme 4**).[22]

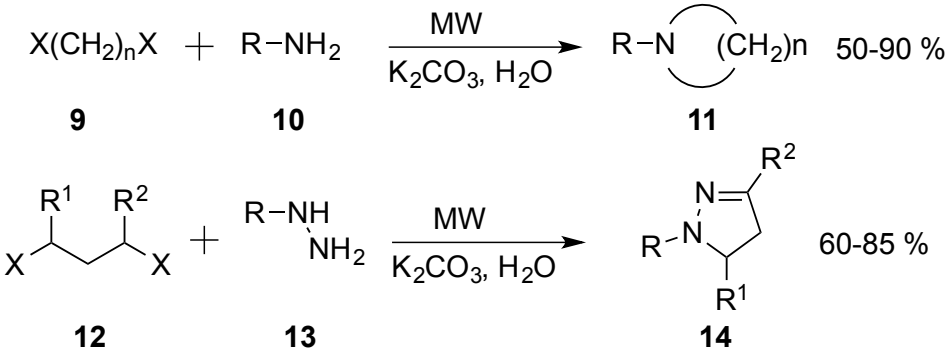

R = H, alkyl, aryl
X = Cl, Br, I, OTs

Scheme 4 Microwave irradiated synthesis of N-heterocycles in aqueous media[21,22]

The selective absorption of microwaves by polar reagents, which are normally insoluble in aqueous media is believed to act as a surrogate phase transfer catalyst. Polyethylene glycol is a benign and cheap reaction solvent, which has been used successfully in microwave promoted Suzuki cross-coupling reactions to deliver simple bi-aryls such as **17**.[23]

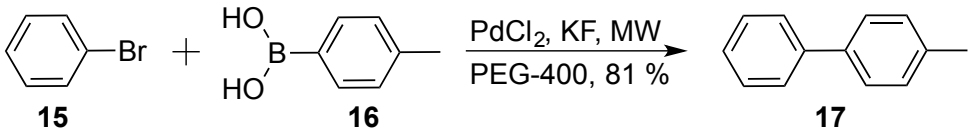

15 **16** **17**

Scheme 5 MW facilitated Suzuki reaction in polyethylene glycol[23]

Nanomaterials have rapidly emerged with wide reaching applications in medicine, electronics, communications, and materials science.[24] Conventional methods of metallic nanoparticle preparation involve strong reducing agents and/or capping agents (i.e. polyvinyl pyrrolidone) in addition to a large amount of organic halide as solvent. Natural oxidants like polyphenols found in tea can function as reductants and have been used in the production of gold and silver nanoparticles and this presents an attractive green alternative to conventional synthesis.[25]

A limitation of nanoparticles is that they are prone to aggregation, which drastically reduces activity due to decreased effective surface area. Stabilising agents are therefore required to retain activity and extend shelf life but significantly contribute to waste streams. Developments in green stabilising agents have meant that biodegradable polymers and biocatalyst stabilisers are viable options.[26]

1.1.3. Biorenewable materials

The ability to effectively utilise renewable resources in fuel and materials production will be a key factor in mitigating the increasing danger posed by climate change.[27] Biomass is a sustainable resource comprised chiefly of lignocellulose and triglycerides that has seen increased adoption from industry in the last decade with emerging dedicated biorefineries.[28] In addition to biofuels and chemicals, refineries providing greener materials such as bio-derived plastics can lower costs and reduce carbon footprint.[29]

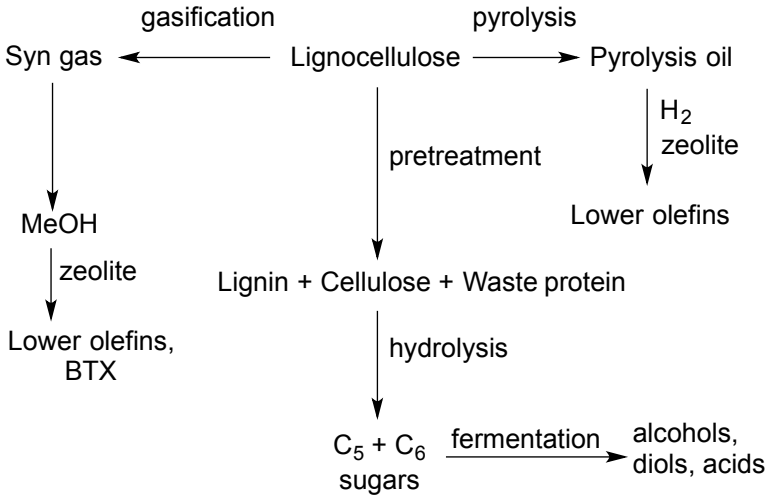

Scheme 6 Primary conversion options for lignocellulose[3]

Lignocellulose from plant biomass is comprised of polymeric sugars and aromatic lignin. It is extremely abundant in nature and being inedible, its use in manufacturing doesn't compete with other materials derived from foodcrops such as starch and vegetable oil. Processing lignocellulose is more challenging than crop based feedstocks and involves depolymerisation and then deoxygenation.[30] The first step can be carried out by thermochemical treatment (pyrolysis/gasification) or hydrolysis (**Scheme 6**). This is usually carried out in water although ionic liquids can dissolve lignocellulose[31] and, with water, has potential for chemocatalytic[32] and biocatalytic hydrolysis.[33]

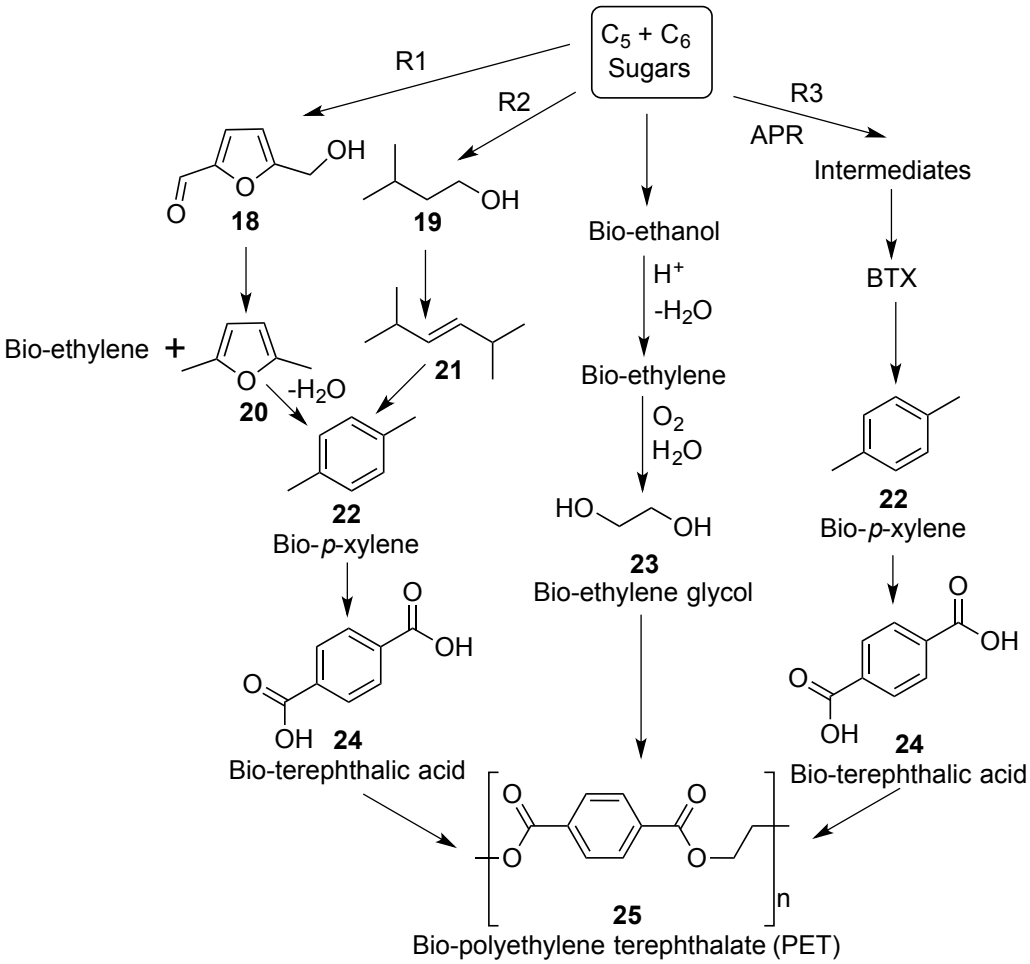

Scheme 7 Paths to bio-derived PET[3]

Polyethylene terephthalate (PET) is an industrial polymer utilised ubiquitously in plastic bottles and accounts for a significant percentage of plastics produced globally (>50 million tonnes). The components of PET are terephthalic acid and ethylene glycol, which themselves are produced from ethylene and crude oil-derived xylene. Development of biobased counterparts from hexose and pentose have led to partial (~30 %) and fully plant based PET bottles. Three routes to bio-*p*-xylene are depicted above (**Scheme 7**). Route 1 (R1) involves the addition of bioethylene to biomass-derived 2,5-dimethylfuran in a zeolite catalysed Diels-Alder cyclisation with loss of water. [34,35] The second and third routes both involve industrial processes from Gevo[36] and Virent respectively. Gevo's patented process involves fermentation of sugars to produce bio-isobutanol **19**, which then undergoes dehydration and metathesis to deliver the C8 alkene **21**. Dehydrocyclisation using a specific catalyst then yields *p*-xylene. The Virent process involves aqueous phase reforming (APR) and dehydrocyclisation to deliver a

mixture of benzene, toluene and various xylenes (BTX) from which *p*-xylene can be isolated.

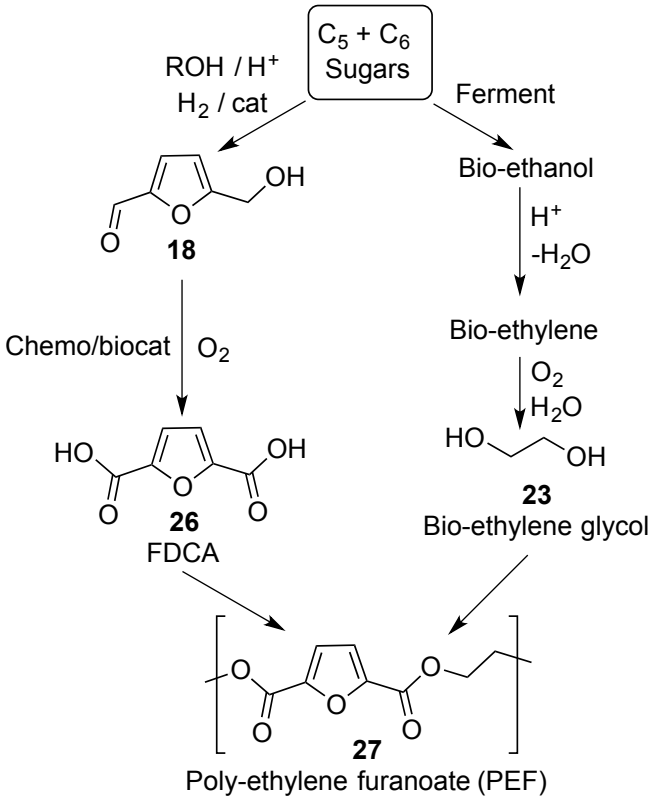

Scheme 8 Path to bio-polyethylene furanoate[37]

Alternatively, a replacement bio-derived polymer, poly-ethylene furanoate (PEF) has been developed by Avantium (**Scheme 8**), where terephthalic acid is replaced by furandicarboxylic acid (FDCA), which is also obtained from hexose sugars through acid catalysed dehydration followed by oxidation.[37] FDCA is readily formed from the less stable intermediate hydroxymethyl furfural (HMF)[28] and is recognised as a key sugar-based platform chemical by the US Department of Energy.[38]

1.2. Enzyme biocatalysts

Enzymes have been utilised in fermentation processes to produce alcohol and foodstuffs throughout history. The first reported synthetic use of enzymes occurred in 1858 when Louis Pasteur isolated optically pure (-)-tartaric acid through selective consumption of the opposite enantiomer by *Penicillium glaucum* mould.[39] This is also considered the first example of an enzyme driven resolution. Later work by Eduard Buchner at the end of the 19th century demonstrated that biotransformations didn't

require living cells by successfully fermenting sugar with yeast cell extract thereby identifying enzymes as independently acting units.[40]

Owing to their chemo-, regio- and stereoselectivity, enzymes have become great assets available to a synthetic chemist for greening synthesis.[41] Biocatalysts operate optimally in aqueous media under ambient conditions at neutral pH, are biodegradable and safe. This results in catalysts that often preclude the use of organic solvent and harsh temperature/pressure. Many enzymes (i.e. lipases, proteases) are also functional in organic solvent. This has been exploited by industry where many processes utilise solvents for their ease of product extraction. Enzymes can also bypass conventional synthetic protection/deprotection strategies due to their chemoselectivity, which increases atom economy.

1.2.1. Enzyme structure and function

Enzymes are macromolecules consisting of a typically globular protein and may also possess one or multiple co-factors. Deconstruction reveals a distinct four-tier hierarchy of structure; primary, secondary, tertiary and quaternary (**Figure 1**).[42] Primary structure consists of a specific sequence of α-amino acids connected through strong peptide bonds in an order defined by the protein's genetic code. The dual hydrogen donating and accepting character present in amides leads to H-bonding between neighbouring amino acids. This produces secondary structures, the most common of which are α-helixes and β-sheets.

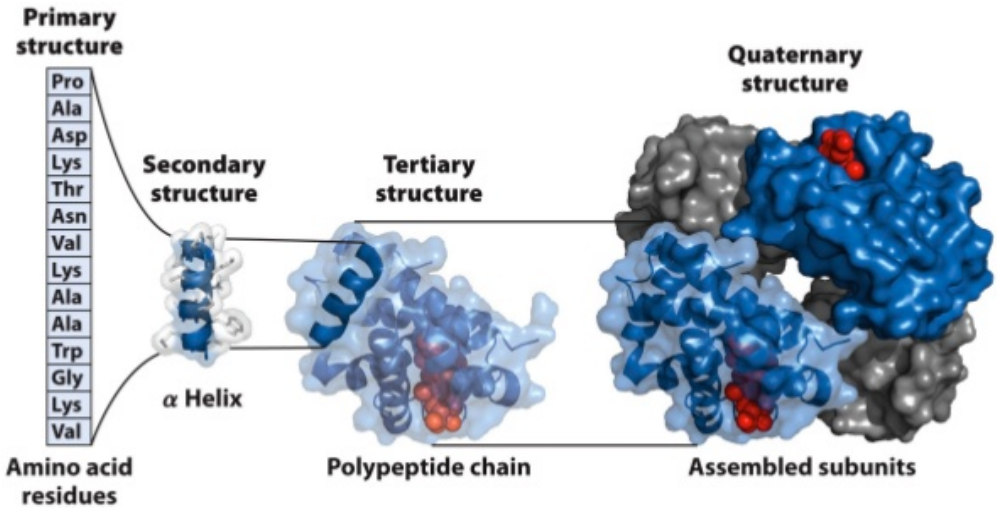

Figure 1 Protein structure starting from primary through quaternary[42]

A single peptide backbone containing secondary structures folds into a compact and stable tertiary structure. This is driven by the lower energy obtained by isolating alkyl and other non-polar hydrophobic residues internally. Conversely, polar hydrophilic residues are situated towards the surface of the protein to interact with water. Additional bonding interactions including; π-π stacking, Van der Waals forces, salt bridges and cysteine di-sulfide bridges contribute to give a globular 3D shape. Higher order quaternary structures arise as a result of these additional interactions occurring between separate ordered tertiary structures.

Co-factors consist of inorganic ions and organic co-enzymes, which can be loosely or covalently bound and assist in the activity of an enzyme.[41] Tightly bound co-factors termed prosthetic groups function at the active site to facilitate reactions.

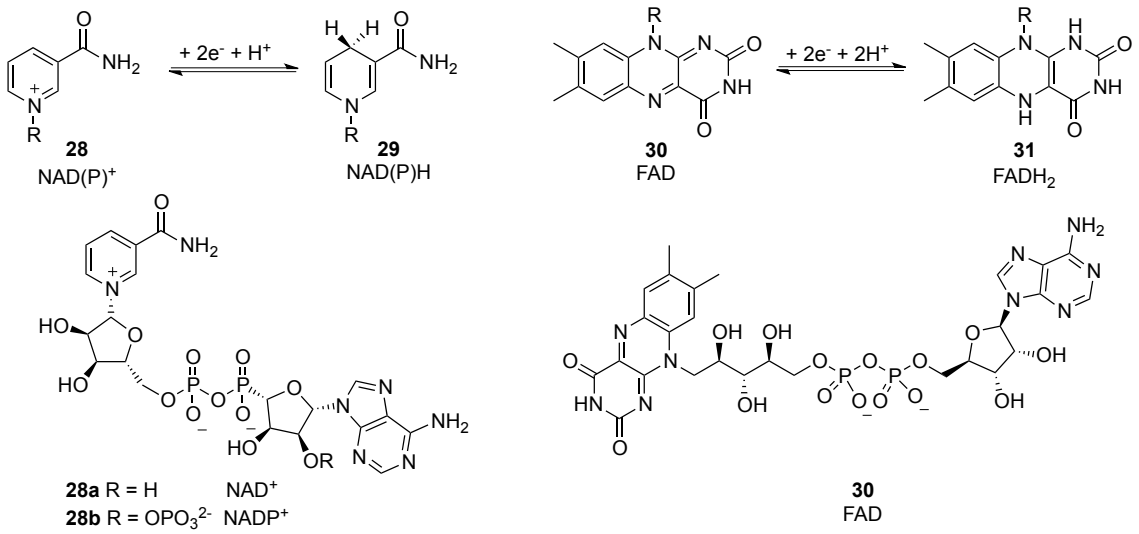

Scheme 9 Interconversion of oxidised and reduced $NAD(P)^+$ and FAD

Metals such as iron, cobalt, molybdenum and copper are common inorganic prosthetic groups, while NAD(P)H and FADH are important for electron transport and metabolism (**Scheme 9**). Co-factors function by assisting in processes the enzyme cannot carry out alone such as metabolism and electron transfer. Co-enzymes are also not considered part of the main protein, as they are transient and frequently recycled.

1.2.2. Mechanisms of enzyme activity

Enzymes function similarly to other catalysts in that they increase the rate without affecting the equilibrium of a given reaction. Enzymes in particular can increase the rate of a reaction by many orders of magnitude.[42]

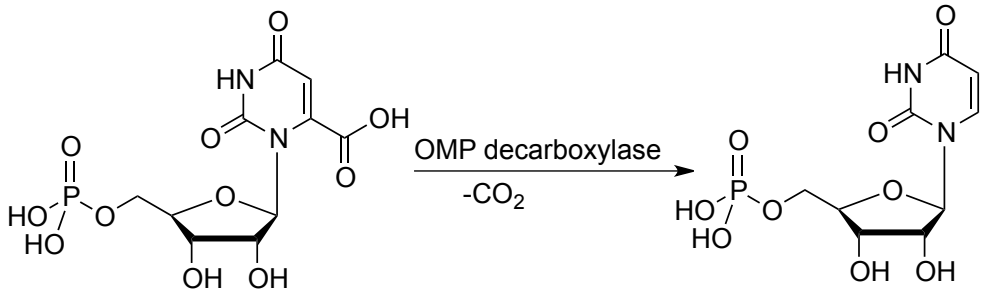

31 **32**

Scheme 10 UMP biosynthesis through OMP decarboxylase

Orotidine 5'-phosphate decarboxylase catalyses the biosynthesis of uridine monophosphate **32** (UMP) and is an extremely efficient catalyst with a rate enhancement of 10^{17} (**Scheme 10**). Other notable examples of rate enhancement include urease (10^{14}) and phosphoglucomutase (10^{12}).

$$E + S \underset{k_{-1}}{\overset{k_1}{\rightleftharpoons}} ES \xrightarrow{k_2} E + P$$

Figure 2 Single enzyme-substrate reaction where E = enzyme, S = substrate, ES = enzyme-substrate complex and P = product

A standard enzyme-catalysed reaction can be represented in a simplified manner as depicted above (**Figure 2**), where the formation of product from the enzyme-substrate complex is assumed to be the rate-limiting step.

$$V_0 = \frac{V_{max}[S]}{K_m + [S]}$$

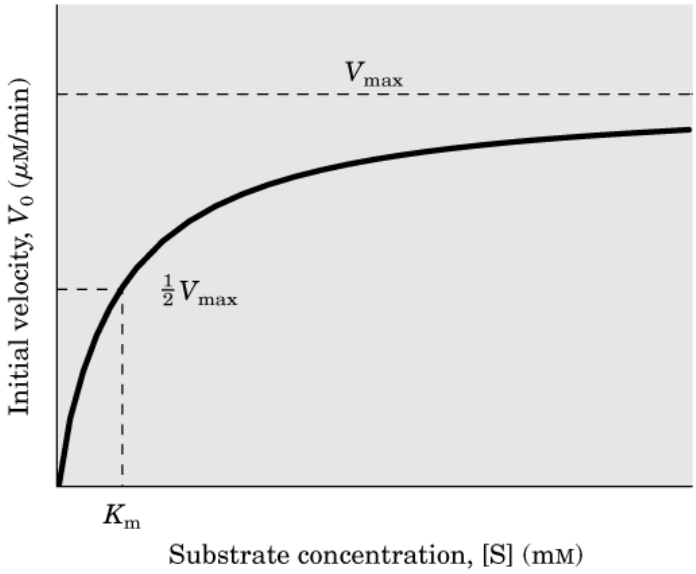

Figure 3 Michaelis-Menten rate equation and saturation curve[43]

The Michaelis-Menten model is a simple and popular method of enzyme kinetics, relating reaction rate to substrate concentration for a single enzyme and substrate (**Figure 3**).[43] Key terms described by the rate equation are: initial rate V_0, the maximal rate V_{max}, initial substrate concentration [S] and the Michaelis constant K_m. Additional parameters derived from this include the catalyst rate constant k_{cat} and the enzyme specificity constant k_{cat}/K_m. These parameters can be experimentally measured and are often used to compare the activity between enzymes on a given substrate.

Enzyme catalysis is accomplished through reducing the activation energy by either providing an alternate low-energy pathway or reducing the transition state energy, both of which enable the reaction to proceed faster (**Figure 4**).[42]

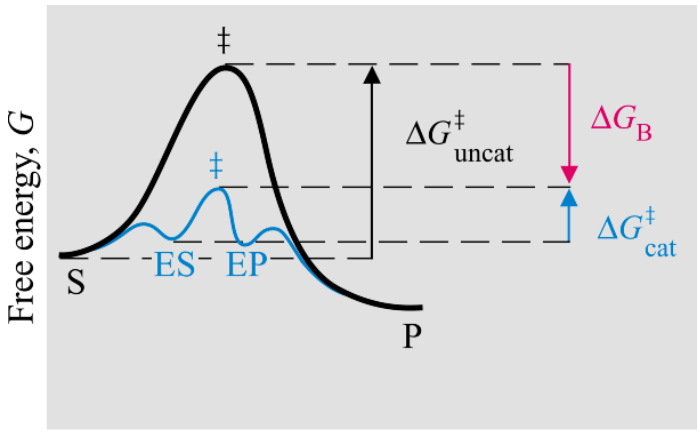

Figure 4 Reaction coordinate vs free energy (black = non-enzyme catalysed, blue = enzyme catalysed)[42]

Like other catalysts, enzymes remain unchanged after taking part in a chemical process. A distinguishing feature of biocatalysed reactions is that they take place in an enzymes active site; an internal compartment containing surface amino acid residues involved in chemical transformation and substrate binding. Here an enzyme-substrate complex is formed providing a lower energy pathway.

Emil Fischer originally postulated the formation of such complexes to be completely complimentary in 1894.[44] It is now known that the lock and key hypothesis would actually result in a poor enzyme. This is because an enzyme that is completely complementary to a substrate would stabilise the ground state ES complex and be unable to overcome the energy required to reach the transition state (**Figure 4**).

Instead, to overcome the issue of ΔG, Linus Pauling described a natural progression of Fischer's theory where the reaction transition state was stabilised by the enzyme instead.[45] While much lower, the required energy input to form the transition state is provided by the binding energy from additional interactions between the substrate and active site.

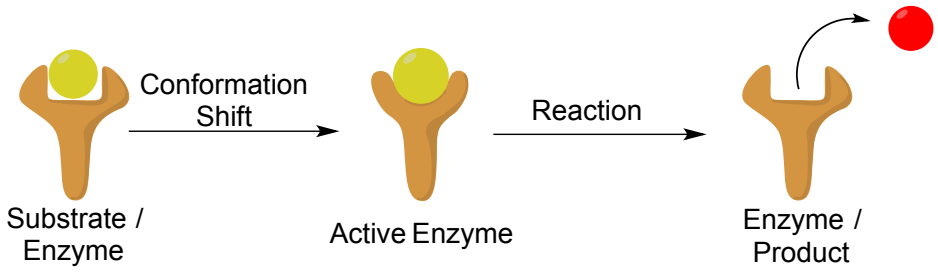

Figure 5 Induced fit enzyme model

Daniel Koshland proposed the currently favoured induced fit model in 1958 postulating that a change in the enzyme's active site occurs in response to the substrate.[46] Initially, weak hydrogen bonding and hydrophobic/ionic interactions between a substrate and enzyme trigger a conformational change. This provides additional complementary positioned residues, which, through further interactions, stabilise the transition state (**Figure 5**).

Other considerations for lowering activation energy involve the spatial properties of the active site. Reducing the entropy of the system involves aligning substrates and catalytic residues at a restricted and favourable orientation in the binding pocket. The binding of the substrate to the active site from the bulk water phase has an

accompanying entropy cost. As the system becomes more ordered, the free energy of the system is increased but is paid for by the binding energy obtained during catalysis.

The space within the active site also contributes to enzymes having a high degree of stereo- and enantioselectivity. In 1948, Alexander Ogston suggested that prochiral molecules could react asymmetrically, provided the active site had a defined asymmetrical structure.[47] This led to the three-point attachment rule, which was first postulated to explain why only one type of radiolabelled α-ketoglutarate was detected from the reaction of aconitase with citrate; a symmetrical molecule (**Scheme 11**).

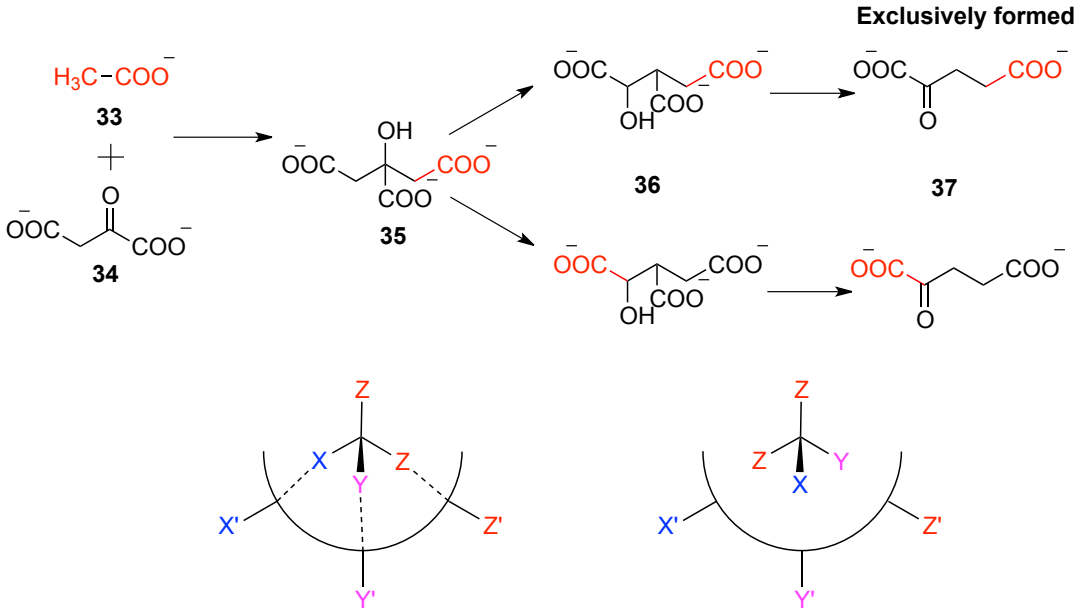

Scheme 11 Top – Incorporation of labelled (red) acetate into α-ketoglutarate **Bottom** – Complementary vs non-complementary fit of substrate to active site.[42]

A carbon (red) labelled acetate **33** was condensed with unlabelled oxaloacetate **34** to produce prochiral citrate **35**. Formation of isocitrate **36** followed by oxidative decarboxylation yielded α-ketoglutarate **37**. Only products from the upper path were observed when analysing the product. The selectivity could be rationalised if the *gem* hydroxyl and carboxylate groups interacted at specific residues within the active site, effectively anchoring the substrate to always react at the same position.

1.2.3. Methods of enzyme application in preparative biocatalysed reactions

Enzymes can be employed as whole-cells, cell free extracts or isolated preparations. Initially workers were limited to whole-cells and crude extracts, nevertheless this still allowed advances in enzyme mediated asymmetric catalysis. For

example the formation of (*R*)-mandelonitrile in 1912 from benzaldehyde and acetonitrile was achieved using (oxynitrilase containing) extract of bitter almonds.[48] Microbial strains later discovered to contain alcohol dehydrogenases were utilised in seminal work by Prelog for the stereoselective reduction of ketones.[49] Regio- and stereoselective oxidative hydroxylation of progesterone by *Aspergillus niger* and *Rhizopus arrhizus* (CP450's) led to a chemo-bio approach to the synthesis of hydrocortisone which previously required 40 distinct chemical steps.[50,51]

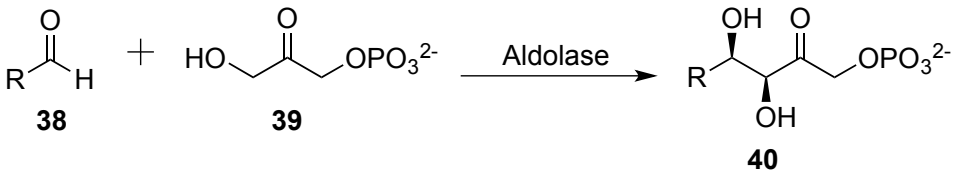

Scheme 12 Stereoselective adduct formation from rabbit liver aldolase.[52]

With the advent of improved methods of protein purification from the 1950's onward, the possibility of using isolated enzymes was realised. This resulted in the utilisation of biocatalysts for stereoselective transformations with unnatural substrates. A particularly noteworthy transformation emerged from the Whitesides group in 1985 (**Scheme 12**), where an isolated rabbit liver aldolase enabled the stereoselective addition of aldehydes and ketones to give chiral diols with high diastereoselectivity.[52]

Despite the availability of isolated enzymes, whole-cells have seen continued use particularly where industrial scale up is concerned. For example L-DOPA, a drug used in Parkinson's disease, is manufactured using a tyrosine-phenol lyase from *E. herbicola* (Ajinomoto, Japan)[53] and nicotinamide, a vitamin used for acne and niacin deficiency, is produced by a nitrile hydratase from *R. rhodocrous* (Lonza, Switzerland).[54] In several cases, where isolated enzymes are used, external redox co-factors (i.e. NAD^+/NADH, $NADP^+$/NADPH) and/or energy in the form of ATP are required to sustain the system.[41] These co-factors can be prohibitively expensive, particularly where stoichiometric equivalents are required. Conversely, in whole-cell systems, endogenous recycling is achieved through co-enzymes and cellular metabolism. Whole-cells can also protect enzymes from toxic byproducts; for example many organisms produce catalase, which can neutralise hydrogen peroxide that would otherwise deactivate enzyme activity.

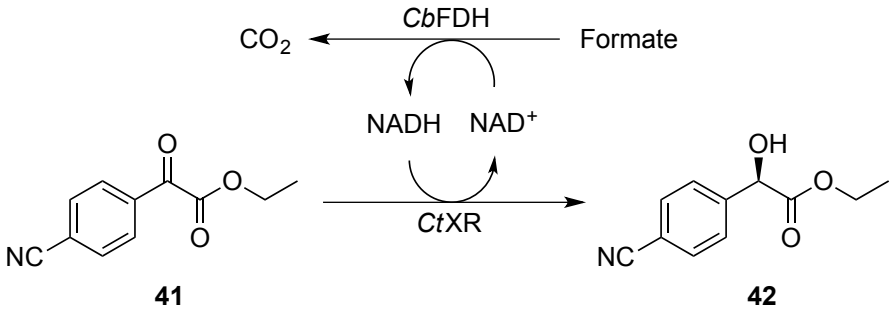

Scheme 13 Co-factor regeneration.[55]

Co-factor regeneration strategies requiring only catalytic amounts of material have been developed using co-enzymes to work in tandem with isolated biocatalysts. For example, (**Scheme 13**) a xylose reductase from *C. tenuis* utilises NADH in the redox process. Instead of supplying stoichiometric quantities of the co-factor, which is unstable in solution, an auxiliary enzyme; formate dehydrogenase from *C. boidinii* was utilised[55]. In this case the formate is considered "sacrificial" as it is solely present to recycle NADH.

Isolated enzyme preparations include solutions, lyophilised powder or immobilised on a solid support. The latter two are simple to use from a synthetic standpoint and have the advantages of cleaner product isolation and generally quicker reactions. Enzyme immobilisation provides a range of possibilities including higher substrate tolerance and, like lyophilisation, can provide greater functionality in organic solvent. Alexander Klibanov reported in 2001 that lipases such as porcine pancreatic lipase were found to retain partial activity in organic solvent in addition to having vastly improved thermal stability.[56] This was exploited in the stereoselective formation of chiral esters; a difficult reaction to perform in aqueous media due to the hydrolysis of esters to their corresponding acids and alcohols.

Ultimately, the type of enzyme system employed will depend on factors including scale, cost and co-factor considerations, in addition to the type of reaction.

1.2.4. Limitations of biocatalysts

Enzymes have evolved to be highly specific for chemical transformations. The great majority of enzymes have operated under physiological conditions. This has resulted in a preference for ambient pH and temperature in an aqueous environment.

Deviating from these comparatively narrow parameters can result in enzyme denaturing/deactivation. A key property of organic molecules is that many are poorly water soluble, this is even exploited during conventional chemical purification in the reaction work up. However, biocatalytic reactions, where water is often required to achieve optimum activity, result in much lower effective substrate concentrations.

The high enantioselectivity can also be a hindrance if the opposite enantiomer is required from a given transformation, a problem easily addressed in conventional catalysis by switching to the enantiomeric ligand. Substrate and product inhibition can also slow the rate of enzyme biotransformations.

Most of these problems have been accepted as limitations of using wild-type proteins, specifically evolved to carry out limited functions required by nature. With the advent of recombinant DNA methods, directed evolution and protein engineering, many of the problems described have been addressed and even more selective and robust proteins can be expressed in much greater quantities than previously possible.

1.3. Protein engineering

Despite clear benefits to employing enzymes in chemical transformations, there are still many limitations with respect to stability, selectivity and the range of reactions that can be carried out. Advances in protein engineering have allowed the modification of residues in structurally relevant sites using a range of targeted evolution methods.

1.3.1. Recombinant DNA for protein expression

An early problem encountered using isolated proteins stemmed from the amount of material naturally expressed. Only small quantities of enzyme could be extracted from microbes, fungi, plants and animals, which presented a major obstacle for generalising the use of biocatalysts in chemical synthesis. This changed with the advent of molecular cloning techniques in the early 1970's, where isolation of restriction endonucleases, DNA polymerases and DNA ligases combined with size exclusion purification techniques allowed heterologous protein expression for the first time. [57,58]

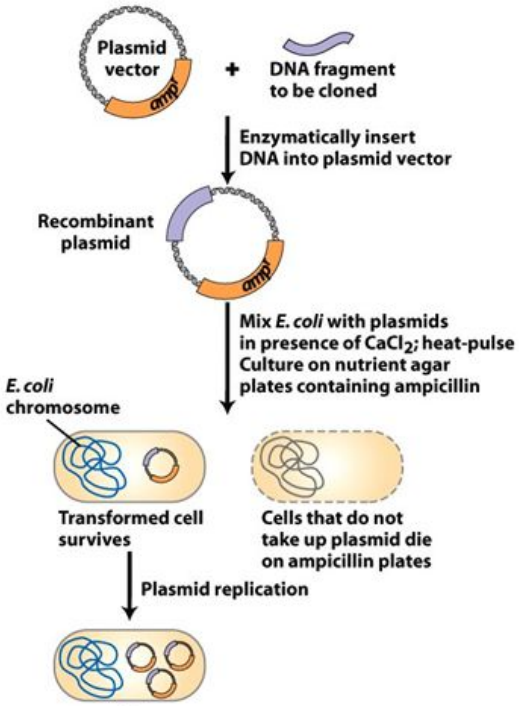

Figure 5 DNA cloning for heterologous expression.[59]

In molecular cloning, a DNA strand containing genetic information to express a given protein is isolated using restriction endonucleases, phosphodiester bond cleaving enzymes, which act specifically at restriction sites on a given plasmid. DNA ligases can then join the strand into a restriction site of vector DNA creating a recombinant plasmid. Inserting the plasmid into a host organism such as *E. coli* results in populations of organisms also producing the recombinant DNA.[59] *E. coli* is often used as a host due to the fact it grows fast, is relatively benign and is amenable to cloning foreign DNA. In addition to cloning DNA, expression strains of *E. coli* have been engineered that accommodate for the unnaturally high protein loads arising from heterologous expression. This allowed for industrial scale production of proteases and lipases, which saw initial use in detergents (Novozyme, Henkel).

1.3.2. The polymerase chain reaction

First developed by Kary Mullis in 1983, the polymerase chain reaction (PCR) revolutionised molecular biology and has become an indispensible tool in protein engineering.[59,60] The technique allows for large scale cloning of DNA through multiple cycles of replication with up to millions of potential copies available from a single sequence. The technique differs from molecular cloning in that it doesn't require

internal cellular machinery; instead utilising a thermostable DNA polymerase and thermal cycling.

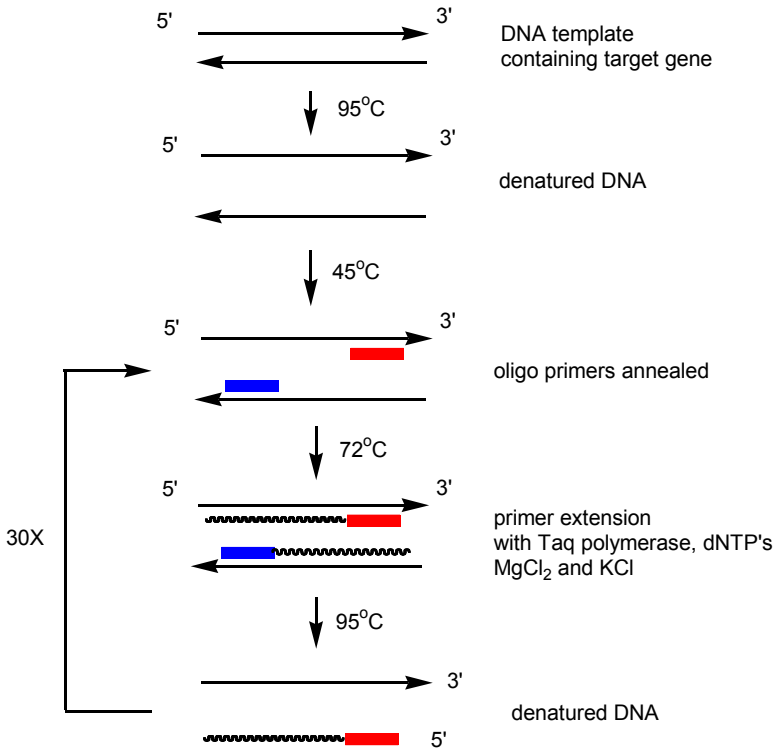

Figure 6 Outline of polymerase chain reaction (PCR)

Firstly, the strand of DNA being replicated also known as the template is denatured and unwound by heating to 95 °C (**Figure 6**). After reducing the temperature to 45 °C complimentary single short strands of oligonucleotides called primers anneal to the template before the separated strands can re-bind. At 72 °C DNA polymerase isolated from thermostable *Thermus aquaticus* (Taq) extends the primers making a copy of the original complementary strand. This process is usually repeated 20-40 times and as DNA is replicated the new strands themselves are used as templates for subsequent cycles resulting in exponential amplification.

PCR being a cheap, reliable and effective way of replicating specific sequences of DNA has resulted in many applications across modern biology, medicine and forensic science. It is a more efficient method of cloning DNA compared to molecular cloning and the DNA produced is also pure. By employing different primers, specific regions of genomic DNA can also be amplified, isolating regions of interest. Amplification of DNA samples has applications in forensic science where only trace amounts of genetic material may be available, the amplified sample can then be analysed through DNA

profiling. Medical applications of PCR include genetic profiling; where regions of an individuals DNA can be analysed to search for known mutations characteristic for a given disease. HIV can also be detected much earlier and treatment quantified using a variant method of PCR coupled with reverse transcriptase (RT-PCR).[61] Instead of screening for antibiotic markers that can take weeks to develop, blood can be screened directly for the viral RNA by amplifying the DNA complement produced by reverse transcriptase.

1.3.3. Site-specific mutagenesis

Site-specific mutagenesis is a structure based genetic engineering technique that involves altering one or more bases in the sequence to replace an amino acid with one of the 19 naturally occurring alternatives. Michael Smith first reported this method in 1978 where mutated DNA was obtained by incorporating complementary oligonucleotides containing base mismatches.[62,63] This technique was initially adopted to improve enzyme stability with applications in synthesis. For example the thermal stability of a 3-isopropylmalate dehydrogenase was improved by introduction of a polar tyrosine residue resulting in additional protein surface hydrogen bonding.[64]

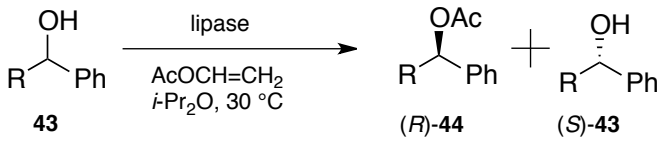

43 (*R*)-**44** (*S*)-**43**

a: R = $(CH_2)_4CH_3$ **b**: R = $(CH_2)_5CH_3$
c: R = $(CH_2)_4CF_3$ **d**: R = $(CH_2)_2(CF_2)_2CF_3$

Scheme 14 Lipase catalysed kinetic resolution of bulky alcohols[65]

This approach was also later used to successfully augment stereoselectivity and catalytic activity. A mutated lipase from *Burkholderia cepacia* displayed a 40-fold greater *E* value and improved rate of reaction compared to the WT enzyme on alcohols with bulky substituents (**Scheme 14**).[65]

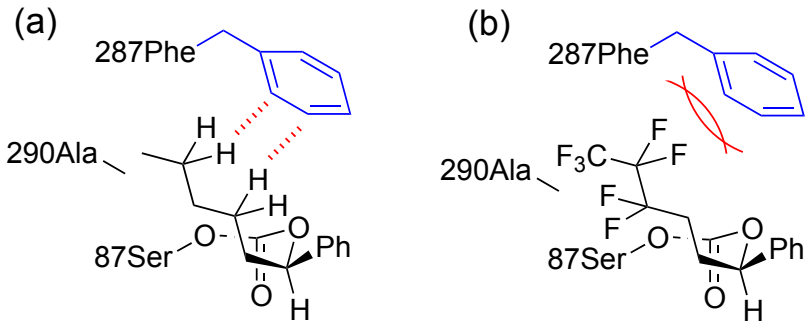

Figure 7 (a) Transition state H-pi interaction between Phe287 and (*R*)-1-phenyl-1-hexanol (b) steric repulsion in partially fluorinated (*R*)-1-phenyl-1-hexanol.[65]

A double mutant (I287F/I290A) was found to have improved activity on (*R*)-1-phenyl-1-hexanol **43a**. Ala290 avoided previous collisions of the alkyl chain with Ile, while Phe287 substitution resulted in attractive H-π interactions. The positive effect of the latter was supported by much poorer activity of the fluorinated analogue where aromatic interactions could not take place (**Figure 7**).

Specific mutagenesis is limited in that knowledge of the individual protein structure is necessary in order to be carried out. Owing to the individual variation and complexity of enzymes in addition to a lack of clear correlation between sequence and function, a general strategy for structural optimisation has yet to be realised.

1.3.4. Random mutagenesis and the dawn of directed evolution

Random mutagenesis can be employed without prior knowledge of the protein structure depending on the technique employed. Error-prone PCR (epPCR) is the most common method of developing random mutations and involves incorporation of incorrect base pairs during DNA replication. This can be achieved by a number of methods including using DNA polymerase lacking a proof reading module thereby being more prone to errors, by increasing the amount of $MgCl_2$ in the reaction, altering the concentration of available dNTPs or using mutator strains. Developed by Pim Stemmer, DNA shuffling is an efficient method for the rapid library expansion that digests mutated DNA strands into oligonucleotides of 50-100 bp that are then combined and extended through conventional PCR.[66] Saturation mutagenesis is another popular method of randomisation at specific residues using degenerate oligonucleotides, however knowledge of the protein structure is required. Early examples of mutagenic libraries produced enzymes possessing greater thermostability[67] and resistance to chemical oxidants.[68]

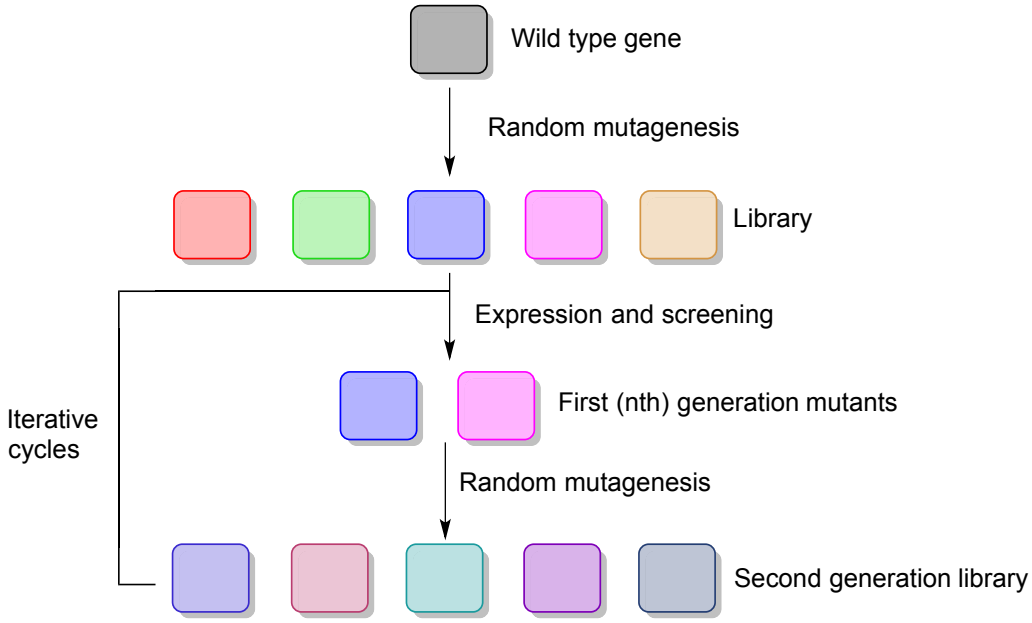

Figure 8 Schematic representing conventional iterative mutagenesis

Directed evolution involves iterative rounds of random mutagenesis following selection of mutants with desired properties (**Figure 8**). The first reported example using successive rounds of mutagenesis improved the thermostability of a kanamycin nucleotidyltransferease from *B. stearothermophilus*.[69] The functioning temperature was increased through two rounds of mutagenesis. Enzymes containing a double mutant tolerated operating temperatures of 70 °C, a considerable improvement over 47 °C for the WT.

However, iterative mutagenesis was not explored further until seven years later with Francis Arnold's seminal work on the protease Subtilisin E.[70] Through 4 rounds of mutagenesis and screening, Arnold's group, developed a variant containing 10 mutations with 256 times the activity of the wild-type enzyme in 60 % DMF. Additionally, it was demonstrated that the mutant could catalyse the synthesis of the peptide poly(L-methionine) in 70 % DMF where the wild-type had no measurable activity. Enzyme catalysed reactions in organic solvent are industrially attractive owing to higher solubility of hydrophobic substrates and suppression of unwanted water-dependent side reactions. Organic solvent often results in loss of enzyme activity. However, in this case mutations around the active site resulted in a mutant enzyme almost as efficient in high concentrations of DMF as the wild-type enzyme in an aqueous environment.

1.3.5. Highlighted examples of directed evolution

Early work focused on improving enzyme thermal stability to be more suited to industrial operating conditions. Proteases in particular were given a great deal of attention due to the need for stable proteins in detergent applications.[71] Additional work was undertaken utilising directed evolution to increase the thermal stability of several different enzymes including esterases[72], peroxidases[73] and amylases.[74]

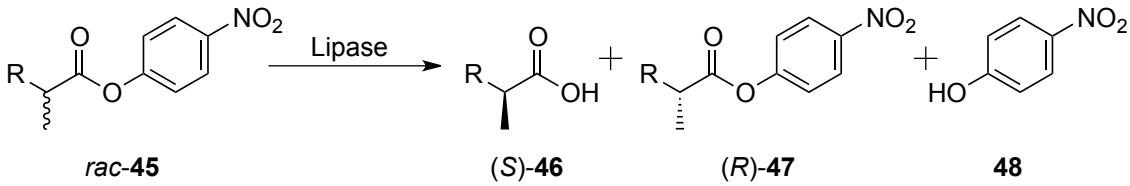

rac-**45** (*S*)-**46** (*R*)-**47** **48**

Scheme 15 Lipase catalysed resolution of chiral ester[75]

Interest in augmenting the catalytic parameters of enzymes for use in organic synthesis was the driving force for the first reported example to improve enantioselectivity (**Scheme 15**).[75] A lipase from *Pseudomonas aeruginosa* used in the kinetic resolution of racemic ester **45** showed marginal selectivity for formation of the *S* product (E = 1.2). Sequential single point mutations through 4 rounds of mutagenesis resulted in a lipase with over 10-fold stereopreference for the *S* isomer.

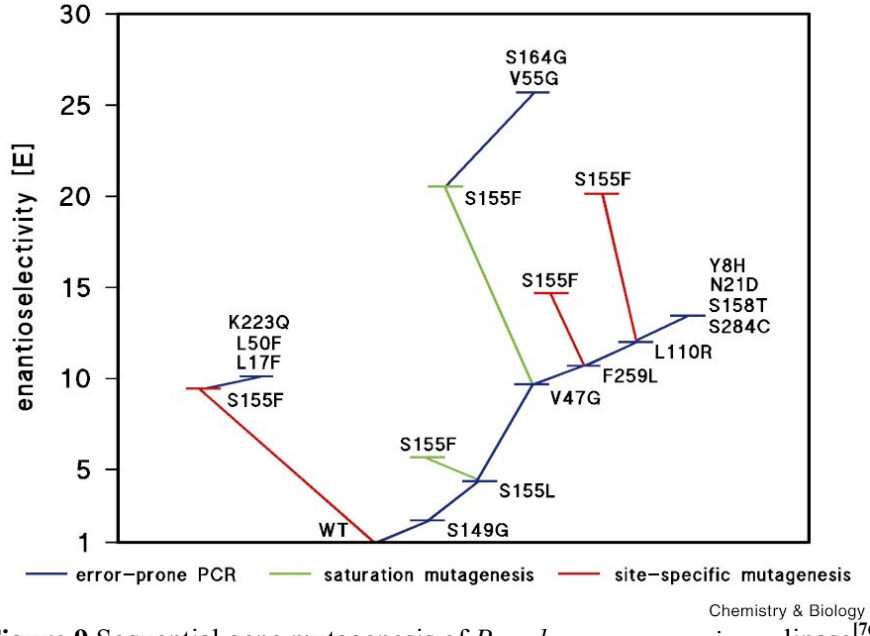

Figure 9 Sequential gene mutagenesis of *Pseudomonas aeruginosa* lipase[76]

This was further improved during subsequent work, which used a combined approach of epPCR, saturation mutagenesis and targeted mutagenesis (**Figure 9**).[76]

After the S115F substitution was found to have a significant effect on the *E* value of the wild-type enzyme, the substitution was introduced in other mutants. What was particularly noteworthy is that the S115F substitution had varying contributions to stereoselectivity depending on other mutations present. The introduction of S115F had a much greater effect on selectivity with V47G compared to F259L, a seemingly more selective mutant. This demonstrated that when using a combined approach, the routes to the most selective enzyme might arise from synergistic effects involving previously less selective variants.

An impressive example using directed evolution to augment both stereoselectivity and substrate specificity concerns a 2-keto-3-deoxy-6-phosphogluconate (KDPG) aldolase from *E. coli*.[77] The wild-type enzyme catalysed the reversible addition of pyruvate to an aldehyde stereoselectively forming a carbon-carbon bond and delivering the phosphorylated precursor **51** to the D-sugar (**Scheme 16**). A combination of epPCR and DNA shuffling was used to screen for variants that accepted non-phosphorylated substrates in addition to showing opposite enantioselectivity for the aldehyde.

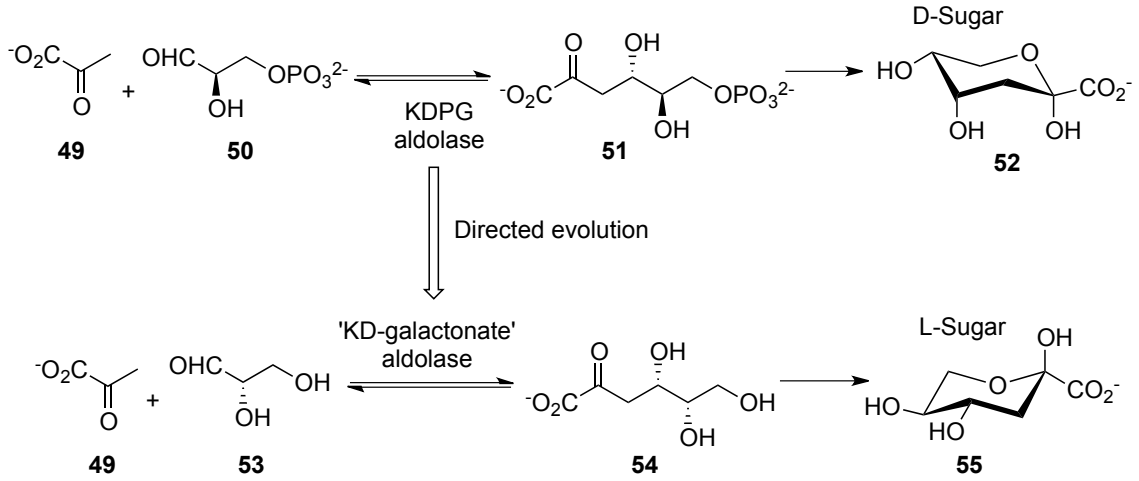

Scheme 16 Directed evolution of a KDPG aldolase to tune stereoselectivity and substrate specificity[77]

Of the initial 2400 mutant population screened, less than 0.5 % showed improved 2-keto-3-deoxy-galactonate (KDG) activity. Four genes found with improved activity were combined using DNA shuffling and the resulting library was assayed with more active mutants being combined and re-screened. A total of four generations were assayed and produced in this manner with a similar approach taken to probe stereoselectivity. The target reaction was screened for using the aldol product **54** as a

substrate and monitoring pyruvate formation with a coupled lactate dehydrogenase (LDH) and following reduction of NADH spectrophotometrically. A resulting variant produced with 4 active mutations (T84A, I92F, V118A and E138V) showed good activity with the non-phosphorylated galactonate and produced the sugar precursor with perfect diastereo control.

Sialic acid aldolase was mutated in a semi-rational approach to extend the substrate scope beyond *N*-acetylmannosamine **56**.[78] Using crystallographic data obtained from the *Haemophilus influenzae* enzyme, which contained 35 % sequence identity and 59 % similarity, three key residues were identified that interacted with an inhibitor 4-oxosialic acid.

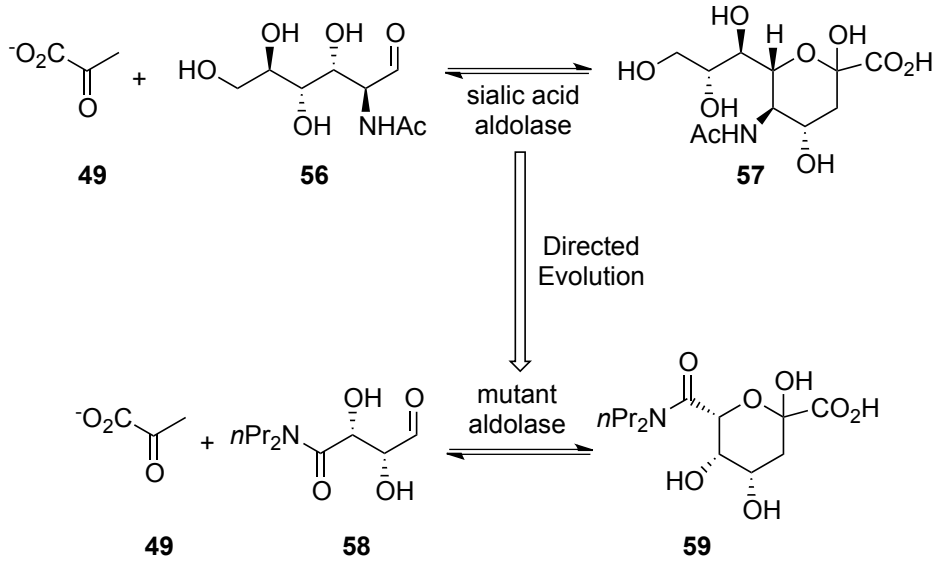

Scheme 17 Directed evolution of an aldolase for synthesis of sialic acid mimetics[78]

The equivalent residues in the *E. coli* enzyme; Asp191 Glu192 and Ser208 underwent saturation mutagenesis and were screened against a synthesised analogue **59** (**Scheme 17**), with the assumption that an active mutant would also catalyse the forward reaction. A singe mutation E192N was observed to have a 50-fold improvement in substrate specificity (k_{cat}/K_M) for **59** over the wild-type enzyme.

A combined deracemisation system consisting of an engineered monoamine oxidase (MAO-N) from *A. niger* and a non-selective chemical reducing agent allowed for the production of enantiomerically pure chiral amines, which are important building blocks in the synthesis of pharmaceuticals (**Scheme 18**).[79]

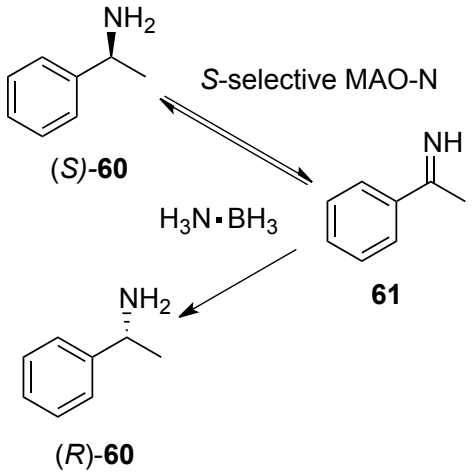

Scheme 18 Dynamic kinetic resolution using a selective amine oxidase and non-selective reducing agent[79]

Depending on the selectivity of the enzyme employed, either isomer could be obtained in high enantiomeric purity from the racemate. This process is a key example of an engineered enzyme used in industrial biocatalysis and was later patented by Ingenza.[80]

1.4. Examples of industrial application for engineered biocatalysts

Protein engineering has delivered selective enzymes that are stable to harsh processing conditions. Their comparatively high activity per unit mass and ease of removal compared to whole-cells has resulted in engineered biocatalysts becoming economically viable in the industrial sector. The stereoselective reduction of ketones using isolated ketoreductases (KREDs) is believed to have largely replaced whole-cell and metal-ligand based approaches.[81]

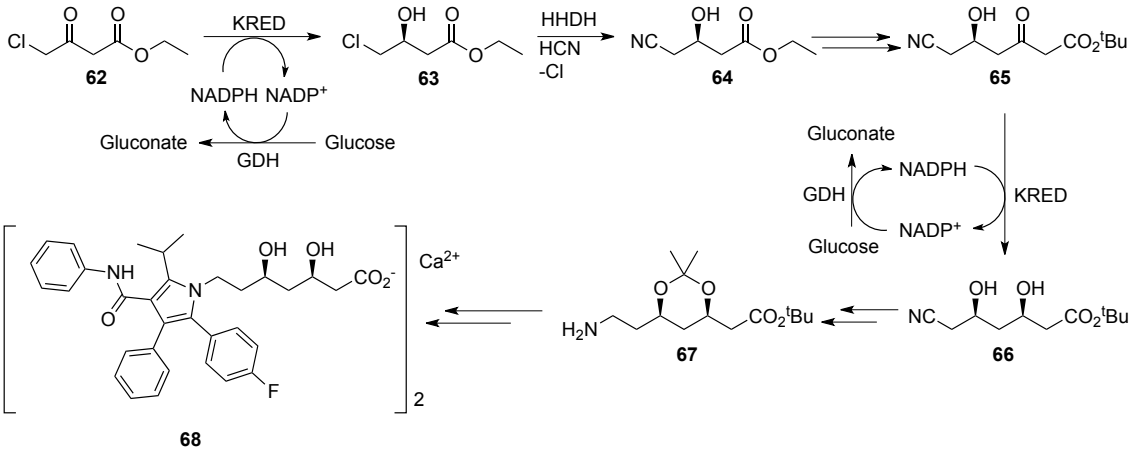

Scheme 19 Enzymatic route to the key side chain of atorvastatin[82]

KREDs have been used in several stages during the synthesis of atorvastatin **68**, an active pharmaceutical ingredient (API) present in Pfizer's blockbuster cholesterol-lowering drug, Lipitor (**Scheme 19**).[82,83] The process highlighted involves 3 biocatalytic steps, two KRED stereoselective reductions providing intermediates **63** and **66** in addition to a halohydrin dehalogenase (HHDH) to form **64**.

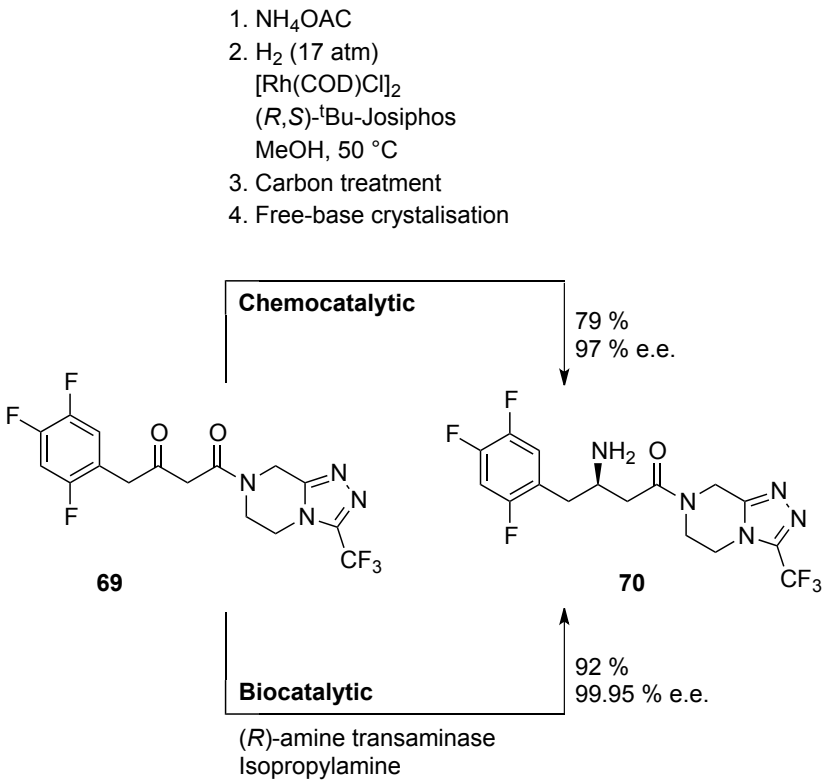

Scheme 20 Chemo/bio routes to sitagliptin[84]

Sitagliptin **70** (marketed as Januvia, Merck), is a drug used to treat hyperglycaemia in patients with type-2 diabetes. The final step of synthesis involves the stereoselective transamination of prositagliptin **69**. A process utilising an engineered *S*-selective transaminase increased the overall yield with greater stereoselectivity in addition to replacing all transition metals.[84] Additionally, the bioctalytic method used much less waste and increased overall process efficiency by up to 53 %.[85]

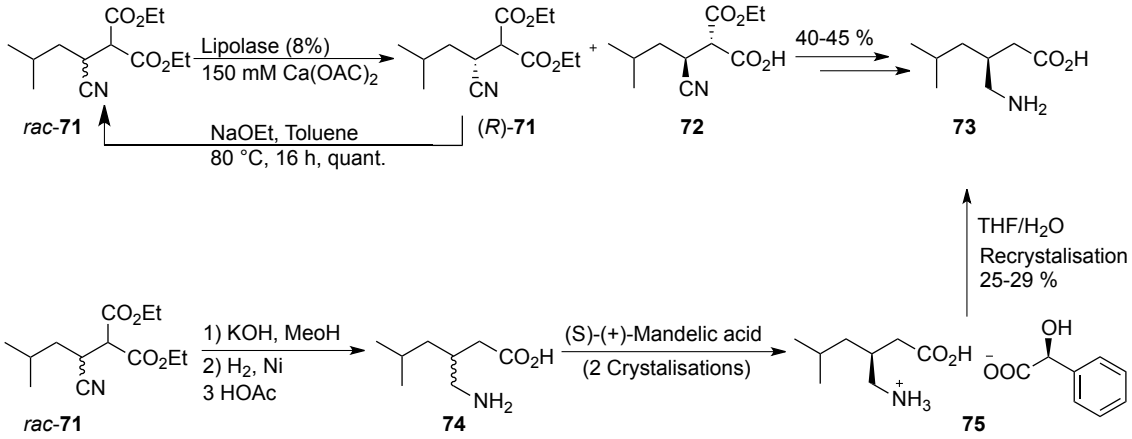

Scheme 21 Comparison of bio/chemo routes to pregabalin[86]

Pregabalin **73** is the API in Lyrica (Pfizer), a drug used in the treatment of epilepsy, neuropathic pain and general anxiety. A chemoenzymatic approach to process optimisation involved the stereoselective hydrolysis of racemic **71** and recycling of the unwanted isomer back to the racemate in a relatively benign manner.[86] The previous process cleaved an ester and reduced the cyano compound to a racemic amine before recrystallizing the desired enantiomer as a mandelic acid salt **75**. The improved process prevented late-stage loss of 50 % product through classical resolution and lowered the *E* factor from 86 to 17, increasing the overall yield up to 40-45 %.

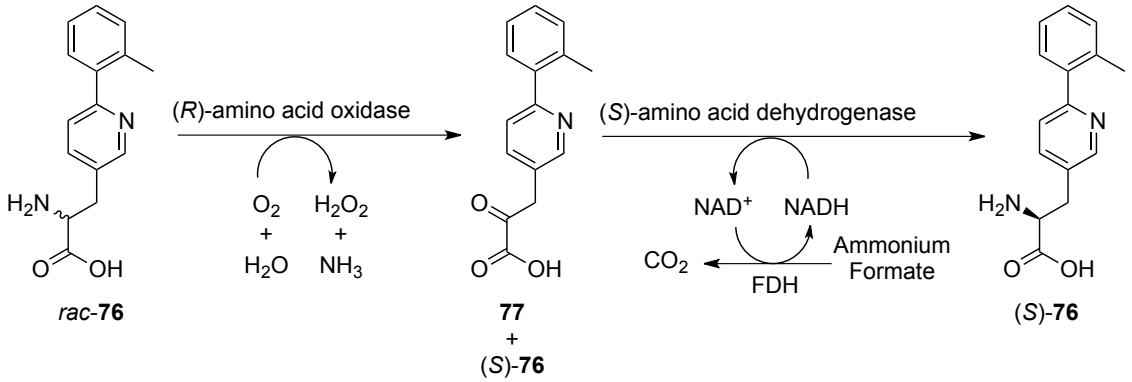

Scheme 22 Deracemization of racemic amino acid drug candidate.[87]

The *S*-amino acid **76** is a key intermediate in a candidate antidiabetic drug being developed by Bristol-Meyers Squibb.[87] A deracemization using a selective *R*-oxidase and *S*-dehydrogenase allowed the desired enantiomer *S*-**76** to be fully resolved.

1.5. Oxidative enzyme transformations

Oxidations are a key reaction in organic synthesis and are used to access many functional groups including: aldehydes, ketones, imines, amides and carboxylic acids. Transition metal based approaches to oxidations have been traditionally adopted, often requiring stoichiometric quantities of oxidant.[88] However, many metal containing oxidants such as Jones/Sarrette (chromium) and Tollen's (Silver) reagent are highly toxic and produce significant waste. Other metal free organic oxidations are available such as the Swern (sulphur) and Dess-Martin (hypervalent iodine) but produce toxic byproducts and are potentially explosive.

The need for more benign methods of chemical oxidation has led to approaches using less toxic metal. Methods using stoichiometric amounts of organic oxidant with a catalytic amount of metal have been successful with palladium[89] and copper.[90] An important discovery by Milstein *et al*.[91] utilised a novel ruthenium pincer catalyst in an oxidative amide coupling with refluxing basic water. This process producing only H_2 as a side product had excellent atom economy and was further utilised for the oxidation of unactivated primary alcohols.[92] Gold nanoparticles using molecular oxygen have also successfully been used in the synthesis of amides.[93] These greener approaches still have inherent limitations related to selectivity, operating temperatures, expensive catalysts and unwanted side-reactions preventing general adoption.

The chemo-, regio- and stereoselectivity of enzymes make bio-oxidations useful for clean formation of product in fewer steps by avoiding unnecessary protection/deprotection. There are many examples of biocatalysed oxidation reactions using a range of enzymes that are comparatively benign and practically metal free.[94]

1.5.1. Classes of oxidative enzymes

Dehydrogenases are amongst the most common enzymes used in oxidation reactions and are the most studied. They catalyse the reversible oxidation of alcohols and amines utilising a $NAD(P)^+$ cofactor. Alcohol dehydrogenases (ADH) have been extensively studied for the oxidation of primary and secondary alcohols.[95] ADH from horse liver (HLADH) was one of the first exploited for use in organic synthesis, due to a broad substrate tolerance and *S*-selectivity.[96]

Oxidase enzymes are also available to catalyse the transformation of alcohols, aldehydes and amines. Most alcohol oxidases (AlcOX) are flavin-dependent where

FAD is the primary hydride acceptor. Glucose oxidase (GluOX) is a very well known flavoenzyme responsible for the oxidation of β-$_D$-glucose, however its substrate scope is significantly limited.[97] A Cu^{2+}-dependent galactose oxidase (GOase) has a comparatively broader substrate scope, which has been further enhanced through protein engineering.[98,99] Laccases are a member of the blue-copper oxidases and generate radicals through the single electron abstraction of phenolic type compounds.[100] Poor redox potentials mean laccase cannot oxidise alcohols alone, however they can re-oxidise activated mediators such as HBT **78**, ABTS **79** and TEMPO **80** (**Scheme 23**). Laccase-mediator-systems (LMS) produce water instead of H_2O_2 as seen in other oxidases. In some cases LMS have replaced hypochlorite as a greener terminal oxidant but low turnover is still a major limitation.[101]

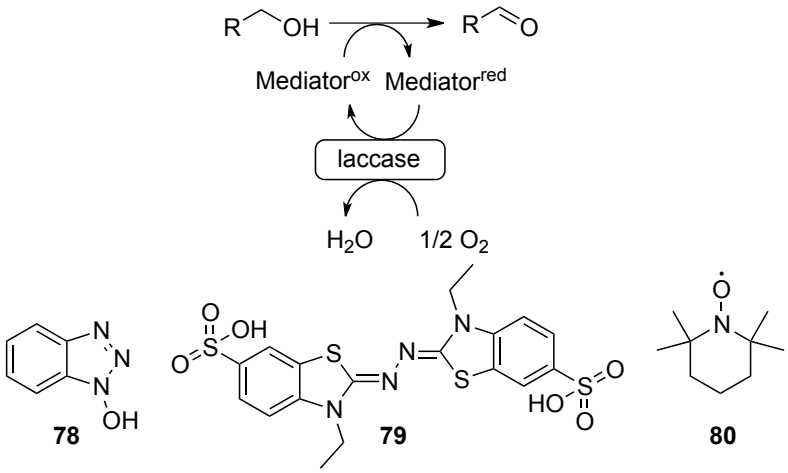

Scheme 23 LMS for alcohol oxidation[100]

Oxygenases catalyse the reductive activation of molecular oxygen, the resulting peroxide and protein bound metal complex can catalyse selective hydroxylations, epoxidations and Baeyer-Villiger reactions.[102,103] Cytochrome P450 monooxygenases utilise an iron-heme complex, where the active species **82** is formed through NAD(P)H mediated reduction of O_2 (**Scheme 24**).[104]

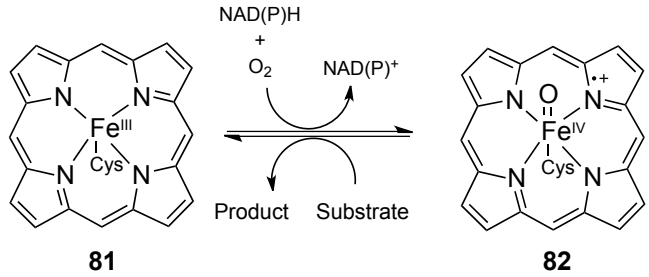

Scheme 24 Simplified P450 monooxygenase active species formation

Peroxidases can perform similar reactions to oxygenases but require hydrogen peroxide to regenerate their active prosthetic group which, in addition to iron, can contain selenium, vanadium or manganese. [105,106] Peroxidase from *Agroybe aegerita* (AaP) has been discovered as a potential replacement for *Caldariomyces fumago* (CPO), a well-documented enzyme for oxidations and oxyfunctionalisations that isn't economically viable for preparative transformations.[107]

1.5.2. Enzymatic alcohol oxidations

Single-step and "through oxidations" of primary alcohols to aldehydes and carboxylic acids are a cornerstone of organic synthesis. Biocatalytic oxidations of this class have accordingly received a great deal of interest. Conversely, oxidation of secondary alcohols destroys chirality and has received less attention due to the lack of complexity in the planar products. However, secondary alcohol oxidation plays an important role in the production of enantiopure alcohols through dynamic kinetic resolutions.[95]

1.5.2.1. Bio-oxidation of primary alcohols to aldehydes

Preventing the over-oxidation of primary alcohols to carboxylic acids is a major challenge due to the reactivity of aldehydes. This is a particular problem in whole-cells, where co-factors are readily regenerated and other oxidative enzymes may be present. An effective solution utilised by Buhler *et al.*[108] for the xylene monooxygenase-facilitated production of 3,4-dimethylbenzaldehyde, involved incorporation of a less polar organic solvent to selectively partition the aldehyde for *in situ* product extraction.

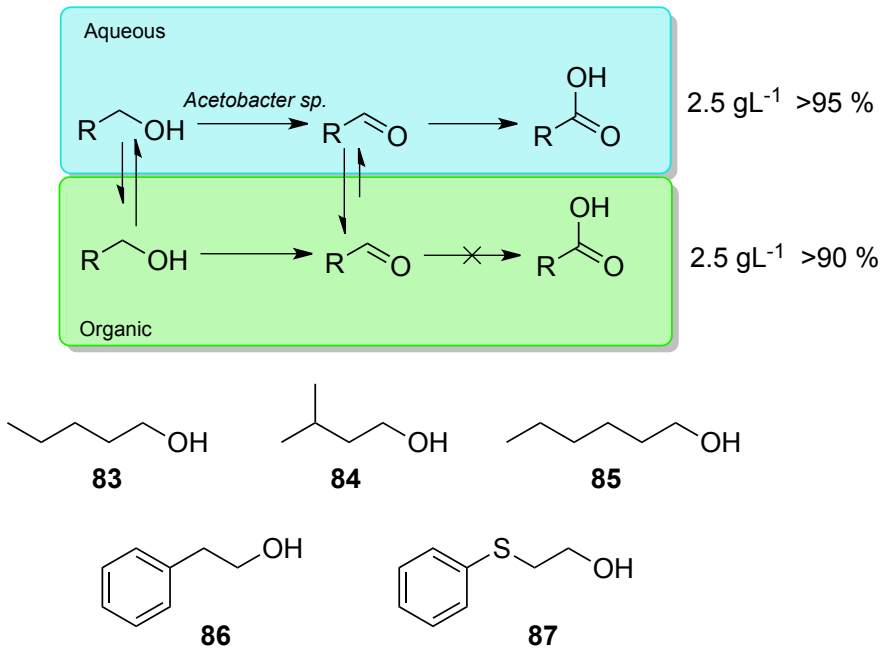

Scheme 25 Reaction engineering for controlled alcohol oxidations.[109]

This process was also used in the selective oxidation of aliphatic and aromatic alcohols using H_2O or H_2O/isooctane with acetic acid bacteria containing ADH (**Scheme 25**).[109] Depending on the reaction conditions employed, the aldehyde or acid could be selectively obtained in excellent yield.

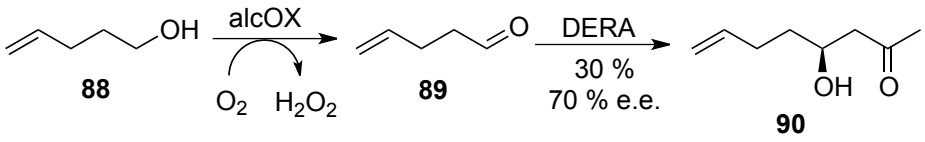

Scheme 26 Two-step one-pot chemo/stereoselective alcohol oxidation and aldol biotransformation[110]

Another method of aldehyde conservation involves a multi-enzyme cascade where the aldehyde is utilised in a second reaction before over-oxidation can occur. A one-pot cascade utilising AlcOx from *Pichia pastoris* and 2-deoxyribo-5-phosphate aldolase (DERA) allowed for the selective oxidation of the alcohol **88**, followed by a stereoselective aldol reaction to deliver **90** in modest yield (**Scheme 26**).[110] The vinyl group also remains intact throughout this process, highlighting the benefits of employing a chemoselective biocatalyst.

LMS have facilitated the successful single oxidation of a range of benzyl alcohols with ABTS[111] and TEMPO[112] in quantitative yields.

1.5.2.2. Bio-oxidation of primary alcohols to carboxylic acids

The biocatalytic oxidation of primary alcohols to carboxylic acids has largely been dominated by whole-cell systems. This is due to the endogenous regeneration of co-factors such as $NAD(P)^+$ that would have to be supplemented through other means in isolated enzymes. Acetic acid bacteria containing ADH III and an aldehyde dehydrogenase (AldDH) have been used for the multi-gram scale "through" oxidations of several alcohols (**Scheme 27**).[113,114] These reactions also displayed stereoselectivity for some chiral substrates allowing for large scale kinetic resolutions.[115-118] Other organisms expressing ADH's have been used in the bio-oxidation of furan alcohols to give the corresponding acids including previously discussed platform chemical candidate FDCA **26** (**Scheme 27**).[119,120]

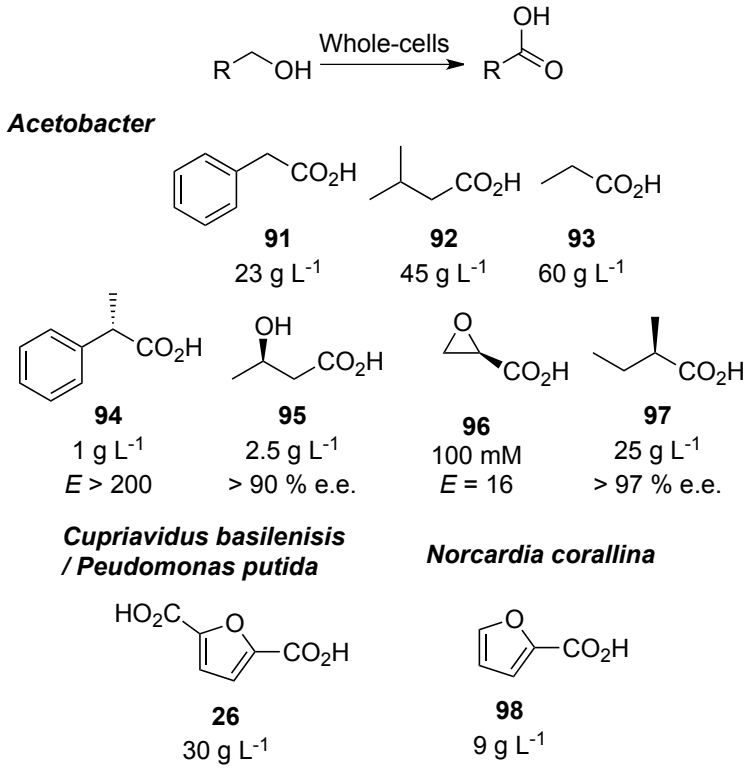

Scheme 27 Examples of whole-cell catalysed "through oxidations" and kinetic resolutions of aliphatic and aromatic alcohols (*E* = enantiomeric ratio).[113-120]

While less prevalent than whole-cells, there are still several examples of processes utilising purified enzymes for the oxidation of primary alcohols. In an early example reported by Wong *et al*., isolated HLADH was used for the selective resolutions of 1,2-diols to α-hydroxy acids (**Scheme 28**).[121]

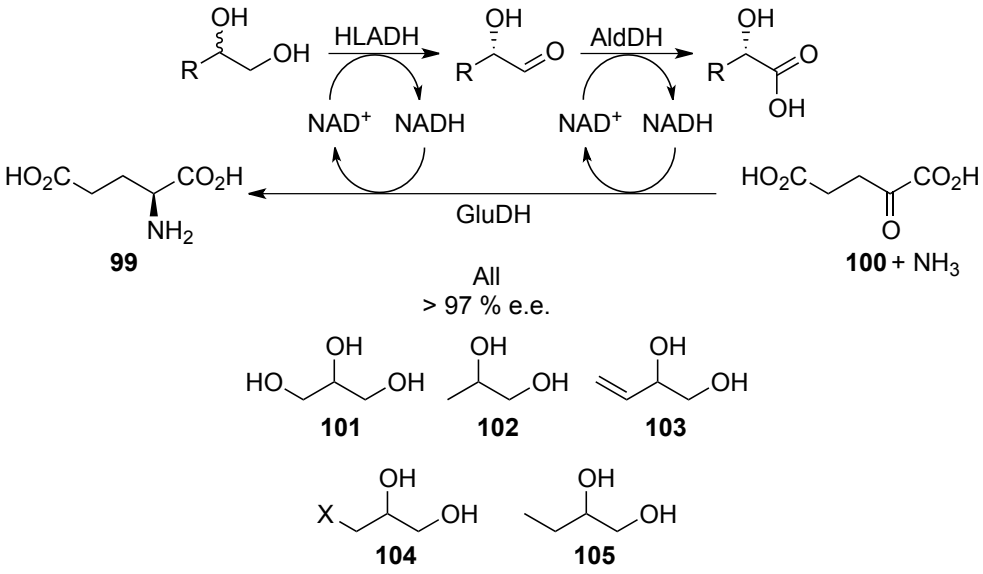

Scheme 28 Isolated HLADH used for kinetic resolution of α-hydroxy acids[121]

Coupled with an AldDH, both enzymes utilised an equivalent of NAD^+, which was regenerated with an α-ketoglutarate/glutamate dehydrogenase (GluDH) system. In addition to 1,2-diols, the HLADH catalysed oxidation of 1,4 and 1,5-diols has led to the formation of enantiopure lactones through the spontaneous cyclisation of the primary aldehyde followed by additional oxidation of the hemiacetal.[122,123]

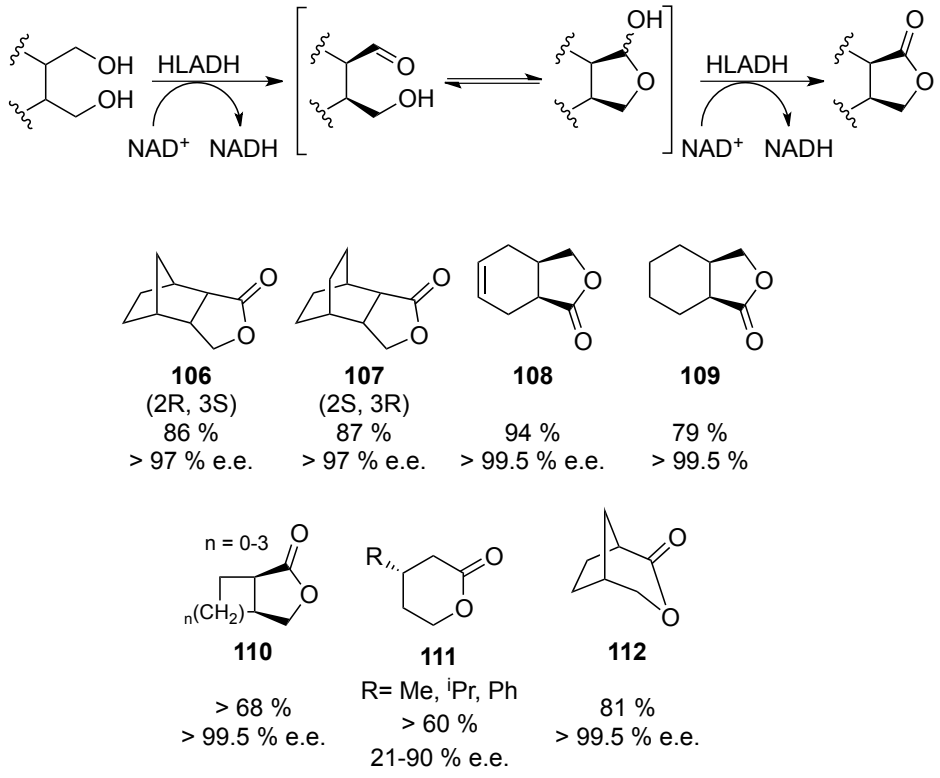

Scheme 29 ADH catalysed desymmetrisation of *meso*- 1,4- and 1,5-diols[122,123]

Lactones were produced at gram scale with good to excellent conversions. The desymmetrisation approach is interesting as, unlike in conventional kinetic resolutions, the desymmetrisation allows for potentially 100 % of a given enantiomer to be formed in the presence of a selective oxidant.

1.5.2.3. Regioselective bio-oxidation of polyols

Enzymatic discrimination of substrates bearing multiple reactive moieties is a highly desirable trait in improving atom efficiency and lowering waste. Regioselective chemical oxidation of carbohydrates has to contend with multiple functional groups, which requires extensive protection/deprotection to avoid unwanted reactions. Many polyol oxidases and dehydrogenases have been used for the oxidation of carbohydrates including galactose[124], glucose[125] and lactose[126] on a preparative scale. Selective polyol oxidases have seen multiple industrial applications. Fructose is commercially used in the food industry for its sweetening properties, but also has important applications as a feedstock for platform chemical replacements (i.e. FDCA). The Cetus process utilises a pyranose-2-oxidase (P2O) followed by chemical dehydrogenation to produce pure fructose from glucose.[127]

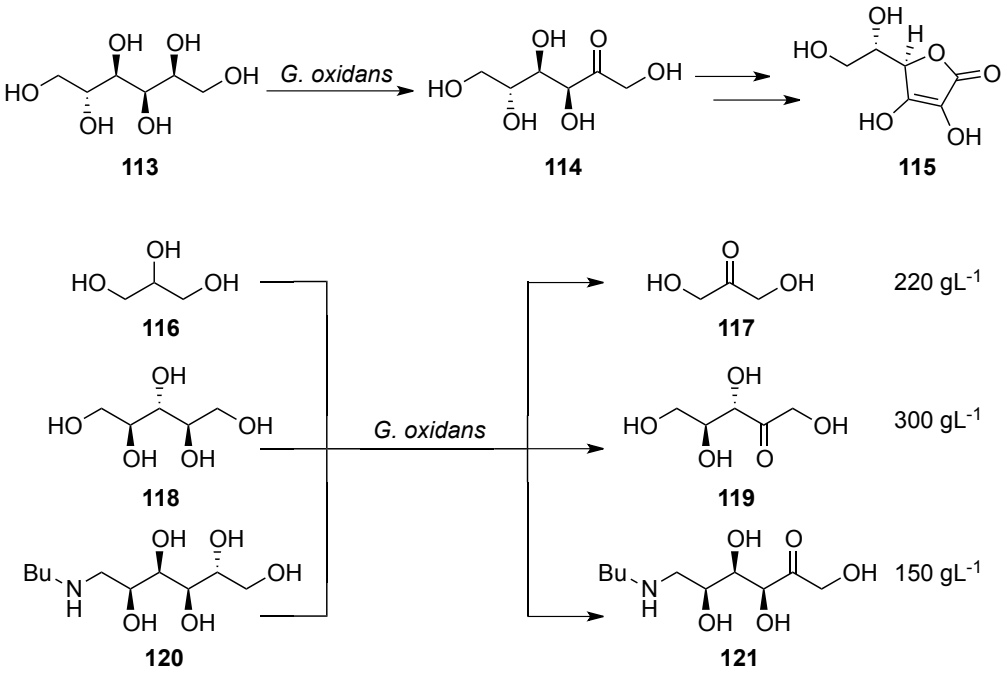

Scheme 30 Microbial *Glucoobacter oxidans* regioselective oxidation of polyols[128-131]

$_L$-Ascorbic acid **115** ($_L$-AA) otherwise more widely known as vitamin C is an important dietary supplement that has been traditionally manufactured using the Reichstein process; a largely chemical method of manufacturing $_L$-AA from $_D$-glucose.[128] An early step in the synthesis involves the fermentation of $_D$-sorbitol **113** to $_L$-sorbose **114** using *Gluconobacter oxidans* (**Scheme 30**), biotechnological advances have also allowed for further microbial substitution of steps.[132] *Gluconobacter oxidans* was also found to regioselectively oxidise a number of polyols including ribitol **118**[130], glycerol **116**[129] and *N*-butylglucamine **120**.[131]

1.5.2.4. Bio-oxidation of secondary alcohols (kinetic resolution)

The oxidation of secondary alcohols isn't considered as synthetically interesting as primary alcohols due to the loss of chiral information. A selective oxidase can allow accumulation of the opposite enantiomer in a kinetic resolution, however a maximum of only 50 % yield can be achieved. Conversely, enantiospecific reduction of a prochiral ketone could result in 100 % conversion. Kroutil *et al*. reported preparative scale kinetic resolutions of several aliphatic and aromatic *S*-alcohols from *Rhodococcus ruber* expressing ADH-A (**Scheme 31**)[133] This was the first example using preparative scale whole cell oxidation of a secondary alcohol tolerating acetone as a co-substrate for NAD^+ regeneration.

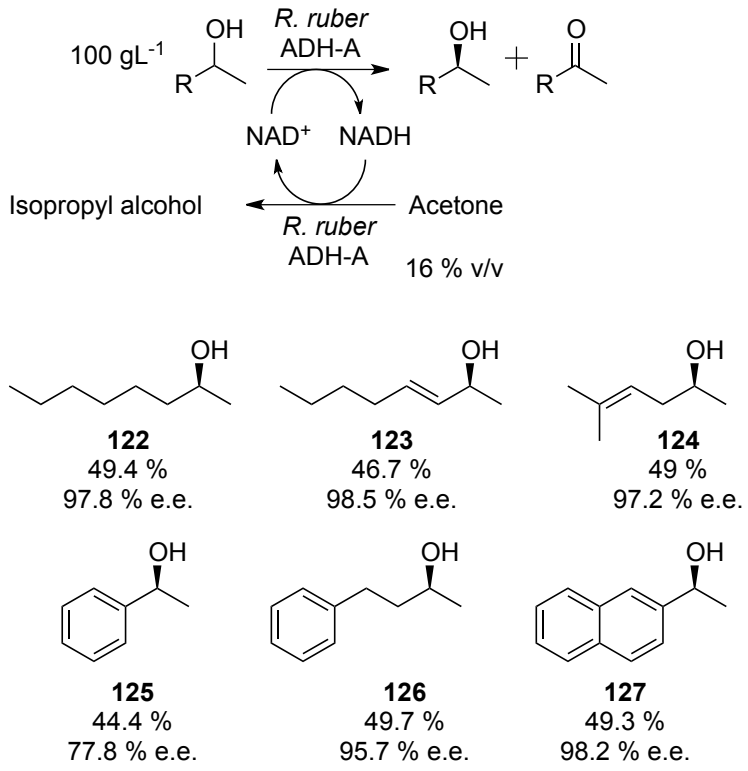

Scheme 31 Kinetic resolution of secondary alcohols using *Rhodococcus ruber*[133]

The "*meso* trick" refers to the selective transformation of a symmetrical prochiral compound to give exclusively one enantiomer. This approach has limited applications, as *meso*-compounds are relatively scarce. Regardless there are examples in the literature describing the desymmetrization of prochiral *meso*-diols using selective dehydrogenases.[116,134]

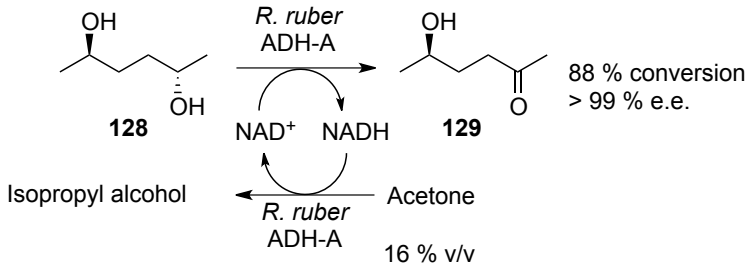

Scheme 32 Desymmetrization of *meso*-2,4-hexanediol using ADH-A from *Rhodococcus ruber*[135]

Further work from Kroutil *et al*. has also demonstrated the *meso* trick on 2,5-hexanediol **128** also using the previously described *Rhodococcus ruber* system (**Scheme 32**).

1.5.2.5 Alcohol deracemizations

As previously discussed (**Scheme 22**), deracemizations are concerned with stereoinversion of the unwanted enantiomer through a selective oxidation/reduction. Ideally, both enzymes should be complementarily stereoselective to a high degree, though a minimum of one stereoselective step is essential. With only one stereoselective enzyme, enrichment of one enantiomer will occur, resulting in more cycles (more co-factor required) to achieve deracemization.

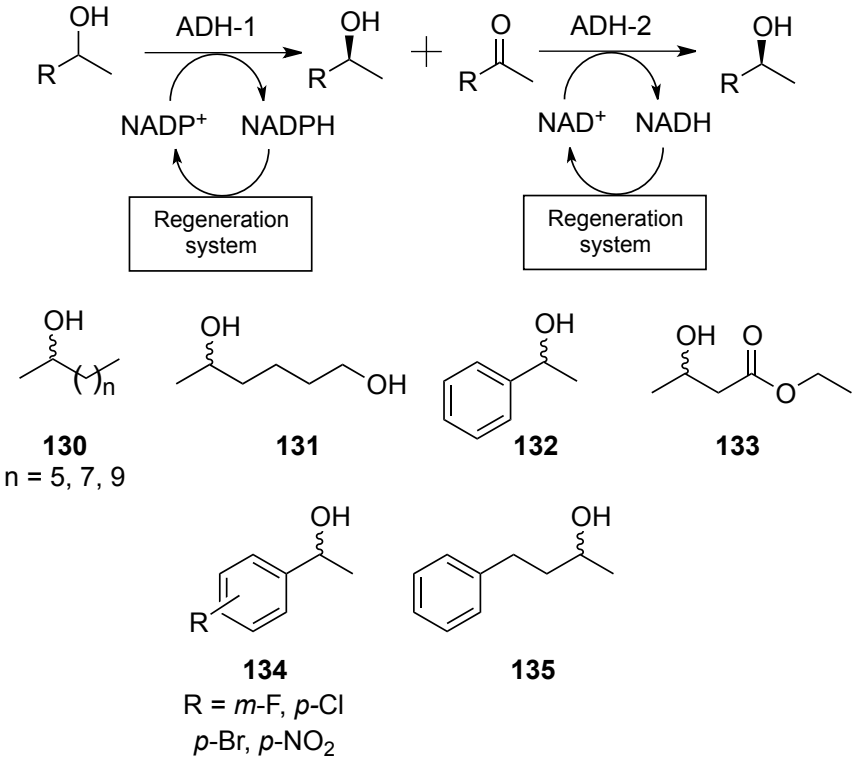

Scheme 33 Selective deracemization of secondary alcohols through stereoinversion[136,137]

A range of simple aliphatic and aromatic secondary alcohols could be deracemized to the desired enantiomer in quantitative conversion through selective ADH oxidative/reductive cascades on a multi-gram scale (**Scheme 33**).[136,137] It is important to note that regeneration systems for the cascades require enzymes utilising different co-factors (i.e. NAD^+/$NADP^+$) to avoid co-factor competition and futile cross-activity.

1.5.3. Enzymatic amine oxidations

1.5.3.1. Amino acid bio-oxidations

Oxidations of $_{L}$-amino acids comprise some of the earliest examples of biocatalytic amine oxidations. Amino acid dehydrogenases (AADH) such as $_{L}$-alanine dehydrogenase[138] are highly $_{L}$-selective and have been used in the successful kinetic resolution of racemic α-amino acids. Much like ADHs, AADHs rely on $NAD(P)^{+}$ recycling to drive the reaction equilibrium. An interesting alternative to the conventional methods of co-factor regeneration involved an electrochemical system using method of NADH re-oxidation with an anode during the stereoinversion of $_{L}$-alanine.[139] The selective oxidation yielded pyruvate, which was recycled through addition of a large excess of ammonia followed by cathodic reduction of the resulting imine.

Amino acid oxidases (AAOx) comparatively have less problematic co-factor dependencies. For example the $_{D}$-AAOx catalysed quantitative conversion of $_{D}$-phenylalanine into phenylpyruvic acid was achieved through bubbling oxygen directly into the reaction.[140] AAOxs also catalyse a wider range of amino acids in high stereoselectivity resulting in valuable catalysts for the production of chiral α-amino acids. The oxidative deamination of cephalosporin C is an industrial example of $_{D}$-AAOx in the production of 7-aminocephalosporonic acid **139**, an important semi-synthetic antibiotic building block. Previously, the highlighted process (**Scheme 34**) was ran alongside a conventional chemical route at GlaxoSmithKline with life cycle assessments claiming up to 60 % reduction in environmental cost.[141]

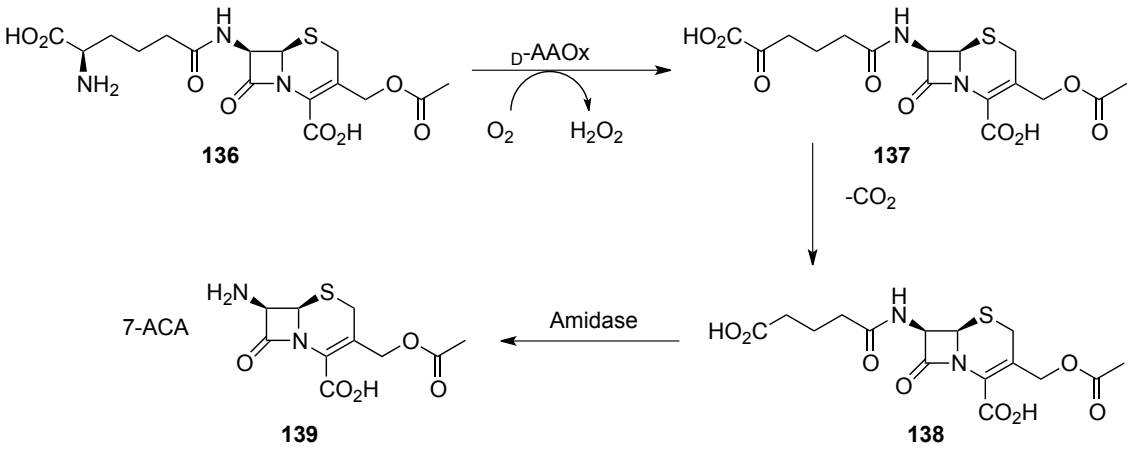

Scheme 34 Industrial enzymatic route to 7-ACA[141]

Deracemizations and DKRs using AAOx for the production of chiral amines have also gained considerable attention. Turner *et al*. developed several one-pot chemo-enzymatic cascades using a stereoselective D- or L-AAOx and a non-selective reducing agent ($NaBH_4$, NH_3-BH_3 or $NaCNBH_3$) to regenerate the racemic starting material for a range of amino acids (**Scheme 35**).[142-144]

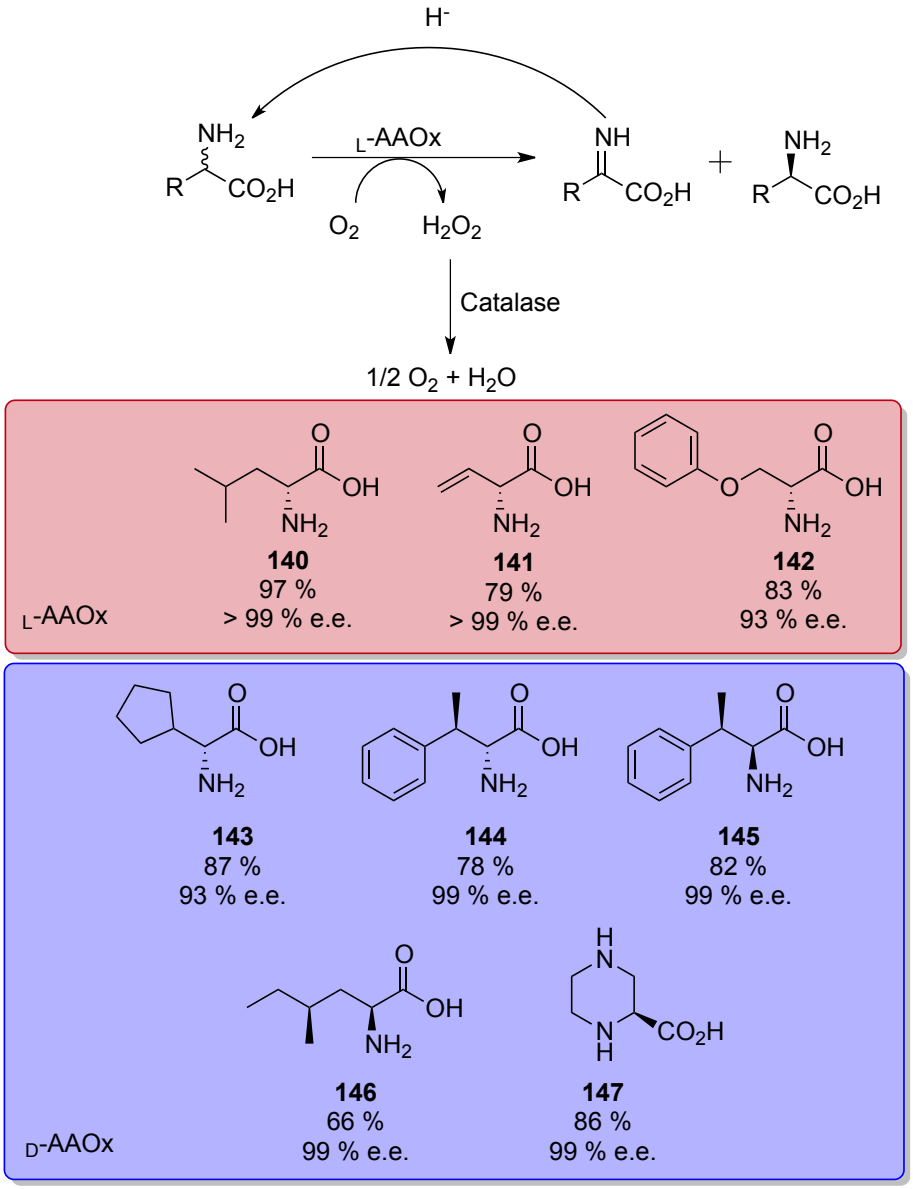

Scheme 35 Chemoenzymatic DKR of chiral amino acids.[142-144]

1.5.3.2. Amine bio-oxidations

While AAOxs have allowed for the production of a range of chiral amino acids, they are limited by their natural substrates and are unable to oxidise amines. As mentioned previously, monoamine oxidases (MAO) are a class of oxidative

flavoenzyme with the ability to facilitate deracemization of a range of primary, secondary and tertiary amines with much work by Turner *et al*. contributing toward industrial commercialization.[79] Furthermore, work in the group of Turner produced a range of mutated variants of MAO from *A. niger* that significantly broadened the substrate scope. Highlights include a variant (D5) able to catalyse the oxidative desymmetrization of various pyrrolidines; subsequent or *in situ* cyanide treatment of the resulting imines yielded a range of substituted prolines with exceptional optical purity.[145] Variants D9 and D11 allowed for the oxidative deracemization of a range of tetrahydro-*β*-carbolines (THBC), a group of natural bio-active alkaloids present in multiple pharmaceutical compounds such as the anti-hypertensive reserpine **150**.[146]

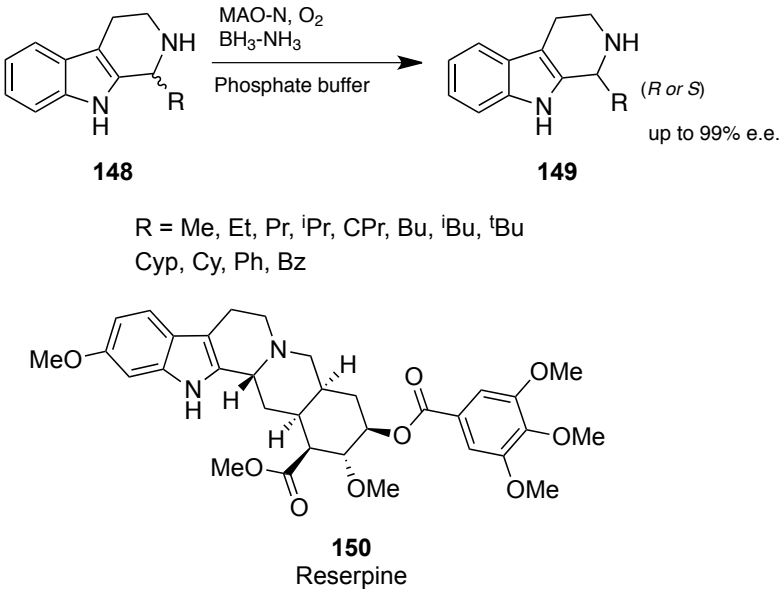

Scheme 36 MAO-N variant catalysed deracemization of THBCs[146]

Strategies for amine oxidation like in the MAO examples often quickly consume the resulting imine through *in situ* chemo reduction or nucleophilic attack; this is to prevent unwanted hydrolysis of the imine in aqueous conditions and subsequent reactivity of the generated aldehyde. There are examples however where aldehyde formation in aqueous conditions has been exploited. MAO initiated oxidation of dopamine followed by spontaneous Pictet-Spengler condensation was used to produce norlaudanosine **153**, a dopamine-uptake inhibitor (**Scheme 37**).[147]

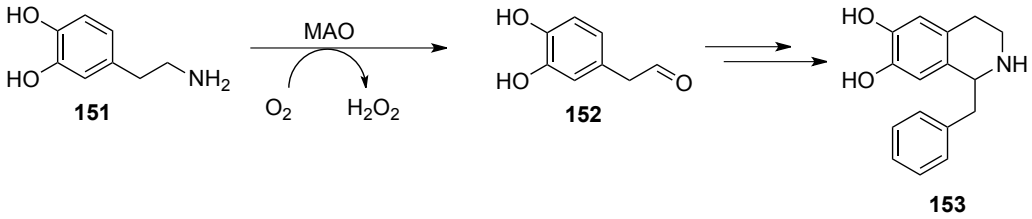

Scheme 37 MAO-triggered Pictet-Spenglar production of norlaudanosine[147]

Transaminases (TAs) have been utilised as tools to access non-racemic α-chiral amines. Kroutil *et al*. have presented two approaches using either a kinetic resolution (with a carbonyl-containing co-substrate as the amine acceptor) or direct asymmetric transamination of the ketone.[148] The latter method is particularly interesting as 100 % of the product is potentially attainable (**Scheme 38**).

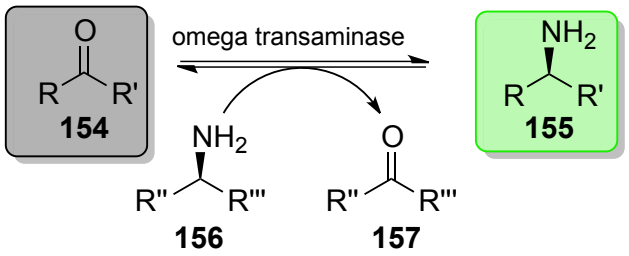

R, R" = H, alkyl, aryl, arylalkyl, alkene
R', R'" = H, alkyl, aryl, arylalkyl, alkene, COOH

Scheme 38 Asymmetric synthesis of chiral amines using transaminase[148]

Reversibility of amino group transfer in addition to substrate inhibition was identified as a key challenge. A solution to the former was approached by Truppo and Turner by using pyruvate as an amino group acceptor coupled with an AAOx, irreversibly oxidising the co-product while regenerating pyruvate (**Scheme 39**).[149]

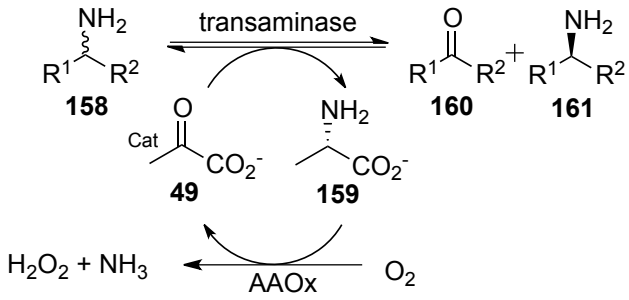

Scheme 39 Racemic amine resolution coupled with catalytic pyruvate and AAOx[149]

1.5.4 Enzymatic aldehyde oxidations

Compared to alcohol oxidations, the bio-oxidations of aldehydes have garnered much less interest and are less studied. The first reported aldehyde bio-oxidation involved the $NAD(P)^+$ dependent oxidation of formaldehyde by HLADH.[150] HLADH will oxidise other aldehydes to the carboxylic acid in presence of equimolar concentrations of $NAD(P)^+$, however the NAD(P)H catalysed reduction of the starting material is an unwanted side reaction.[151] ADH catalysed aldehyde oxidation has been speculated to proceed by the hydrated form of the substrate thereby allowing access to an abstractable hydride by the oxidised nicotinamide co-factor.[152] Other aldehyde oxidations have been described in this chapter previously as a consequence of the through oxidations of alcohols largely by acetic acid bacteria and some isolated ADHs.

Naturally occurring aldehyde oxidising enzymes primarily consist of aldehyde dehydrogenases (AldDHs), which are largely similar to ADHs. The key mechanistic difference between the enzymes involves an active site cysteine residue that catalyses oxidation through a thiohemiacetal and thioester intermediate (**Scheme 40**).[153]

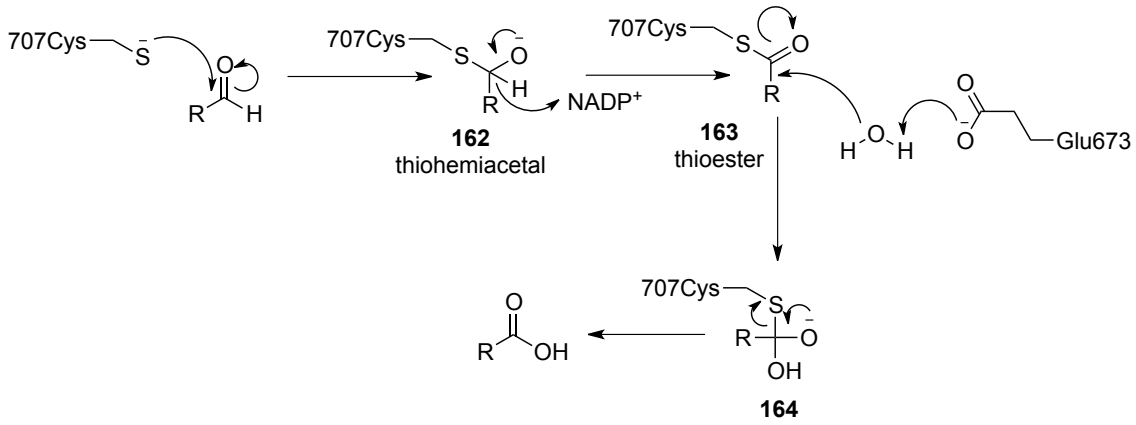

Scheme 40 Proposed mechanism for cysteine catalysed AldDH oxidation[153]

Industrial applications of AldDH are rare. A dual ADH/AldDH coupled disproportionation approach initially employed on a preparative scale for (*Z*,*Z*)-nona-2,4-dienal, was extended to metabolites of linoleic acid for industrial production of detergents and polymers.[154] Aldehydes are not typically substrates for oxidases although a key exception is the xanthine oxidase class of molybdenum hydroxylase enzymes.

1.6. Molybdenum-dependent oxidoreductases

Oxidation of functional groups including aldehydes and *N*-heterocycles by various metabolising enzymes, most notably CYP450's is an important stage in drug metabolism. Oxidation creates a handle for incorporation of more easily excreted bulky groups (glucuronidation, sulfation) in phase II metabolism. Molybdenum hydroxylases are a family of oxidoreductase enzymes widely distributed throughout nature. They are complex flavoproteins, principally involved in the mammalian bioconversion of pharmaceuticals and xenobiotics during phase I metabolism. They exist as monomers or dimers of hetero-trimers and are comprised of a molybdenum cofactor (Moco), FAD and a pair of [Fe-S] containing redox centre electron reservoirs (**Figure 10**).[155]

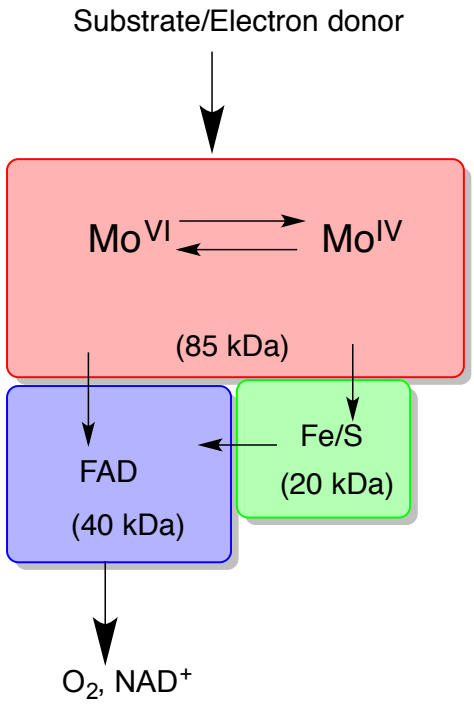

Figure 10 Internal electron transport of molybdenum hydroxylases[155]

The molybdenum is correctly positioned within the active site through a bound pterin moiety, which is assembled and loaded as a Mo-pterin complex (**figure 11**) by the requisite insertase chaperone.[156] Moco containing enzymes are divided into three families depending on the structure of the cofactor: DMSO reductases, xanthine oxidases and sulphite oxidases.[157] In *E. coli*, the xanthine oxidase family is comprised

of xanthine oxidoreductases (XOR) and aldehyde oxidases (AO), which are characterised by a molybdopterin-cytosine-dinucleotide (MCD) cofactor.

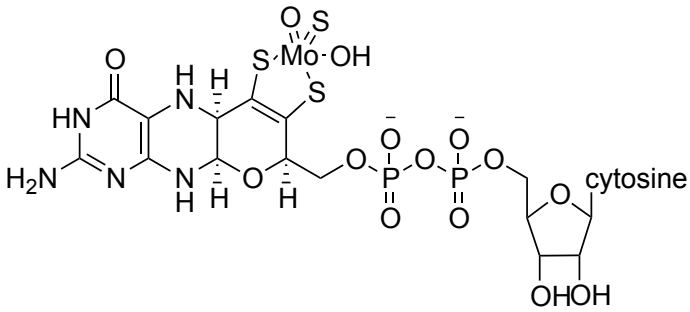

Figure 11 Structure of the pyranopterin molybdenum cofactor (Moco) in the xanthine oxidase family

In the xanthine oxidase family, the molybdenum exists in a distorted square pyramidal configuration with a double bound oxygen group in the apical position. The two pterin sulfurs in addition to a water derived hydroxyl group and terminal Mo=S occupy the equatorial plane. A number of amino acid residues are highly conserved throughout the molybdenum-containing domain and are involved in Moco coordination including Gln211, Phe242, Gly243, Arg350 and Glu692 (*Ec* PaoABC numbering).[157,158]

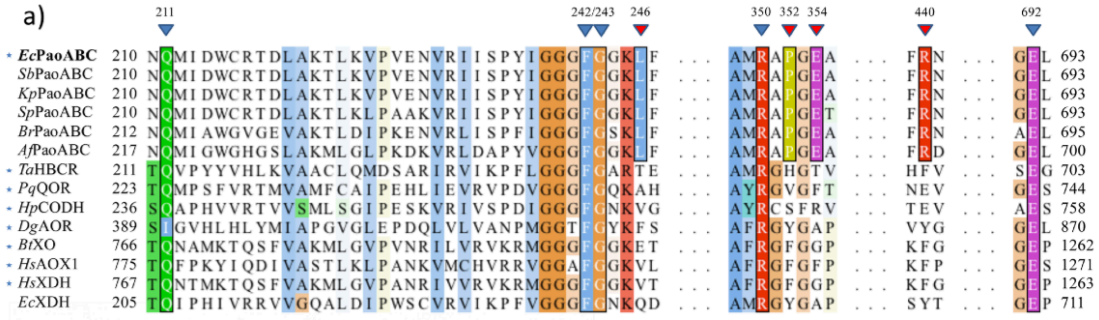

Figure 12 Sequence alignment of Moco domain of 14 bacterial molybdenum hydroxylases including conserved (blue arrows) and non-conserved (red arrows) residues.[158]

Non-conserved residues correlate to differences in substrate binding in the active site domain. Enzymes with preference for aldehyde oxidation lack phenylalanine residues at position 352 and have conserved Leu246, Glu354 and Arg440 residues.

1.6.1. Xanthine oxidase mechanism

Through ^{18}O labelling and EPR experiments, molybdenum hydroxylases have been found to incorporate oxygen from surrounding water during the biooxidation of aldehydes and imines.[157] The generally accepted reaction mechanism begins with co-ordination of the substrate to the Moco redox centre of the enzyme active site. Following deprotonation by a key neighbouring glutamate residue, the Moco-bound hydroxide ion attacks the substrate and electron transfer leads to reduction of Mo(VI) **166** to Mo(IV) **167**. The FAD sub unit in turn becomes reduced, this can occur either directly, or through the Fe-S cluster, which also acts as an electron sink.[159] The Moco then becomes re-oxidised and electrons are passed from reduced flavin to either molecular O_2 (oxidase) or NAD^+ (dehydrogenase).[160] Nucleophilic attack from external water on the electron deficient intermediate **167** delivers the oxidised product while restoring the Mo-pterin (**Scheme 41**).[161]

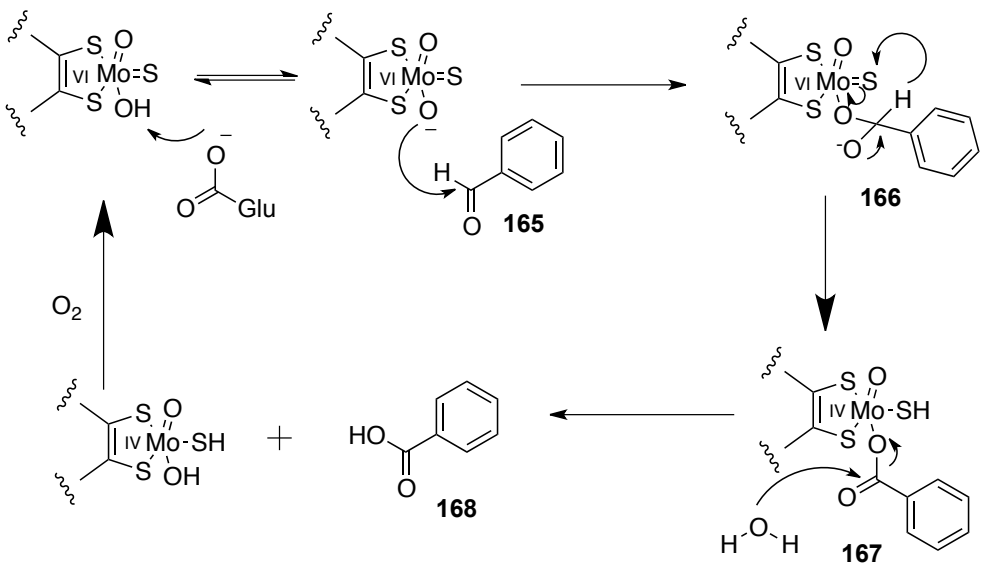

Scheme 41 General molybdenum hydroxylase mechanism for benzaldehyde oxidation[161]

1.6.2. Xanthine oxidoreductase (XOR)

XOR participates in purine catabolism, notably in the formation of xanthine from hypoxanthine and then further oxidation to uric acid (**Scheme 42**).[155]

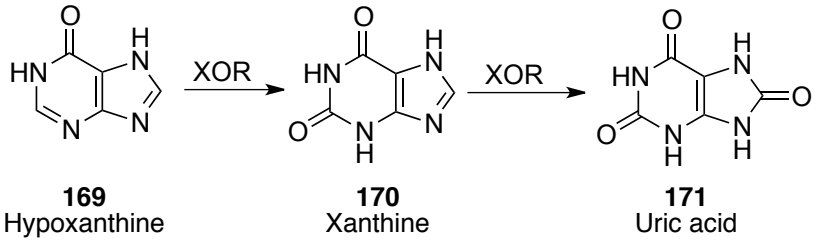

Scheme 42 Hypoxanthine to uric acid XOR biooxidation

XOR is primarily found in the liver but in mammals is more distributed throughout the body and is present in the small intestine and mammary tissue.[162] XOR can exist in two forms from the same gene: xanthine oxidase (XO) and xanthine dehydrogenase (XDH). The subclasses vary in the type of substrates accepted and the cofactor utilised. XO utilises molecular oxygen whereas XDH utilises NAD^+.

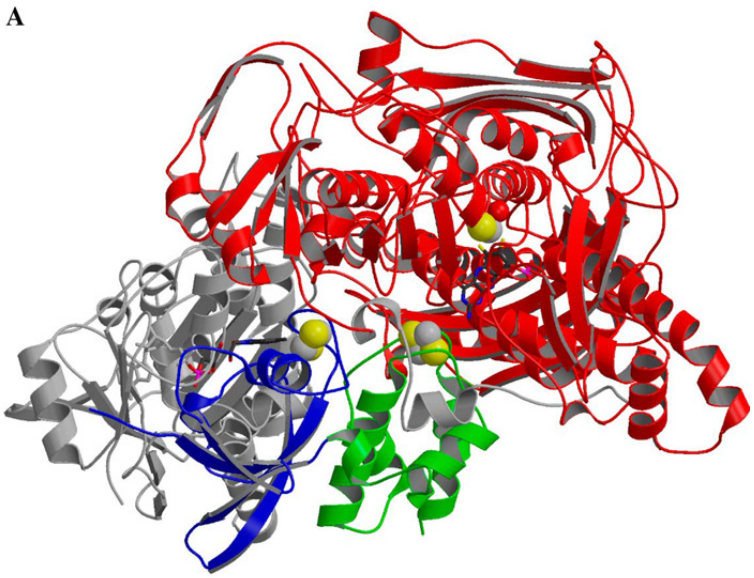

Figure 13 Crystal structure of bovine XOR (PDB id: 1FIQ), grey = FAD domain, green and blue = Fe-S 1 and 2 domains respectively and red = molybdenum substrate binding domain.[163]

Molybdenum hydroxylase Mo-OH groups attack electron deficient carbons alpha to the nitrogen in aromatic *N*-heterocycles. However, xanthine oxidoreductase's substrate scope is comparatively limited compared to aldehyde oxidase. Regardless, XOR has been reported to oxidise a number of imine-containing drug molecules (**Figure 14**). [162,164-167]

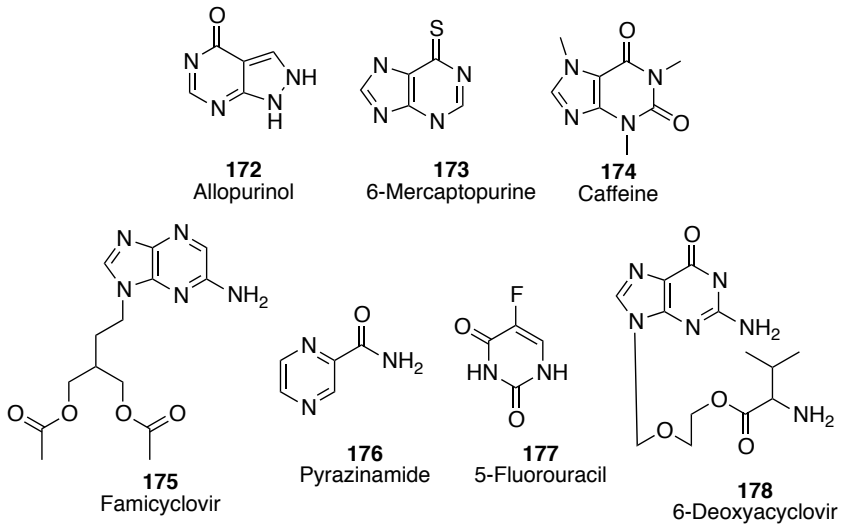

Figure 14 Pharmaceutical compounds metabolised by XORs[162,164-167]

1.6.3. Aldehyde Oxidase (AO)

The other primary class from the xanthine oxidase family, AO is contained within the cytosol of tissues and is found within several living species. It is almost identical to xanthine oxidoreductases in terms of key functional moieties, however AO exists exclusively in a single form, utilising molecular O_2 as an electron acceptor and generally has a broader substrate range for redox biotransformations compared to XOR. AO is known to metabolise a number of aliphatic and aromatic aldehydes to the corresponding carboxylic acids such as retinal into retinoic acid.[168] AO also oxidises a number of imines. In addition to the compounds in **Figure 14**, a range of other substrates including anti-malaria compounds such as Quinine **180** are metabolised (**Figure 15**).

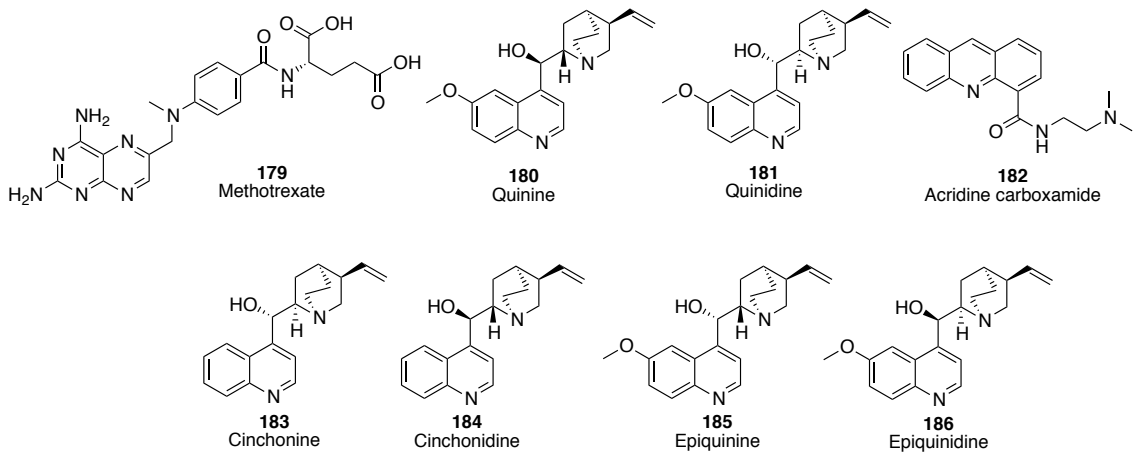

Figure 15 Selection of pharmaceutical compounds metabolised by AO

Periplasmic aldehyde oxidase (PaoABC) from *E. coli* has been identified as an unusual member of the aldehyde oxidase family by Leimkühler and co-workers.[158,169] Kinetic characterisation revealed activity with a broad range of aldehydydes, with a preference for aromatic aldehydes. It is believed that PaoABC plays an important role in the detoxification of aromatic aldehydes in the periplasm. It is the first example of an *E. coli* protein containing a MCD co-factor and the first structurally characterised heterotrimer of the XO family.

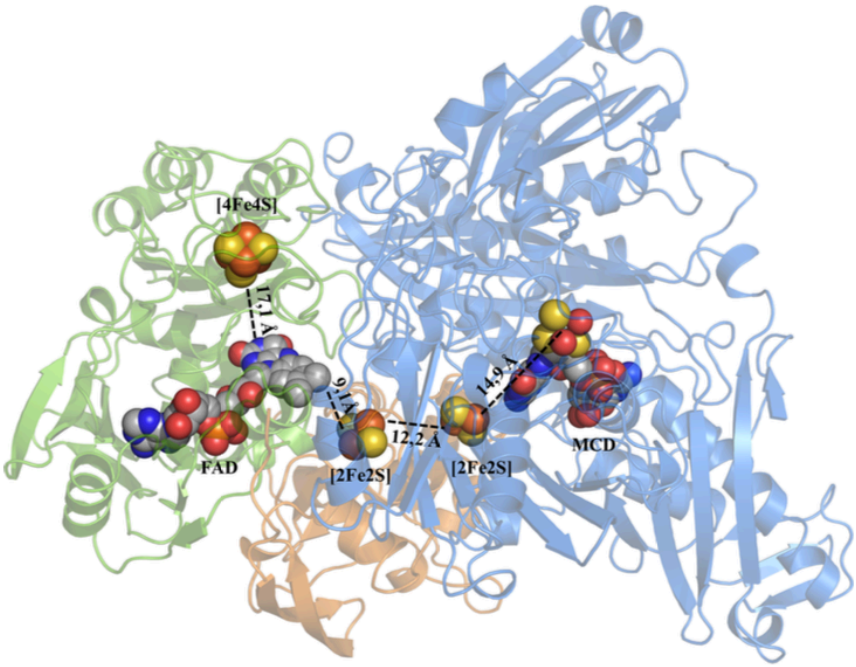

Figure 16 Crystal structure of *E. coli* PaoABC[158]

The crystal structure was similar to those of other characterised members of the XO family however an unexpected [4Fe-4S] cluster was identified in subdomain near to FAD in the protein (green **Figure 16**). This is believed to be involved in regulation of the oxidation state of the FAD during electron transfer.

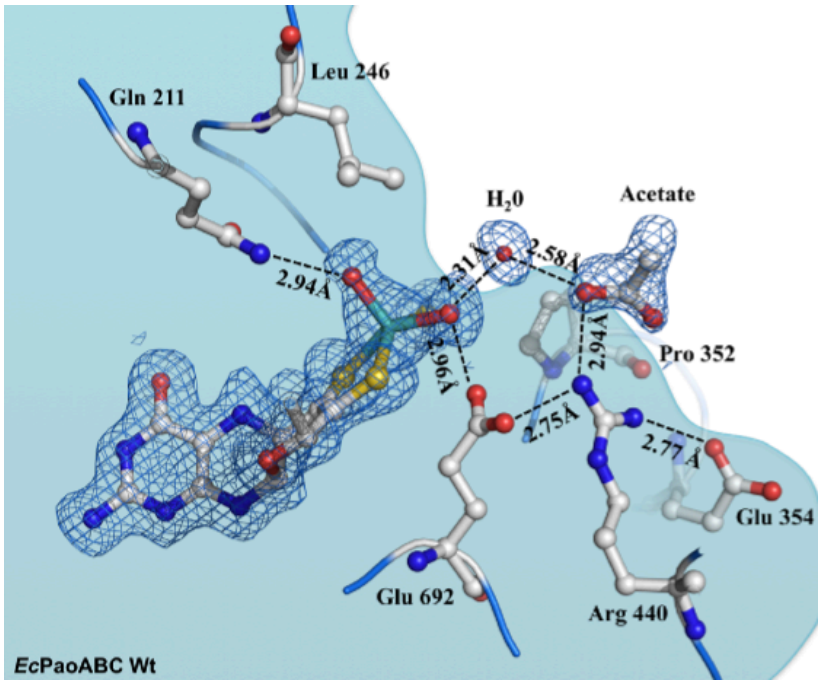

Figure 17 Mo active site region of *E. coli* PaoABC[158]

Crystallographic data revealed that PaoABC contains a wide, shallow groove with short loops at the active site (**Figure 17**). This structure placed the Moco near the surface of the protein and exposed to solvent; a significant structural difference to other XO enzymes, which have the Moco situated at the base of a narrower binding pocket. The broader binding pocket and lack of channel-lining aromatic residues could explain PaoABC's broad spectrum of substrate activity. PaoABC has recently been utilised in a one-pot biocascade for the bioconversion of HMF **18** to the key platform chemical replacement FDCA **26** (**Scheme 43**).[170]

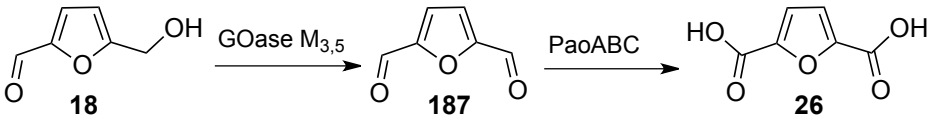

Scheme 43 Dual enzyme one-pot cascade for bioconversion of HMF to FDCA

McKenna *et al*. were able to produce the bioplastic precursor in an isolated yield of ~75 % using PaoABC and an engineered galactose oxidase. In addition, they demonstrated application of the cascade on a range of aliphatic and aromatic alcohols to give the corresponding carboxylic acids in excellent conversions.

1.7. Protein engineering of xanthine oxidases

Molybdo-flavoenzymes (MFE) XOR and AO share some common substrates, but initially only the mechanism of XOR had been described in detail.[171] Mammalian aldehyde oxidase had been previously expressed in *E. coli*, however low catalytic activity of purified proteins relating to low Moco concentrations remained a problem.[172] In order to study the mechanism and biochemical functions of mammalian AO (AOX1), Leimkühler *et al*. developed an expression system for an isoform of mouse aldehyde oxidase (mAOX1).[173] Purified recombinant protein from TP1000 *E. coli* cells containing a *mobAB* knockout (required for MCD assembly) displayed activity comparable to the enzyme isolated from mouse liver. Engineered protein variants indicated positions Glu1265, Val806 and Met884 were crucial to aldehyde oxidase activity. Val806 and Met884 were determined to be responsible for substrate stabilisation while Glu1265 played the central role in the mechanism as previously discussed (**Scheme 44**) (**1.6.1.**).

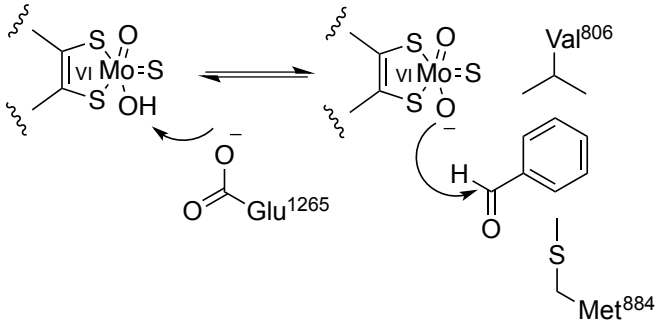

Scheme 44 Key residues in mAOX1

A triple variant E1265Q/V806E/M884R interestingly displayed complete loss of aldehyde activity, while just altering positions Val806 and Met884 drastically reduced aldehyde activity.

Previously, Leimkühler's group had also developed an efficient system for the recombinant *E. coli* expression of a xanthine dehydrogenase from *R. capsulatus*.[174]

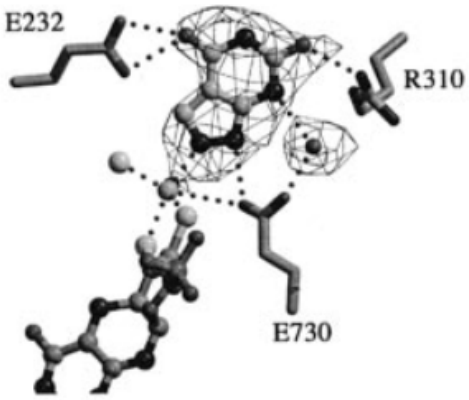

Figure 18 Crystal structure of xanthine-bound *Rc* XDH interacting residues[175]

They later identified the key residues in substrate binding with xanthine in equivalent positions as Glu730 Glu232 and Arg310.[175] Mutating these positions to match the residues present in mAOX1 (E232V/R310M) yielded a XDH protein devoid of purine activity while also displaying a greater specificity for aldehydes.

1.8. Project Aims

Molybdenum-containing enzymes of the xanthine oxidase family catalyse the oxidative hydroxylation of a broad range of aldehydes and aromatic heterocycles. Their use in synthesis until recently has been relatively unexplored; instead literature focusing on enzymatic structural characterisation and roles in metabolism of xenobiotics have been prevalent. Emerging examples of application have shown the potential for green synthesis of carboxylic acids and amides using enzymatic cascades. Many molybdenum hydroxylase enzymes utilise naturally abundant oxygen and water as co-substrates under ambient conditions and do not require diffusible redox cofactors. In addition, mutagenesis of the molybdoenzyme xanthine dehydrogenase from *Rhodobacter capsulatus* has shown that changes in substrate specificity are possible.

Following success in preliminary studies, this work aims to:

- Further investigate cyclic amide forming reactions using single step imine/iminium oxidations with molybdenum-containing oxidoreductases.
- Examine chemoselectivity with substrates containing multiple sites of oxidation.
- Employ an engineered monoamine oxidase variant with a commercially available xanthine dehydrogenase in a novel amine to amide oxidative cascade.
- Investigate protein engineering of an aldehyde oxidase through random and saturation mutagenesis to modulate substrate specificity toward imine oxidation.
- Develop a solid-phase activity assay to screen a library of randomly generated mutants.

In an analogous approach to the work of Leimkühler, an *E. coli* periplasmic aldehyde oxidase (PaoABC) will be the primary candidate for protein engineering with the ultimate goal of producing a robust enzyme for imine to amide biotransformations. PaoABC is oxygen dependent, highly robust and amenable to heterologous expression in *E. coli*.

Results and Discussion

Chapter 2

2.0 Biooxidation of cyclic amines and imines to lactams

2.1. Introduction

Amides are structures found in many organic molecules including pharmaceuticals[176,177] (penicillin, paracetamol) and polymers[178] (Nylon, Kevlar®). The current world population is estimated to be at 7 billion, and with numbers expected to exceed 12 billion by the year 2100 demand for amide-containing goods will only increase.[179] Synthesis has traditionally involved the use of activating agents to combat the poor kinetics of amide formation from its parent molecules. [180,181] This has presented several problems including toxicity and poor atom economy; as a result there are tonnes of waste produced every year, particularly in the pharmaceutical and fine chemical sectors. These obstacles have been formally recognized and atom efficient amide synthesis was regarded as the top challenge for organic chemistry in 2007 by the ACS Green Chemistry Institute®.[182]

The need for more sustainable methods has driven much research with some success. Notable chemical methods for amide formation include the use of boronic acids[183], *N*-heterocyclic carbenes[184-186], Pd[89], Cu/Ag[90], Ru[91] and gold nanoparticles.[93] These chemo-catalytic methods, while having good atom economy, also have shortcomings including the requirement for organic solvents, high temperature and pressure and expensive and non-renewable catalysts. These methods hamper industrial scale-up, and more sustainable green methods of amide synthesis are needed.

The synthesis of amides from amines *via* an imine intermediate is rare in the literature and uses harsh conditions (i.e. *m*-CPBA).[187] Engineered monoamine oxidase (MAO) enzymes reported by Turner *et al*. have displayed a spectrum of activity for amine oxidation.[145,146] Additionally, molybdenum hydroxylases have been documented to oxidise a number of imine containing compounds.[161,162] Whilst mammalian AO benefits from having broad substrate specificity, attempts to express the fully active enzyme in *E.coli* have had limited success, limiting the availability of purified AO.[172] Conversely, *R. capsulatus* XDH can be expressed in *E. coli* with little difficulty and can

undergo mutagenesis to change its substrate specificity. This has been successful with AO type activity found for XDH E232V and XDH E232V / R310M variants compared to the wild type as reported by Leimkühler *et al*.[173]

A commercial source of *E. coli* XDH (Sigma-Aldrich) has become available. *Ec* XDH uses oxygen as a terminal electron acceptor, producing H_2O_2. *Ec* XDH is marketed as "xanthine oxidase microbial", however it is referred to as a dehydrogenase here as it will accept NAD^+ as a cofactor. Oxidases have a clear advantage over dehydrogenases in that molecular oxygen is used as the oxidant. Unfortunately, the crystal structure for *Ec* XDH is unknown but homologue *Rc* XDH E232V is believed to interact with purines through active site-flanking phenylalanines in the substrate channel.[188] Aromatic π-π interactions between phenylalanine and DHIQ could stabilise the transition state and lower activation energy.

XOR enzymes used alone or in combination with MAO hold great potential as biocatalysts for oxidative formation of amides. As outlined in the oxidative cascade below, an amine **188** could be selectively oxidised to the imine **189**, which is then a substrate for XOR to produce the corresponding amide **190** (**Scheme 45**).

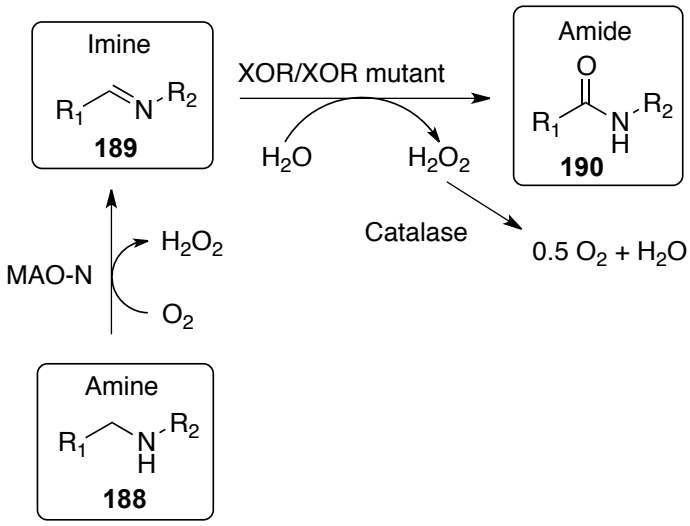

Scheme 45 Tandem biocatalytic approach to amide formation

This work aims to facilitate the atom efficient conversion of amines to amides using such a biocatalytic approach. A MAO variant and XDH will be utilised to demonstrate proof of concept. Additionally, single step biooxidations of cyclic imine/iminium substrates will be investigated and compared to chemical methods. The

chemoselectivity of molybdenum hydroxylases on imine-containing substrates with multiple sites of oxidation will also be assessed.

Imines/iminiums formed through cascades in this project were generated *in situ* using an engineered monoamine oxidase, MAO-N D9 provided by our collaborator Nick Turner (Manchester, UK). Cascades and single-step imine oxidations were facilitated by *Rc* XDH E232V and *Ec* PaoABC provided by our other collaborator Silke Leimkühler (Potsdam, GER). Initial reactions on the project performed by Dr Carnell had some success with the formation of lactams from tetrahydroisoquinolines (THIQs) (**Scheme 46**), where a one-pot enzyme cascade with MAO-N D9 and XDH E232V formed the lactam in reasonable yield.[189]

In this case, the XDH E232V oxidation was facilitated by 2,6-dichlorophenolindophenol (DCPIP) **195**, which is a redox mediator and 1 or 0.5 eq. of $K_3Fe(CN)_6$ acting as a terminal electron acceptor. *Rc* XDH E232V is a NAD^+ utilising enzyme. Using catalytic quantities, the co-factor can in principle be regenerated using NADH oxidase.[190] However, the combination of catalytic DCPIP (10 mol%) and $K_3Fe(CN)_6$ (due to the low aqueous solubility of DCPIP) as electron acceptors worked well.

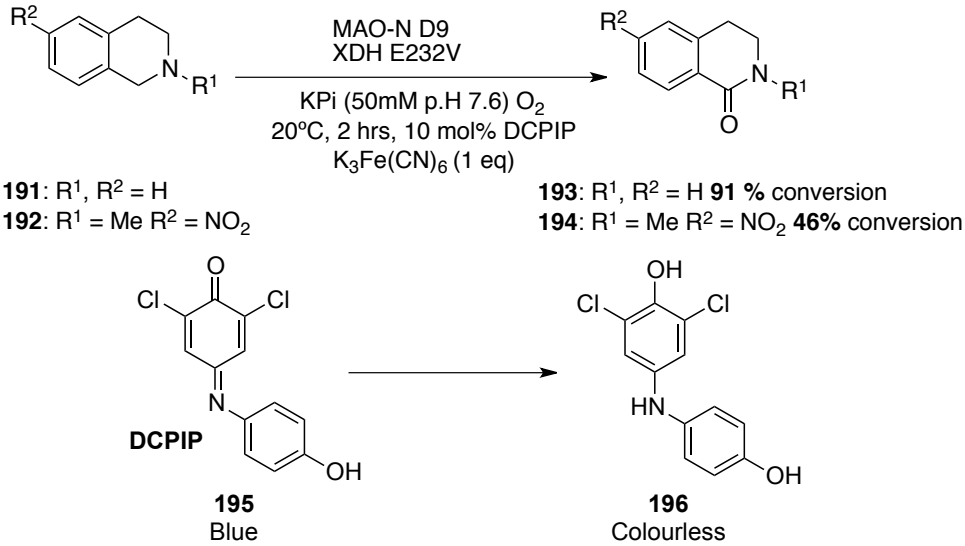

Scheme 46 Initial THIQ cascades[189]

2.1.1. Monitoring reaction conversions by HPLC

Reaction conversions for enzyme biotransformations were monitored by HPLC. Transformations were verified by comparing the retention times observed with samples of authentic standards of starting materials and products under the same conditions. Where standards were not commercially available, they were synthesised. In order to confirm that the relative intensities observed on HPLC traces were indicative of the amounts present, 1:1 standards (by NMR analysis) of the lactam and amine were analysed by HPLC (section 5.3.5.). Transformations where an intermediate iminium ion was formed such as substrate **201** (**Table 4**) were treated with a reducing agent prior to analysis to ensure no substrate remained in the aqueous phase.

2.2. Initial biotransformation of DHIQ with XORs

We initially focused on the biotransformations of 3,4-dihydroisoquinoline (DHIQ) **197** using both *E. coli* XDH and *Rc* XDH E232V. *Ec* XDH is commercially available, while sources of MAO-N D9 were comparatively limited. The *E. coli mob* locus is required for synthesising active molybdenum co-factor molybdopterin-guanine-dinucleotide (MGD) in molybdoenzymes. XOR enzymes possess the cytosine analogue (MCD), and thus require a modified strain of *E. coli* to heterologously express active protein. Palmer *et al*. developed a TP1000 strain of *E. coli* with a kanamycin resistance cassette and a *mobAB* knockout resulting in MCD assembly.[191] To avoid continuous expression and purification of enzyme by our collaborators, initial trials were run for the imine to amide stage of oxidation. Whole cell trials (growing and resuspended) were probed using whole cells (*E.coli* TP1000) expressing XDH E232V. DHIQ was added directly to the growing and re-suspended cells and incubated for three hours at 37 °C. The amide was observed from NMR analysis of the crude product. However, difficulty in product purification precluded determination of an accurate conversion or product isolation.

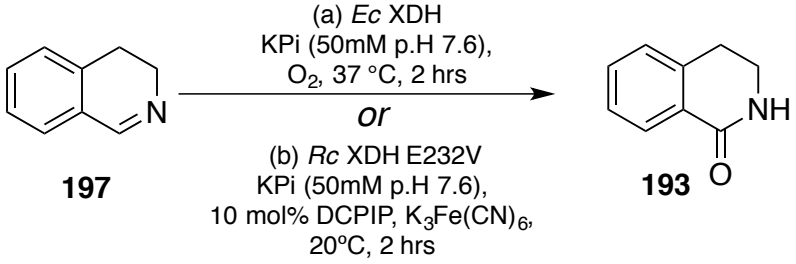

Scheme 47 DHIQ oxidation using isolated enzymes

Using the isolated enzymes proved to be more successful. Bioconversion reactions using isolated *Rc* XDH E232V (with DCPIP-$K_3Fe(CN)_6$) or commercially available *Ec* XDH (with O_2) were performed in potassium phosphate buffer (50 mM, pH 7.6) with DHIQ **197** (final substrate concentration of 1 mM). The redox dye DCPIP characteristically decolourised upon reduction indicating enzyme activity. The *Ec* XDH biotransformation was followed by normal phase HPLC and showed full conversion to the product after 3 h. Efforts to scale up the reaction to 10 and 50 mM substrate concentration were less effective with much less of the product observed (24 % and 5 % respectively) this was thought to be due to substrate / product inhibition at larger concentrations.

HPLC analysis of *Ec* XDH reactions required an authentic chemical standard of the lactam **193** for comparison. The standard was not commercially available so was synthesised by conventional acid chloride coupling to give the carbamate ester **200** followed by acid catalysed cyclisation as described by Kurouchi *et al*.[192]

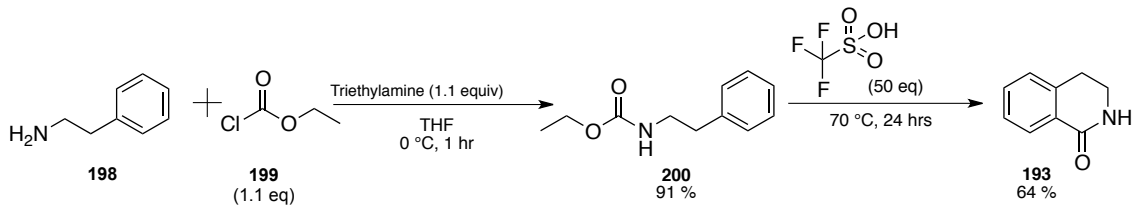

Scheme 48 Chemical route to lactam **193**[192]

2.3. MAO-N D9 & *Ec* XDH / *Rc* XDH E232V cascades

Following the successful biotransformation of DHIQ using *Ec* XDH, an enzyme cascade using MAO-N D9 and *Ec* XDH with the substrate 1,2,3,4-tetrahydroisoquinoline (THIQ) **191** was next examined at 1 mM (**Table 1** entry 1). HPLC analysis showed quantitative conversion to the lactam. The substrate concentration was increased to 10 mM (entries 2-4), which still showed moderate amounts of conversion. For substrate concentrations of 30 mM (entries 5-7) and 50 mM (entries 8-10) conversions were comparatively poor.

Table 1 Oxidative cascades of THIQ using MAO-N D9 and *Ec* XDH[a]

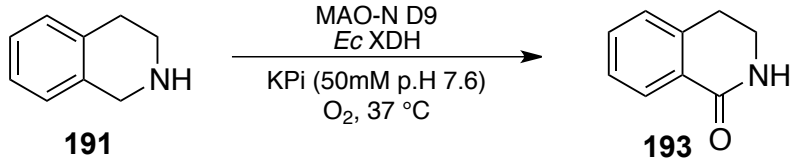

191 **193**

Entry	Molarity (mM)	Time (h)	Conversion (%)
1	1	5	100
2	10	1	39
3	"	3	30
4	"	5	34
5	30	1	13
6	"	3	11
7	"	5	10
8	50	1	7
9	"	3	9
10	"	5	7

[a]Reaction conditions: Incubated at 37 °C with agitation at 180 RPM. Potassium phosphate buffer (50 mM, pH 7.6), total volume 1000 µL. 10, 30 & 50 µL **191** (in DMF), 50 µL MAO-N D9 (14 mg/ml) and 100 µL *Ec* XDH (1 mg/ml). HPLC Conditions: Diacel OJ-H column, 1 ml/min, 10 % IPA/Hexane at 230 nm. (") signifies a repeat of the above value in a given column.

Reduced conversion at lower substrate concentrations was thought to be due to deactivation of the enzyme by the hydrogen peroxide formed during the reaction. Continuing with 10 mM **191**, a series of biotransformation cascades were run using catalase as a peroxide scavenger.

Table 2 Catalase supplemented oxidative cascades of THIQ using MAO-N D9 and *Ec* XDH[a]

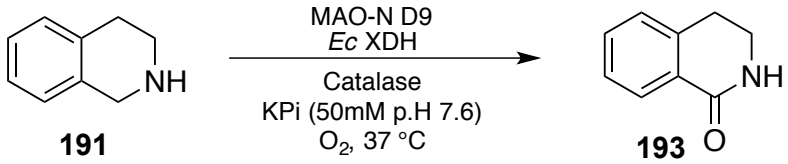

191 **193**

Entry	Molarity (mM)	Catalase conc. (mg ml^{-1})	Time (h)	Conversion (%)
1	10	1.1	2	90
2	"	"	4	96
3	"	"	7	97
4	"	0.55	2	50
5	"	"	4	64
6	"	"	6	67
7[b]	"	1.1	6	30
8	20	"	2	22
9	"	"	4	23
10	"	"	6	28

[a]Reaction conditions: Incubated at 37 °C with agitation at 180 RPM. Potassium phosphate buffer (50 mM, pH 7.6), total volume 1000 µL. 10 & 20 µL **191** (1 M in DMF), 50 µL MAO-N D9 (14 mg/ml), 100 µL *Ec* XDH (1 mg/ml) and catalase 333 or 167 µL (3.3 mg/ml). HPLC Conditions: Diacel OJ-H column, 1 ml/min, 10 % IPA/Hexane at 230 nm. [b]No aeration. (") signifies a repeat of the above value in a given column.

The observed conversions (**Table 2**) indicated that both substrate inhibition and peroxide inactivation were playing a role in lower conversions. Catalase provided near quantitative conversions by 4 h at 10 mM THIQ concentration. Increasing substrate concentration to 20 mM resulted in a significant drop in conversion. Additionally, lowering the concentration of catalase by half had a deleterious effect on conversion of 10 mM THIQ.

The necessity for regular aeration is demonstrated in these transformations, where despite the addition of catalase, lack of aeration led to lower conversion (**Table 2** entry 7). To ensure high degrees of atmospheric oxygen saturation, Eppendorf tube reaction vessels were exposed to air then manually shaken for a few seconds every 30 min.

Table 3 Peroxide scavenger screens on 10 mM THIQ MAO-N D9 and *Ec* XDH cascade[a]

Additive	Conversion to lactam
Control	2.5 %
Catalase	55.2 %
Superoxide Dismutase	5.6 %
Peroxidase	26.1 %

[a]Reaction conditions: Incubated at 37 °C with agitation at 180 RPM. Potassium phosphate buffer (50 mM, pH 7.6), total volume 1000 µL. 10 µL **186** (1 M in DMF), 50 µL MAO-N D9 (14 mg/ml), 100 µL *Ec* XDH (1 mg/ml) and additive 167 µL (3.3 mg/ml). HPLC Conditions Diacel OJ-H column, 1 ml/min, 10 % IPA/Hexane at 230 nm.

Two additional peroxide scavengers, peroxidase and superoxide dismutase were assayed for improved activity with **191** (10 mM) in place of catalase. Assays were run at the same concentration and conditions with catalase remaining the most effective.

Catalase was then utilised in a series of THIQ analogue cascades using MAO-N D9 and *Ec* XDH (**Table 4**) or *Rc* XDH E232V (**Table 5**). The results obtained using THIQ (**Table 2** entries 1-4) and *N*-methyl THIQ **201** (**Table 4** entries 5-8) were published as part of a so-called "catalytic toolbox" where a series of water-based bio-chemo and bio-bio cascades contributed towards the green synthesis of carboxylic acids / amides from alcohols and lactams from cyclic amines.[189]

Table 4 Cascade biooxidation of THIQ analogues with MAO-N D9 and *Ec* XDH[a]

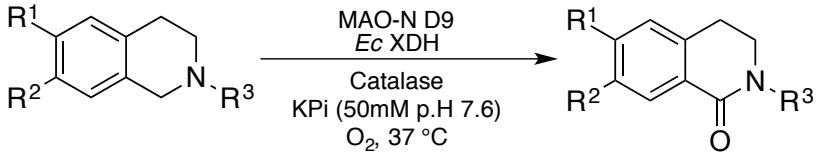

192: $R^1 = NO_2$, R^2 = H, R^3 = Me
201: R^1 = H, R^2 = H, R^3 = Me
202: R^1 = OMe, R^2 = OMe, R^3 = H

194: $R^1 = NO_2$, R^2 = H, R^3 = Me
203: R^1 = H, R^2 = H, R^3 = Me
204: R^1 = OMe, R^2 = OMe, R^3 = H

Entry	Substrate	Molarity (mM)	Time (h)	Conversion (%)[b]
1[c,d]	**192**	1	5	0
2[d]	"	10	2	"
3[d]	"	"	4	"
4[d]	"	"	6	"
5[c,d]	**201**	1	6	91
6[d]	"	10	2	64
7[d]	"	"	4	82
8[d]	"	"	6	100
9	**202**	1	"	0

[a]Reaction conditions: Incubated at 37 °C with agitation at 180 RPM. Potassium phosphate buffer (50 mM, pH 7.6), total volume 300 µL. 0.3 & 3 µL **192**, **201** and **202** (1M in DMF), 17 µL MAO-N D9 (14 mg/ml), 33 µL *Ec* XDH or (1 mg/ml) and catalase 100 µL (3.3 mg/ml). HPLC Conditions Diacel OJ-H column, 1 ml/min, 10 % IPA/Hexane at 230 nm. [b]Conversion calculated from peak areas of HPLC analysis using authentic standards of the amine:lactam in a 1:1 ratio by NMR (Section 5.3.5.). [c]Absence of catalase. [d]Before extraction, the reaction was shaken with ammonia borane complex for 3 hours. (") signifies a repeat of the above value in a given column.

Unfortunately substrates **192** and **202** appeared to display no conversion with *E. coli* XDH. *N*-methyl THIQ **201**, on the other hand showed excellent conversions over 6 h at both 1 and 10 mM (**Table 4** entries 5-8). For *N*-methyl THIQ **201** conversions, the lactam showed greater absorbance intensity than was actually present (approx. eight fold, section 5.3.5.). Accordingly, the conversions (**Tables 4** and **5**) have been normalised to reflect this. Additionally *N*-substituted analogues **192** and **201** were shaken with ammonia-borane complex to reduce any unconverted iminium, as it would partition into the aqueous layer during extraction and give unrepresentative results.

Table 5 Cascade biooxidation of THIQ analogues with MAO-N D9 and *Rc* XDH E232V[a,b]

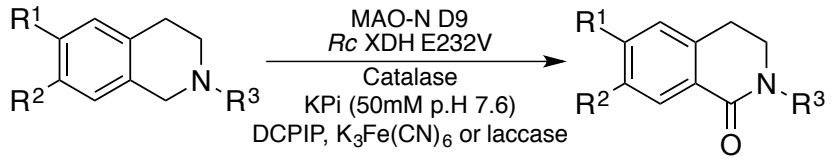

192: $R^1 = NO_2$, $R^2 = H$, $R^3 = Me$ **194**: $R^1 = NO_2$, $R^2 = H$, $R^3 = Me$
201: $R^1 = H$, $R^2 = H$, $R^3 = Me$ **203**: $R^1 = H$, $R^2 = H$, $R^3 = Me$

Entry	Substrate	Molarity (mM)	Time (h)	Conversion (%)[c]
1[d]	**192**	1	6	0
2[e]	"	"	"	"
3[f]	"	"	"	"
4[e]	**201**	"	"	97
5[f]	"	"	"	32

[a]Reaction conditions: Incubated at 37 °C with agitation at 180 RPM. Potassium phosphate buffer (50 mM, pH 7.6), total volume 300 µL. 0.3 & 3 µL **192** and **201** (1 M in DMF), 17 µL MAO-N D9 (14 mg/ml), 33 µL *Rc* XDH E232V (1 mg/ml) DCPIP 30 µL (10 mM) and catalase 100 µL (3.3 mg/ml). HPLC Conditions Diacel OJ-H column, 1 ml/min, 10 % IPA/Hexane at 230 nm. [b]Before extraction, the reaction was shaken with ammonia borane complex for 3 hours. [c]Conversion calculated from peak areas of HPLC analysis using authentic standards of the amine:lactam in a 1:1 ratio by NMR (see experimental). [d]Absence of catalase. [e]10 mol % $K_3Fe(CN)_6$. [f]laccase 1.5 U. (") signifies a repeat of the above value in a given column.

Rc XDH E232V was examined with substrates **192** and **201** at 1 mM. Laccase was also tested as a biological alternative to iron ferricyanide as an electron sink. Substrate **192** continued to display no activity with *Rc* XDH E232V, while **201** had greater conversion with iron ferricyanide compared to laccase (**Table 5** entries 4-5). Interestingly the lack of **192** oxidation is in contrast to a working bio-chemocatalytic approach using MAO-N D9 and H_2O_2/CuI.[189] This could suggest that the presence of the nitro group in the 6-position of THIQ was interfering with substrate oxidation in *Ec* XDH / *Rc* XDH E232V through either steric repulsion in the substrate channel or the electron withdrawing nature of the *para*-nitro group sufficiently deactivated the oxidation by reduction of conjugation in the imine intermediate.

2.3.1. Synthesis of *N*-methyl THIQ standards

In order to confirm the biotransformation products for substrate **201** (**Table 4 / 5)**, comparison to authentic chemical standards were made using HPLC. The starting material **201** was synthesised by methylation and subsequent reduction of the resulting DHIQ iminium iodide salt **205**.[193,194]

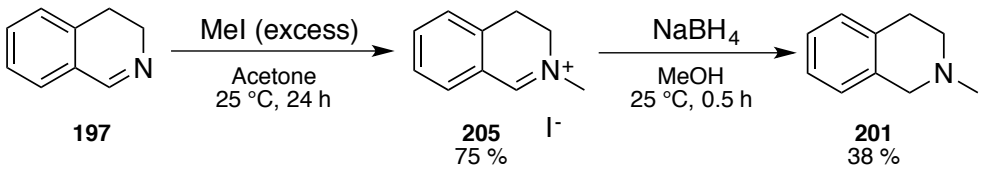

Scheme 49 Synthesis of *N*-methyl THIQ[193,194]

The iminium intermediate **205** was also used to synthesise the lactam standard **203**.[195]

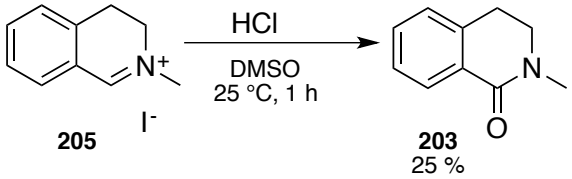

Scheme 50 Synthesis of *N*-methyl THIQ lactam[195]

The requirement of HCl for the oxidation to occur is thought to be due to oxysulfonium intermediate, which, upon protonation, cannot undergo the reverse transformation due to the unavailability of the nitrogen electron pair. O-S bond cleavage followed by deprotonation (or vice-versa) yields the lactam.

2.4. pH-dependence of biotransformations by *Ec* XDH

The work that ensued examined the dependence of solvent pH on degree of conversion. Beedham *et al*.[162] first reported that imine substrates required basic media to observe activity with xanthine oxidase. This was also supported by Kitamura *et al*.[155], who reported that XOR enzymes in general appeared to function most efficiently at more basic pH (9-10).

Table 6 THIQ analogue bioconversion dependence on pH[a]

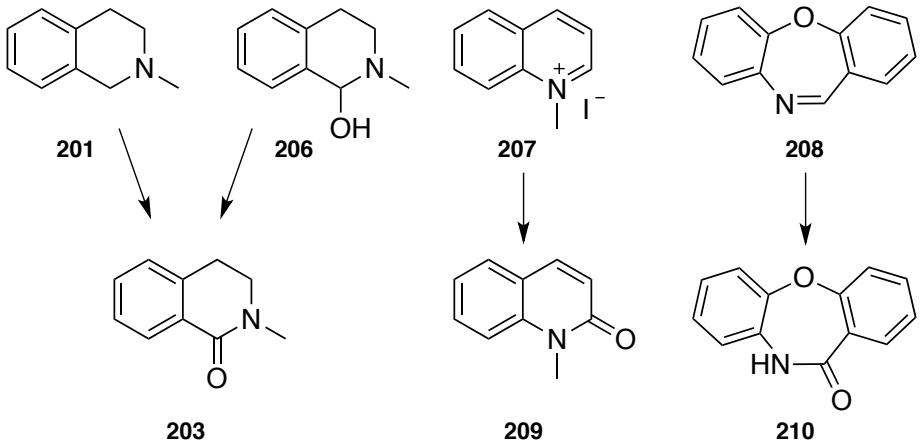

Entry	Substrate	Conversion pH 7 (%)[d]	Conversion pH 8 (%)[d]
1[b]	**201**	82	100
2[c]	**206**	100	"
3[c]	**207**	75	"
4[c]	**208**	86	"

[a]Reaction conditions: Incubated at 37 °C with agitation at 180 RPM for 16 h. Potassium phosphate buffer (100 mM, pH 7 or 8), total volume 300 µL. 3 µL **201** and **206-208** (1 M in DMF), 100 µL catalase (3.3 mg/ml). [b]17 µL MAO-N D9 (14 mg/ml), 33 µL *Ec* XDH (1 mg/ml) and [c] 33 µL *Ec* XDH (1 mg/ml). HPLC Conditions Diacel OJ-H column, 1 ml/min, 10 % IPA/Hexane at 230 nm. [d]Conversion calculated from peak areas of HPLC analysis using authentic standards of the amine:lactam in a 1:1 ratio by NMR (see experimental). (") signifies a repeat of the above value in a given column.

Prior transformations had been run at pH 7.6 so pH 7 and 8 as the closest integers were selected to examine the effect of small changes in pH on conversion. Comparing the cascade of **201** and single step oxidations of **206-208** at pH 7 and 8 overnight revealed higher conversion at more basic pH, supporting what had been reported previously. We observed that the hydroxyl-containing pseudobase **206** was also fully converted at lower pH. A shorter reaction time may provide a better comparison of the effect of pH on conversion for faster acting substrates. Beedham stipulated that the formation of lactams from nicotine and azapetine proceeded through pseudobase intermediates.[162] Having observed improved conversions in slightly basic media, pH 8 buffer was used on additional imine containing substrates going forward.

2.4.1. Synthesis of standards for pH dependence study

A publication by Leonard *et al*. in the late 1940s outlined a relatively mild method for the synthesis of the pseudobase **206** involving washing and filtering the iodide salt **205** with water followed by the addition of aqueous sodium hydroxide, further filtration and extraction into ether.[196]

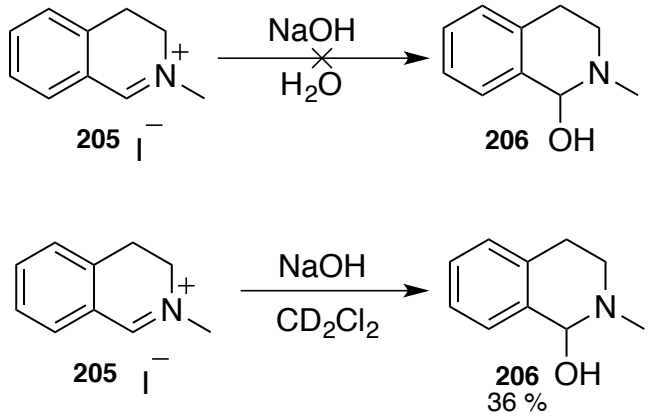

Scheme 51 Initial unsuccessful attempt at forming the pseudobase[196] and the successful method from Hanquet *et al*.[197]

This was unsuccessful when attempted; the process was designed for an industrial scale and the many filtrations on a small scale resulted in a mixture, which could not be separated. A similar method utilising a biphasic reaction mixture has been outlined by Hanquet *et al*.[197] This method was adapted, using deuterated dichloromethane to allow analysis of the reaction mixture directly following separation of the organic layer. NMR analysis showed complete conversion.

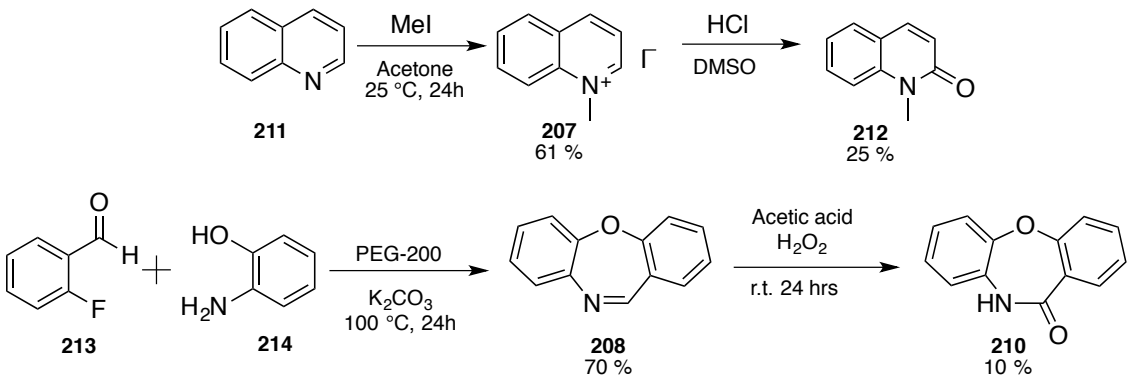

Scheme 52 Synthesis of quinolinium substrate, dibenzo[b,f][1,4]oxazepine and bicyclic lactam standards[193,195,198,199]

In analogous methods to that which were used to prepare THIQ *N*-Me iodide salt and lactam by Gray *et al*.[193] and Ruchiwarat *et* al.[195], the quinoline salt **207** and lactam **212** were successfully made in 61 % and 25 % yield respectively. Interestingly, biocatalytic conversions of **207** and **208** to **209** and **210** respectively (**Table 6**) were much greater than the corresponding chemical methods used to produce the authentic standards (**Scheme 52**). Jorapour *et al.*[198] described a method of forming oxazepine type compounds using polyethylene glycol. This was used to access dibenzo[b,f][1,4]oxazepine **208** and an oxidation described by Brewster *et* al.[199] was employed to produce the corresponding lactam **210** proceeding in comparatively poorer yield (**Scheme 52**) .

2.5. Additional bicyclic imine analogues

Selectivity at multiple sites for imine oxidation was initially assessed using 10 mM quinoxaline **215** and *Ec* XDH where the mono oxidised product **216** was observed (**Scheme 53**).

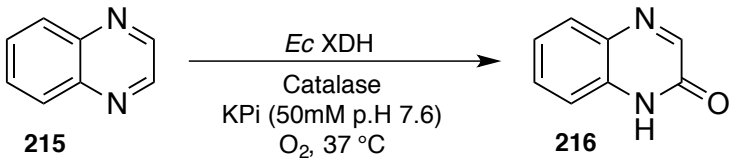

Scheme 53 *Ec* XDH quinoxaline oxidation

Initially believed to be the observed product, the di amide **217**, derived from quinoxaline **215** was not commercially available and therefore synthesised following a procedure by Troian-Gautier *et al*. (**Scheme 54**).[200]

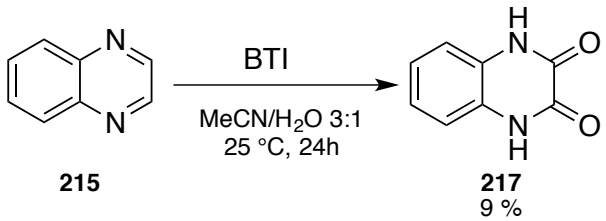

Scheme 54 Quinoxaline di amide forming oxidation[200]

An additional group of bicyclic imines (**211**, **218** and **219**) were screened using a series of XOR enzymes (PaoABC mutants for entries **5** & **6** will be introduced in Chapter 4) to investigate the chemoselectivity in the presence of multiple imine sites (**Table 7**).

Table 7 Bicyclic imine screen with XORs at pH8[a]

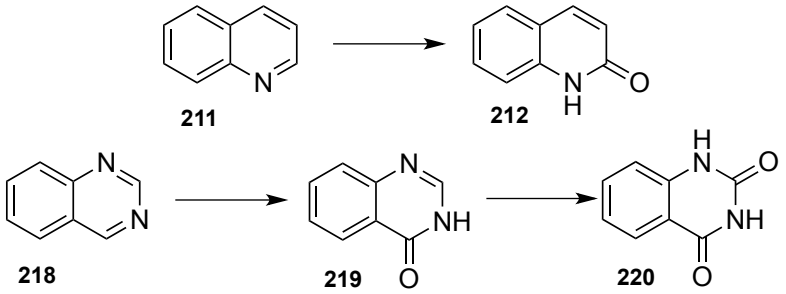

Entry	Enzyme	211	218	219
		Conversion[b] (%)	**Conversion[b] (%)**	**Conversion[b] (%)**
1	*Ec* XDH	58 (2-OH)	100 (di)	100
2	*Ec* PaoABC	0	100 (mono)	0
3	*Bovine* XO	"	100 (di)	100
4	*Rc* XDH E232V	75 (2-OH)	74 (mono)	0
5	*Ec* PaoABC L246E	0	0	"
6	*Ec* PaoABC T318R	"	67 (mono)	"

[a]Reaction conditions: Incubated at 37 °C with agitation at 250 RPM for 16 h. Potassium phosphate buffer (100 mM, pH 8), total volume 1000 µL. 10 µL **211**, **218** and **219** (1 M in DMF), 100 µL XOR (1 mg/ml) and catalase 100 µL (3.3 mg/ml). [b]Reaction centrifuged (5000 RPM, 1 min) and filtered before monitoring conversion by NMR (appendix). (") signifies a repeat of the above value in a given column

Due to the poor solubility of the products, transformations were monitored *via* NMR (DMSO-d6). *Ec* PaoABC displayed a preference for mono oxidation of quinazoline **218**; this preference was shared by *Rc* XDH E232V and *Ec* PaoABC mutant T318R with partial conversions (no di amide was observed) while L246E switched off activity. Conversely, *Ec* XDH and *Bovine* XO fully converted quinazoline **218** to the diamide. This was confirmed by separately assaying the mono amide **219**. Quinoline **211** was oxidised by both *Ec* XDH and *Rc* XDH E232V to give lactam **212** rather than the oxidation in the 4-position.

The same XOR enzymes employed in **Table 7** were used to assay another group of substrates under the same conditions (**Scheme 55**).

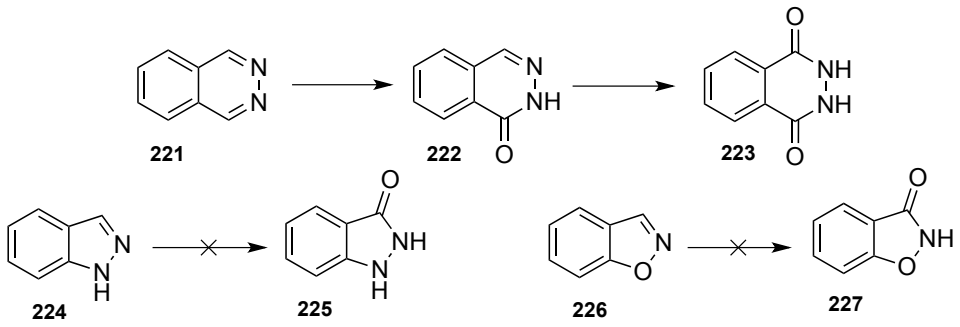

Scheme 55 Unsuccessful XOR substrate screen

Control reactions for substrates **221** and **222** revealed that they underwent auto-oxidation under reaction conditions. 5-membered ring-containing substrates **224** and **226** also displayed no conversion.

2.6. Conclusion

In summary we have developed a novel two-step enzymatic cascade for the formation of lactams from cyclic amines in a one-pot reaction. Biocatalytic formation of amides is inherently green and has the advantage of ease of use and atom efficiency. Two oxygen-dependent enzymes, monoamine oxidase-N D9 and *Ec* xanthine dehydrogenase function in water at ambient temperature (25-37 °C) and near neutral pH. The cascade has also been demonstrated using an external electron acceptor with xanthine dehydrogenase E232V from *Rhodobacter*. The enzymes have been previously utilised in separate processes, MAO-N D9 was used in the de-racemisation of chiral amines and an *Rc* XDH mutant E232V was shown to have increased aldehyde oxidase activity, however they have not been previously combined. Similarly *Ec* XDH, while commercially available, has not been previously used in biotransformations.

Initial limitations to cascade conversions caused by build up of harmful H_2O_2 were overcome through the incorporation of catalase to the reaction. The apparent reduction in conversion at higher substrate concentration remained a limitation however.

The imine/iminium oxidation stage has been further investigated using a range of molybdenum hydroxylases for chemoselectivity with respect to multiple sites of oxidation. Selectivity for mono oxidation was observed in quinoxaline **215** and quinazoline **218** where chemical methods of quinoxaline oxidation gave the fully oxidised product.

Changes in conversions of additional cyclic imines from tuning the pH were also investigated, which confirmed a preference for slightly basic media. This compared favourably to chemocatalytic methods used in synthesis, which required high temperature and harsh conditions.

Chapter 3

3.0. Random mutagenesis of *Ec* PaoABC and development of a solid-phase oxidase activity assay

3.1. Introduction

Directed evolution is a powerful technique used to access structurally modified enzymes, which may impart such properties as increased solvent or temperature tolerance, wider substrate range or improved chemo-, regio- or stereoselectivity. epPCR is a method of introducing random mutations throughout a defined region of a protein sequence that has the advantage of not requiring the crystal structure. There have been many successful examples utilising this technique following the work of Francis Arnold[72] as discussed previously.

Our collaborator, Silke Leimkühler reported the isolation of *Ec* PaoABC, which is the first MCD-containing MFE isolated from *E. coli*.[169] It catalyses the bio-oxidation of a wide range of aliphatic and aromatic aldehydes and is thought to play a role in mammalian detoxification of xenobiotics, particularly aromatic aldehydes. It is extremely robust and can be heterologously over-expressed using bacterial hosts in the laboratory, which is vital for effective isolation and mutation studies. Application of *Ec* PaoABC has been demonstrated in the synthesis of a range of carboxylic acids in addition to FDCA, a key platform chemical.[170] Successful mutagenesis of molybdenum hydroxylases to demonstrate the reliance of the protein mechanism on specific amino acid residues had been carried out.[173] In addition, mutagenesis for modulation of substrate specificity has been demonstrated previously by Leimkühler.[173]

Many established bioassays such as western blots, can detect the presence of various antibodies through a colorimetric reaction. An antibody-coupled peroxidase enzyme, upon interaction with hydrogen peroxide, mediates the oxidation of a redox dye. Work in the group of our collaborator, Nick Turner used a variation of this process to screen for improved mutations of galactose oxidase (GOase).[99] This involved lysing a plate containing bacterial colonies on a nitrocellulose membrane, then saturating the membrane with a solution containing the dye, a substrate and horseradish peroxidase (HRP). Substrate oxidation would generate H_2O_2 within the bacterial colony, triggering HRP mediated oxidation of the dye to a coloured, insoluble product.

3.2. *Ec* PaoABC random mutagenesis

Through site-directed mutagenesis, Leimkühler's group shifted the substrate specificity of a xanthine dehydrogenase to that of an aldehyde oxidase. We postulated that through mutagenesis, it could be possible to alter the specificity of an aldehyde oxidase to that of a xanthine dehydrogenase with the aim of producing an imine oxidase.

As discussed previously, *Ec* PaoABC is a temperature stable, robust, oxygen-dependent enzyme with a broad substrate range. As it is oxygen dependent, it doesn't require stoichiometric co-factors or recycling systems. It is also easily expressed in host organisms such as *E.coli* and this made it a strong candidate for mutagenesis. Samples of isolated *Ec* PaoABC enzyme and bacterial cultures of TP1000 x *Ec* PaoABC were kindly provided by our collaborator, Silke Leimkühler (Potsdam, GER).

At the outset, the crystal structure for PaoABC had not been elucidated so we aimed to exploit a random mutagenesis approach using epPCR and develop a suitable method for screening mutant libraries. Using the sequence data for the Moco-containing PaoC subunit, a homology model was assembled using the Phyre2 web portal for protein modelling, prediction and analysis to help identify which region of PaoC to mutate.[201] The Phyre2 tool compares a submitted sequence against databases of characterised protein crystal structures and constructs a homology model of best estimation based on similar proteins available on the database at the time.

```
  1 mkfdkpagen pidqlkvvgr phdridgplk ttgtaryaye wheeapnaay gyivgsaiak
 61 grltaldtda aqkapgvlav itasnagalg kgdkntarll ggptiehyhq aialvvaetf
121 eqaraaaslv qahyrrnkga ysladekqav nqppedtpdk nvgdfdgaft saavkidaty
181 ttpdqshmam ephasmavwd gnkltlwtsn gmidwcrtdl aktlkvpven vriispyigg
241 gfggkllflrs dallaalaar avkrpvkvml prpsipnntt hrpatlqhlr igadqsgkit
301 aisheswsgn lpggtpetav qqsellyaga nrhtglrlat ldlpegnamr apgeapglma
361 leiaidelae kagidpvefr ilndtqvdpa dptrcfsrrq lieclrtgad kfgwkqrnat
421 pgqvrdgewl vghgvaagfr nnlleksgar vhleqngtvt vetdmtdigt gsytilaqta
481 aemlgvpleq vavhlgdssf pvsagsggqw gantstsgvy aacmklremi asavgfdpeq
541 sqfadgkitn gtrsatlhea taggrltaee siefgtlske yqqstfaghf vevgvhsatg
601 evrvrrmlav caagrilnpk tarsqvigam tmgmgaalme elavddrlgy fvnhdmagye
661 vpvhadipkq evifldtdtp isspmkakgv gelglcgvsa aianavynat girvrdypit
721 ldklldklpd vv
```

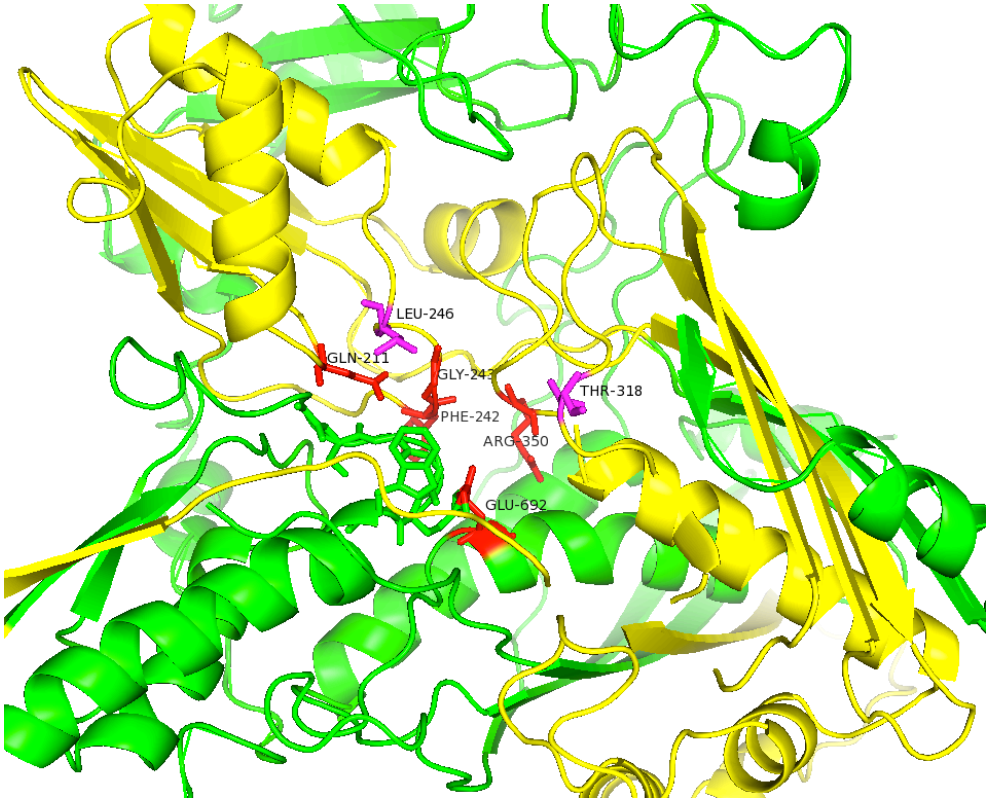

Figure 19 Top - AA sequence of PaoC subunit. Yellow - region selected for mutation, purple – residues involved in substrate binding red – highly conserved residues. Bottom - Phyre2 generated homology model of *Ec* PaoABC[201]

Based on the estimated structure of the model, we selected a region of approximately 300 amino acid residues for mutagenesis. The area of sequence selected for mutation and the corresponding regions in the PaoC model are highlighted in (**Figure 19**). Key residues Gln211, Phe242 and Gly243 involved in MCD coordination and catalytic Glu 692 are highlighted in red, while residues Leu246 and Thr318, displayed in purple, were later found to correspond (*via* structure-based sequence alignment) to Glu232 and Arg310 in *Rc* XDH, known to be important for substrate binding. According to the estimated structure of PaoC, the selected area for mutation appeared to cover a reasonable range of residues around the active site. Importantly, the

essential Glu692 residue was well outside the mutation region, which minimised the risk of producing inactive mutants. *Ec* PaoABC pMN100 with an ampicillin resistance gene[169] was isolated and purified from samples of *E. coli* TP1000[191] x pMN100 PaoABC provided and used as a template for mutagenesis.

A commercially available "Genemorph II" mutagenesis kit from Agilent was used for introducing random mutations within the selected region. Primers were designed flanking the outsides of the desired mutation region to ensure the all of the highlighted region was included (green **Figure 20**). PCR with the included "Mutazyme II" DNA polymerase resulted in amplification of the desired region with random mutations. A high rate of mutation (9-16 mutations / kb) was selected by using a lower concentration plasmid to be amplified (100 ng). Low concentrations of plasmid result in more replication cycles with increased accumulation of errors.

```
451   AATCAGCCGCCGGAA GACACGCCCGACAAA AACGTCGGTGACTTT GACGGGGCTTTCACC TCCGCTGCGGTGAAG
151    N  Q  P  P  E   D  T  P  D  K   N  V  G  D  F   D  G  A  F  T   S  A  A  V  K
526   ATTGATGCTACCTAC ACGACCCCGGACCAG AGCCATATGGCGATG GAGCCGCATGCCTCG ATGGCCGTCTGGGAT
176    I  D  A  T  Y   T  T  P  D  Q   S  H  M  A  M   E  P  H  A  S   M  A  V  W  D
601   GGAAATAAGCTTACC CTCTGGACCTCAAAT CAGATGATTGACTGG TGCCGCACCGATCTG GCAAAAACGCTGAAA
201    G  N  K  L  T   L  W  T  S  N   Q  M  I  D  W   C  R  T  D  L   A  K  T  L  K
676   GTTCCCGTGGAGAAT GTGCGTATTATCTCC CCGTATATCGGCGGA GGGTTTGGCGGCAAG CTGTTCCTGAGAAGC
226    V  P  V  E  N   V  R  I  I  S   P  Y  I  G  G   G  F  G  G  K   L  F  L  R  S
751   GATGCGCTGCTGGCG GCCCTCGCCGCCCGA GCGGTGAAACGTCCG GTTAAAGTGATGCTC CCCCGCCCCTCTATT
251    D  A  L  L  A   A  L  A  A  R   A  V  K  R  P   V  K  V  M  L   P  R  P  S  I
826   CCCAATAACACCACG CACCGCCCCGCCACC CTTCAGCACTTGCGT ATCGGTGCCGACCAG AGCGGGAAAATCACC
276    P  N  N  T  T   H  R  P  A  T   L  Q  H  L  R   I  G  A  D  Q   S  G  K  I  T
901   GCTATCTCACATGAA AGCTGGTCTGGAAAC CTGCCCGGCGGCACG CCGGAAACGGCGGTA CAGCAAAGCGAATTA
301    A  I  S  H  E   S  W  S  G  N   L  P  G  G  T   P  E  T  A  V   Q  Q  S  E  L
976   CTCTACGCCGGGGCG AATCGTCATACCGGC CTGCGGCTCGCCACG CTTGATTTGCCGGAA GGGAACGCCATGCGT
326    L  Y  A  G  A   N  R  H  T  G   L  R  L  A  T   L  D  L  P  E   G  N  A  M  R
1051  GCGCCCGGCGAAGCC CCCGGTCTGATGGCG CTCGAAATCGCGATC GACGAACTGGCGGAA AAAGCGGGCATCGAT
351    A  P  G  E  A   P  G  L  M  A   L  E  I  A  I   D  E  L  A  E   K  A  G  I  D
1126  CCCGTCGAGTTTCGC ATCCTGAATGACACT CAGGTTGACCCCGCC GACCCGACGCGCTGC TTCTCTCGCCGTCAG
376    P  V  E  F  R   I  L  N  D  T   Q  V  D  P  A   D  P  T  R  C   F  S  R  R  Q
1201  CTTATCGAGTGCTTG CGCACCGGAGCGGAT AAATTTGGCTGGAAG CAGCGCAACGCCACA CCCGGACAGGTGCGC
401    L  I  E  C  L   R  T  G  A  D   K  F  G  W  K   Q  R  N  A  T   P  G  Q  V  R
1276  GACGGGGAGTGGCTA GTCGGCCACGGTGTT GCGGCGGGCTTTCGC AATAATCTGCTGGAA AAATCGGGTGCTCGG
426    D  G  E  W  L   V  G  H  G  V   A  A  G  F  R   N  N  L  L  E   K  S  G  A  R
1351  GTTCACCTCGAACAA AACGGCACCGTTACC GTAGAAACGGACATG ACCGACATTGGCACC GGCAGCTACACCATT
```

Figure 20 Nucleobase and corresponding AA sequence of mutation region of PaoC indicating primer sites (green)

The second stage involved annealing the mutated PaoC sequence back to the template and amplifying the mutated PCR product in an additional PCR reaction. The product contained a library of mutations within the indicated region of PaoC, which was then transformed into a cloning strain of ultracompetent cells and selectively grown on ampicillin-containing agar plates for plasmid isolation. A random sampling of 10

colonies was taken out of ~3000 produced and the corresponding plasmids were sequenced to evaluate the efficiency of mutagenesis.

Table 8 Mutagenesis sampling results

Entry	Base Mutation	AA Mutation	Mutation rate (mutations / kb)
1	T806C	M269T	3.75
	T1050C	R350R *Silent*	
	G1104C	L368L *Silent*	
2	-	-	-
3	T1145C	L382P	2.5
	T1302C	G434G *Silent*	
4	T678C	V226V *Silent*	2.5
	C1307T	A436V	
5	G592A	V198I	3.75
	C1043T	A348V	
	C1064G	A355G	
6	T646A	C216S	3.75
	C873T	I291I *Silent*	
	C1263T	P421P *Silent*	
7	-	-	-
8	-	-	-
9	-	-	-
10	G1036C	G346R	3.75
	G1092A	A364A *Silent*	
	C1206A	I402I *Silent*	

Region of PaoC DNA amplified: 827bp (-) indicates WT sequence detected

Due to the time-consuming nature of culturing sampled colonies and manual plasmid isolation, 10 colonies were selected to assess the degree of mutagenesis. Of the colonies containing mutations, an average of 2.5 base substitutions and 1 AA substitution per kb was determined. This is significantly less than the 9-16 bp claimed in the kit instructions, but given the number of silent mutations a rate of 1 AA substitution would theoretically result in 6000 potential mutants over a range of 300

AAs. 3000 colonies could provide coverage of approximately half the available sequence space if the amount of wild type colonies were consistent so the library was taken forward for screening. For each screen ~3000 colonies were grown from TP1000 *E. coli* transformed with the plasmid library to express the variants generated. Mutagenesis could be further improved through using lower template concentration in addition to increasing the number of PCR cycles.

3.3. Development of a solid-phase aldehyde oxidase assay

A solid-phase screen for detecting improved mutants of GOase for the enantioselective oxidation of a range of 1-phenylethanol analogues was developed by Turner.[99] The assay indirectly detects the presence of hydrogen peroxide produced by oxidase enzymes through the colour change of a redox dye in the presence of peroxidase. 3,3'-diaminobenzidine (DAB) was employed as the redox dye whereupon oxidation, a pink colouration would be observed within a bacterial colony through an HRP mediated reaction. In order to successfully assay the bacterial colonies, cultures were grown on a nitrocellulose membrane before being assayed.

To effectively express *Ec* PaoABC on a nitrocellulose membrane, 0.035 mM IPTG and 4 mM sodium molybdate per 200 ml of the nutrient agar were determined to be the optimal concentrations after several trials. The membrane was then overlaid and bacterial culture applied before incubating overnight at 37 °C. Submerging the membrane-bound bacterial colonies in liquid N_2 (3 x ~3 seconds) sufficiently lysed them for screening. Prior to actual screening, membranes were pre-soaked in phosphate buffer containing HRP to remove any endogenous peroxide.

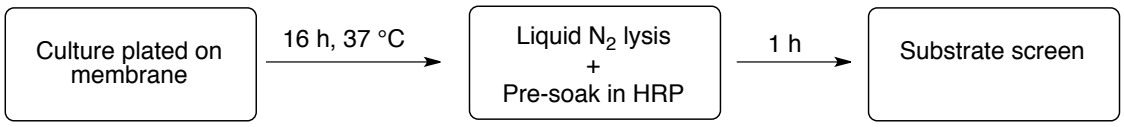

Scheme 56 Simplified solid-phase screen workflow

Before screening mutant libraries, some trials were conducted using DAB to detect the oxidation of benzaldehyde with WT *Ec* PaoABC. Benzaldehyde was selected as a simple aldehyde with known activity.[169] While initial results seemed encouraging, the dye was forming an imine adduct (**Scheme 57**) with benzaldehyde as indicated by

the yellow colouration on white filter paper (**Figure 21**). This was also confirmed by NMR.

Figure 21 *Ec* PaoABC benzaldehyde screen using DAB as a dye

This ultimately resulted in DAB being unsuitable for screening. In addition to interfering with the substrate, it was unknown if the peroxide was detected as a result from oxidation of the substrate, or the imine adduct. Instead an alternative redox dye 4-chloronapthol (4-CN) was selected for screening (**Scheme 58**).

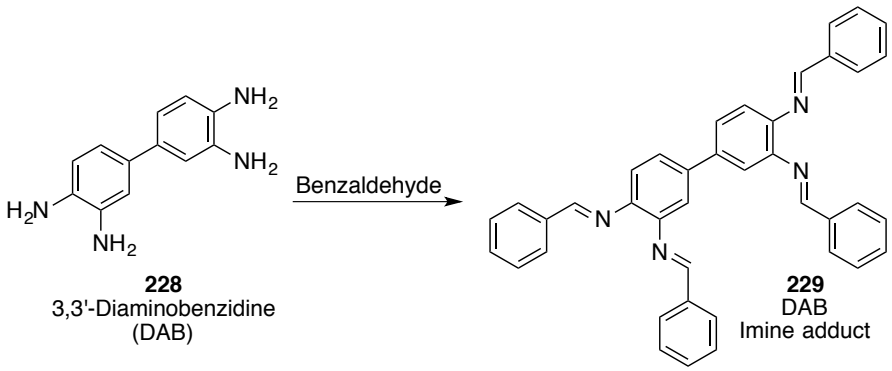

Scheme 57 Formation of DAB imine adduct

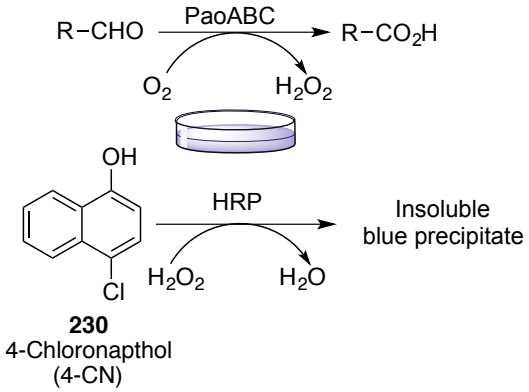

Scheme 58 HRP mediated 4-CN solid phase screen

The dye also had the benefit of not auto-oxidizing over extended periods of time as DAB does and reacted positively with benzaldehyde (**Figure 22**).

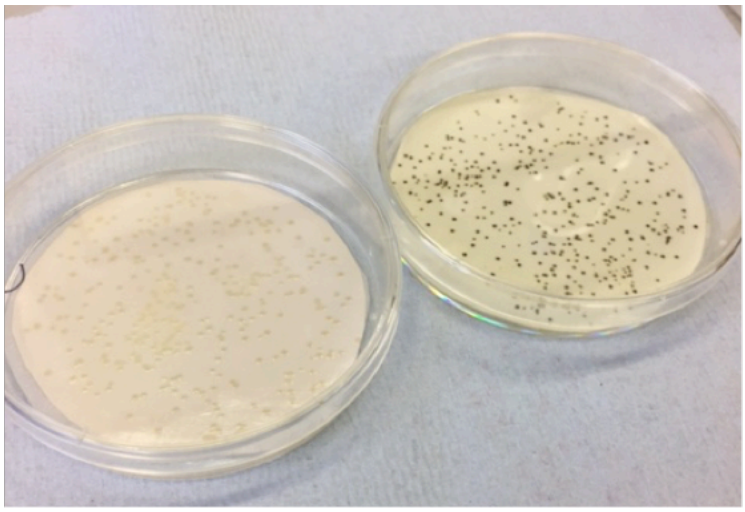

Figure 22 Plates showing *Ec* PaoABC colonies, 4-chloronapthol (16.8 mM) and HRP (1.4 mg/ml): left – no substrate, right – 10 mM benzaldehyde

In addition the solid-phase screen could tolerate up to 50 % DMF as a co-solvent after pre-soaking in order to fully solubilise the dye and substrate. Additionally, a liquid screen was run to check if the 4-CN dye interacted with benzaldehyde in a similar fashion to DAB. Unlike DAB the test appeared to show no immediate reaction without the addition of isolated *Ec* PaoABC whereupon an immediate colour change was observed (**Figure 23**).

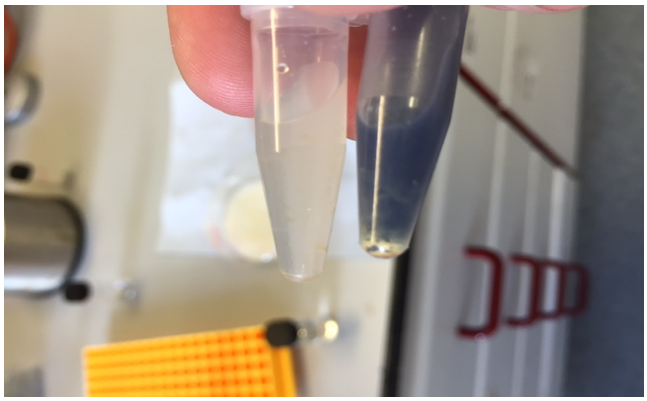

Figure 23 Liquid screen of 4-CN (16.8 mM) containing benzaldehyde (10 mM) and HRP (1.4 mg/ml): left - no PaoABC, right – 2 µl PaoABC (16 mg/ml)

With a suitable detection system in place, DHIQ was screened as a model imine substrate against the whole mutant library (~3000 colonies) of *Ec* PaoABC however no hits were observed. Following this initial setback it was decided to instead check for improved aldehyde oxidase activity among mutants. Initially benzaldehyde was selected as a substrate; plates containing the mutant library (~3000 colonies) were screened in addition to a plate containing just the WT enzyme as a control. However, this substrate underwent rapid oxidation, which made screening for potential improved mutants problematic. A more slowly oxidised substrate, phenylacetaldehyde (PAA) had been previously trialled in DAB screenings before the dye was revealed to be acting on the substrate and was determined to be a more suitable substrate. A faster mutant L443Q taking only 40 min to show activity (compared to 1.5 h for the WT) under DAB assay conditions was isolated. This mutant was then re-assessed using the new dye (**Figure 24**).

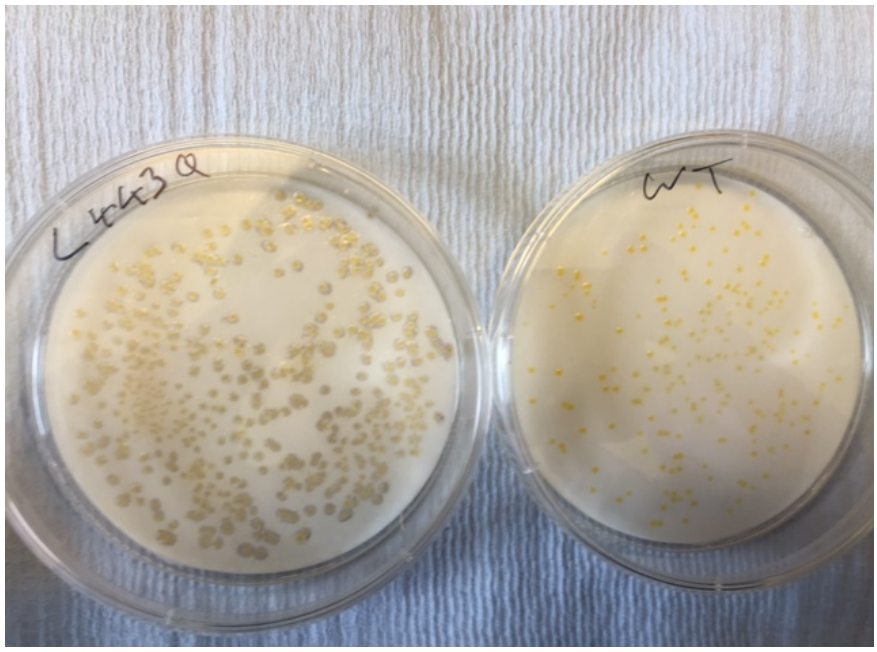

Figure 24 25 mM PAA 4-CN screen comparing L443Q mutant (left) to WT PaoABC (right) at 40 min

The isolated mutant was further verified using the new dye system by co-plating the WT PaoABC with L443Q and analysing the sequences of 5 sampled colonies, which gave fast colour change (**Figure 25**).

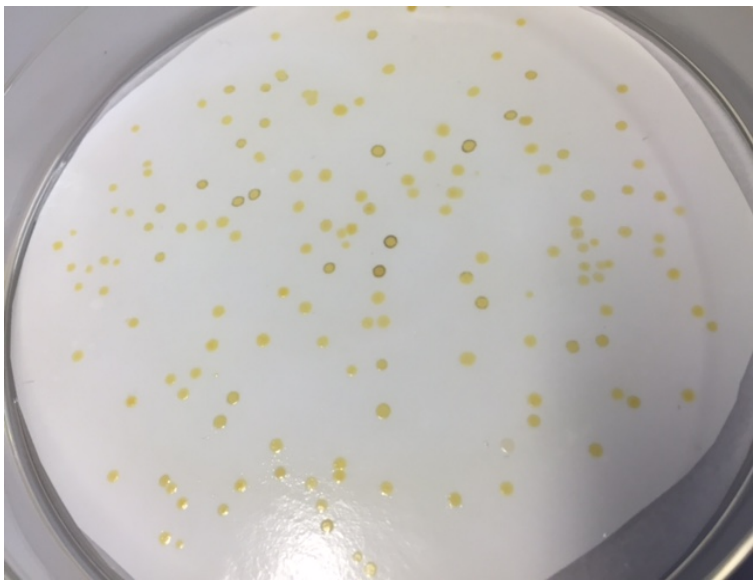

Figure 25 Mixed L443Q / WT PaoABC assay using 25 mM PAA at 30 min.

The sequence of all 5 selected samples contained the mutation indicating PaoABC L443Q was indeed an improved mutant for the oxidation of PAA and validating the plate screen.

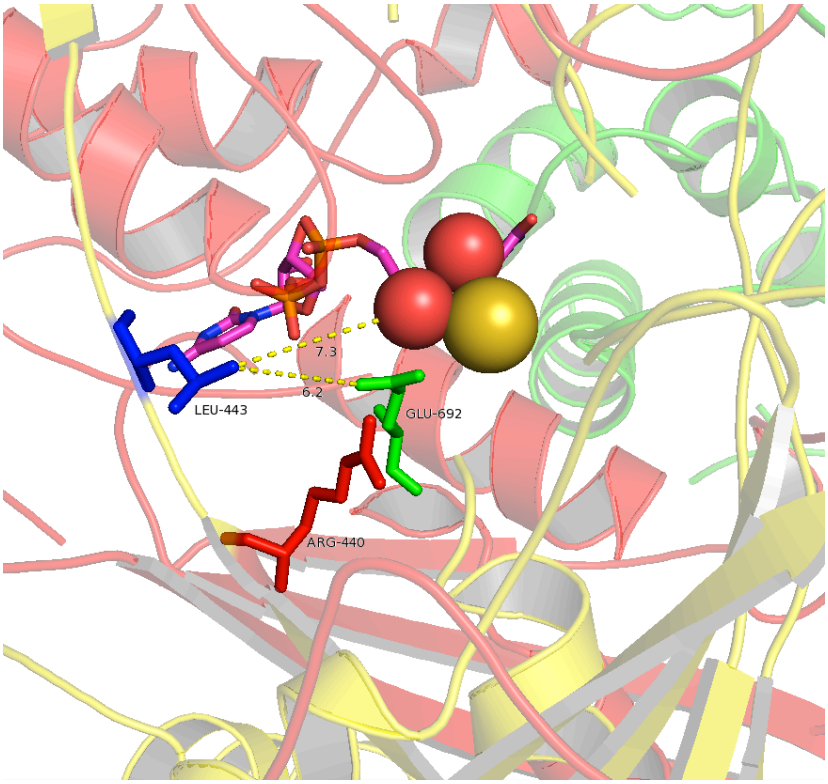

Figure 26 Active site of *Ec* PaoABC L443 residue (blue) R440 (red) and E692 (green) from published crystal structure Spheres represent the pterin-bound apical Mo=O and hydroxyl ligand (red), in addition to the Mo=S (yellow).[158]

Following the publication of the crystal structure of *Ec* PaoABC, it was revealed that L443 was situated reasonably close (7.3 Å) to the active site.[158] In addition to substrate interaction *via* hydrogen bonding, the mutated residue may also increase enzymatic activity through bonding interactions (6.2 Å away) with the key Glu692 residue. Arg440 was determined to activate Glu692 through charged interactions by Leimkühler.[158]

3.3.1. Methods of enzyme purification and characterisation

PaoABC WT and mutants were purified by first obtaining the cell-free extract of the mature culture through sonication and centrifugation. The plasmid harbouring the *PaoABC* gene had a polyhistidine-tag fused to the N-terminus of the PaoA sub unit. Polyhistidine-tags allow for ease of separation from the cell free extract by HiTrap affinity chromatography, where a nickel sepharose resin stationary phase binds to histidine, which can then be eluted by displacement using an imidazole gradient. The

final step involved buffer exchange to remove the imidazole using a de-salting PD-10 column.

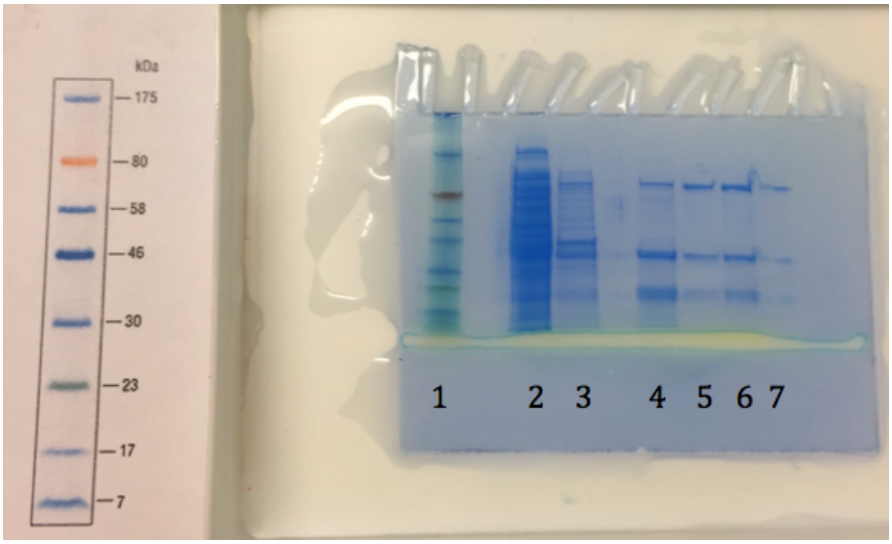

Figure 27 Pure PaoABC obtained by affinity chromatography. Lane 1: protein ladder, lane 2: flow through, lane 3: wash, lane 4: standard, lane5/6/7: dilution gradient of purified protein.

The purified protein (WT PaoABC and mutant) was analysed by denaturing PAGE, co-running an authentic sample provided by our collaborators. Gels contained characteristic bands corresponding to the three sub-units at 85 (Moco), 40 (FAD) and 20 (Fe-S) kDa. The purified protein could also be pre-identified by a characteristic bronze hue afforded by the molybdenum.

3.3.2. Kinetic evaluation of PaoABC L443Q

After observing positive results on the solid phase plate screen, kinetic characterisation was performed on isolated PaoABC L443Q vs WT PaoABC for PAA oxidation. WT PaoABC and mutants were expressed in *E. coli* TP1000 cells grown using ampicillin selection. Isolated proteins were purified by Hi-Trap nickel affinity chromatography as previously discussed. Work in the group of our collaborator Nick Turner used a spectrophotometric method to characterise the kinetics of *R*-selective amine oxidases.[202] The adopted method of characterisation here uses a similar principle to that of the solid-phase screen by monitoring the formation of H_2O_2. A dye consisting of 4-aminoantipyrene **231** and 2,4,6-tribromo-3-hydroxy-benzoic acid **232** forms an adduct **233** upon oxidation that remains soluble in aqueous media with an absorbance maximum of 510 nm (**Scheme 59**).

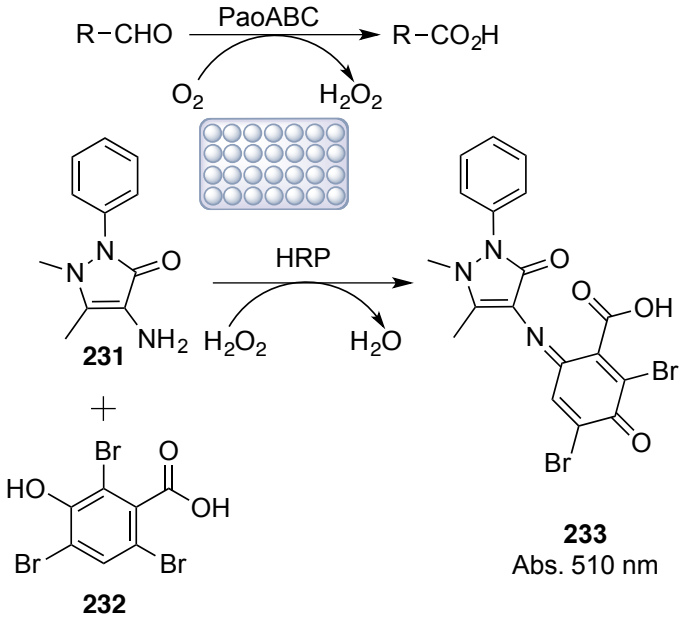

Scheme 59 4-aminoantipyrene coupled-enzyme liquid phase assay[202]

The rate of transformation was spectrophotometrically monitored in a 96 well plate assay. Steady state kinetics were calculated by plotting rate (measured in triplicate) against substrate concentration (8 values typically between 8 and 0.002 mM) and V_{max} and K_m values extracted using non-linear regression analysis with a fit to the Michaelis-Menten equation (V_{max}.[S]/K_m+[S]).

Table 9 Kinetic parameters of WT PaoABC *vs* L443Q for PAA oxidation[a]

Enzyme	K_m (mM)	V_{max} (umol min^{-1} mg^{-1})	k_{cat} (min^{-1})	k_{cat}/K_m (min^{-1} mM^{-1})
WT	**5.4 x 10^{-2}**	**1.2**	**160**	**2900**
	(± 1.1 x 10^{-2})	(± 8.1 x 10^{-2})	(± 11)	(± 630)
L443Q	**4.3 x 10^{-2}**	**1.3**	**180**	**4100**
	(± 4.8 x 10^{-3})	(± 4.8 x 10^{-2})	(± 6.5)	(± 470)

[a]Reaction conditions: Readings made at 30 °C at 510 nm over 8 min. The rate of production of hydrogen peroxide was detected by HRP (microbial, Sigma) and 4-amino antipyrine / 2,4,6-tribromo-3-hydroxybenzoic acid dye (ε = 29400 L mol^{-1} cm^{-1}). Typically eight different substrate concentrations were examined (8 mM down to 0.0015 mM).

Both enzymes exhibited classical Michaelis-Menten kinetics behaviour (**Appendix**). L443Q displayed a modest improvement in V_{max}, K_m, and k_{cat}, which led to

an improvement in substrate specificity for PAA. While the results appear to validate the solid-phase screen, the perceived degree of colouration on the plate is greater than the improvement in kinetics.

3.4. Solid-phase assay limitations

3.4.1. Screening mutant library for improved imine oxidase activity

Having discovered an improved aldehyde oxidase mutant PaoABC L443Q, we next turned our attention to generating an "imine oxidase". We therefore didn't re-assess the library with PAA using 4-CN as a screen.

Enzymes for purine oxidation such as XORs are well documented, however enzymes for selective imine oxidation would be novel. Shifting the substrate specificity from aldehyde to imine is an extremely attractive concept, which would result in a biocatalyst geared toward the green synthesis of amides.

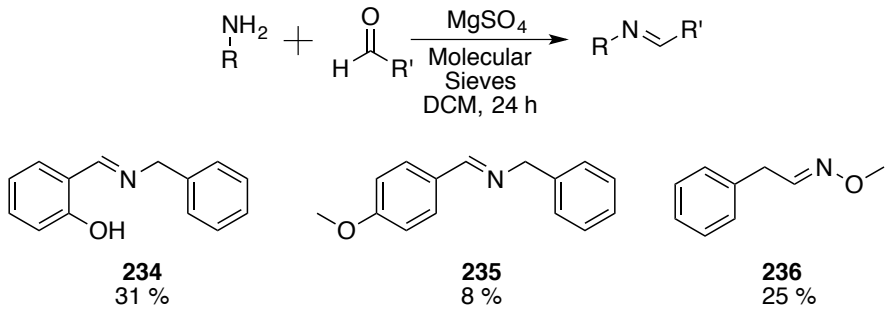

Scheme 60 Dehydration reactions to form aliphatic imines

A small group of aliphatic imines were synthesised using a simple dehydration (**Scheme 60**) with $MgSO_4$ and molecular sieves. Prior to screening, the substrates were analysed by NMR in buffer to determine the ratio of imine to aldehyde (**Table 10**).

Table 10 NMR analysis of aliphatic imines

Entry	Substrate	% Aldehyde	% Imine
1	**234**	50	50
2	**235**	18	82
3	**236**	5	95

Substrates were added to 90 % KPi 100 mM pH 8 and 10 % deuterated acetonitrile. Water suppression NMR was used to determine the ratio of aldehyde to imine in buffer.

Aliphatic imines are known to be unstable in aqueous conditions. It was hypothesised that short imines with neighbouring aromatic groups could stabilise the imine, however aldehyde was detected in each of the synthesised aliphatic imines. This would be problematic during screening as PaoABC would have a clear preference for oxidising the aldehyde and the rest of the imine would equilibrate as the aldehyde was oxidised. This was confirmed in a liquid phase transformation of **234** with WT PaoABC where only the acid and amine were detected (see experimental **5.4.4.**).

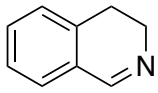

197
3,4-Dihydroisoquinoline

Figure 28 DHIQ - model imine substrate for PaoABC mutagenesis

3,4-dihydroisoquinoline (DHIQ) remains exclusively in the imine form under aqueous conditions due to the combined stability of the cyclic structure and conjugation with the aromatic system. PaoABC was found to display limited activity with DHIQ (**Table 11**). As can be seen, *E. coli* XDH is a better catalyst for this substrate

Table 11 Kinetic parameters of WT PaoABC *vs Ec* XDH for DHIQ **197** oxidation[a]

Enzyme	K_m (mM)	V_{max} (umol min^{-1} mg^{-1})	k_{cat} (min^{-1})	k_{cat}/K_m (min^{-1} mM^{-1})
PaoABC	**1.6**	**9.1×10^{-4}**	**0.12**	**0.08**
	(± 0.26)	(± 5.4×10^{-5})	(± 7.3×10^{-3})	(± 0.01)
E. coli XDH	**3.2**	**5.5×10^{-2}**	**7.5**	**2.3**
	(± 0.41)	(± 3.1×10^{-3})	(± 0.42)	(± 0.33)

[a]Reaction conditions: Readings made at 30 °C at 510 nm over 24 min. The rate of production of hydrogen peroxide was detected by HRP (microbial, Sigma) and 4-amino antipyrine / 2,4,6-tribromo-3-hydroxybenzoic acid dye (ε = 29400 L mol^{-1} cm^{-1}). Typically eight different substrate concentrations were examined (8 mM down to 0.02 mM).

It was reasoned that improving existing activity for a given substrate would be much more likely than introducing new substrate specificity. Solid-phase assays on membranes expressing the WT PaoABC for a range of DHIQ concentrations (1-25 mM)

displayed no visually observable colour change. These trials were repeated on membranes expressing the mutant library but no observable oxidation occurred. It could be reasoned that the poor activity of PaoABC for DHIQ could be the limiting factor of the plate screen. For PAA, WT PaoABC has a k_{cat} / K_m of ~2900, this still required over an hour to observe a colour change in the assay. It is also unlikely that a single mutant at a random position would improve this significantly. Therefore, in order to identify mutants with slightly improved DHIQ specificity, a saturation mutagenesis approach was taken where mutants could be analysed by the more sensitive spectrophotometric method.

3.4.2. Phenylacetaldehyde (PAA) background oxidation

It was found that during the solid-phase screening that benzaldehyde and PAA both underwent microbial background oxidation. This was observed on a control plate with membrane bound bacterial colonies grown without induction media and intentionally not expressing the PaoABC protein. The oxidation was believed to be microbial due to the lack of colour change elsewhere on the membrane outside of the bacterial colonies. The rapid oxidation of benzaldehyde largely bypassed this having any impact on screening. For PAA this background activity took longer than cells expressing the WT PaoABC (~3 h vs 1.5 h), and as all mutants would be exposed to this oxidation it was determined there would be no bias. Screening for less active mutants of PaoABC on a given aldehyde may be obstructed using this method however.

A small but consistent amount of background absorbance was detected during liquid phase kinetic screening of WT PaoABC vs L443Q on the oxidation of PAA. This was overcome by manually correcting the absorbance values by subtracting absorbance values of control runs with no PaoABC present. This was done before calculating the kinetic parameters presented (see experimental). DHIQ displayed no background oxidation.

3.5. Conclusion

A region of the Moco containing PaoC subunit of PaoABC has been successfully mutated using a random mutagenesis approach. The region of interest was determined using a homology model of PaoC. The region was amplified with a controlled rate of mutation using epPCR. Commercial sequencing of randomly sampled colonies confirmed successful mutations with a frequency of 2.5 base substitutions per kb of template which was lower than the expected rate. In the event of a single AA mutation across the region of 300 residues, screening ~3000 colonies could provide a reasonable coverage of the theoretical 6000 mutants.

The mutant L443Q was obtained with an apparent improvement in aldehyde oxidase activity; initially identified from an ultimately unsuitable screen, this mutant was verified with reproducible results using an alternative screening system. The improved mutant was further studied in a kinetic assay and shown to possess a small improvement in kinetic properties for the substrate phenylacetaldehyde. L443 lies in close proximity to the Moco active site and the mutation from an aliphatic leucine to a polar glutamine may result in hydrogen bonding interaction thereby activating the carbonyl group in the substrate.

The solid-phase screen appeared to be unsuitable for aliphatic imines, which are prone to aldehyde formation under aqueous conditions. Additionally cyclic imines like DHIQ failed to give clear results in the initial solid phase screen of the library. This could be due to very low baseline activity of DHIQ with WT PaoABC and the lack of improved (or significantly improved) mutants generated in the library for imine oxidation.

In Chapter 4, a saturation mutagenesis approach focusing on key substrate binding residues will be pursued with kinetic characterisation of isolated mutants using PAA and DHIQ as substrates following publication of the PaoABC crystal structure.

Chapter 4

4.0. Saturation mutagenesis of *Ec* PaoABC L246 and T318 & kinetic evaluation

4.1. Introduction

Provided structural data of an enzyme is known, site-directed and saturation mutagenesis are effective methods of probing the specific effect of amino acid substitutions at a given position. Residues around the active site are most frequently targeted as they play roles in substrate binding or intermediate stabilisation. Residues like glutamate in xanthine oxidoreductases can also be critical to the catalytic mechanism of the enzyme. There are several examples discussed previously of successful site-directed mutagenesis approaches, whether in combination with other mutagenesis methods (**Figure 9**) or used at anticipated positions of interest (**Scheme 16**).

PaoABC is an exceptional member of the xanthine oxidase family of molybdenum-containing enzymes and has only recently been structurally characterised.[158] As such, targeted mutation has been limited to studies directly concerning its mechanism.[169] Saturation mutagenesis of this enzyme is also not reported in the literature.

4.2. *Ec* PaoABC L246 and T318 targeted mutagenesis and kinetic evaluation

Structure-based sequence alignment of *Ec* PaoABC with *Rc* XDH, another structurally characterised XOR enzyme showed several highly conserved residues concerned with Moco binding and catalytic activity (**Figure 12**). Among the non-conserved residues are two, known to be involved with substrate binding in *Rc* XDH, E232 and R310. Leimkühler previously reported increased "aldehyde oxidase like" activity when substituting these residues with those found in mouse aldehyde oxidase (mAOX1) through structural alignment (E232V and R310M).[173]

Sequence alignment of PaoABC for these substrate interacting residues revealed L246 & T318 of PaoC as equivalent positions to E232 & R310 in *Rc* XDH and V806 & M884 in mAOX1. Structurally, *Ec* PaoABC L246 lies close to *Rc* XDH E232 while *Ec* PaoABC T318 is comparatively further apart from *Rc* XDH R310 (**Figure 29**).

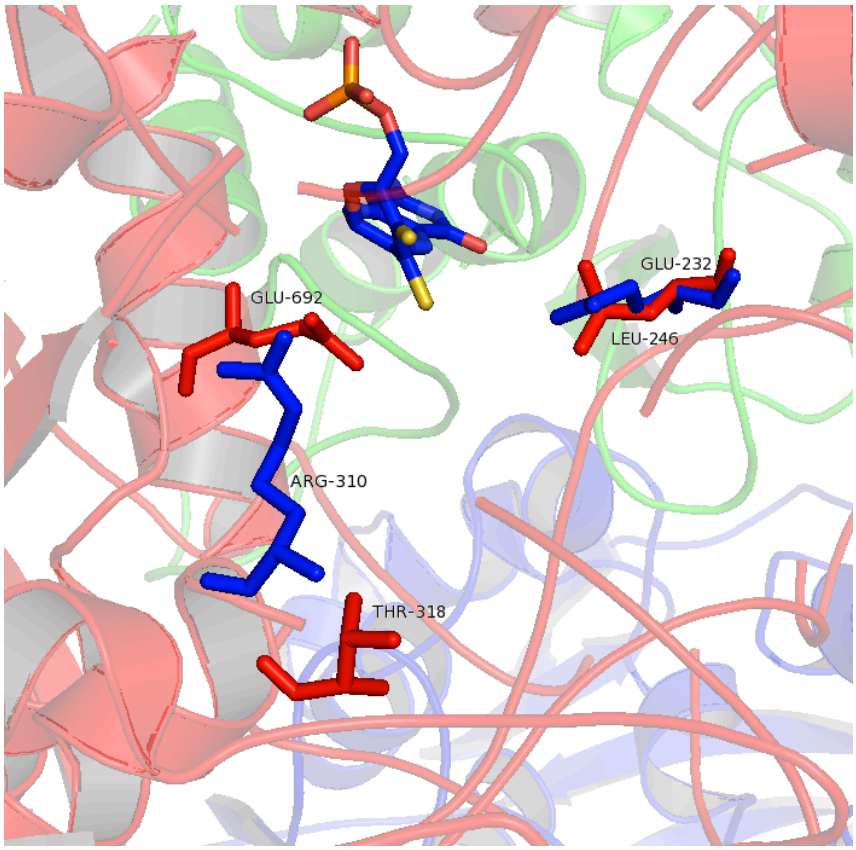

Figure 29 Structural overlay of substrate binding residues of *Ec* PaoABC (red) and *Rc* XDH (blue) using published crystal structures (*Ec* PaoABC PDB id: 5G5G, *Rc* XDH PDB id: 1JRO).[158,175]

Given the importance of analogous residues in other molybdenum enzymes we aimed to mutate these positions and directly analyse the effect of residue substitutions on the kinetics. This method bypassed the requirement for a solid phase assay, which proved problematic for DHIQ as a substrate.

Prior to saturation mutagenesis, we designed primers for site-specific mutations L246E, T318R and then made the double mutant L246E/T318R from the L246E mutant. Mutations were carried out using the "Quick Change II" mutagenesis kit from Agilent. Successful mutants were verified through sequencing of isolated plasmids by Eurofins Genomics (Ebersburg, Germany). PCR reactions were initially unsuccessful, attempts to remedy this included reducing the template concentrations (higher primer to template ratio) and altering the annealing temperature (in case of non-specific binding). The inclusion of 3 % DMSO as an additive in PCR reactions ultimately resulted in successful mutagenesis based on sequencing. DMSO is often used with GC rich sequences to destabilise secondary structure formation, which would otherwise interfere with PCR.

The single mutants and double mutant were then successfully expressed and purified in TP1000 *E. coli* before kinetic analysis (**Table 12**). Phenylacetaldehyde (PAA) and 3,4-dihydroisoquinoline (DHIQ) remained the substrates for aldehyde and imine screening due to existing PaoABC activity and a working procedure for kinetic analysis.

Table 12 Kinetic parameters of mutants for PaoABC PAA oxidation[a]

Enzyme	K_m (mM)	V_{max} (umol min^{-1} mg^{-1})	k_{cat} (min^{-1})	k_{cat}/K_m (min^{-1} mM^{-1})
WT	**5.4 x 10^{-2}**	**1.2**	**160**	**2900**
	(± 1.1 x 10^{-2})	(± 8.1 x 10^{-2})	(± 11)	(± 630)
L246E	**n.d.**	**n.d.**	**n.d.**	**n.d.**
T318R	**1.0 x 10^{-2}**	**0.22**	**31**	**3000**
	(± 2.3 x 10^{-3})	(± 5.4 x 10^{-3})	(± 0.70)	(± 670)
L246E/T318R	**2.5**	**0.66**	**90**	**37**
	(± 0.30)	(± 5.2 x 10^{-2})	(± 7.1)	(± 5.0)

[a]Reaction conditions: Readings made at 30 °C at 510 nm over 8 min. The rate of production of hydrogen peroxide was detected by HRP (microbial, Sigma) and 4-amino antipyrine / 2,4,6-tribromo-3-hydroxybenzoic acid dye (ε = 29400 L mol^{-1} cm^{-1}). Typically eight different substrate concentrations were examined (8 mM down to 0.0015 mM). n.d. = no absorbance detected

L246E had no detectable PAA activity while T318R lowered k_{cat} but almost completely retained PAA specificity. The double mutant had half the V_{max} and both K_m and k_{cat} were negatively affected. Mutations at these residues were clearly having a direct effect on the activity of the enzyme. Kinetic screens of the single and double mutants with DHIQ yielded no observable activity, so a saturation mutagenesis approach at the two residues was taken.

4.3. *Ec* PaoABC saturation mutagenesis

Saturation mutagenesis involves designing primers with degenerate codons at positions encoding residues to be mutated. Degenerate codons are designed with a mix of potential oligonucleotide combinations at a given position. Depending on the combinations of nucleobases employed, all 20 naturally occurring amino acids are

potentially available for substitution. Additionally, three termination codons exist (TAA, TAG, GTA), which encode for stopping protein synthesis. Adopting a partially degenerate codon such as NNK can mitigate the risk of introducing termination codons. This approach still allows potential access to all amino acids while reducing the chance of getting a termination codon by 3.

Table 13 Degenerate codon table

Degenerate codon	No. of codons	No. of amino acids	No. of stops	Amino acids encoded
NNN	64	20	3	All 20
NNK / NNS	32	20	1	All 20
NDT	12	12	0	RNDCGHILFSYV
DBK	18	12	0	ARCGILMFSTWV
NRT	8	8	0	RNDCGHSY

Zheng *et al*. developed a variation of saturation mutagenesis using the "QuickChange II" Agilent kit.[203] The strategy utilises primers with overlapping regions at the codon to be mutated. Primers were designed with overhanging regions (blue and yellow **Figure 30**) at opposite ends to minimise primer self-annealing seen in complementary primers. Degenerate primers with NNN containing codons at L246 and T318 were used.

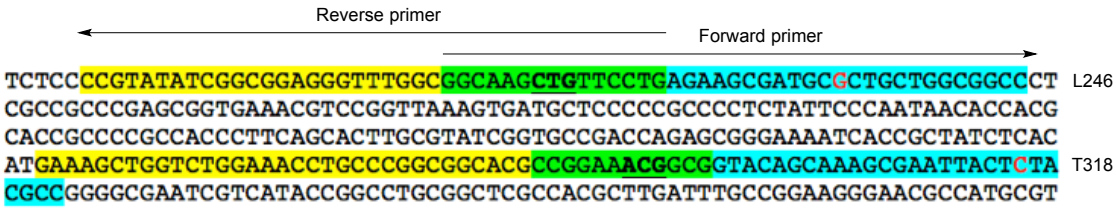

Figure 30 Template AA sequence of PaoC bold and underlined codons coding for L246 (CTG) and T318 (ACG) blue = forward primer, yellow = reverse primer, green = overlapping region, red base = controlled silent forward mutation

As outlined in the method, the primers contained an overhang of at least 8 residues in each direction in addition to a silent forward mutation to confirm successful mutation. The aim was to use this improved method of mutagenesis to efficiently generate mutants at L246 and T318. Following the described protocol, a 50 ng scale

mutagenesis PCR reaction was run, transforming the PCR product in XL-10 Gold ultracompetent cells. Following incubation the culture was plated onto LB agar resulting in no growth for either reaction. Following this, the PCR was attempted again using DMSO as an additive and using a greater volume of PCR product to transform. This also resulted in no growth. An additional attempt was made, increasing the number of cycles in the PCR, the template size (100 ng) and primer conc. (10x i.e. ~1 ug) also to no avail. Redesigned overhanging primers with NNKs instead of NNNs were explored with little improvement.

Having had little success with the overhanging strategy for generating a range of variants at L246 and T318, an additional kit advertised as more suited to saturation mutagenesis, the "Quick Change Multi" site directed mutagenesis kit (Agilent) was used. The protocol recommended the use of complementary primers, so primers containing NNKs were designed and PCR was run with the inclusion of 5 % DMSO. This approach was successful and generated approximately 60 individual colonies in total, which were sampled, cultured and purified in order to be identified by sequencing. The colonies sequenced contained several silent mutations, termination codons and repeats. 4 individual mutants for L246 and 6 for T318 were identified. These combined with the site-specific mutations covered multiple amino acid types (**Table 13**). Unfortunately only 25 % of the potentially available mutants were isolated. NNK degenerate codons would still have allowed for all 20 potential amino acid substitutions. This suggests mutagenesis was successful but there may have been problems with transformation efficiency.

Table 14 L246 and T318 mutants

AA type	L246 mutant	T318 mutant
Aliphatic	L246G	T318G
-	L246V	T318P
-	-	T318L
Acidic	L246E	T318E
Basic	L246H	T318R
Hydroxyl	L246S	T318S
Amide	-	T318N

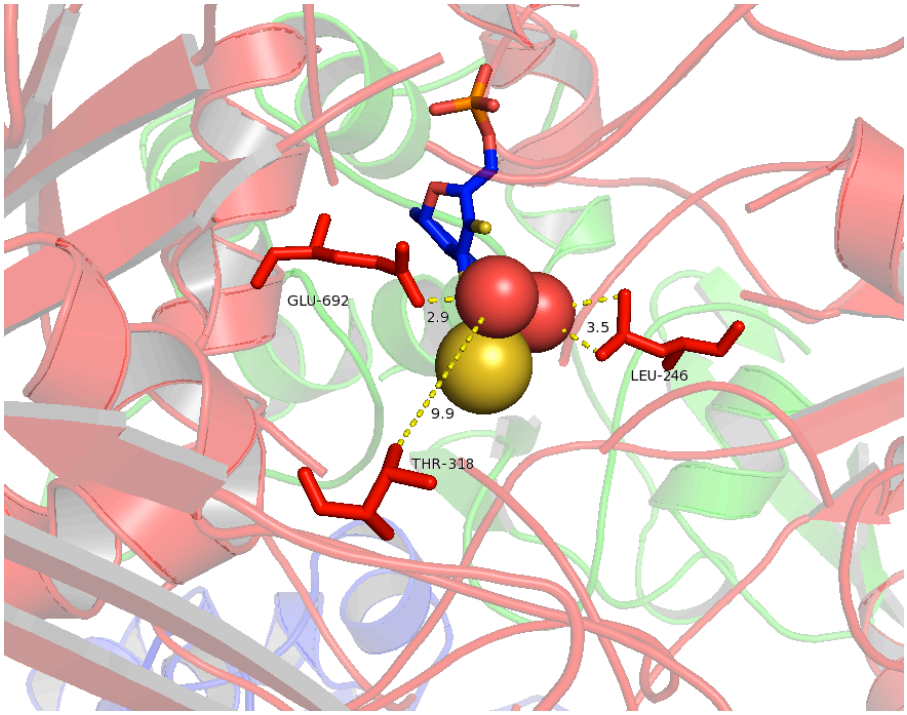

Figure 31 Positions of L246, T318 and key catalytic E692 in PaoABC crystal structure. Spheres represent the pterin-bound apical Mo=O and hydroxyl ligand (red), in addition to the Mo=S (yellow).[158]

L246 lies close to the Moco (3.5 Å), while T318 is further away (9.9 Å). Site-directed mutagenesis has demonstrated both positions have an effect on PaoABC activity, although whether this is a direct effect or through secondary interactions is unknown. Of the novel identified mutants, all were successfully expressed and purified except for T318N. Several attempts to express the protein were made with no visual indication of molybdenum present during purification (molybdenum containing enzymes have a characteristic bronze hue in solution). As the sole example of an amide containing mutation it is possible that T318N could have interfered with Moco insertion.

4.4. Kinetic evaluation of mutants

The kinetic assay using 4-aminoantipyrene and 2,4,6-tribromo-3-hydroxybenzoic acid was further utilised in the characterisation of saturation mutants.

4.4.1. PaoABC L246 mutant kinetics for phenylacetaldehyde (PAA)

Table 15 Kinetic parameters of PaoABC L246 saturation mutants for PAA oxidation[a]

Mutant	K_m (mM)	V_{max} (umol min^{-1} mg^{-1})	k_{cat} (min^{-1})	k_{cat}/K_m (min^{-1} mM^{-1})
WT PaoABC	**5.4×10^{-2}**	**1.2**	**160**	**290**
	(± 1.1×10^{-2})	(± 8.1×10^{-2})	(± 11)	(± 630)
L246G	**5.8×10^{-2}**	**4.8×10^{-2}**	**6.6**	**110**
	(± 9.6×10^{-3})	(± 2.1×10^{-3})	(± 0.30)	(± 19)
L246V	**5.1**	**1.0**	**140**	**27**
	(± 1.8)	(± 0.27)	(± 37)	(± 12)
L246H	**n.d.**	**n.d.**	**n.d.**	**n.d.**
L246S	**3.2**	**0.66**	**90**	**29**
	(± 0.75)	(± 0.11)	(± 15)	(± 8.0)

[a]Reaction conditions: Readings made at 30 °C at 510 nm over 8 min. The rate of production of hydrogen peroxide was detected by HRP (microbial, Sigma) and 4-amino antipyrine / 2,4,6-tribromo-3-hydroxybenzoic acid dye (ε = 29400 L mol^{-1} cm^{-1}). Typically eight different substrate concentrations were examined (8 mM down to 0.0015 mM). n.d. = no absorbance detected

L246H, a charged amino acid substitute was found to have no measurable activity with PAA, while each active mutation at L246 lowered the k_{cat}/K_m of PaoABC for PAA compared to the WT. L246V retained the majority of k_{cat} however this mutation also saw a marked increase in K_m. A similar outcome was observed for L246S, with a more pronounced drop in k_{cat}. L246G, another aliphatic substitution largely retained the K_m but lost almost all k_{cat}. No mutants had an improved V_{max}.

4.4.2. T318 mutant kinetics for phenylacetaldehyde (PAA)

Table 16 Kinetic parameters of PaoABC T318 saturation mutants for PAA oxidation[a]

Mutant	K_m (mM)	V_{max} (umol min^{-1} mg^{-1})	k_{cat} (min^{-1})	k_{cat}/K_m (min^{-1} mM^{-1})
WT	**5.4×10^{-2}** ($\pm 1.1 \times 10^{-2}$)	**1.2** ($\pm 8.1 \times 10^{-2}$)	**160** ($\pm$ 11)	**2900** ($\pm$ 630)
T318G	**2.9×10^{-2}** ($\pm 2.4 \times 10^{-3}$)	**0.20** ($\pm 2.8 \times 10^{-3}$)	**27** ($\pm$ 0.40)	**930** ($\pm$ 78)
T318P	**2.6×10^{-2}** ($\pm 2.4 \times 10^{-3}$)	**0.17** ($\pm 2.6 \times 10^{-3}$)	**24** ($\pm$ 0.40)	**900** ($\pm$ 85)
T318L	**2.5×10^{-2}** ($\pm 7.3 \times 10^{-3}$)	**0.11** ($\pm 6.1 \times 10^{-3}$)	**15** ($\pm$ 0.80)	**610** ($\pm$ 180)
T318E	**1.9×10^{-2}** ($\pm 1.4 \times 10^{-3}$)	**0.19** ($\pm 2.2 \times 10^{-3}$)	**15** ($\pm$ 0.30)	**610** ($\pm$ 180)
T318S	**1.8×10^{-2}** ($\pm 6.9 \times 10^{-3}$)	**0.14** ($\pm 8.7 \times 10^{-3}$)	**20** ($\pm$ 0.30)	**1100** ($\pm$ 430)

[a]Reaction conditions: Readings made at 30 °C at 510 nm over 8 min. The rate of production of hydrogen peroxide was detected by HRP (microbial, Sigma) and 4-amino antipyrine / 2,4,6-tribromo-3-hydroxybenzoic acid dye (ε = 29400 L mol^{-1} cm^{-1}). Typically eight different substrate concentrations were examined (8 mM down to 0.0015 mM).

In comparison to L246, T318 mutations had a lesser effect on PAA k_{cat}/K_m although activity (k_{cat}) was significantly reduced. The lower specificity observed could be in relation to the increased distance from the active site compared to L246. The hydroxyl moiety in T318 may be playing a significant catalytic role through hydrogen bonding, similarly to R440 in *E. coli* XDH. Interestingly the activity was not retained for the similar serine side chain in T318S and no improvement in k_{cat} was observed in any of the other mutations at T318. Every mutant displayed a reduction in K_m.

4.4.3. L246 mutant kinetics for 3,4-dihydroisoquinoline (DHIQ)

Saturation mutants were additionally assayed for DHIQ activity similarly to the site-specific mutants to look for a variant with improved imine oxidase activity.

Table 17 Kinetic parameters of PaoABC L246 saturation mutants for DHIQ oxidation[a]

Mutant	K_m (mM)	V_{max} (umol min^{-1} mg^{-1})	k_{cat} (min^{-1})	k_{cat}/K_m (min^{-1} mM^{-1})
E. coli XDH	**3.2** (± 0.40)	**5.5 x 10^{-2}** (± 3.1 x 10^{-3})	**7.5** (± 0.40)	**2.3** (± 0.33)
WT PaoABC	**1.6** (± 0.26)	**9.1 x 10^{-4}** (± 5.4 x 10^{-5})	**0.12** (± 7.3 x 10^{-3})	**0.08** (± 0.01)
L246G	**0.24** (± 4.7 x 10^{-2})	**3.9 x 10^{-3}** (± 2.9 x 10^{-4})	**0.54** (± 3.9 x 10^{-2})	**2.2** (± 0.47)
L246V	**n.d.**	**n.d.**	**n.d.**	**n.d.**
L246E	**n.d.**	**n.d.**	**n.d.**	**n.d.**
L246H	**n.d.**	**n.d.**	**n.d.**	**n.d.**
L246S	**0.22** (± 3.4 x 10^{-2})	**1.8 x 10^{-3}** (± 8.5 x 10^{-5})	**0.25** (± 1.2 x 10^{-2})	**1.1** (± 0.18)

[a]Reaction conditions: Readings made at 30 °C at 510 nm over 24 min. The rate of production of hydrogen peroxide was detected by HRP (microbial, Sigma) and 4-amino antipyrine / 2,4,6-tribromo-3-hydroxybenzoic acid dye (ε = 29400 L mol^{-1} cm^{-1}). Typically eight different substrate concentrations were examined (8 mM down to 0.02 mM). n.d. = no absorbance detected.

A general observation as previously noted pertains to the rate of DHIQ oxidations. The kinetic assay was run for triple the length of time compared with PAA (24 min vs 8 min). Valine, glutamic acid and histidine substitutions were all inactive, while L246G is a very interesting mutant. It has 6 times lower K_m, 4 times greater V_{max}, 4.5 times faster k_{cat} and consequently a 28-fold improvement in specificity for DHIQ. This is comparable to *Ec* XDH and suggests a switch in substrate specificity. Glycine substitution at L246 may provide improved steric freedom for DHIQ to bind to the active site. There may also be other interactions that leucine was previously obstructing.

The other active mutant, L246S has a comparable K_m to L246G and improved V_{max}, k_{cat} and k_{cat}/K_m compared to WT PaoABC.

4.4.4. T318 mutant kinetics for 3,4-dihydroisoquinoline (DHIQ)

Table 18 Kinetic parameters of PaoABC T318 saturation mutants for DHIQ oxidation[a]

Mutant	K_m (mM)	V_{max} (umol min^{-1} mg^{-1})	k_{cat} (min^{-1})	k_{cat}/K_m (min^{-1} mM^{-1})
E. coli XDH	**3.2** (± 0.40)	**5.5 x 10^{-2}** (± 3.1 x 10^{-3})	**7.5** (± 0.42)	**2.3** (± 0.33)
WT	**1.6** (± 0.26)	**9.1 x 10^{-4}** (± 5.4 x 10^{-5})	**0.12** (± 7.3 x 10^{-3})	**0.08** (± 0.01)
T318G	**2.3** (± 0.35)	**6.9 x 10^{-4}** (± 3.9 x 10^{-5})	**0.090** (± 5.3 x 10^{-3})	**0.04** (± 6.5 x 10^{-3})
T318P	**3.7** (± 1.2)	**9.9 x 10^{-4}** (± 1.5 x 10^{-4})	**0.13** (± 2.0 x 10^{-2})	**0.04** (± 0.01)
T318L	**n.d.**	**n.d.**	**n.d.**	**n.d.**
T318E	**2.7** (± 0.93)	**9.8 x 10^{-4}** (± 1.8 x 10^{-5})	**0.13** (± 2.4 x 10^{-2})	**0.05** (± 0.01)
T318S	**4.1** (± 0.57)	**9.9 x 10^{-4}** (± 6.5 x 10^{-5})	**0.13** (± 2.1 x 10^{-2})	**0.03** (± 5.0 x 10^{-3})

[a]Reaction conditions: Readings made at 30 °C at 510 nm over 24 min. The rate of production of hydrogen peroxide was detected by HRP (microbial, Sigma) and 4-amino antipyrine / 2,4,6-Tribromo-3-hydroxybenzoic acid dye (ε = 29400 L mol^{-1} cm^{-1}). Typically eight different substrates concentrations were examined (8 mM down to 0.02 mM). n.d. = no absorbance detected.

In contrast to L246 mutants where kinetic values were measured for DHIQ, all mutations at T318 had higher K_m values and much lower specificity toward DHIQ. All mutantations similarly lowered k_{cat} compared to WT PaoABC.

4.5 Conclusion

A site-directed mutagenesis method has been used to produce *Ec* PaoABC mutants L246E, T318R and L246E/T318R in an inverse approach to Leimkühler's "XOR to AO" activity mutations. Kinetics revealed a distinct drop in k_{cat}/K_m for mutants compared with the WT. Unfortunately, the equivalent increase in DHIQ activity was not observed in the mutants. This may be in part due to differences in the protein's substrate binding area, particularly with respect to lack of aromatic stabilising residues and tight binding channel.[158] Despite the lack of imine activity, the drastic change in kinetics suggested L246 and T318 play a significant role in enzyme activity.

In order to screen a range of substitutions at these positions, a saturation mutagenesis approach was undertaken and successfully implemented after a number of experimental hurdles were overcome. Examples of aliphatic, acidic, basic and hydroxyl amino acid substitutions were introduced at both positions. None of the mutations improved substrate specificity for PAA, since variants had reduced k_{cat} and higher K_m.

L246G and L246S, the only mutants active with DHIQ both displayed much less substrate specificity for PAA compared with the WT. Our best example, L246G exhibited a switch in substrate specificity by having 26-fold less k_{cat}/K_m for PAA than the WT, while having 28-fold greater k_{cat}/K_m for DHIQ compared with the WT. This result in particular is exciting, as the specificity is almost that of xanthine dehydrogenase. Additionally, the other active mutant L246S obtained suggests potential for further improvement of PaoABC for imine oxidation.

Further work should aim to explore the rest of the potential amino acid substitutions at both positions (i.e. aromatic, amide or sulphur containing residues) in addition to screening other cyclic amines/imines.

Chapter 5

5. Experimental Section

5.1. Chemical Experimental

5.1.1. Chemicals

Unless stated otherwise, all reagents were commercially available. Solvents for extraction and FCC were technical grade. Reported solvent mixtures for both TLC and FCC were volume/volume mixtures. Solvents were analytical or HPLC grade and purchased dried over molecular sieves where necessary.

5.1.2. Analytical methods

Analytical thin layer chromatography (TLC) was performed on Whatman F254 precoated silica gel plates (250 μm thickness). Visualization was accomplished with a UV light and/or a KMnO4 solution. Flash column chromatography (FCC) was performed using Whatman Silica Gel 60Å (230-400 mesh). Normal and reverse phase HPLC was performed on an Agilent system (Santa Clara, CA, USA) equipped with a G1379A degasser, G1312A binary pump, a G1329 well plate autosampler unit, a G1315B diode array detector and a G1316A temperature controlled column compartment. The University of Liverpool analytical services department provided Mass spectrometry. ^{1}H NMR and ^{13}C NMR were recorded on Bruker AV 500 MHz & Bruker DPX 400 MHz NMR spectrometers in the indicated deuterated solvents. For ^{1}H NMR $CDCl_3$ was set to 7.26 ppm ($CDCl_3$ singlet) and for ^{13}C NMR to 77.66 ppm ($CDCl_3$ centre of triplet). All values for ^{1}H NMR and ^{13}C NMR chemical shifts for deuterated solvents were obtained from Cambridge Isotope Labs. Data are reported in the following order: chemical shift in ppm (δ), integration, (multiplicity, which are indicated by br (broadened), s (singlet), d (doublet), t (triplet), q (quartet), m (multiplet)) and coupling constants (*J*, Hz).

5.2. General Biology Experimental

5.2.1. Enzymes and competent cells

E. coli XDH (sold as xanthine oxidase, microbial), *Bovine* milk xanthine oxidase, catalase and horseradish peroxidase were purchased from Sigma-Aldrich. MAO-N D9 was kindly provided by Professor N. Turner, Manchester Institute of Biotechnology, University of Manchester. PaoABC, XDH E232V and competent *E. coli* TP1000 cells were kindly provided by Professor S. Leimkühler, Institute of Biochemistry and Biology, University of Potsdam. The *E. coli* TP1000 mutant strain used for WT/mutant PaoABC and XDH E232V expression is a derivative of MC4100 with a kanamycin cassette inserted in the *mobAB* gene region.[191] Ultracompetent cells used for PaoABC mutant cloning include XL 10-Gold and XL 1-Blue, purchased from Agilent Technologies and used according to the manufacturers instructions.

5.2.2. DNA and protein methods

5.2.2.1. Plasmids

All PaoABC plasmids were isolated from bacterial cultures using a commercial plasmid mini-prep kit (Qiagen). Plasmids for XDH variant E232V (pSL207) and PaoABC (pMN100) were provided pre-cloned, using a pTrcHis vector (Invitrogen) with a His6-tag fused to the N-terminus of XDHA and PaoA subunits for affinity purification. WT and mutant PaoABC plasmids in addition to XDH E232V were transformed into *E. coli* TP1000 (Δ*mobAB*) competent cells. DNA mutagenesis was performed using a Prime Gradient thermal cycler (Techne) and PCR products were transformed into cloning strains XL 10-Gold or XL 1-Blue ultracompetent cells (Agilent Technologies). Primer synthesis for mutagenesis reactions and plasmid sequencing were performed by Eurofins Genomics (Ebersburg, Germany).

5.2.2.2. Cultures and protein expression

Bacterial colonies were grown on LB agar (Miller) containing 100 μg / ml ampicillin and 50 μg / ml kanamycin at 37 °C for 18 h in a static incubator. Cultures for plasmid isolation were prepared from a single colony using 5 ml LB broth (Miller) containing 100 μg / ml ampicillin and grown for 18 h at 37 °C with shaking at 250 RPM. Starter cultures for protein expression were prepared by single colony (TP1000 x PaoABC or XDH E232V) inoculation of 50 ml of LB (Miller) containing 100 μg / ml ampicillin, supplemented with 1 mM sodium molybdate and 10 μM isopropyl thio-β-$_D$-galactoside

(IPTG). Starter cultures were incubated in non-baffled flasks in a static incubator at 37 °C for 48 h. Main cultures were inoculated using 1 ml of starter culture in 500 ml LB (Miller) with 1 mM sodium molybdate and 10 μM IPTG. XDH E232V was grown for 24 h at 30 °C with shaking at 130 RPM, while PaoABC was grown for 24 h at 22 °C with shaking at 120 RPM. Cells were spun down and stored as pellets at -80 °C.

5.2.2.3. Protein purification

Cell pellets were thawed and resuspended in phosphate buffer (0.1 M, pH 7.6) containing 300 mM NaCl and 10 mM imidazole. DNase I (1 U / ml lysate) was added and cell lysis was performed by sonication (20 s on, 20 s off x20 cycles) using a Soniprep 150 plus (MSE UK Ltd.). Cell debris was removed by centrifugation at 17000 G for 30 minutes. The lysate was loaded onto a HisTrap 1mL FastFlow affinity column (GE Healthcare) and the column washed with 10 mL resuspension buffer containing 20 mM imidazole. The protein was then eluted using 2 ml resuspension buffer containing 0.3 M imidazole and buffer exchanged into Tris-HCl (50 mM, pH 7.5) containing 1 mM ethylenediaminetetraacetic acid (EDTA) using a PD-10 Sephadex column (GE Healthcare). Purified protein was quantified spectrophotometrically using a NanoDrop Lite (Thermo Fisher Scientific, USA). Purity was analysed by SDS-PAGE using pre-cast Tris/glycine 4 – 20% Tris-Hepes gel, (NuSep) stained with “Instant Blue” (Expedion).

5.2.2.4. Kinetics

The initial rates were followed on a TECAN Spark 10M spectrophotometer at 30 °C and 510 nm. A 1:1 ratio was assumed in the oxidation of substrate : production of hydrogen peroxide. The rate of production of hydrogen peroxide was detected by HRP (microbial, Sigma) and 4-amino antipyrine / 2,4,6-tribromo-3-hydroxybenzoic acid dye (ε = 29400 L mol^{-1} cm^{-1}). The dye was made up by adding 100 µl 4-amino antipyrine (100 mg / mL) and 30 µL (20 mg / mL) 2,4,6-tribromo-3-hydroxybenzoic acid to 10 mL of pH 8.0 potassium phosphate buffer. Substrates were dissolved in DMF to 0.5 M then diluted in buffer. Typically eight different substrate concentrations were examined (8 mM down to 0.0015 mM). HRP was dissolved in 0.1 M potassium phosphate buffer, pH 8.0, to give 1.4 mg / mL concentration. To a 96 well plate 50 µL HRP, 50 µL dye and 33 µL purified enzyme (typically 0.025 – 1 mg / mL) were added. The assay was started by adding 67 µL substrate. Rate was measured in triplicate and plotted against substrate concentration and V_{max} and K_M The kinetic parameters, k_{cat} and K_M, were calculated by using curve-fitting software Sigma Plot kinetics module (Systat Software Inc.) to fit the data to the Michaelis-Menten equation $V_{max}.[S]/K_M+[S]$. The errors represent the 95% confidence interval of the variance in the fit.

5.2.2.5. PAA background correction

Blank samples for PAA assays were run and background absorbance was removed. This allowed for accurate determination of kinetics in improved mutants while correcting perceived activity in poor mutants.

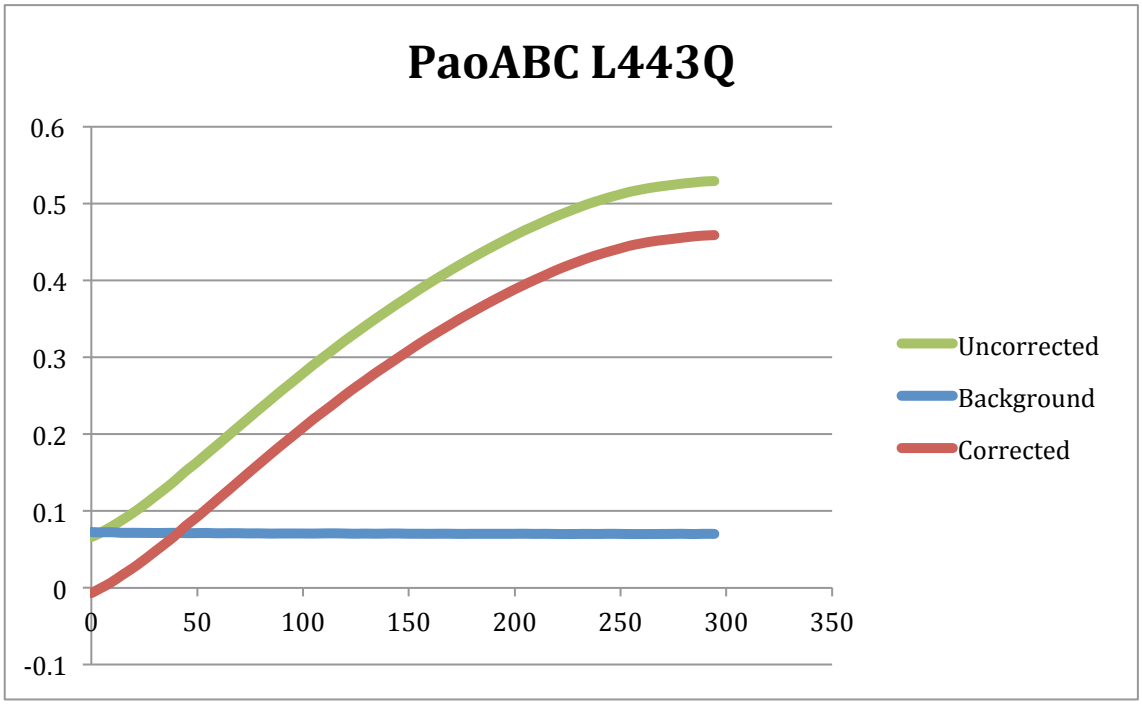

Figure 32 L443Q background PAA correction

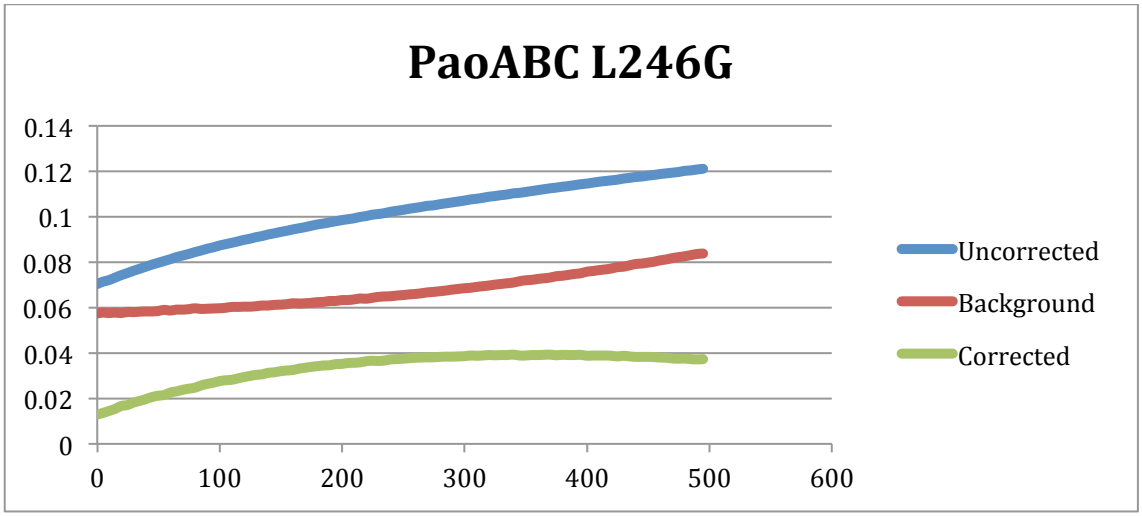

Figure 33 L246G background PAA correction

5.3. Chapter 2 Experimental

5.3.1. General HPLC

Table 18 Imine substrate retention times and conditions

Entry	Substrate	Retention Time (Min)	Conditions
1	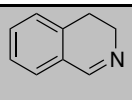	5.1	A
2	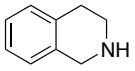	5.7	A
3	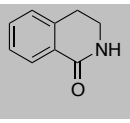	9.1	A
4	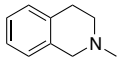	5.1	A
5	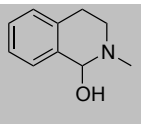	8.1	A
6	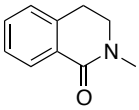	9.4	A
7	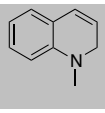	5.3	A
8	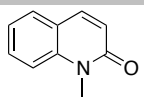	11.4	A
9	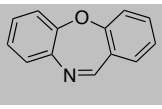	12.2	A
10	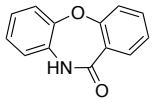	9.7	A
11	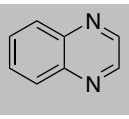	4.3	B
12	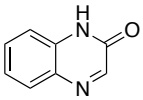	2.9	B
13	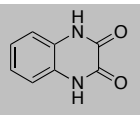	2.4	B

Column conditions – A: Normal phase Diacel OJ-H chiral column, 90:10 hexane:isopropyl alcohol, 1 ml/min UV 230 nm. B: Reverse phase Thermo Fischer Scientific C-18 column, 70:30 deionised water (containing 0.1 % trifluoroacetic acid): Acetonitrile 1 ml/min UV 254 nm.

5.3.2. General Biotransformation Procedures

General procedure for imine/iminium biotransformations (10 mM) using *Rc* XDH E232V

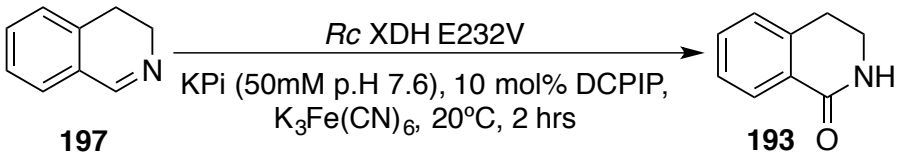

To an Eppendorf tube, the substrate in DMF (3 µl, 1 M), potassium ferricyanide (30 µl, 10 mM), dichloroindophenol (30 µl, 10 mM) xanthine dehydrogenase mutant E232V (33 µl, 1 mg/ml) in potassium phosphate buffer (50 mM, pH 7.6) catalase (100 µl, 3.3 mg/ml, pH 7.6) and potassium phosphate buffer (117 µl, 50 mM, pH 7.6) were added. The Eppendorf was then incubated at 37 °C and shaken with extractions taken as necessary. The reaction mixture/extracts were extracted with dichloromethane and analysed via HPLC on a Diacel OJH chiral column HPLC (conditions: 10% IPA / hexane, 1 ml/min at 230 nm).

General procedure for imine/iminium biotransformations (10 mM) using *Ec* XDH

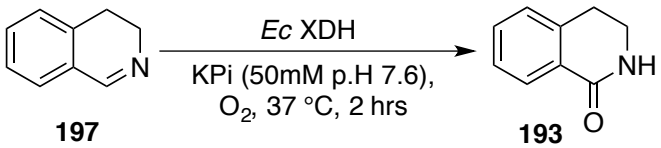

To an Eppendorf tube, the substrate in DMF (3 µl, 1 M), *Ec* XDH (33 µl, 1.1 mg/ml) in potassium phosphate buffer (50 mM, pH 7.6), catalase (100 µl, 3 mg/ml, pH 7.6) and potassium phosphate buffer (147 µl, 50 mM, pH 7.6) were added. The Eppendorf was then incubated for required time at 37 °C and shaken with extractions taken as necessary. The reaction mixture/extracts was extracted with dichloromethane and analysed via HPLC on a Diacel OJH column (conditions: 10% IPA / hexane, 1 ml/min at 230 nm).

General procedure for MAO-N D9 / *Ec* XDH cascades (1-10 mM)

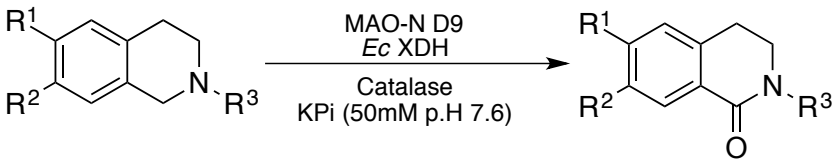

191: R^1 = H, R^2 = H, R^3 = H
192: R^1 = NO_2, R^2 = H, R^3 = Me
201: R^1 = H, R^2 = H, R^3 = Me
202: R^1 = OMe, R^2 = OMe, R^3 = H

193: R^1 = H, R^2 = H, R^3 = H
194: R^1 = NO_2, R^2 = H, R^3 = Me
203: R^1 = H, R^2 = H, R^3 = Me
204: R^1 = OMe, R^2 = OMe, R^3 = H

To an Eppendorf tube, the substrate in DMF (3 µl, 1 M), MAO-N D9 (30 µl, 14 mg/ml) xanthine oxidase (100 µl, 1.1 mg/ml) in potassium phosphate buffer (50 mM, pH 7.6), catalase (100 µl, 3 mg/ml pH 7.6) and potassium phosphate buffer (67 µl, 50 mM, pH 7.6) were added. The Eppendorf tube was then incubated for the required time at 37 °C and shaken. The reaction mixture was extracted with dichloromethane and analysed via HPLC (conditions: 10% IPA / hexane, 1 ml/min at 230 nm).

General procedure for MAO-N D9 / *Rc* XDH E232V cascades (1 mM)

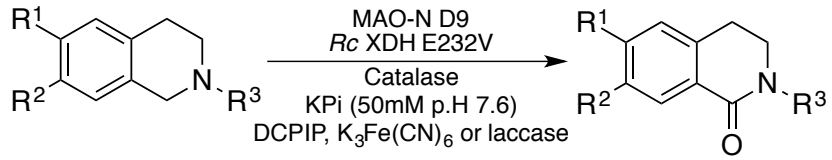

192: R^1 = NO_2, R^2 = H, R^3 = Me
201: R^1 = H, R^2 = H, R^3 = Me

194: R^1 = NO_2, R^2 = H, R^3 = Me
203: R^1 = H, R^2 = H, R^3 = Me

To an Eppendorf tube, the substrate in DMF (0.3 µl, 1M), MAO-N D9 (50 µl, 14 mg/ml), XDH E232V (33 µl, 1 mg/ml) in potassium phosphate buffer (50 mM, pH 7.6), potassium ferricyanide (30 µl, 10 mM) or laccase (1.5 U), dichloroindophenol (30 µl, 10 mM) catalase (100 µl, 3 mg/ml pH 7.6) and potassium phosphate buffer (127 µl, 50 mM, pH 7.6) were added. The Eppendorf tube was then incubated for the required time at 37 °C and shaken. The reaction mixture was extracted with dichloromethane and analysed via HPLC on a Diacel OJH column (conditions: 10% IPA / hexane, 1 ml/min at 230 nm).

5.3.4. Chemical synthesis

Synthesis of ethyl (2-phenylethyl)carbamate

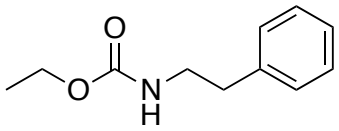

200

To a solution of phenethylamine (2.5 ml, 20.0 mmol) and triethylamine (3 ml, 22.0 mmol, 1.1 equiv) in DMF (75 ml), ethyl chloroformate (1.7 ml, 22.0 mmol, 1.1 equiv) was slowly added at 0 °C with stirring for 1 hr. Water (250 ml) was added, and the whole was extracted with ethyl acetate (3 x 50 ml). The organic phase was washed with brine and dried with magnesium sulfate before evaporating the solvent *in vacuo*. The crude oil was purified via column chromatography using 20% ethyl acetate / n-hexane to give a clear oil (3.03 g, 85 %). NMR ^{1}H (400 MHz, $CDCl_3$) δ 7.32-7.18 (5 H, m, Ar-*H*), 4.71 (1 H, s (br), N*H*), 4.13-4.07 (2 H, q, *J* = 7 Hz, CH_2), 3.46-3.41 (2 H, t, *J* = 7 Hz, CH_2), 2.82-2.79 (2 H, t, *J* = 7 Hz, CH_2), 1.24-1.20 (3 H, t, *J* = 7 Hz, CH_3). ^{13}C (100 MHz, $CDCl_3$) δ 156.6, 138.8, 128.8, 128.6, 126.5 60.7, 42.1, 36.2, 14.6. *m/z* 194 ($[M+H]^+$, 100).

Synthesis of 3,4-dihydroisoquinolin-1(2*H*)-one

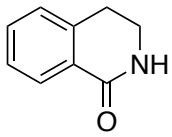

193

To phenethylcarbamic acid ethyl ester (344 ul, 2.04 mmol), trifluoromethanesulfonic acid (9 ml, 101.7 mmol, 50 equiv) was slowly added at 0 °C. The reaction mixture was heated to 70 °C with stirring for 24 hr. The whole was then poured into ice water (200 ml) and extracted with dichloromethane (3 X 100 ml). The organic phase was washed with brine and dried over sodium sulfate. Following evaporation of the solvent *in vacuo* the crude residue was purified via column chromatography using 50% ethyl acetate / n-hexane to give a pale residue (197.5 mg, 64 %). NMR ^{1}H (400 MHz, $CDCl_3$) δ 8.08-8.06 (1 H, d, *J* = 8 Hz, Ar-*H*) 7.47-7.43 (1 H, t, *J* = 7 Hz, Ar-*H*), 7.37-7.33 (1 H, t, *J* = 7 Hz, Ar-*H*) 7.23-7.21 (1 H, d, *J* = 8 Hz, Ar-*H*), 7.49 (1 H, s, N*H*), 3.60-3.56 (2 H, td, *J* =

7, 3 Hz, CH_2), 3.01-2.09 (2 H, t, J = 7 Hz, CH_2). ^{13}C (100 MHz, $CDCl_3$) δ 166.6, 138.9, 132.1, 129.0, 127.9, 127.3, 127.1, 40.2, 28.3. *m/z* 148 ([M+H]$^+$, 100).

Synthesis of 2-methyl-3,4-dihydroisoquinolinium iodide

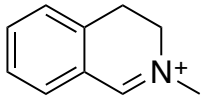

205 I^-

3,4-dihydroisoquinoline (100 mg, 0.76 mmol) was dissolved in acetone (10 ml) and an excess of iodomethane (60 ul) was added. The mixture was left to stir overnight at room temperature, after which the solvent was evaporated *in vacuo* to give a yellow solid (157 mg, 75 %). NMR ^{1}H (400 MHz, $CDCl_3$) δ 10.03 (1 H, s, C*H*), 8.05-8.04 (1 H, d, J = 8 Hz, aromatic), 7.72-7.68 (1 H, t, J = 8 Hz, Ar-*H*), 7.47-7.43 (1 H, t, J = 8 Hz, Ar-*H*), 7.37-7.35 (1 H, d, J = 8 Hz, Ar-*H*), 4.14-4.10 (2 H, t, J = 8 Hz, CH_2), 4.02 (3 H, s, CH_3), 3.42-3.38 (2 H, t, J = 8 Hz, CH_2). ^{13}C (101 MHz, $CDCl_3$) δ 166.6, 138.0, 135.6, 134.4, 128.6, 128.3, 124.5, 51.0, 48.7, 25.4. *m/z* 274 ([M+H]$^+$, 30).

Synthesis of 2-methyl-1,2,3,4-tetrahydroisoquinoline

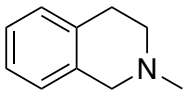

201

2-methyl-3,4-dihydroisoquinoline (147.1 mg, 1 mmol) was dissolved in methanol (10 ml). To this, sodium borohydride (73.5 mg, 2 equivalents) was added and the solution was stirred at room temperature for 2 hours after which, the methanol was evaporated *in vacuo*. The resulting residue was extracted with water and diethyl ether, dried over magnesium sulfate and evaporated *in vacuo* to give a yellow oil (56 mg, 38 %). NMR ^{1}H (400 MHz, $CDCl_3$) δ 7.13-7.09 (3 H, m, Ar-*H*), 7.02-7.00, (1 H, m, Ar-*H*), 3.58 (2 H, s, CH_2), 2.94-2.91 (2 H, t, J = 6 Hz, CH_2), 2.74-2.67 (2 H, t, J = 6 Hz, CH_2), 2.46 (3 H, s, CH_3). ^{13}C NMR (101 MHz, $CDCl_3$) δ 134.7, 133.8, 128.7, 126.4, 126.1, 125.6, 58.0, 52.9, 46.2, 29.2. *m/z* 148 ([M+H]$^+$, 100).

Synthesis of 2-methyl-3,4-dihydroisoquinolin-1(2*H*)-one

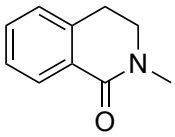

203

2-methyl-3,4-dihydroisoquinolinium iodide (100 mg, 0.4 mmol) was dissolved in DMSO (3.7 ml), to which concentrated hydrochloric acid (0.53 ml) was added. The solution was left to stir for an hour at room temperature. 3 M sodium hydroxide (3 ml) was added and the solution was worked up with distilled water and diethyl ether before being purified by column chromatography (2 % methanol/dichloromethane) to give a residue (14.8 mg, 25 %). NMR ^{1}H (400 MHz, $CDCl_3$) δ 8.09-8.07 (1H, d, *J* = 8 Hz, Ar-*H*), 7.42-7.38 (1H, t, *J* = 8 Hz, Ar-*H*), 7.35-7.31 (1H, t, *J* = 8 Hz, Ar-*H*), 7.17-7.15 (1H, d, *J* = 8 Hz, Ar-*H*), 3.58-3.55 (2H, t, *J* = 7 Hz, CH_2), 3.15 (3H, s, CH_3) 3.02-2.99 (2H, t, *J* = 7 Hz, CH_2). ^{13}C NMR (101 MHz, $CDCl_3$) δ 164.8, 138.0, 131.5, 129.4, 128.1, 127.0, 126.9, 48.1, 35.2, 27.9. *m/z* 162 ($[M+H]^+$, 100).

Synthesis of 2-methyl-1,2,3,4-tetrahydroisoquinolin-1-ol

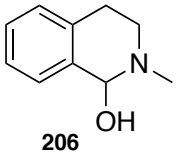

206

N-Methyl-tetrahydroisoquinolinium iodide (100 mg, was dissolved in dichloromethane (3 ml) and stirred for 15 min and cold NaOH (3 ml, 3 M) was added and left to stir at room temperature for 2 hours. The turbid reaction was extracted using dichloromethane and water. Following drying over $MgSO_4$, the dichloromethane was removed *in vacuo* to give an oil. (21 mg, 36 %). NMR ^{1}H (400 MHz, CD_2Cl_2) δ 7.37-7.33 (1H, m, Ar-*H*), 7.20-7.16 (2H, m, Ar-*H*), 7.07-7.04 (1H, m, Ar-*H*), 4.86 (1H, s, C*H*), 4.23 (1H, s (br), O*H*), 3.02-2.97 (1H, m, *H*CH), 2.80-2.77 (2H, t, *J* = 6 Hz, CH_2), 2.61-2.56 (1H, m, HC*H*), 2.36 (3H, s, CH_3). ^{13}C NMR (101 MHz, CD_2Cl_2) δ 138.0, 135.1, 128.6, 128.2, 128.0, 126.3, 85.5, 46.8, 41.2, 28.8. *m/z* 130 ([M – H_2O + CH_3], 100),

Synthesis of N-Me quinolinium iodide

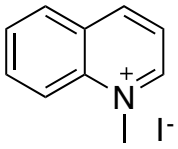

207

Quinoline (1 g, 0.77 mmol) was dissolved in acetone (50 ml) and an excess of iodomethane (2 ml) was added. The mixture was left to stir overnight at room temperature, after which the solvent was evaporated *in vacuo* and the resulting brown solid was filtered and washed with cold hexane to give a yellow solid (1.29 g, 61 %). NMR ^{1}H (400 MHz, DMSO) δ 9.53-9.51 (1H, dd, *J* = 6, 1 Hz, Ar-*H*), 9.30-9.29 (1H, d, *J* = 8 Hz, Ar-*H*), 8.54-8.52 (1H, dd, *J* = 9, 1 Hz, Ar-*H*), 8.51-8.49 (1H, dd, *J* = 8, 1 Hz, Ar-*H*), 8.32-8.29 (1H, td, *J* = 8, 2 Hz, Ar-*H*), 8.20-8.17 (1H, dd, *J* = 8, 6 Hz, Ar-*H*), 8.09-8.06 (1H, td, *J* = 8, 1 Hz, Ar-*H*), 4.65 (3H, s, C*H*$_3$). ^{13}C NMR (101 MHz, DMSO) δ 150.7, 147.5, 138.8, 135.9, 130.8, 130.4, 129.7, 122.5, 119.6, 45.9. *m/z* 258 ([M – CH_3], 2), 130 ([M – I + CH_3]$^+$).

Synthesis of 1-methylquinolin-2(1H)-one

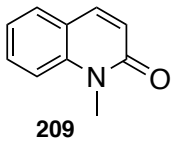

209

1-methyl-quinolinium iodide (100 mg, 0.4 mmol) was dissolved in DMSO (4 ml), to which concentrated hydrochloric acid (0.5 ml) was added. The solution was left to stir for an hour at room temperature. 3 M sodium hydroxide (3 ml) was added and the solution was worked up with distilled water and diethyl ether before being purified by column chromatography (2 % methanol/dichloromethane) to give a residue (14.8 mg, 25 %). NMR ^{1}H (400 MHz, $CDCl_3$) δ 7.69-7.67 (1H, d, *J* = 9 Hz, Ar-*H*), 7.59-7.56 (2H, m, Ar-*H*), 7.39-7.37 (1H, dd, *J* = 8, 1 Hz, Ar-*H*), 7.26-7.23 (1H, td, *J* = 8, 1 Hz, Ar-*H*), 6.73-6.71 (1H, d, *J* = 9 Hz, Ar-*H*), 3.15 (3H, s, C*H*$_3$). ^{13}C NMR (101 MHz, $CDCl_3$) δ 164.8, 138.0, 131.5, 129.4, 128.1, 127.0, 126.9, 48.1, 35.2, 27.9. *m/z* 160 ([M+H]$^+$, 100).

Synthesis of dibenzo[*b*,*f*][1,4]oxazepine

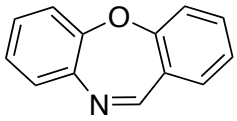

208

2-Fluorobenzaldehyde (105 ul, 1 mmol), 2-aminophenol (120 mg, 1.1 mmol), polyethylene glycol (2 ml) and potassium carbonate (138 mg, 1.1 mmol) were added to a round bottom flask and heated at 100 °C overnight. After work up with dichloromethane and water the crude product was purified via flash column chromatography (10 % hexane/ethyl acetate) to give an orange solid (136 mg, 70 %). NMR ^{1}H (400 MHz, $CDCl_3$) δ 8.53 (1H, s, NC*H*), 7.50-7.46 (1H, td, *J* = 8, 2 Hz, Ar-*H*), 7.40-7.37 (2H, td, *J* = 8, 2 Hz, Ar-*H*), 7.27-7.19 (3H, m, Ar-*H*), 7.18-7.15 (2H, td, *J* = 9, 2 Hz, Ar-*H*), ^{13}C NMR (101 MHz, $CDCl_3$) δ 160.6, 160.5, 152.7, 140.5, 133.4, 130.1, 129.3, 128.8, 127.4, 125.7, 125.1, 121.4, 120.7. *m/z* 196 ($[M+H]^+$, 100).

Synthesis of dibenzo[*b*,*f*]oxazepine lactam

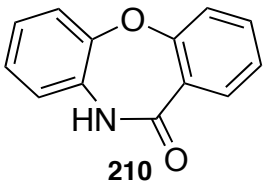

210

Dibenzo[*b*,*f*][1,4]oxazepine (200 mg, 1 mM) was stirred overnight at room temperature in a solution of acetic acid (1.8 ml) and hydrogen peroxide (0.6 ml). The reaction was diluted with brine and extracted with chloroform (3 x 25 ml), the extracts were dried over sodium sulfate and concentrated before purification *via* flash column chromatography (30% EtOAc/Hexane) to furnish a white solid (21.3 mg, 10%) NMR ^{1}H (400 MHz, $CDCl_3$) δ 8.48 (1H, s, N*H*), 7.99-7.97 (1H, dd, 8, 2 Hz, Ar-*H*), 7.57-7.53 (1H. td, *J* = 8, 2 Hz, Ar-*H*), 7.30-7.28 (3H, m, Ar-*H*), 7.17-7.15 (2H, m, Ar-*H*), 7.10-7.08 (1H, m, Ar-*H*). ^{13}C NMR (101 MHz, $CDCl_3$) δ 167.6, 159.8, 151.1, 134.6, 132.1, 130.7, 126.1, 126.0, 125.4, 125.2, 121.8, 121.4, 121.0. *m/z* 212 ($[M+H]^+$, 100).

Syntheisis of 1,4-dihydroquinoxaline-2,3-dione

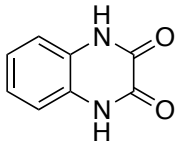

217

Quinoxaline (65 mg, 0.5 mM) was dissolved in a 3:1 mixture of MeCN/H_2O (11 ml and 4 ml). To this, [Bis(trifluoroacetoxy)iodo]benzene (237 mg, 0.5 mM) was added and the reaction was left to stir overnight at room temperature. The reaction mixture was then concentrated under vacuum and filtered; washing with water, MeCN and diethyl ether to give a brown solid (7 mg, 9 %). NMR ^{1}H (400 MHz, $CDCl_3$) δ 11.91 (2H, s, N-*H*), 7.14-7.07 (4H, aromatic, Ar-*H*). ^{13}C NMR (101 MHz, $CDCl_3$) δ 155.7, 126.1, 123.6, 115.7. *m/z* 163 ($[M+H]^+$, 100).

5.3.5. NMR UV absorbance calibration

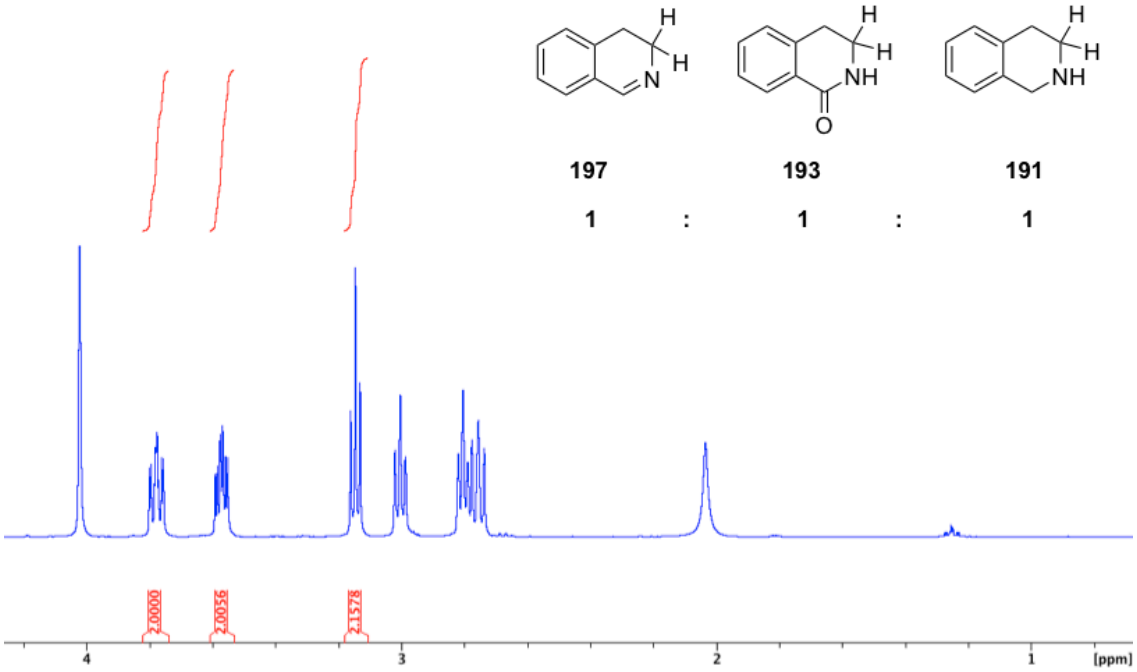

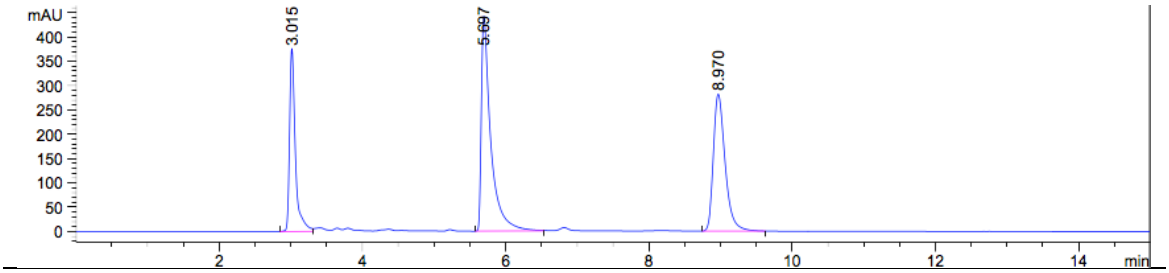

Peak	Retention time (min)	Area (%)	Calibration (x)
Imine **197**	3.02	22.5	1.93
Amine **201**	5.70	43.1	1.00
Amide **203**	9.00	34.3	1.26

Figure 34 Calibration of HPLC response for ca. 1:1:1 of **197**:**201**:**203** (-CH_2 triplets) by NMR. HPLC conditions: Diacel OJ-H column; 1.0 mL/min; UV 230 nm; eluent = hexane/iPrOH 90:10.

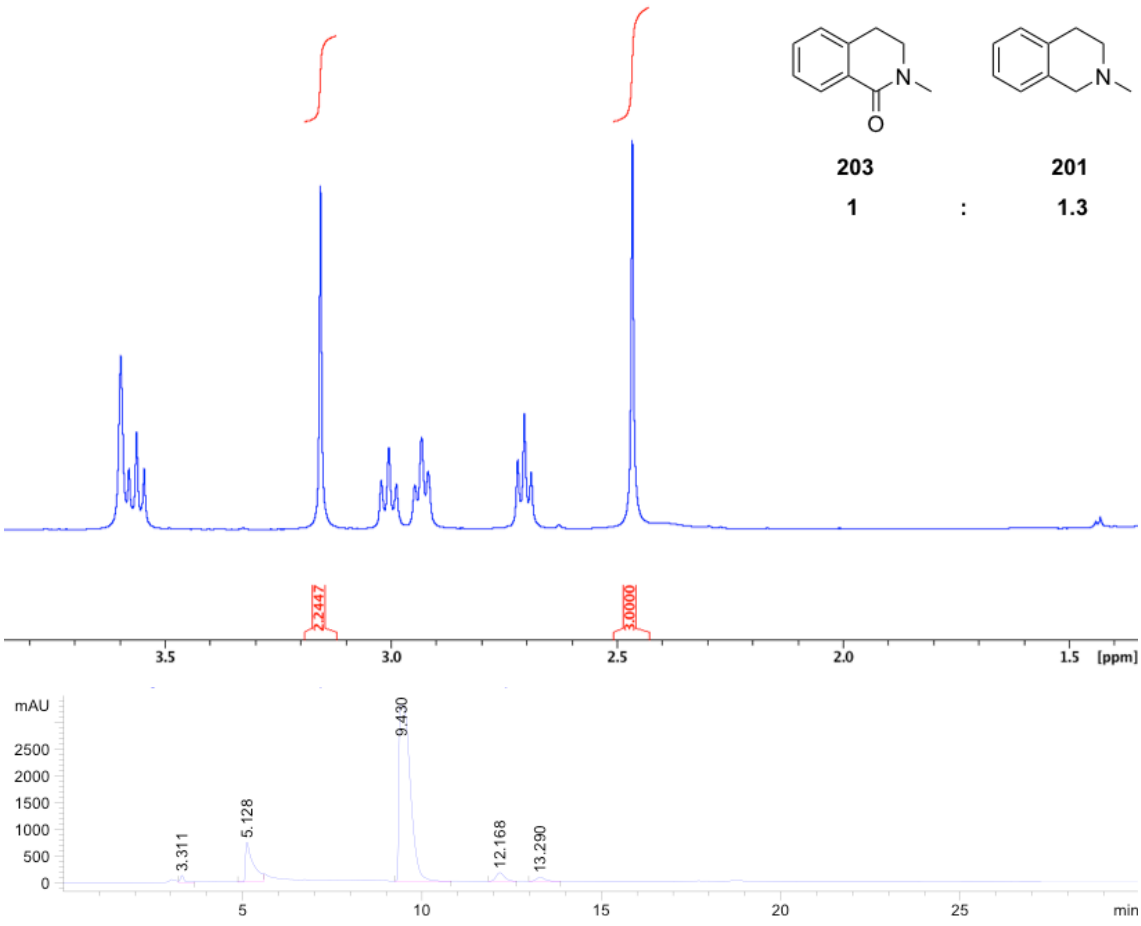

Peak	Retention time (min)	Corrected Area (%)	Calibration (x)
Amine **201**	5.13	14.0	6.14
Amide **203**	9.43	86.0	1.00

Figure 35 Calibration of HPLC response for ca. 1:1 of **196**:**198** (-NCH_3 singlets) by NMR. HPLC conditions: Diacel OJ-H column; 1.0 mL/min; UV 230 nm; eluent= hexane/iPrOH 90:10.

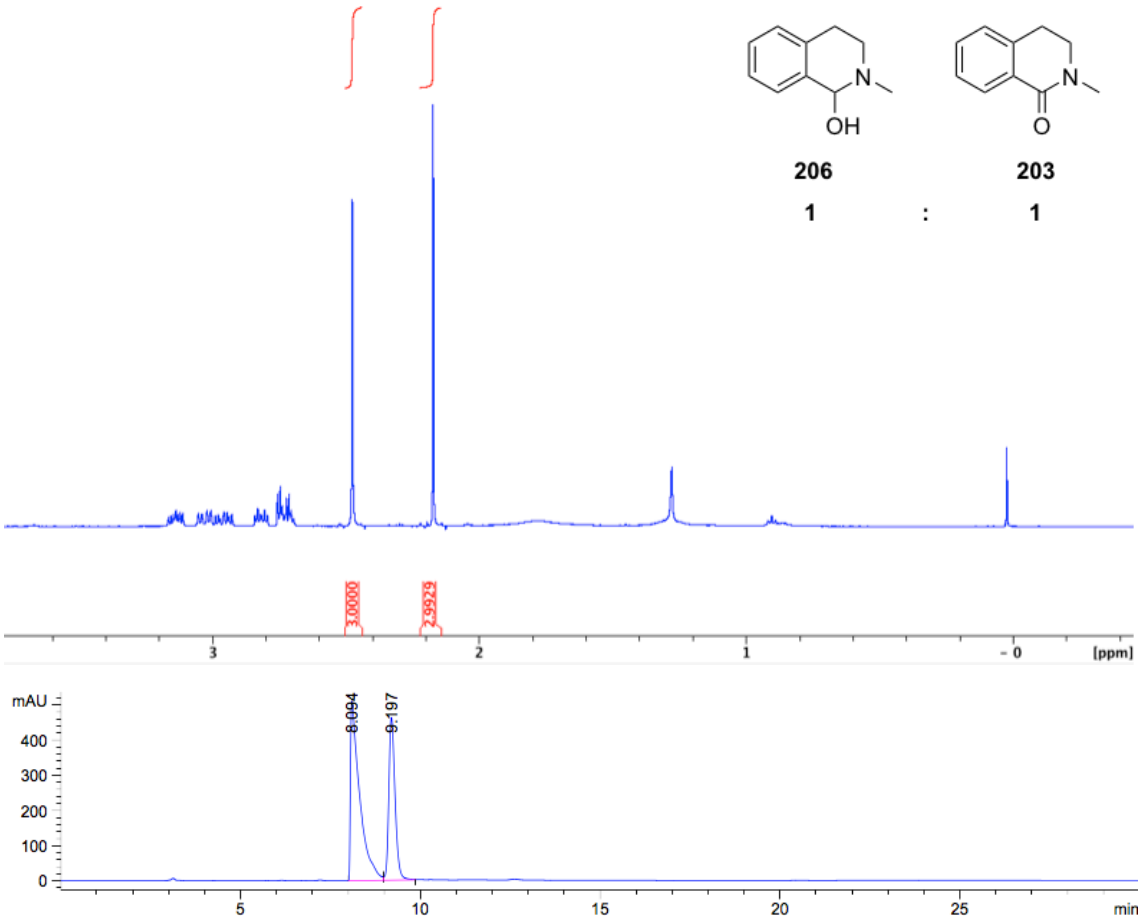

Peak	Retention time (min)	Area (%)	Calibration (x)
Hydroxyl **206**	8.09	62.2	1.00
Amide **203**	9.20	37.8	1.65

Figure 36 Calibration of HPLC response for ca. 1:1 of **201**:**198** (-NCH_3 singlets) by NMR. HPLC conditions: Diacel OJ-H column; 1.0 mL/min; UV 230 nm; eluent= hexane/iPrOH 90:10.

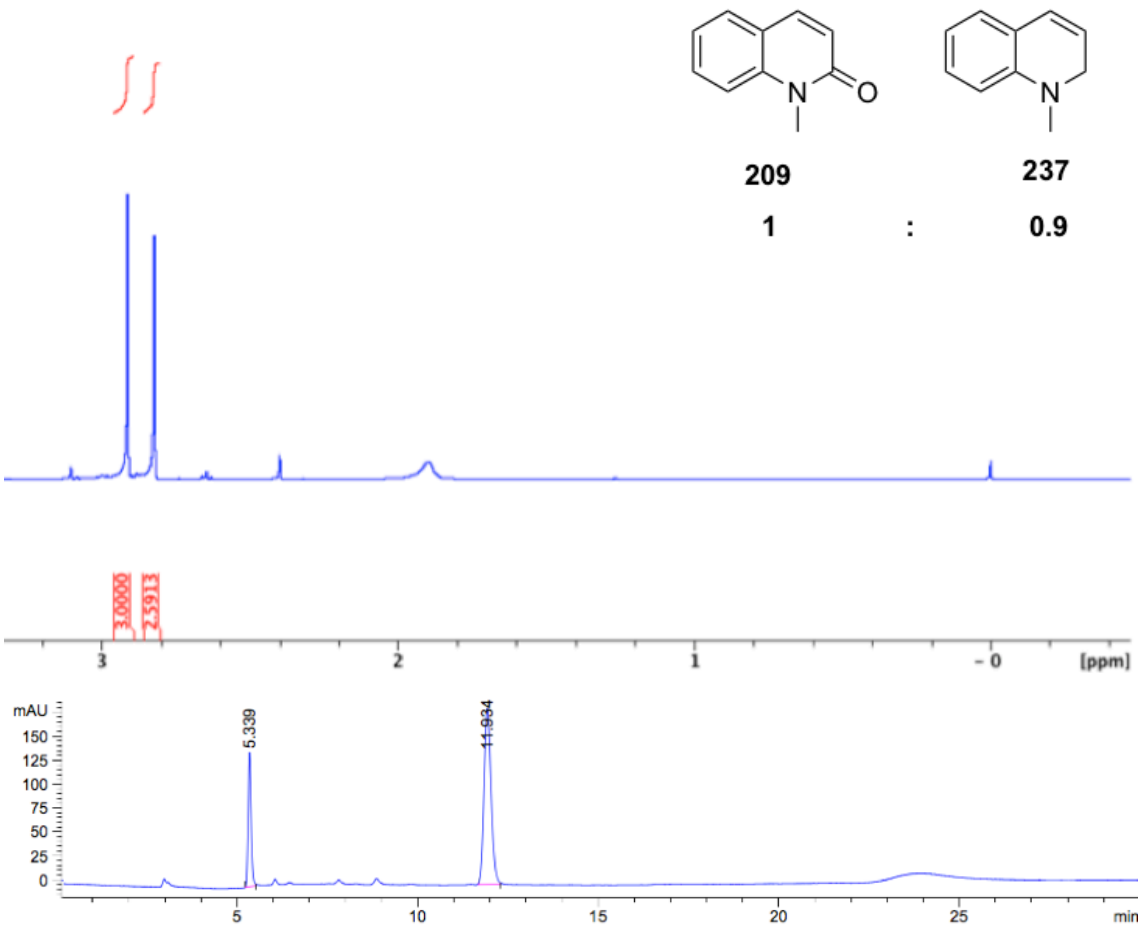

Peak	Retention time (min)	Corrected Area (%)	Calibration (x)
Amine **237**	5.3	28.2	2.55
Amide **209**	11.9	71.8	1.00

Figure 37 Calibration of HPLC response for ca. 1:1 of **237**:**209** (-NCH_3 singlets) by NMR. HPLC conditions: Diacel OJ-H column; 1.0 mL/min; UV 230 nm; eluent= hexane/iPrOH 90:10.

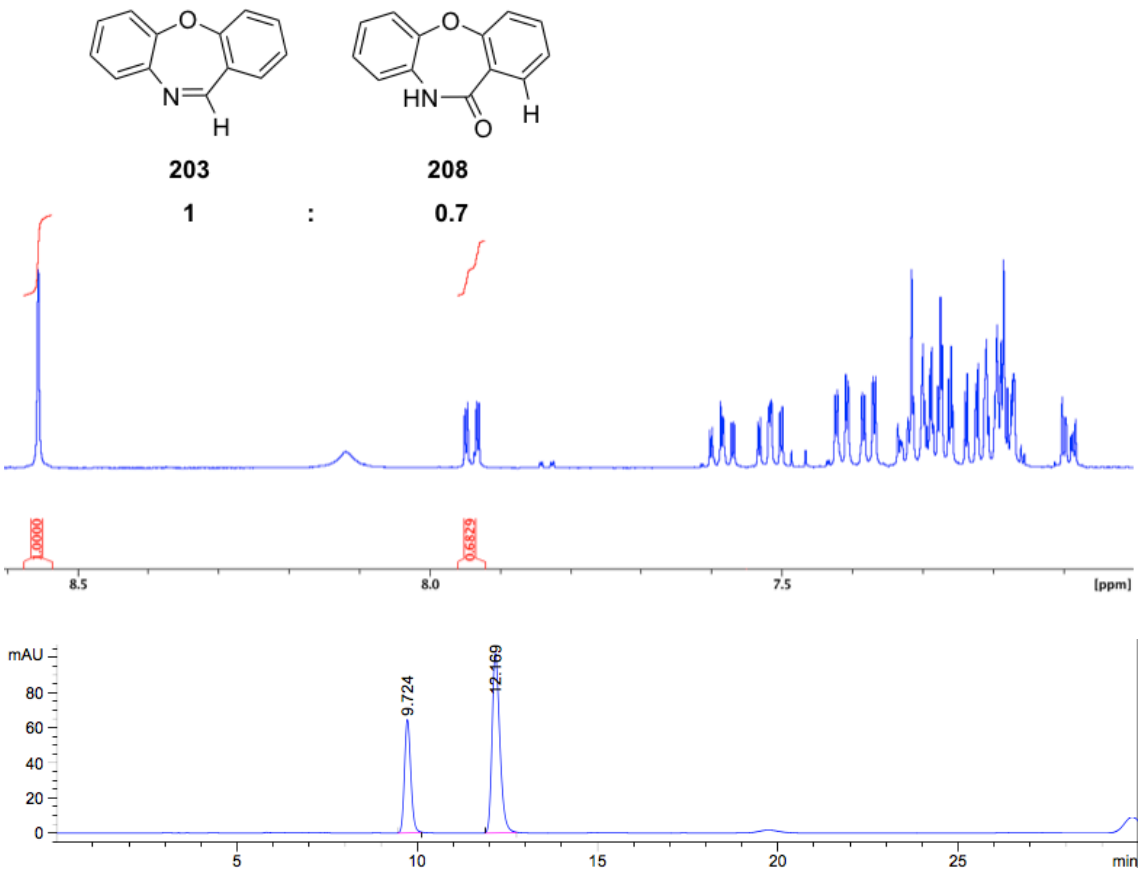

Peak	Retention time (min)	CorrectedArea (%)	Calibration (x)
Imine **203**	12.2	51.7	1.00
Amide **208**	9.7	48.3	1.07

Figure 38 Calibration of HPLC response for ca. 1:1 of **203**:**208** (-CH singlet) by NMR. HPLC conditions: Diacel OJ-H column; 1.0 mL/min; UV 230 nm; eluent= hexane/iPrOH 90:10.

5.3.6. Bicyclic imine screen with XORs

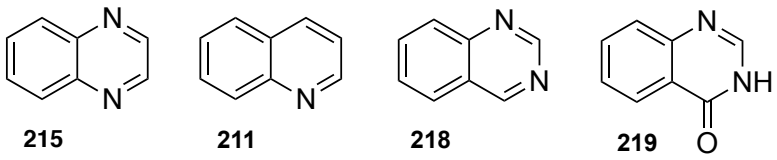

To an Eppendorf tube, the substrate in DMF (10 µl, 1 M), XOR (100 µl, 1 mg/ml) in potassium phosphate buffer (100 mM, pH 8), catalase (100 µl, 3 mg/ml pH 8) and potassium phosphate buffer (798 µl, 100 mM, pH 8) were added. In the case of *Rc* XDH E232V potassium phosphate buffer (598 µl, 100 mM, pH 8), potassium ferricyanide (100 µl, 10 mM), DCPIP (100 µl, 10 mM). The Eppendorf tube was then incubated for the required time at 37 °C and shaken. The reaction mixture was centrifuged, filtred and analysed via RP-HPLC (**215**) Thermo Fischer Scientific C-18 column, 70:30 deionised water (containing 0.1 % trifluoroacetic acid): Acetonitrile UV 254 nm. NMR in DMSO-d6 compared **211**, **218** and **219** with authentic standards (Appendix).

5.4. Chapter 3 Experimental

5.4.1. Libraries

Libraries were made by designing primers at the selected regions of the Moco containing PaoC subunit (residue 184 - 458) and following the protocol from the "GeneMorph II EZclone Domain Mutagenesis Kit" (Agilent Technolgies).

5.4.1.1. Mutant megaprimer synthesis

Forward primer = 5'-GCG GTG AAG ATT GAT GCT AC-3'.
Reverse primer = 5'-CCA ATG TCG GTC ATG TCC G-3'.

The PCR reaction was made up of the following: 10x Mutazyme II reaction buffer (5 µl), PaoABC template plasmid (4.4 µl, 235 ng/µl), forward primer (1 µl, 125 ng/µl), reverse primer (1 µl, 125 ng/µl), dNTP mix (1 µl, 40 mM), Mutazyme II DNA polymerase (1 µl, 2.5 U/µl) and dH_2O (37.6 µl). The following thermal cycle program was used.

Table 19 Megaprimer PCR program

Segment	Number of cycles	Temperature (° C)	Duration
1	30	95	30 sec
		55	30 sec
		72	1 min
2	1	72	10 min

The megaprimer was isolated through agarose gel electrophoresis and purified by excising the band and using a DNA purification kit from Agilent.

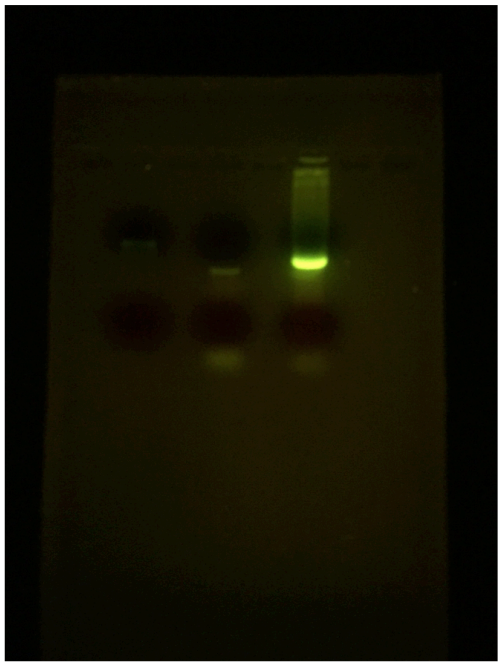

Figure 39 Agarose gel containing megaprimer band

5.4.1.2. Mega primer cloning reaction

The PCR reaction was made up of the following: 2x EZClone enzyme mix (25 µl), PaoABC template plasmid (2.1 µl, 23.5 ng/µl), megaprimer (22 µl, 11.36 ng/µl) and EZClone solution (3 µl). The following thermal cycle program was used.

Table 20 cloning PCR program

Segment	Number of cycles	Temperature (° C)	Duration
1	1	95	1 min
2	25	95	50 sec
		60	50 sec
		78	17 min

DPN I restriction enzyme (1 µl) was added to PCR products and incubated at 37 °C for 2 h following mixing and centrifugation (1 min, 5000 RPM). The mixture (1.5 µl) was added to an aliquot (45 µl) of thawed XL10-Gold ultra competent cells. The cells were left on ice for 30 min and heat-pulsed (42 °C 30 seconds). Transformed cells were incubated in NZY^+ broth for an hour prior to plating on Highbond-N membranes.

5.4.2. Solid phase screen

The solid phase screen was used both to screen libraries and to confirm isolated mutants for activity. *E. coli* TP1000 (Δ*mobAB*) was transformed with either a library, the wildtype or a single/double mutant. The transformation reaction was plated on a membrane (HyBond-N) on LB containing 100 µg / mL ampicillin, 1 mM IPTG and grown / induced overnight at 37 °C after which membranes were kept frozen at -20 °C until use. Membranes were freeze-thawed three times (using liquid N_2) before being placed on filter paper containing 0.14 mg / mL Horse-radish peroxidase (HRP) (Sigma) in pH 8.0, 0.1 M potassium phosphate buffer. The membranes were left at room temperature for 1 hour. This ensured removal of any cellular H_2O_2. The membrane was the transferred to another filter paper containing a solution of 0.1 mg / mL HRP, 3,3'-Diaminobenzidine (DAB) (1 tablet per 15 mL, SigmaFast, Sigma) or 4-chloronapthol (4-CN) 16.8 mM, and 1-20 mM substrate. Colonies which turned dark red (DAB) / dark blue (4-CN) indicated oxidation of the substrate. For screening a panel of conditions, the membrane was cut into smaller pieces and each piece placed on a filter paper.

5.4.3 Synthesis of acyclic imines

5.4.3.1 Synthesis of 2-[(*E*)-(benzylimino)methyl]phenol

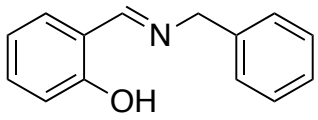

234

Salicaldehyde (4.3 ml, 40.1 mM) and benzylamine (3.7 ml, 40.1 mM) were added to DCM (20 ml) and molecular sieves. Stirring overnight followed by filtration and removal of solvent afforded a white solid (2.66 g, 31 %) NMR ^{1}H (500 MHz, CD_2Cl_2) δ 14.30 (1H, s, OH) 8.47 (1H, s, *H*C=N) 7.38-7.27 (7H, m, Ar-*H*), 6.92-6.88 (2H, m, Ar-*H*), 4.80 (2H, s CH_2). ^{13}C NMR (101 MHz, $CDCl_3$) δ 165.7, 161.2, 138.3, 132.5, 131.5, 132.5, 128.8, 127.9, 127.5, 119.0, 118.7, 117.2, 63.3. *m/z* 212 ($[M+H]^+$, 100).

5.4.3.2. Synthesis of *N*-[(*E*)-(4-methoxyphenyl)methylidene]-1-phenylmethanamine

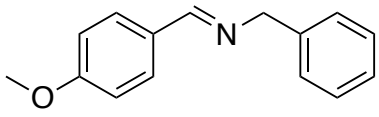

235

4-methoxybenzaldehyde (4.5 ml, 36.6 mmol) and benzylamine (3.8 ml, 36.6 mM) were added to DCM (20 ml) and molecular sieves. Stirring overnight followed by filtration and removal of solvent afforded a white solid (0.68 g, 8 %) NMR ^{1}H (500 MHz, CD_2Cl_2) δ 8.33 (1H, s, *H*C=N), 7.72-7.70 (2H, d, *J*= 8 Hz, Ar-*H*), 7.37-7.36 (4H, m, Ar-*H*), 7.30-7.27 (1H, m, Ar-*H*), 6.96-6.92 (2H, d, *J* = 8 Hz, Ar-*H*), 4.74 (2H, s, N-CH_2), 3.83 (3H, s, CH_3). ^{13}C NMR (101 MHz, $CDCl_3$) δ 139.6, 129.9, 129.2, 128.5, 127.9, 126.9, 114.0, 65.0, 55.4. *m/z* 226 ($[M+H]^+$, 100).

5.4.3.3. Synthesis of (1*E*)-*N*-methoxy-2-phenylethanimine

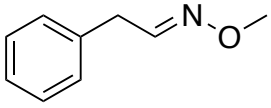

236

Phenylacetaldehyde (0.48 ml, 4 mM), methoxyamine hydrochloride (0.35 mg, 4 mM)

and triethylamine (0.58 ml, 4 mM) were added to DCM (20 ml) and molecular sieves. Stirring overnight followed by filtration and removal of solvent afforded a white solid (142 mg, 25 %). NMR ^{1}H (500 MHz, CD_2Cl_2) Rotamers E/Z 55/45 δ 7.45-7.43 (1H, t, *J* = 7 Hz, C-*H*), 7.32-7.29 (4H, m, Ar-*H*), 7.25-7.20 (6H, m, Ar-*H*), 6.78-6.76 (1H, t, *J* = 6 Hz, C-*H*), 3.94 (3H, s, CH_3), 3.86 (3H, s, CH_3), 3.67 (2H, d, *J* = 6 Hz, CH_2), 3.52 (2H, d, *J* = 7 Hz, CH_2). ^{13}C NMR (101 MHz, $CDCl_3$) δ 149.7, 149.2, 136.9, 136.4, 128.8, 126.9, 126.6, 61.8, 61.4, 35.9, 32.3. *m/z* 150 ([M+H]$^+$, 100).

5.4.4. Acyclic 224 imine transformation with *Ec* PaoABC

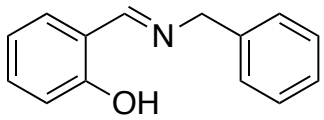

234

To an Eppendorf tube, **234** in DMF (3 µl, 1 M), PaoABC (33 µl, 3 mg/ml) in potassium phosphate buffer (100 mM, pH 8), catalase (100 µl, 3 mg/ml pH 8) and potassium phosphate buffer (164 µl, 100 mM, pH 8) were added. The Eppendorf tube was then incubated for 5 h at 37 °C and shaken. The reaction mixture was centrifuged, filtred and analysed via RP-HPLC conditions: Thermo Fischer Scientific C-18 column, 70:30 deionised water (containing 0.1 % trifluoroacetic acid): Acetonitrile UV 254 nm.

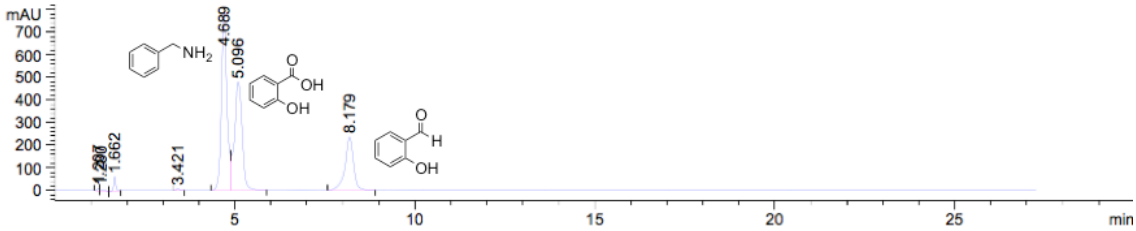

Figure 40 RP-HPLC of **224** and PaoABC

5.5. Chapter 4 Experimental

5.5.1. Site directed mutagenesis

Site directed mutations were made by designing primers with the required mutations at the appropriate regions following instructions from the "QuickChange II Site-Directed Mutagenesis Kit" (Agilent Technologies).

L246E

Forward primer = 5'-GAG GGT TTG GCG GCA AGG AAT TCC TGA GAA GCG ATG C-3'

Reverse primer = 5'-GCA TCG CTT CTC AGG AAT TCC TTG CCG CCA AAC CCT C-3'.

T318R

Forward primer = 5'-CCT GCC CGG CGG CAC GCC GGA AAG GGC GGT ACA GC-3'

Reverse Primer = 5'-GCT GTA CCG CCC TTT CCG GCG TGC CGC CGG GCA GG-3'

The PCR reactions for L246E and T318R were made up of the following: 10x reaction buffer (5 µl), PaoABC template plasmid (2 µl, 25 ng/µl), forward primer (1 µl, 125 ng/µl), reverse primer (1 µl, 125 ng/µl), dNTP mix (1 µl), *PfuUltra* HF DNA polymerase (1 µl, 2.5 U/µl), DMSO (3 µl) and dH_2O (36 µl). The following thermal cycle program was used.

Table 21 Site-directed mutagenesis PCR program

Segment	Number of cycles	Temperature (° C)	Duration
1	1	95	30 sec
2	25	95	30 sec
		55	1 min
		68	8.6 min

The double mutant was produced by substituting the WT template for purified L246E plasmid using T318R primers.

DPN I restriction enzyme (1 µl) was added to PCR products and incubated at 37 °C for 2 h following mixing and centrifugation (1 min, 5000 RPM). The mixture (1.5 µl) was added to an aliquot (45 µl) of thawed XL10-Gold ultra competent cells. The cells were left on ice for 30 min and heat-pulsed (42 °C 30 seconds). Transformed cells were incubated in NZY^+ broth for an hour prior to plating on Highbond-N membranes.

5.5.2. Saturation mutagenesis

Site saturation libraries were produced by designing primers with degenerate codons at the L246 and T318 positions of the Moco containing PaoC subunit and following the protocol from the "QuickChange II Multi Site-Directed Mutagenesis Kit" (Agilent Technolgies).

L246

Forward primer = 5'-GTT TGG CGG CAA GNN KTT CCT GAG AAG CGA TGC CCT GCT GGC GGC C-3'

Reverse primer = 5'-CTT CTC AGG AAM NNC TTG CCG CCA AAC CCT CCG CCG ATA TAC GG-3'

T318

Forward primer = 5'-CCC GGC GGC ACG CCG GAA NNK GCG GTA CAG CAA AG-3'

Reverse primer = 5'-CTT TGC TGT ACC GCM NNT TCC GGC GTG CCGCCG GG-3'

The PCR reactions for L246 and T318 saturation mutagenesis were made up of the following: 10x QuickChange multi reaction buffer (10 µl), PaoABC template plasmid (1 µl, 325 ng/µl), QuickSolution (0.5 µl) forward primer (1 µl, 125 ng/µl), reverse primer (1 µl, 125 ng/µl), dNTP mix (1 µl), QuickChange multi enzyme blend (1 µl) and DMSO (5 µl) dH_2O (79 µl). The following thermal cycle program was used.

Table 22 Saturation mutagenesis PCR program

Segment	Number of cycles	Temperature (° C)	Duration
1	1	95	1 min
2	30	95	1 min
		55	1 min
		65	17.2 min

DPN I restriction enzyme (2 µl) was added to PCR products and incubated at 37 °C for 3 h following mixing and centrifugation (1 min, 5000 RPM). The mixture (1.5 µl) was added to an aliquot (45 µl) of thawed XL10-Gold ultra competent cells. The cells were left on ice for 30 min and heat-pulsed (42 °C 30 seconds). Transformed cells were incubated in NZY^+ broth for an hour prior to plating on Highbond-N membrane.

References

[1] R. S. Varma, *Green Chem.,* **2014**, *16*, 2027–15.
[2] R. A. Sheldon, *Green Chem.,* **2007**, *9*, 1273–12.
[3] R. A. Sheldon, *Green Chem.,* **2014**, *16*, 950–963.
[4] M. T. Reetz, *J. Am. Chem. Soc.,* **2013**, *135*, 12480–12496.
[5] U. T. Bornscheuer, G. W. Huisman, R. J. Kazlauskas, S. Lutz, J. C. Moore, K. Robins, *Nature.,* **2012**, *485*, 185–194.
[6] J. A. Linthorst, *Found Chem.,* **2009**, *12*, 55–68.
[7] M. L. Burnett, *Environ Manage.,* **1998**, *22*, 213–224.
[8] P. T. Anastas, J. C. Warner, *Green Chemistry: Theory and Practice*, Oxford University Press, **1998**.
[9] A. K. Bose, M. S. Manhas, S. Pednekar, S. N. Ganguly, H. Dang, W. He, A. Mandadi, *Tetrahedron Lett.* **2005**, *46*, 1901–1903.
[10] K. Tanaka, S. Kishigami, F. Toda, *J. Org. Chem.,* **1991**, *56*, 4333–4334.
[11] R. Thorwirth, A. Stolle, B. Ondruschka, *Green Chem.,* **2010**, *12*, 985–7.
[12] F. Toda, K. Kiyoshige, M. Yagi, *Angew. Chem. Int. Ed.,* **1989**, *28*, 320–321.
[13] R. R. Deshmukh, R. Rajagopal, K. V. Srinivasan, *Chem. Commun.,* **2001**, 1544–1545.
[14] V. V. Namboodiri, R. S. Varma, *Org. Lett.,* **2002**, *4*, 3161–3163.
[15] R. B. N. Baig, R. S. Varma, *Chem. Soc. Rev.,* **2012**, *41*, 1559–1584.
[16] K. H. Park, S. Watanabe, M. A. Kakimoto, Y. Imai, *Polymer Journal.,* **1993**, *25*, 209–213.
[17] B. R. Vaddula, R. S. Varma, J. Leazer, *Tetrahedron Lett.,* **2013**, *54*, 1538–1541.
[18] M. Ješelnik, S. Polanc, M. Kocevar, R. S. Varma, *Chem. Commun.,* **2001**, 1716–1717.
[19] R. S. Varma, D. Kumar, P. J. Liesen, *J. Chem. Soc., Perkin Trans., 1* **1998**, 4093–4096.
[20] R. S. Varma, V. V. Namboodiri, *Chem. Commun.,* **2001**, 643–644.
[21] Y. Ju, R. S. Varma, *Org. Lett.,* **2005**, *7*, 2409–2411.
[22] Y. Ju, R. S. Varma, *Tetrahedron Lett.,* **2005**, *46*, 6011–6014.
[23] V. V. Namboodiri, R. S. Varma, *Green Chem.,* **2001**, *3*, 146–148.
[24] G. Adlakha-Hutcheon, R. Khaydarov, R. Korenstein, R. Varma *et al*, *Nanomaterials, Nanotechnology*, Springer Netherlands, Dordrecht, **2009**.
[25] M. N. Nadagouda, R. S. Varma, *Green Chem.,* **2008**, *10*, 859–4.
[26] J. Virkutyte, R. S. Varma, *Chem. Sci.,* **2011**, *2*, 837–846.
[27] R. A. Sheldon, *Chem. Soc. Rev.,* **2012**, *41*, 1437–1451.
[28] P. Gallezot, *Chem. Soc. Rev.,* **2012**, *41*, 1538–1558.
[29] E. de Jong, A. Higson, P. Walsh, M. Wellisch, *Biofuels, Bioprod. Bioref.,* **2012**, *6*, 606–624.
[30] J. P. Lange, *Biofuels, Bioprod. Bioref.,* **2007**, *1*, 39–48.
[31] E. C. Achinivu, R. M. Howard, G. Li, H. Gracz, W. A. Henderson, *Green Chem.,* **2014**, *16*, 1114–1119.
[32] R. Rinaldi, R. Palkovits, F. Schüth, *Angew. Chem. Int. Ed.,* **2008**, *47*, 8047–8050.
[33] Z. Qiu, G. M. Aita, M. S. Walker, *Bioresour. Technol.,* **2012**, *117*, 251–256.
[34] P. T. M. Do, J. R. McAtee, D. A. Watson, R. F. Lobo, *ACS Catal.,* **2013**, *3*,

41–46.
[35] C. C. Chang, S. K. Green, C. L. Williams, P. J. Dauenhauer, W. Fan, *Green Chem.,* **2014**, *16*, 585–588.
[36] M. W. Peters, *Renewable Xylenes Produced From Biological C4 and C5 Molecules*, **2012**, WO2012061372A1.
[37] P. Imhof, J. C. van der Waal, *Catalytic Process Development for Renewable Materials*, Degruyter, **2013**.
[38] J. J. Bozell, G. R. Petersen, *Green Chem.,* **2010**, *12*, 539–17.
[39] Pasteur, L. *C. R. Acad. Sci.,* **1858** *46* **,** 615.
[40] E. Buchner, *Ber. Dtsch. Chem. Ges.,* **1897**, *30*, 1110–1113.
[41] K. Faber, *Biotransformations in Organic Chemistry*, Springer Science & Business Media, Berlin, Heidelberg, **2012**.
[42] D. L. Nelson, M. M. Cox, *Lehninger Principles of Biochemistry*, **2013**.
[43] U. Deichmann, S. Schuster, J. P. Mazat, A. Cornish Bowden, *FEBS J.,* **2013**, *281*, 435–463.
[44] E. Fischer, *Ber. Dtsch. Chem. Ges.,* **1894**, *27*, 1–4.
[45] L. Pauling, *Nature,* **1948**, *161*, 707–709.
[46] D. E. Koshland, *Proc. Natl. Acad. Sci. U.S.A.,* **1958**, *44*, 98-104.
[47] A. G. Ogston, *Nature,* **1948**, *162*, 963.
[48] L. Rosenthaler, *Arch. Pharm. Pharm. Med. Chem.,* **1908**, *246*, 365–366.
[49] V. Prelog, *Pure Appl. Chem.*, **1964**, *9*, 119-130.
[50] D. H. Peterson, H. C. Murray, *J. Am. Chem. Soc.,* **1952**, *74*, 1871–1872.
[51] R. B. Woodward, F. Sondheimer, D. Taub, K. Heusler, W. M. McLamore, *J. Am. Chem. Soc.,* **1952**, *74*, 4223–4251.
[52] G. M. Whitesides, C.-H. Wong, *Angew. Chem. Int. Ed. Engl.,* **1985**, *24*, 617–638.
[53] T. Koyanagi, T. Katayama, H. Suzuki, A. Onishi, K. Yokozeki, H. Kumagai, *Biosci. Biotechnol. Biochem.,* **2014**, *73*, 1221–1223.
[54] T. Nagasawa, C. D. Mathew, J. Mauger, H. Yamada, *Appl. Environ. Microbiol.,* **1988**, *54*, 1766–1769.
[55] R. Kratzer, M. Pukl, S. Egger, B. Nidetzky, *Microb. Cell. Fact.,* **2008**, *7*, 37–12.
[56] A. M. Klibanov, *Nature,* **2001**, *409*, 241–246.
[57] D. A. Jackson, R. H. Symons, P. Berg, *Proc. Natl. Acad. Sci. U.S.A.,* **1972**, *69*, 2904–2909.
[58] S. N. Cohen, A. C. Y. Chang, H. W. Boyer, R. B. Helling, *Proc. Natl. Acad. Sci. U.S.A.,* **1973**, *70*, 3240–3244.
[59] H. F. Lodish, *Molecular Cell Biology*, Freeman **2012**.
[60] K. B. Mullis, *Angew. Chem. Int. Ed. Engl.,* **1994**, *33*, 1209–1213.
[61] D. R. Kuritzkes, *J. Infect. Dis.* **2004**, *190*, 2047–2054.
[62] C. A. Hutchison, S. Phillips, M. H. Edgell, S. Gillam, P. Jahnke, M. Smith, *J. Biol. Chem.,* **1978**, *253*, 6551–6560.
[63] M. Smith, *Angew. Chem. Int. Ed.,* **1994**, *33*, 1214–1221.
[64] T. Oshima, *Curr. Opin. Struct. Biol.,* **1994**, *4*, 623–628.
[65] T. Ema, S. Kamata, M. Takeda, Y. Nakano, T. Sakai, *Chem. Commun.,* **2010**, *46*, 5440–5442.
[66] W. P. C. Stemmer, *Nature,* **1994**, *370*, 389–391.
[67] M. Matsumura, S. Aiba, *J. Biol. Chem.,* **1985**, *260*, 15298–15303.
[68] D. A. Estell, T. P. Graycar, J. A. Wells, *J. Biol. Chem.,* **1985**, *260* 6518-6521.

[69] H. Liao, T. McKenzie, R. Hageman, *Proc. Natl. Acad. Sci. U.S.A.,* **1986**, *83*, 576–580.
[70] K. Chen, F. H. Arnold, *Proc. Natl. Acad. Sci. U.S.A.,* **1993**, *90*, 5618–5622.
[71] J. Minshull, J. E. Ness, M. Welch, L. Giver, M. Bueno, J. R. Cherry, T. V. Borchert, W. P. C. Stemmer, *Nat., Biotechnol.* **1999**, *17*, 1–4.
[72] L. Giver, J. Kim, S. Kim, A. Gershenson, P. O. Freskgard, S. Yoon, E. Hong, F. H. Arnold, Y. Ryu, *Proc. Natl. Acad. Sci.,* **1998**, *95*, 12809–12813.
[73] J. R. Cherry, M. H. Lamsa, P. Schneider, J. Vind, A. Svendsen, A. Jones, A. H. Pedersen, *Nat. Biotechnol.,* **1999**, *17*, 379–384.
[74] T. H. Richardson, X. Tan, G. Frey, W. Callen, M. Cabell, D. Lam, J. Macomber, J. M. Short, D. E. Robertson, C. Miller, *J. Biol. Chem.,* **2002**, *277*, 26501–26507.
[75] M. T. Reetz, A. Zonta, K. Schimossek, K.-E. Jaeger, K. Liebeton, *Angew. Chem. Int. Ed.,* **1997**, *36*, 2830–2832.
[76] K. Liebeton, A. Zonta, K. Schimossek, M. Nardini, D. Lang, B. W. Dijkstra, M. T. Reetz, K. E. Jaeger, *Chem. Biol.,* **2000**, *7*, 709–718.
[77] S. Fong, T. D. Machajewski, C. C. Mak, C. Wong, *Chem, Biol.,* **2000**, *7*, 873–883.
[78] T. Woodhall, G. Williams, A. Berry, A. Nelson, *Angew. Chem. Int. Ed.,* **2005**, *44*, 2109–2112.
[79] M. Alexeeva, A. Enright, M. J. Dawson, M. Mahmoudian, N. J. Turner, *Angew. Chem. Int. Ed.,* **2002**, *41*, 3177–3180.
[80] M. Alexeeva, *Deracemisation of Amines*, **2007**, US7208302.
[81] J. C. Moore, D. J. Pollard, B. Kosjek, P. N. Devine, *Acc. Chem. Res.,* **2007**, *40*, 1412–1419.
[82] S. K. Ma, J. Gruber, C. Davis, L. Newman, D. Gray, A. Wang, J. Grate, G. W. Huisman, R. A. Sheldon, *Green Chem.,* **2010**, *12*, 81–86.
[83] S. Panke, M. Wubbolts, *Curr. Opin. Chem Biol.,* **2005**, *9*, 188–194.
[84] C. K. Savile, J. M. Janey, E. C. Mundorff, J. C. Moore, S. Tam, W. R. Jarvis, J. C. Colbeck, A. Krebber, F. J. Fleitz, J. Brands, et al., *Science* **2010**, *329*, 305–309.
[85] A. A. Desai, *Angew. Chem. Int. Ed.,* **2011**, *50*, 1974–1976.
[86] C. A. Martinez, S. Hu, Y. Dumond, J. Tao, P. Kelleher, L. Tully, *Org. Process Res. Dev.,* **2008**, *12*, 392–398.
[87] Y. Chen, S. L. Goldberg, R. L. Hanson, W. L. Parker, I. Gill, T. P. Tully, M. A. Montana, A. Goswami, R. N. Patel, *Org. Process Res. Dev.,* **2011**, *15*, 241–248.
[88] T. Punniyamurthy, S. Velusamy, J. Iqbal, *Chem. Rev.,* **2005**, *105*, 2329–2364.
[89] Y. Tamaru, Y. Yamada, Z.-I. Yoshida, *Synthesis,* **1983**, *1983*, 474–476.
[90] W. J. Yoo, C. J. Li, *J. Am. Chem. Soc.,* **2006**, *128*, 13064–13065.
[91] C. Gunanathan, Y. Ben-David, D. Milstein, *Science,* **2007**, *317*, 790–792.
[92] E. Balaraman, E. Khaskin, G. Leitus, D. Milstein, *Nat. Chem.,* **2013**, *5*, 122–125.
[93] J. F. Soulé, H. Miyamura, S. Kobayashi, *J. Am. Chem. Soc.,* **2011**, *133*, 18550–18553.
[94] F. Hollmann, I. W. C. E. Arends, K. Buehler, A. Schallmey, B. Bühler, *Green Chem.,* **2011**, *13*, 226.
[95] W. Kroutil, H. Mang, K. Edegger, K. Faber, *Adv. Synth. Catal.* **2004**, *346*,

125–142.
[96] A. J. Irwin, J. B. Jones, *J. Am. Chem. Soc.,* **1976**, *98*, 8476–8482.
[97] S. B. Bankar, M. V. Bule, R. S. Singhal, L. Ananthanarayan, *Biotechnol. Adv.,* **2009**, *27*, 489–501.
[98] J. W. Whittaker, *Arch. Biochem. Biophys.,* **2005**, *433*, 227–239.
[99] F. Escalettes, N. J. Turner, *ChemBioChem.,* **2008**, *9*, 857–860.
[100] S. Riva, *Trends Biotechnol.,* **2006**, *24*, 219–226.
[101] R. A. Sheldon, *Chem. Commun.,* **2008**, *35*, 3352–14.
[102] W. J. H. van Berkel, N. M. Kamerbeek, M. W. Fraaije, *J. Biotechnol.,* **2006**, *124*, 670–689.
[103] H. M. Dudek, M. W. Fraaije, *Curr. Opin. Chem. Biol.,* **2010**, *14*, 138–144.
[104] M. Winkler, A. Glieder, M. W. Fraaije, *J. Biotechnol.,* **2010**, *146*, 9–24.
[105] G. Mugesh, W.-W. du Mont, H. Sies, *Chem. Rev.,* **2001**, *101*, 2125–2180.
[106] M. Kuwahara, J. K. Glenn, M. A. Morgan, M. H. Gold, *FEBS Lett.,* **2001**, *169*, 247–250.
[107] M. Hofrichter, R. Ullrich, *Appl. Microbiol. Biotechnol.,* **2006**, *71*, 276–288.
[108] B. Buhler, B. Witholt, B. Hauer, A. Schmid, *Appl. Environ. Microbiol.,* **2002**, *68*, 560–568.
[109] R. Villa, A. Romano, R. Gandolfi, J. Gago, F. Molinari, *Tetrahedron Lett.,* **2002**, *43*, 6059–6061.
[110] A. Siebum, A. van Wijk, R. Schoevaart, T. Kieboom, *J. Mol. Catal. B: Enzym.,* **2006**, *41*, 141–145.
[111] A. Potthast, T. Rosenau, C. L. Chen, J. S. Gratzl, *J. Mol. Catal. A: Chem.,* **1996**, *108*, 5–9.
[112] M. Fabbrini, C. Galli, P. Gentili, D. Macchitella, *Tetrahedron Lett.,* **2001**, *42*, 7551–7553.
[113] R. Gandolfi, K. Cavenago, R. Gualandris, J. V. Sinisterra Gago, F. Molinari, *Proc. Biochem.,* **2004**, *39*, 749–753.
[114] F. Molinari, R. Villa, F. Aragozzini, P. Cabella, M. Barbeni, F. Squarcia, *J. Chem. Technol. Biotechnol.,* **1997**, *70*, 294–298.
[115] A. Geerlof, J. A. Jongejan, T. J. van Dooren, P. C. Racemakers-Franken, W. J. van den Tweel, J. A. Duine, *Enzyme Microb. Technol.,* **1994**, *16*, 1059–1063.
[116] A. Romano, R. Gandolfi, P. Nitti, M. Rollini, F. Molinari, *J. Mol. Catal. B: Enzym.,* **2002**, *17*, 235–240.
[117] R. Gandolfi, A. Borrometi, A. Romano, J. Gago, F. Molinari, *Tetrahedron: Asymmetry,* **2002**, *13*, 2345–2349.
[118] F. Molinari, R. Gandolfi, R. Villa, E. Urban, A. Kiener, *Tetrahedron: Asymmetry,* **2003**, *14*, 2041–2043.
[119] F. Koopman, N. Wierckx, J. H. de Winde, H. J. Ruijssenaars, *Bioresour. Technol.,* **2010**, *101*, 6291–6296.
[120] H. I. Perez, N. Manjarrez, A. Solis, H. Luna, M. A. Ramirez, J. Cassani, *Afr. J. Biotechnol.,* **2009**, *8*, 2279–2282.
[121] C. H. Wong, J. R. Matos, *J. Org. Chem.,* **1985**, *50*, 1992–1994.
[122] K. P. Lok, I. J. Jakovac, J. B. Jones, *J. Am. Chem. Soc.,* **1985**, *107* 2521-2526.
[123] A. J. Irwin, J. B. Jones, *J. Am. Chem. Soc.,* **1977**, *99* 556-561.
[124] K. Parikka, M. Tenkanen, *Carbohydr. Res.,* **2009**, *344*, 14–20.
[125] S. P. Yao, D. S. Lu, Q. Wu, Y. Cai, S.-H. Xu, X.-F. Lin, *Chem. Commun.,* **2004**, *0*, 2006–2007.

[126] A. van Wijk, A. Siebum, R. Schoevaart, T. Kieboom, *Carbohydr. Res.,* **2006**, *341*, 2921–2926.
[127] J. Geigert, S. L. Neidleman, D. S. Hirano, *Carbohydr. Res.,* **1983**, *113*, 159–162.
[128] J. Boudrant, *Enzyme Microb. Technol.,* **1990**, *12*, 322–329.
[129] R. Bauer, N. Katsikis, S. Varga, D. Hekmat, *Bioprocess Biosyst Eng.,* **2005**, *28*, 37–43.
[130] C. De Muynck, C. Pereira, W. Soetaert, E. Vandamme, *J. Biotechnol.,* **2006**, *125*, 408–415.
[131] B. H. Landis, J. K. McLaughlin, R. Heeren, R. W. Grabner, P. T. Wang, *Org. Process Res. Dev.,* **2002**, *6*, 547–552.
[132] R. D. Hancock, R. Viola, *Trends. Biotechnol,* **2002**, *20*, 299–305.
[133] W. Stampfer, B. Kosjek, C. Moitzi, W. Kroutil, K. Faber, *Angew. Chem. Int. Ed.,* **2002**, *41*, 1014–1017.
[134] L. G. Lee, G. M. Whitesides, *J. Org. Chem.,* **1986**, *51*, 25–36.
[135] K. Edegger, H. Mang, K. Faber, J. Gross, W. Kroutil, *J. Mol. Catal. A: Chem.,* **2006**, *251*, 66–70.
[136] C. V. Voss, C. C. Gruber, W. Kroutil, *Angew. Chem. Int. Ed.,* **2008**, *47*, 741–745.
[137] C. V. Voss, C. C. Gruber, K. Faber, T. Knaus, P. Macheroux, W. Kroutil, *J. Am. Chem. Soc.,* **2008**, *130*, 13969–13972.
[138] A. Chang, M. Scheer, A. Grote, I. Schomburg, D. Schomburg, *Nucleic Acids Res.* **2009**, *37*, D588–D592.
[139] A. Anne, C. Bourdillon, S. Daninos, J. Moiroux, *Biotechnol. Bioeng.,* **1999**, *64*, 101–107.
[140] R. Fernandez-Lafuente, V. Rodriguez, *Enzyme and Microb. Technol.,* **1998**, *23*, 28–33.
[141] R. K. Henderson, C. Jiménez-González, *Ind. Biotechnol.,* **2008**, *4*, 180–192.
[142] F. R. Alexandre, D. P. Pantaleone, P. P. Taylor, I. G. Fotheringham, D. J. Ager, N. J. Turner, *Tetrahedron Lett.,* **2002**, *43*, 707–710.
[143] T. M. Beard, N. J. Turner, *Chem. Commun.,* **2002**, 246–247.
[144] A. Enright, F.-R. Alexandre, G. Roff, I. G. Fotheringham, M. J. Dawson, N. J. Turner, *Chem. Commun.,* **2003**, *35*, 2636–2637.
[145] V. Köhler, K. R. Bailey, A. Znabet, J. Raftery, M. Helliwell, N. J. Turner, *Angew. Chem. Int. Ed.,* **2010**, *49*, 2182–2184.
[146] D. Ghislieri, N. J. Turner, *Top. Catal.,* **2013**, *57*, 284–300.
[147] L. K. Hoover, M. Moo Young, R. L. Legge, *Biotechnol. Bioeng.,* **1991**, *38*, 1029–1033.
[148] D. Koszelewski, K. Tauber, K. Faber, W. Kroutil, *Trends. Biotechnol.,* **2010**, *28*, 324–332.
[149] M. D. Truppo, N. J. Turner, J. D. Rozzell, *Chem. Commun.,* **2009**, *350*, 2127–3.
[150] R. H. Abeles, H. A. Lee, *J. Biol. Chem.,* **1960**, *235*, 1499–1503.
[151] J. A. Hinson, R. A. Neal, *J. Biol. Chem.,* **1972**, *247*, 7106–7107.
[152] G. T. M. Henehan, N. J. Oppenheimer, *Biochem.,* **2002**, *32*, 735–738.
[153] Y. Tsybovsky, H. Donato, N. I. Krupenko, C. Davies, S. A. Krupenko, *Biochem.,* **2007**, *46*, 2917–2929.
[154] A. Nunez, T. A. Foglia, G. J. Piazza, *Biotechnol. Appl. Biochem.,* **1999**, *29*, 207–212.

[155] S. Kitamura, K. Sugihara, S. Ohta, *Drug Metab. Pharmacokinet.,* **2006**, *21*, 83–98.
[156] K. V. Rajagopalan, J. L. Johnson, *J. Biol. Chem.,* **1992**, *267*, 10199–10202.
[157] R. Hille, J. Hall, P. Basu, *Chem. Rev.,* **2014**, *114*, 3963–4038.
[158] M. A. S. Correia, A. R. Otrelo-Cardoso, V. Schwuchow, K. G. V. Sigfridsson Clauss, M. Haumann, M. J. Romão, S. Leimkühler, T. Santos-Silva, *ACS Chem. Biol.,* **2016**, *11*, 2923–2935.
[159] T. Nishino, K. Okamoto, *J. Inorg. Biochem.,* **2000**, *82*, 43–49.
[160] M. J. Barber, M. P. Coughlan, K. V. Rajagopalan, L. M. Siegel, *Biochem.,* **1982**, *21*, 3561–3568.
[161] D. C. Pryde, D. Dalvie, Q. Hu, P. Jones, R. S. Obach, T.-D. Tran, *J. Med. Chem.,* **2010**, *53*, 8441–8460.
[162] C. Beedham, *Drug Metab. Rev.,* **1985**, *16*, 119–156.
[163] R. Hille, *Arch. Biochem. Biophys.,* **2005**, *433*, 107–116.
[164] T A Krenitsky, *Proc. Natl. Acad. Sci. U.S.A.,* **1984**, *81*, 3209–3213.
[165] K. Rowland, L. Lennard, J. S. Lilleyman, *Xenobiotica.,* **1999**, *29*, 615–628.
[166] S. E. Fowles, S. K. Pratt, J. Laroche, W. T. Prince, *Eur. J. Clin. Pharmacol.,* **1994**, *46*, 355–359.
[167] Y. Moriwaki, T. Yamamoto, Y. Nasako, S. Takahashi, M. Suda, K. Hiroishi, T. Hada, K. Higashino, *Biochem. Pharmacol.,* **1993**, *46*, 975–981.
[168] W. Ambroziak, G. Izaguirre, R. Pietruszko, *J. Biol. Chem.,* **1999**, *274*, 33366–33373.
[169] M. Neumann, G. Mittelstädt, C. Iobbi-Nivol, M. Saggu, F. Lendzian, P. Hildebrandt, S. Leimkühler, *FEBS J.,* **2009**, *276*, 2762–2774.
[170] S. M. McKenna, S. Leimkühler, S. Herter, N. J. Turner, A. J. Carnell, *Green Chem.,* **2015**, *17*, 3271–3275.
[171] R. Hille, H. Sprecher, *J. Biol. Chem.,* **1987**, *262*, 10914–10917.
[172] M. Adachi, K. Itoh, A. Masubuchi, N. Watanabe, Y. Tanaka, *J. Biochem. Mol. Biol.,* **2007**, *40*, 1021–1027.
[173] S. Schumann, M. Terao, E. Garattini, M. Saggu, F. Lendzian, P. Hildebrandt, S. Leimkühler, *PLoS One.,* **2009**, *4*, e5348.
[174] S. Leimkuhler, *J. Biol. Chem.,* **2003**, *278*, 20802–20811.
[175] S. Leimkühler, A. L. Stockert, K. Igarashi, T. Nishino, R. Hille, *J. Biol. Chem.,* **2004**, *279*, 40437–40444.
[176] A. Fleming, *Bull. World Health Organ.,* **2001**, *79*, 780–11.
[177] A. Bertolini, A. Ferrari, A. Ottani, S. Guerzoni, R. Tacchi, S. Leone, *CNS Drug. Rev.,* **2006**, *12*, 250–275.
[178] Y. S. Lee, E. D. Wetzel, N. J. Wagner, *J. Mater. Sci.,* **2003**, *38*, 2825–2833.
[179] P. Gerland, A. E. Raftery, H. Sevčíková, N. Li, D. Gu, T. Spoorenberg, L. Alkema, B. K. Fosdick, J. Chunn, N. Lalic, et al., *Science.,* **2014**, *346*, 234–237.
[180] V. R. Pattabiraman, J. W. Bode, *Nature.,* **2011**, *480*, 471–479.
[181] R. M. Lanigan, T. D. Sheppard, *Eur. J. Org. Chem.,* **2013**, *2013*, 7453–7465.
[182] D. J. C. Constable, P. J. Dunn, J. D. Hayler, G. R. Humphrey, J. L. Leazer Jr, R. J. Linderman, K. Lorenz, J. Manley, B. A. Pearlman, A. Wells, et al., *Green Chem.,* **2007**, *9*, 411–420.
[183] P. Tang, *Org. Synth.,* **2005**, *81*, 262.
[184] S. De Sarkar, A. Studer, *Org. Lett.,* **2010**, *12*, 1992–1995.
[185] J. W. Bode, R. M. Fox, K. D. Baucom, *Angew. Chem. Int. Ed.,* **2006**, *45*,

1248–1252.
[186] H. U. Vora, T. Rovis, *J. Am. Chem. Soc.,* **2007**, *129*, 13796–13797.
[187] H. Hussain, A. Al-Harrasi, I. R. Green, I. Ahmed, G. Abbas, N. U. Rehman, *RSC Adv.,* **2014**, *4*, 12882–12917.
[188] J. J. Truglio, K. Theis, S. Leimkühler, R. Rappa, K. V. Rajagopalan, C. Kisker, *Structure* **2002**, *10*, 115–125.
[189] B. Bechi, S. Herter, S. M. McKenna, C. Riley, S. Leimkühler, N. J. Turner, A. J. Carnell, *Green Chem.,* **2014**, *16*, 4524–4529.
[190] B. R. Riebel, P. R. Gibbs, W. B. Wellborn, A. S. Bommarius, *Adv. Synth. Catal.* **2002**, *344*, 1156–1168.
[191] T. Palmer, C. L. Santini, C. Iobbi-Nivol, D. J. Eaves, D. H. Boxer, G. Giordano, *Mol. Microbiol.* **1996**, *20*, 875–884.
[192] H. Kurouchi, K. Kawamoto, H. Sugimoto, S. Nakamura, Y. Otani, T. Ohwada, *J. Org. Chem.* **2012**, *77*, 9313–9328.
[193] R. W. Gray, A. A. S. Dreiding, *Helv. Chim. Acta.,* **1980**, *63*, 315–319.
[194] G. Palmisano, G. Lesma, M. Nali, B. Rindone, S. Tollari, *Synthesis.,* **1985**, *1985*, 1072–1074.
[195] S. Ruchiwarat, *Tetrahedron Lett.,* **1984**, *25*, 3479–3480.
[196] N. J. Leonard, G. W. Leubner, *J. Am. Chem. Soc.,* **1949**, *71*, 3408–3411.
[197] G. Hanquet, X. Lusinchi, P. Milliet, *Tetrahedron Lett.,* **1987**, *28*, 6061–6064.
[198] Y. R. Jorapur, G. Rajagopal, P. J. Saikia, R. R. Pal, *Tetrahedron Lett.,* **2008**, *49*, 1495–1497.
[199] K. Brewster, R. A. Chittenden, J. M. Harrison, T. D. Inch, C. Brown, *J. Chem. Soc., Perkin Trans., 1* **1976**, 1291.
[200] L. Troian-Gautier, J. De Winter, P. Gerbaux, C. Moucheron, *J. Org. Chem.,* **2013**, *78*, 11096–11101.
[201] S. Mezulis, C. M. Yates, M. N. Wass, M. J. E. Sternberg, L. A. Kelley, *Nat. Protoc.* **2015**, *10*, 845–858.
[202] R. S. Heath, M. Pontini, B. Bechi, N. J. Turner, *ChemCatChem.,* **2014**, *6*, 996–1002.
[203] L. Zheng, *Nucleic Acids Res.,* **2004**, *32*, e115–e115.

Appendix

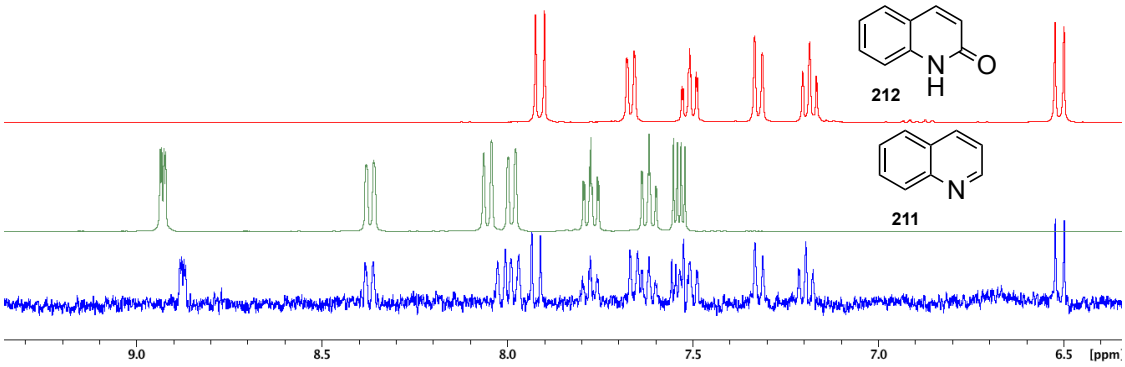

Figure 41 Aromatic region NMR standards **211** and **212** and *Ec* XDH in DMSO-d6

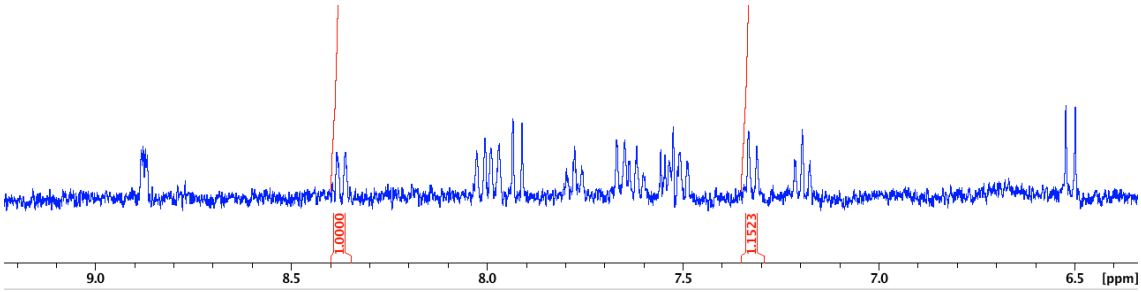

Figure 42 *Ec* XDH quinoline **211** : 2-hydroxyquinoline **212** = 1:1.15

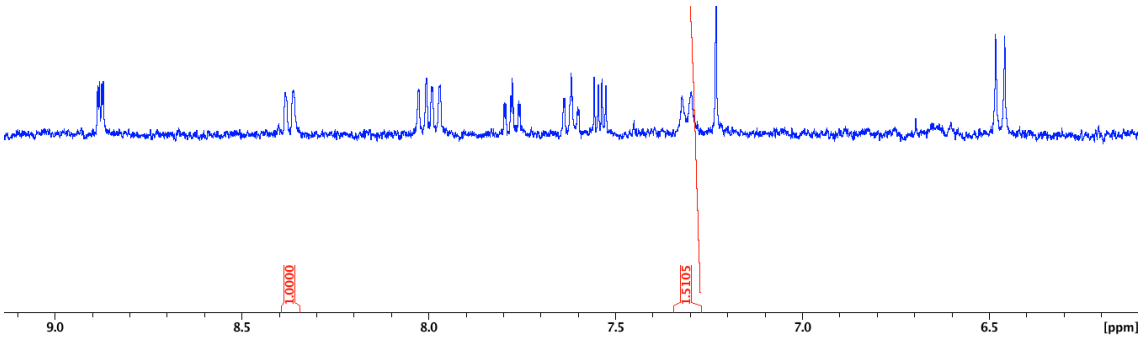

Figure 43 *Rc* XDH E232V quinoline **211** : 2-hydroxyquinoline **212** = 1:1.5

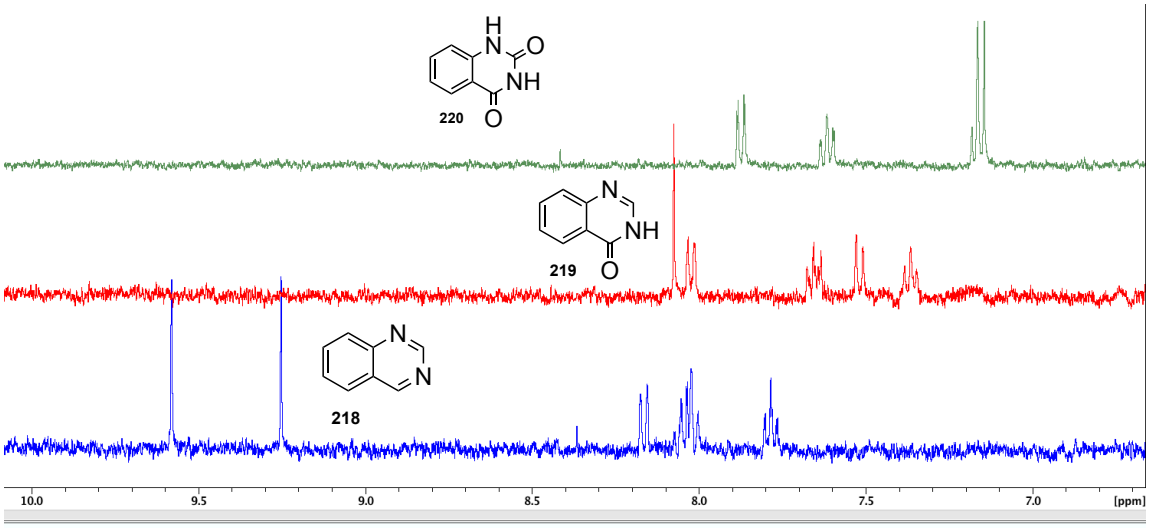

Figure 44 Aromatic region NMR standards of **218**, **219**, **220**, in DMSO-d6

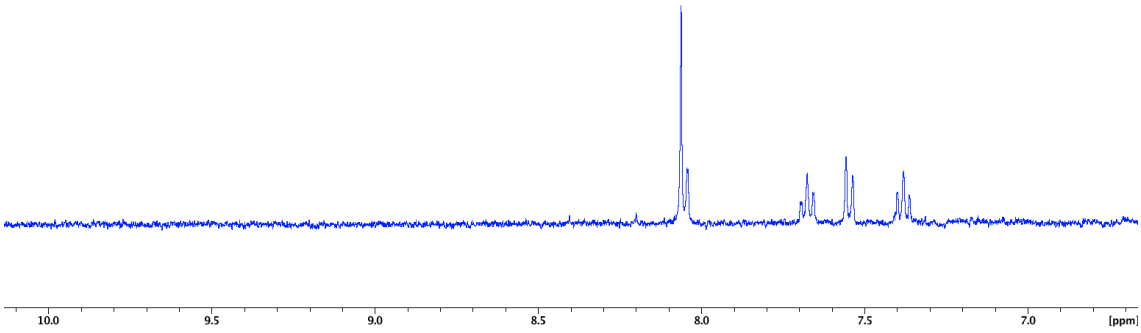

Figure 45 PaoABC **218** trace in DMSO-d6

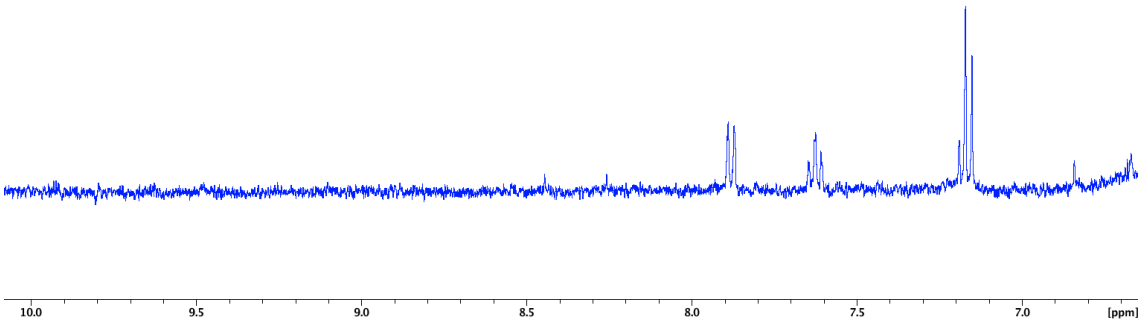

Figure 46 *Ec*XDH / *Bovine* XO **218** trace in DMSO-d6

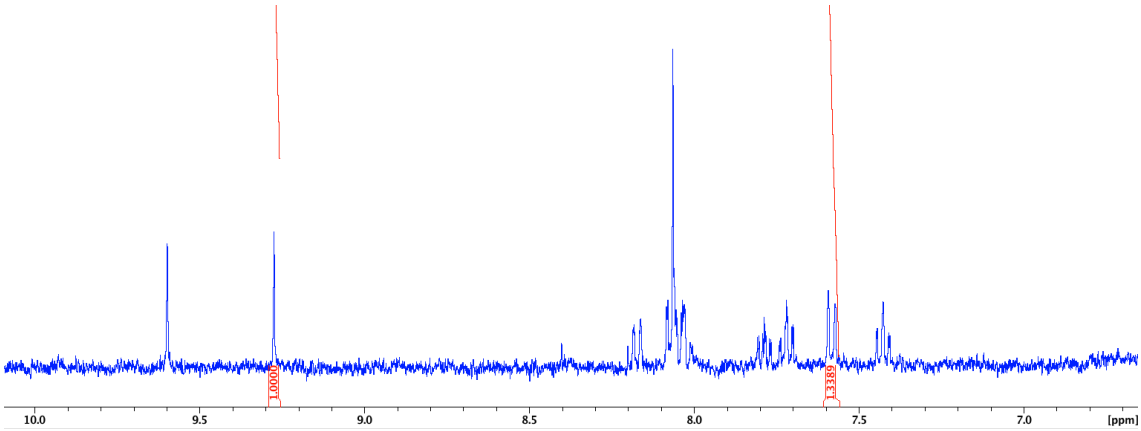

Figure 47 *Ec* PaoABC T318R quinazoline **218** : **219** = 1:1.34

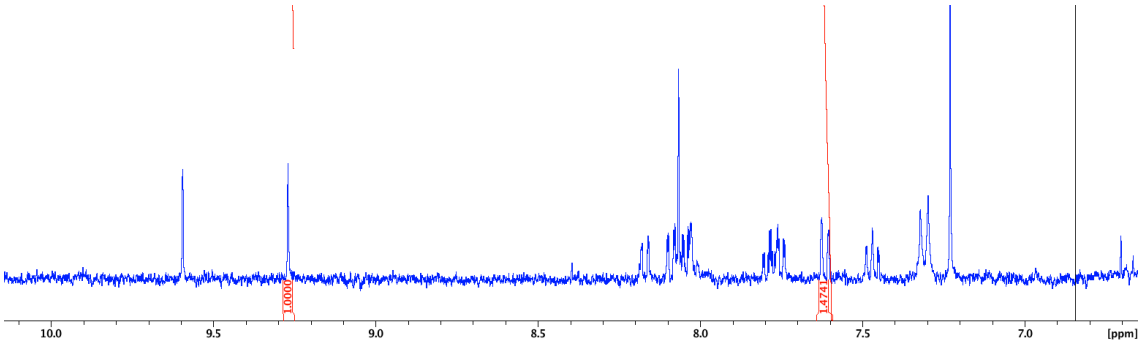

Figure 48 *Rc* XDH E232V quinazoline **218** : **219** = 1:1471

Phenylacetaldehyde – WT PaoABC

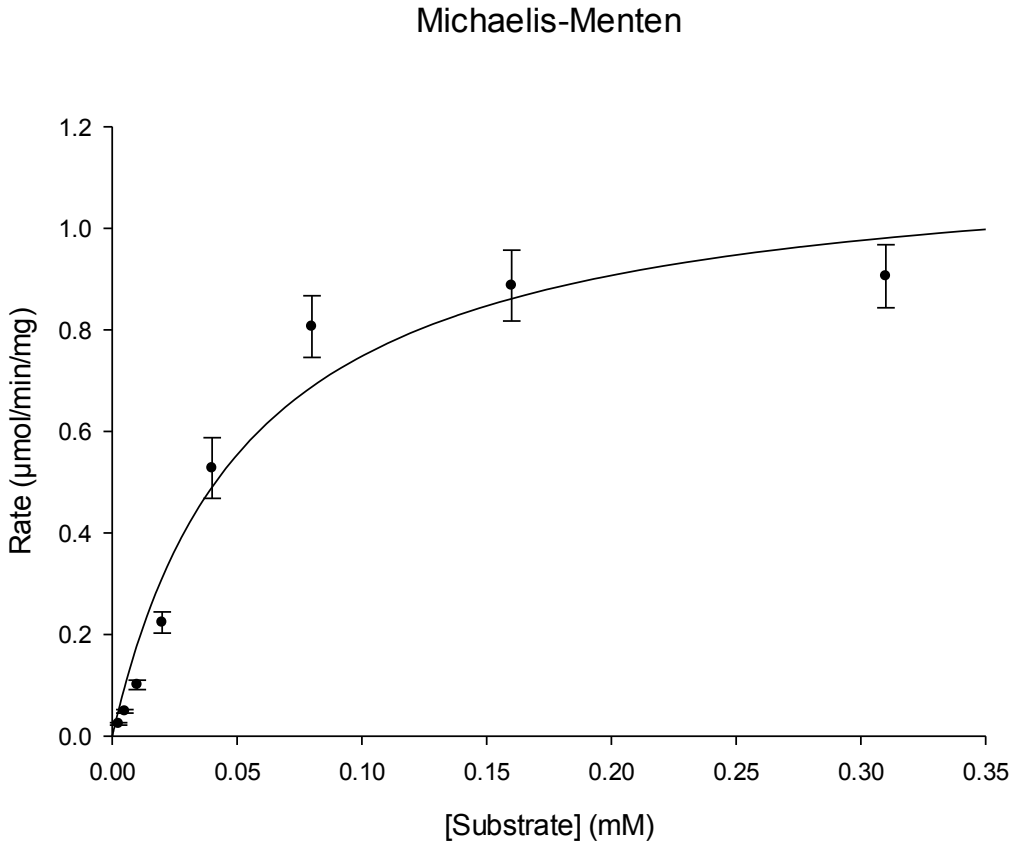

Vmax = 1.2
Km = 0.05385

Calculation

Pao MW = 136357.7 g mol^{-1} (mg $mmol^{-1}$) = **136.36 mg $umol^{-1}$**

Vmax unit = **umol min^{-1} mg^{-1}** Km unit = **mM**

kcat = 1.1515 x 136.36 = **157.0 min^{-1} (± 11.0)**

kcat/Km = **2916 (± 627) min^{-1} mM^{-1}**

Parameters

	Value	±Std. Error	95% Conf. Interval
Vmax	**1.15**	**$8.10x10^{-2}$**	0.98 to 1.32
Km	**$5.39x10^{-2}$**	**$1.10x10^{-2}$**	$3.12x10^{-2}$ to $7.65x10^{-2}$

Phenylacetaldehyde – PaoABC L443Q

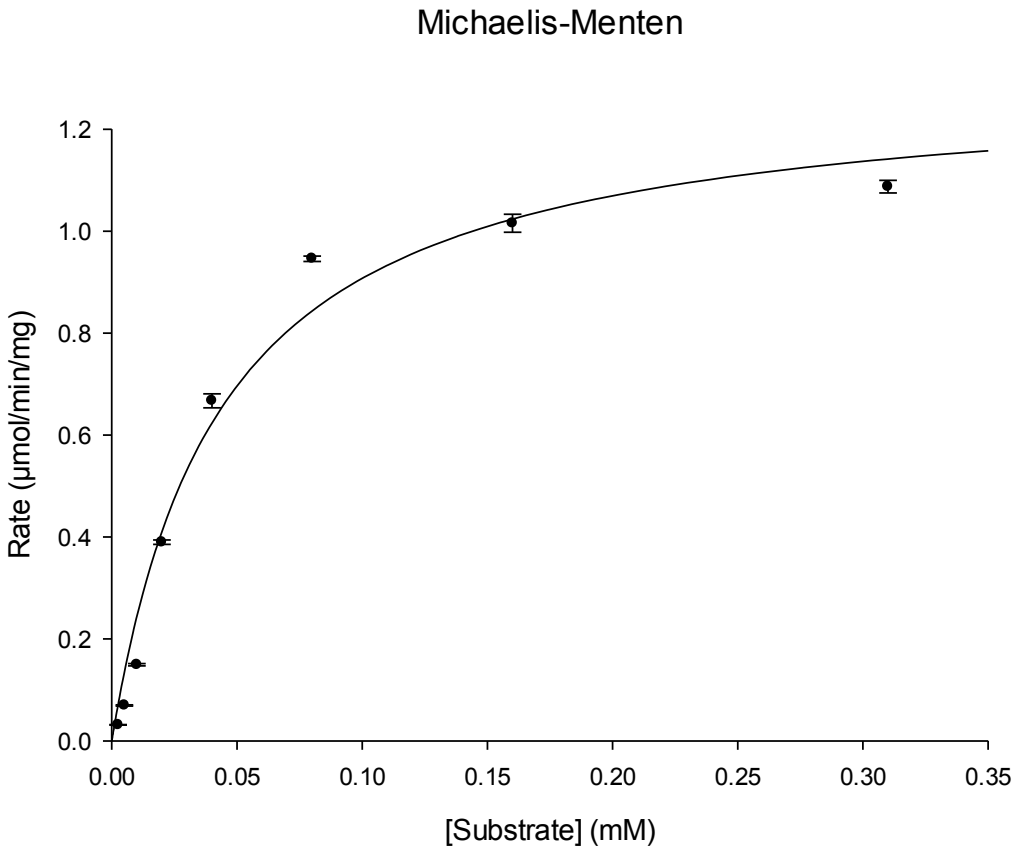

Vmax = 1.3
Km = 0.04338

Calculation

Pao MW = 136357.7 g mol^{-1} (mg $mmol^{-1}$) = **136.36 mg $umol^{-1}$**

Vmax unit = **umol min^{-1} mg^{-1}** Km unit = **mM**

kcat = 1.3013 x 136.36 = **177.4 min^{-1} (± 6.5)**

kcat/Km = **4080 (± 474) min^{-1} mM^{-1}**

Parameters

	Value	±Std. Error	95% Conf. Interval
Vmax	**1.30**	**$4.80x10^{-2}$**	1.20 to 1.40
Km	**$4.34x10^{-2}$**	**$4.80x10^{-3}$**	$3.34x10^{-2}$ to $5.34.x10^{-2}$

Phenylacetaldehyde – PaoABC L246E

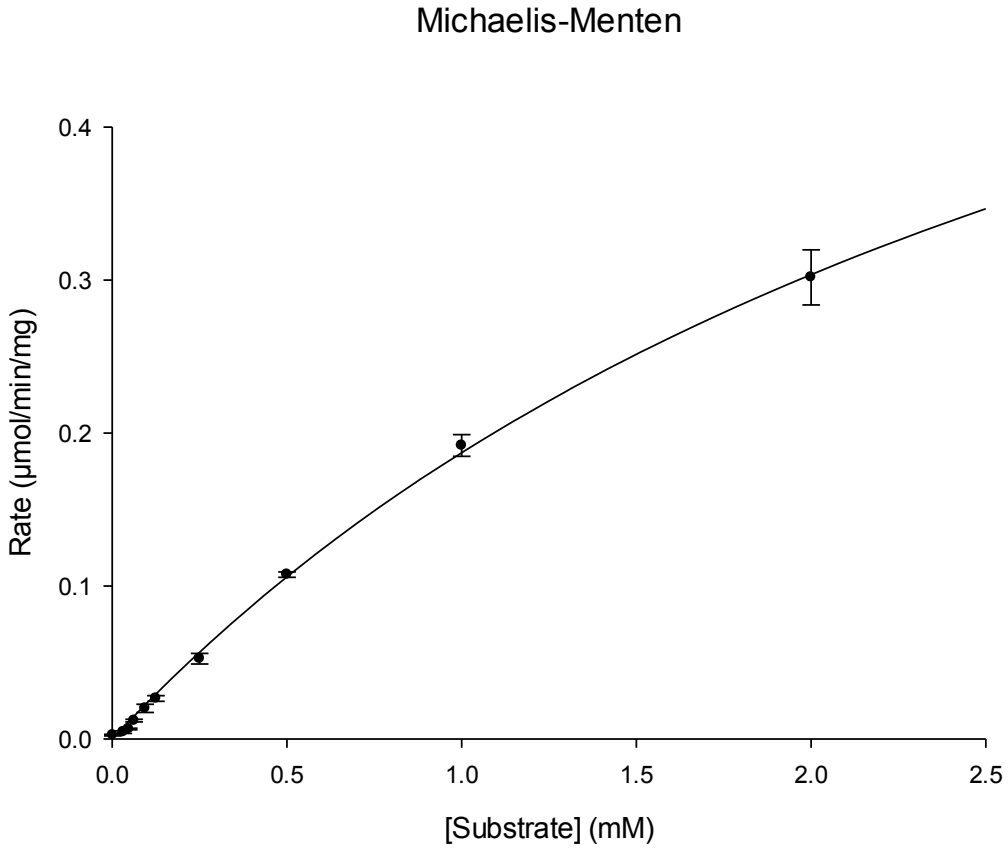

Vmax = 0.8023
Km = 3.3

Calculation

Pao MW = 136357.7 g mol^{-1} (mg $mmol^{-1}$) = **136.36 mg $umol^{-1}$**

Vmax unit = **umol min^{-1} mg^{-1}** Km unit = **mM**

kcat = 0.8023 x 136.36 = **109.4 min^{-1} (± 11.9)**

kcat/Km = **33 (± 6) min^{-1} mM^{-1}**

Parameters

	Value	±Std. Error	95% Conf. Interval
Vmax	**0.80**	**$8.76x10^{-2}$**	0.62 to 0.98
Km	**3.29**	**0.52**	2.23 to 4.34

Phenylacetaldehyde – PaoABC T318R

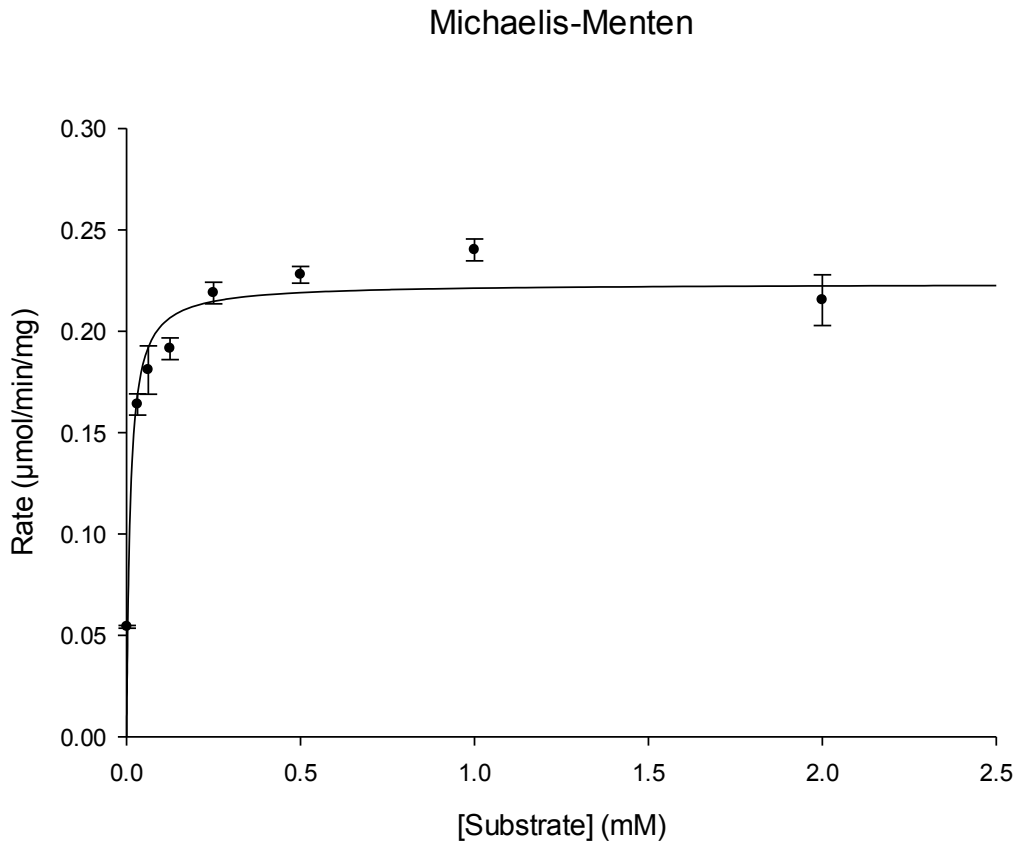

Vmax = 0.2235
Km = 0.01014

Calculation

Pao MW = 136357.7 g mol^{-1} (mg $mmol^{-1}$) = **136.36 mg $umol^{-1}$**

Vmax unit = **umol min^{-1} mg^{-1}** Km unit = **mM**

kcat = 0.2235 x 136.36 = **30.5 min^{-1} (± 0.7)**

kcat/Km = **3020 (± 672) min^{-1} mM^{-1}**

Parameters

	Value	±Std. Error	95% Conf. Interval
Vmax	**0.22**	**$5.40x10^{-3}$**	0.21 to 0.24
Km	**$1.01x10^{-2}$**	**$2.30x10^{-3}$**	$5.38x10^{-3}$ to $1.49x10^{-2}$

Phenylacetaldehyde – PaoABC L246E/T318R

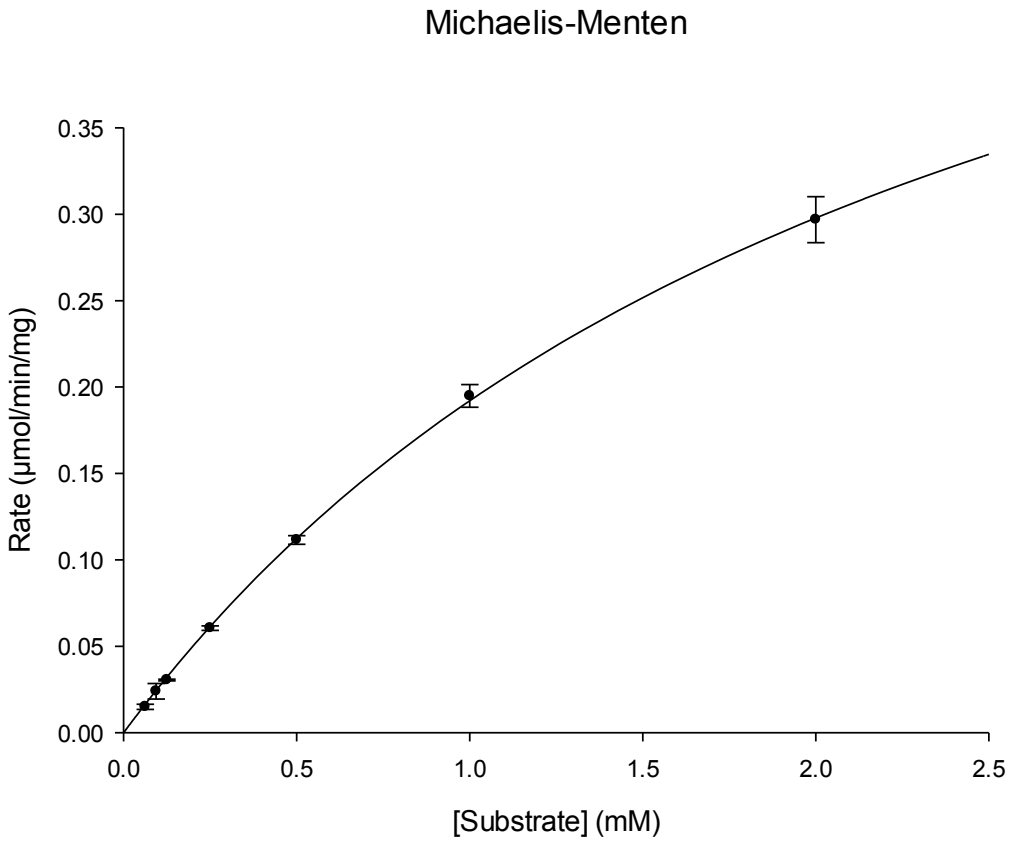

Vmax = 0.6621
Km = 2.4

Calculation

Pao MW = 136357.7 g mol^{-1} (mg $mmol^{-1}$) = **136.36 mg $umol^{-1}$**

Vmax unit = **umol min^{-1} mg^{-1}** Km unit = **mM**

kcat = 0.6621 x 136.36 = **90.3 min^{-1} (± 7.1)**

kcat/Km = **37 (± 5) min^{-1} mM^{-1}**

Parameters

	Value	±Std. Error	95% Conf. Interval
Vmax	**0.66**	**$5.20x10^{-2}$**	0.55 to 0.77
Km	**2.45**	**0.30**	1.82 to 3.08

Phenylacetaldehyde – PaoABC L246G

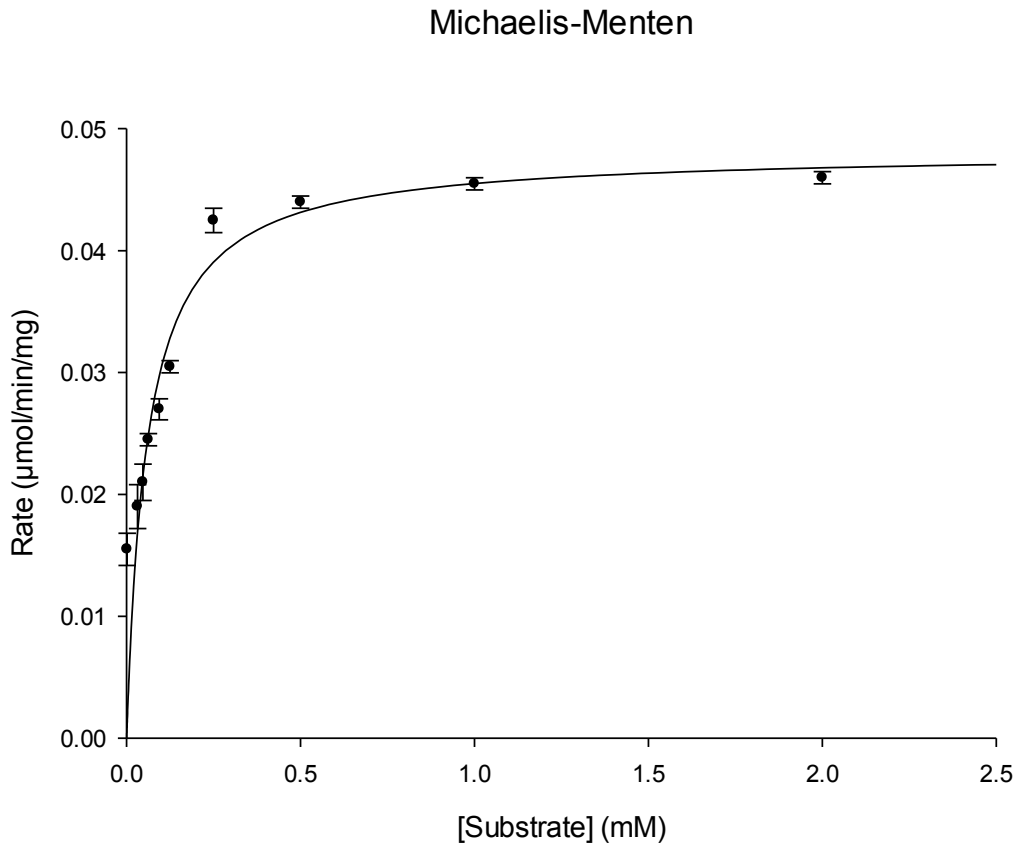

Vmax = 0.04815
Km = 0.05806

Calculation

Pao MW = 136357.7 g mol^{-1} (mg $mmol^{-1}$) = **136.36 mg $umol^{-1}$**

Vmax unit = **umol min^{-1} mg^{-1}** Km unit = **mM**

kcat = 0.0481 x 136.36 = **6.6 min^{-1} (± 0.3)**

kcat/Km = **114 (± 19) min^{-1} mM^{-1}**

Parameters

	Value	±Std. Error	95% Conf. Interval
Vmax	**$4.81x10^{-2}$**	**$2.10x10^{-3}$**	$4.40x10^{-2}$ to $5.20x10^{-2}$
Km	**$5.81x10^{-2}$**	**$9.60x10^{-3}$**	$3.84x10^{-2}$ to $7.77x10^{-2}$

Phenylacetaldehyde – PaoABC L246V

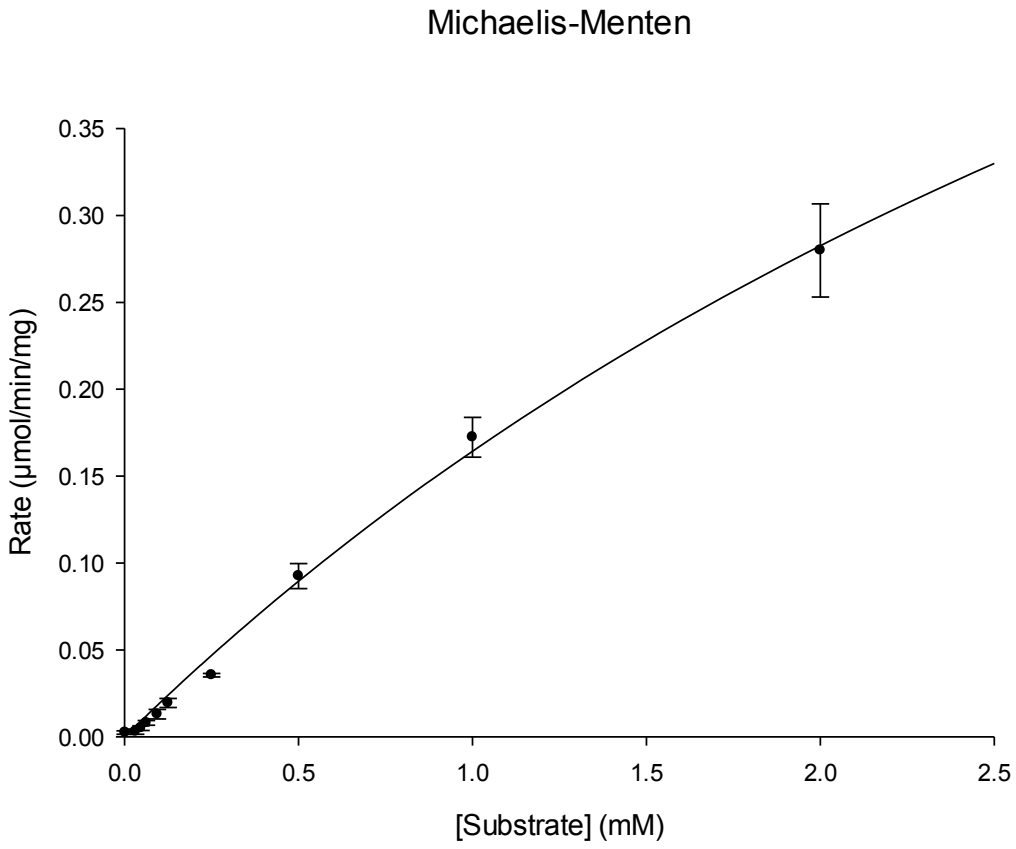

Vmax = 1.
Km = 5.1

Calculation

Pao MW = 136357.7 g mol^{-1} (mg $mmol^{-1}$) = **136.36 mg $umol^{-1}$**

Vmax unit = **umol min^{-1} mg^{-1}** Km unit = **mM**

kcat = 1.004 x 136.36 = **136.9 min^{-1} (± 36.8)**

kcat/Km = **27 (± 12) min^{-1} mM^{-1}**

Parameters

	Value	±Std. Error	95% Conf. Interval
Vmax	**1.00**	**0.27**	0.44 to 1.56
Km	**5.11**	**1.81**	1.40 to 8.81

Phenylacetaldehyde – PaoABC L246S

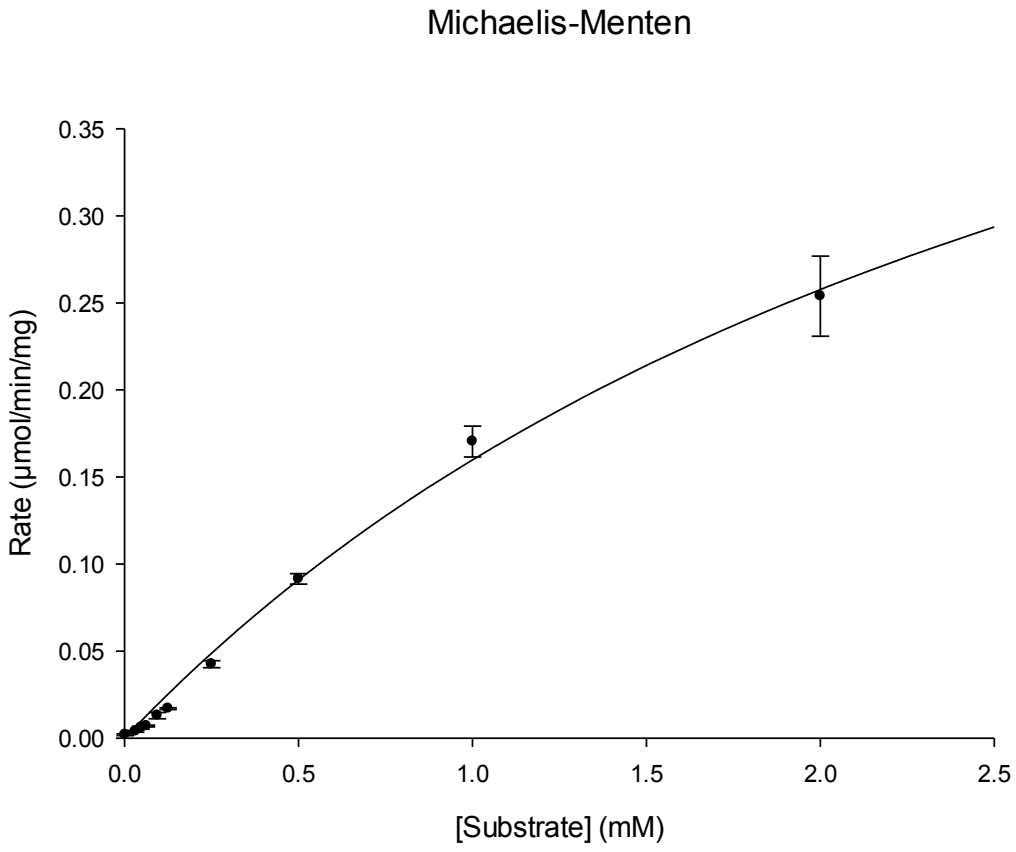

Vmax = 0.6632
Km = 3.1

Calculation

Pao MW = 136357.7 g mol^{-1} (mg $mmol^{-1}$) = **136.36 mg $umol^{-1}$**

Vmax unit = **umol min^{-1} mg^{-1}** Km unit = **mM**

kcat = 0.663 x 136.36 = **90.4 min^{-1} (± 15.0)**

kcat/Km = **29 (± 8) min^{-1} mM^{-1}**

Parameters

	Value	±Std. Error	95% Conf. Interval
Vmax	**0.66**	**0.11**	0.44 to 0.89
Km	**3.15**	**0.75**	1.62 to 4.68

Phenylacetaldehyde – PaoABC T318G

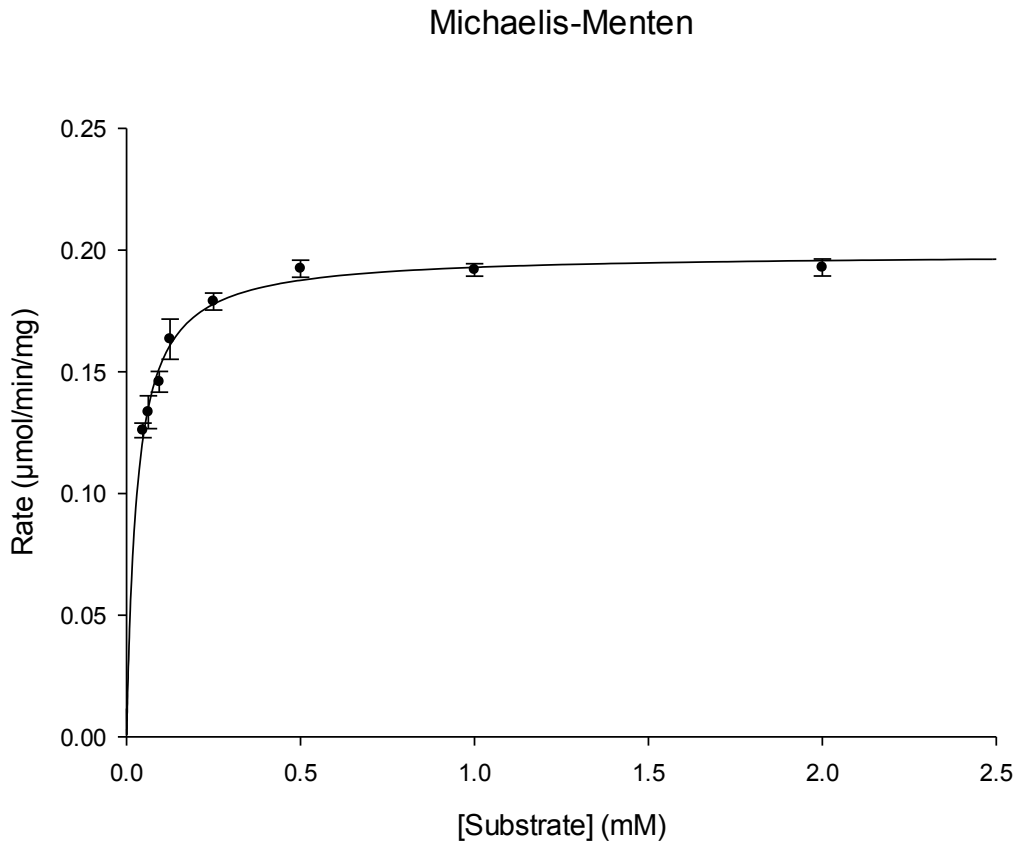

Vmax = 0.1986
Km = 0.02912

Calculation

Pao MW = 136357.7 g mol^{-1} (mg $mmol^{-1}$) = **136.36 mg $umol^{-1}$**

Vmax unit = **umol min^{-1} mg^{-1}** Km unit = **mM**

kcat = 0.199 x 136.36 = **27.1 min^{-1} (± 0.4)**

kcat/Km = **932 (± 78) min^{-1} mM^{-1}**

Parameters

	Value	±Std. Error	95% Conf. Interval
Vmax	**0.20**	**$2.82x10^{-3}$**	0.19 to 0.20
Km	**$2.91x10^{-2}$**	**$2.39x10^{-3}$**	$2.42x10^{-2}$ to $3.41x10^{-2}$

Phenylacetaldehyde – PaoABC T318P

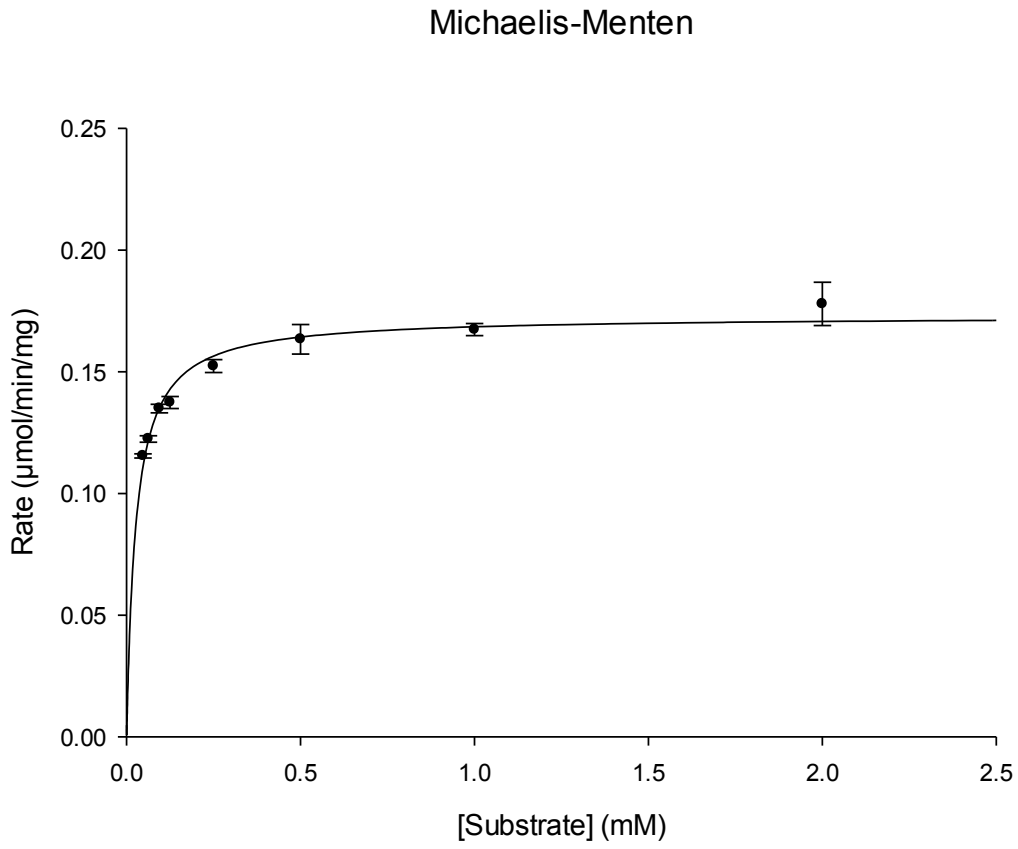

Vmax = 0.1729
Km = 0.02621

Calculation

Pao MW = 136357.7 g mol^{-1} (mg $mmol^{-1}$) = **136.36 mg $umol^{-1}$**

Vmax unit = **umol min^{-1} mg^{-1}** Km unit = **mM**

kcat = 0.173 x 136.36 = **23.6 min^{-1} (± 0.4)**

kcat/Km = **900 (± 85) min^{-1} mM^{-1}**

Parameters

	Value	±Std. Error	95% Conf. Interval
Vmax	**0.17**	**$2.63x10^{-3}$**	0.17 to 0.18
Km	**$2.62x10^{-2}$**	**$2.43x10^{-3}$**	$2.12x10^{-2}$ to $3.13x10^{-2}$

Phenylacetaldehyde – PaoABC T318L

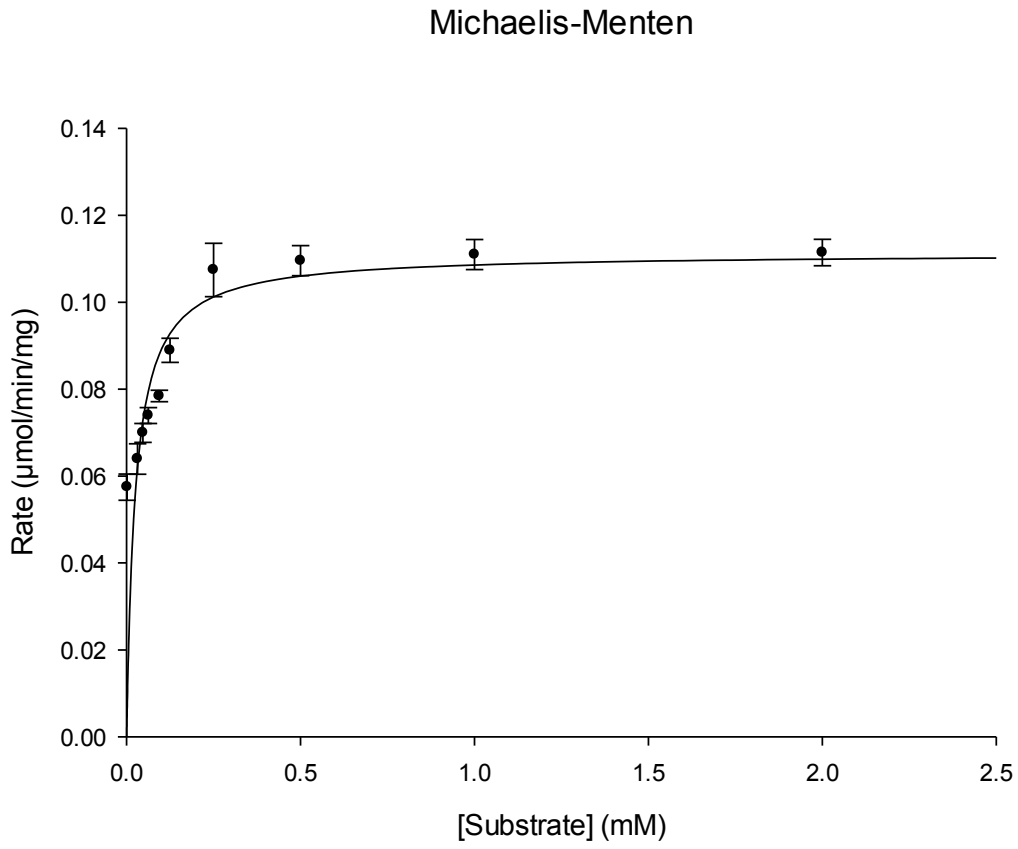

Vmax = 0.1113
Km = 0.02476

Calculation

Pao MW = 136357.7 g mol^{-1} (mg $mmol^{-1}$) = **136.36 mg $umol^{-1}$**

Vmax unit = **umol min^{-1} mg^{-1}** Km unit = **mM**

kcat = 0.111 x 136.36 = **15.1 min^{-1} (± 0.8)**

kcat/Km = **610 (± 183) min^{-1} mM^{-1}**

Parameters

	Value	±Std. Error	95% Conf. Interval
Vmax	**0.11**	**$6.05x10^{-3}$**	$9.89x10^{-2}$ to 0.12
Km	**$2.48x10^{-2}$**	**$7.30x10^{-3}$**	$2.12x10^{-2}$ to $3.13x10^{-2}$

Phenylacetaldehyde – PaoABC T318E

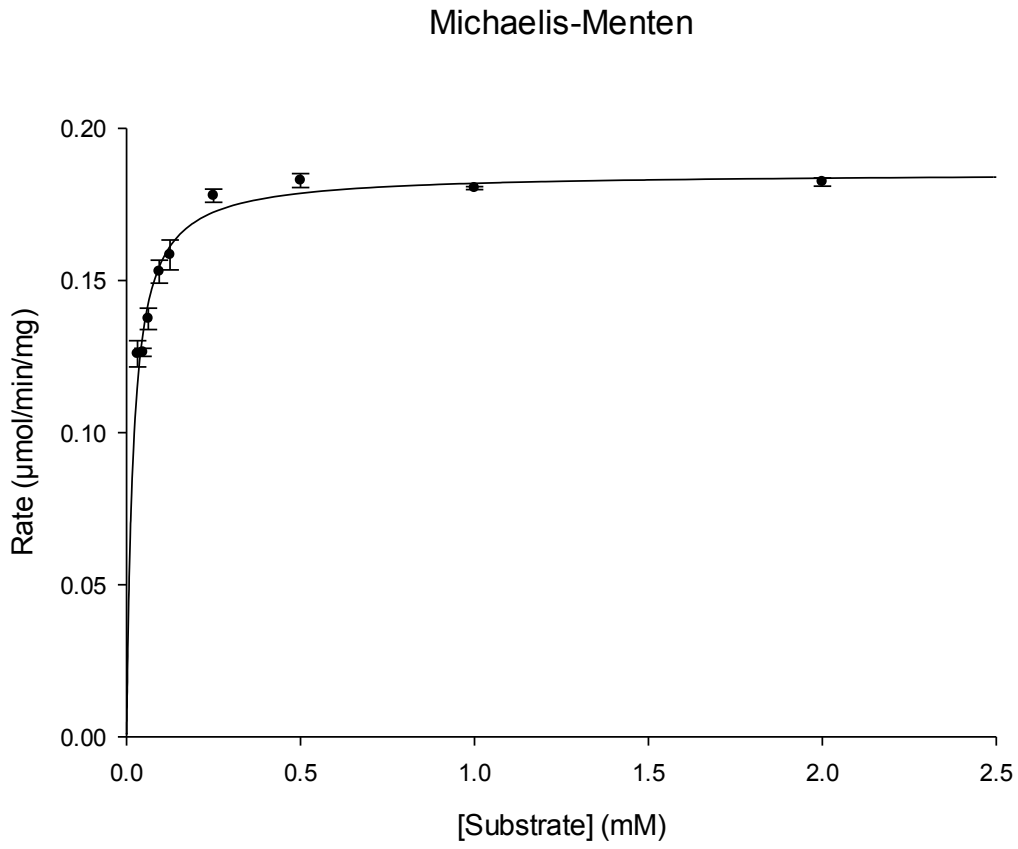

Vmax = 0.1854
Km = 0.01866

Calculation

Pao MW = 136357.7 g mol^{-1} (mg $mmol^{-1}$) = **136.36 mg $umol^{-1}$**

Vmax unit = **umol min^{-1} mg^{-1}** Km unit = **mM**

kcat = 0.111 x 136.36 = **15.1 min^{-1} (± 0.3)**

kcat/Km = **610 (± 183) min^{-1} mM^{-1}**

Parameters

	Value	±Std. Error	95% Conf. Interval
Vmax	**0.19**	**$2.22x10^{-3}$**	0.18 to 0.19
Km	**$2.48x10^{-2}$**	**$7.30x10^{-3}$**	$1.57x10^{-2}$ to $2.16x10^{-2}$

Phenylacetaldehyde – PaoABC T318S

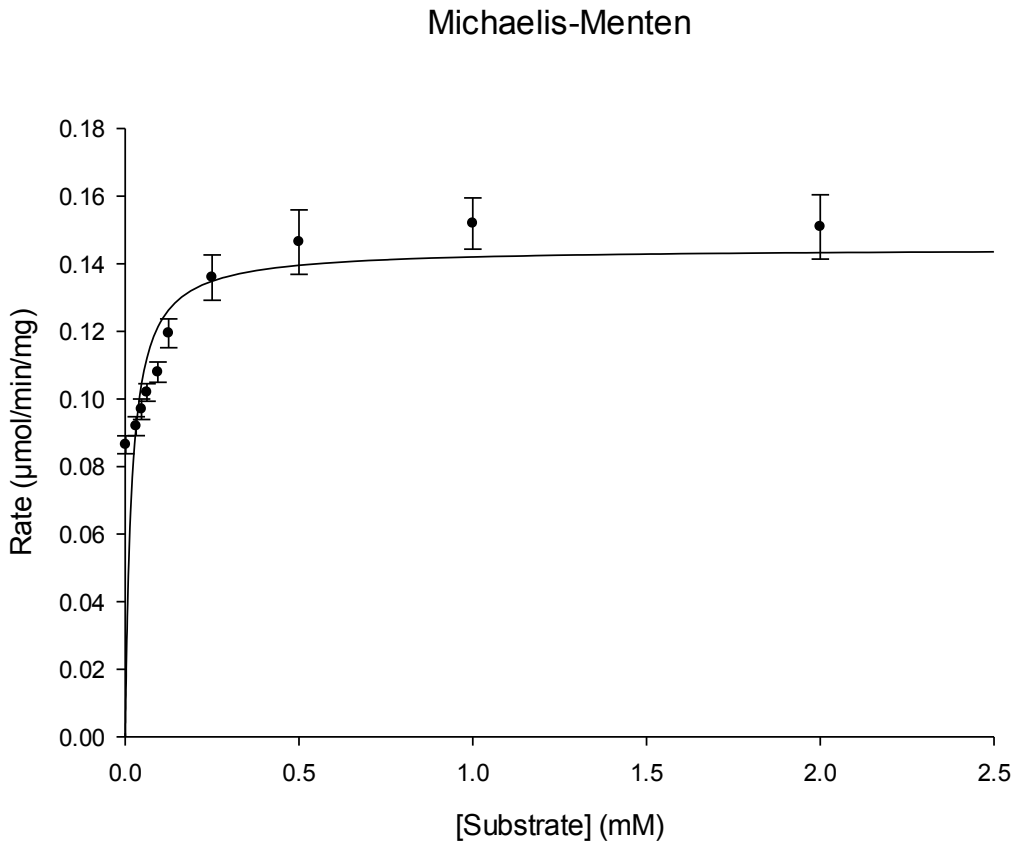

Calculation

Pao MW = 136357.7 g mol^{-1} (mg $mmol^{-1}$) = **136.36 mg $umol^{-1}$**

Vmax unit = **umol min^{-1} mg^{-1}** Km unit = **mM**

kcat = 0.145 x 136.36 = **19.8 min^{-1} (± 0.3)**

kcat/Km = **1098 (± 429) min^{-1} mM^{-1}**

Parameters

	Value	±Std. Error	95% Conf. Interval
Vmax	**0.14**	**$8.72x10^{-3}$**	0.13 to 0.16
Km	**$1.80x10^{-2}$**	**$6.94x10^{-3}$**	$3.76x10^{-3}$ to $3.22x10^{-2}$

Dihydroisoquinoline – *Ec*XDH

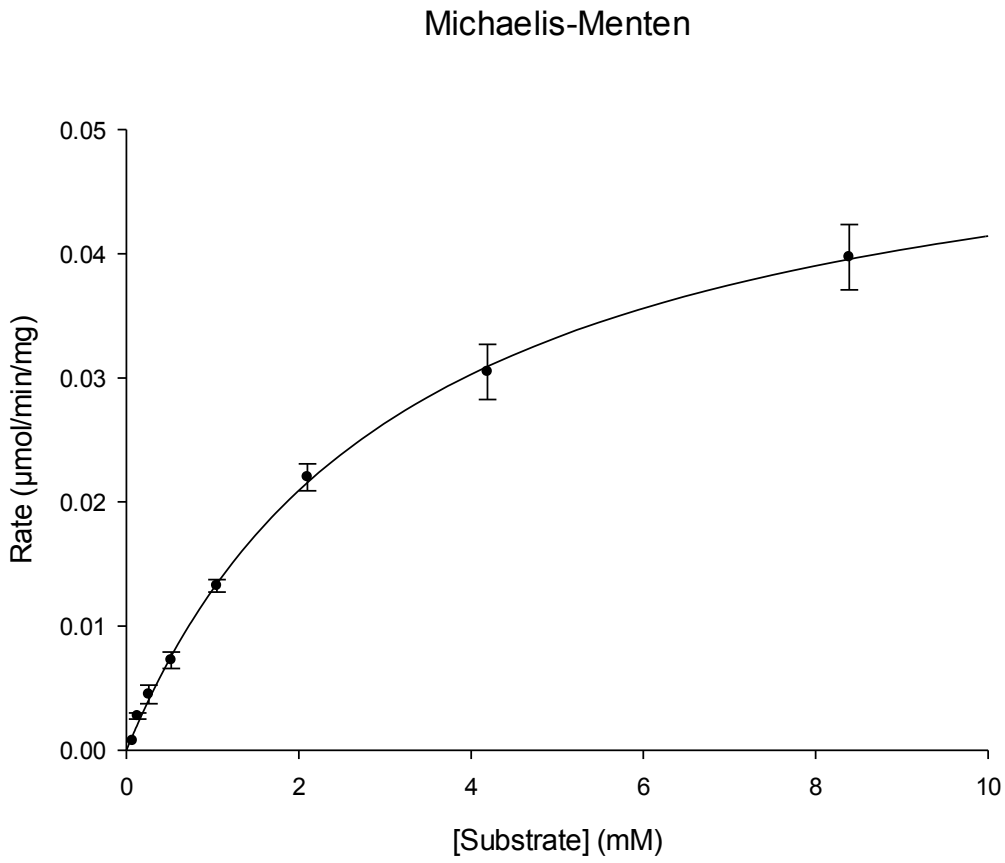

Calculation

Pao MW = 136357.7 g mol^{-1} (mg $mmol^{-1}$) = **136.36 mg $umol^{-1}$**

Vmax unit = **umol min^{-1} mg^{-1}** Km unit = **mM**

kcat = 0.0549 x 136.36 = **7.49 min^{-1} (± 0.42)**

kcat/Km = **2.34 (± 0.33) min^{-1} mM^{-1}**

Parameters

	Value	±Std. Error	95% Conf. Interval
Vmax	**$5.49x10^{-2}$**	**$3.09x10^{-3}$**	$4.80x10^{-2}$ to $6.12x10^{-2}$
Km	**3.20**	**0.41**	2.32 to 4.02

Dihydroisoquinoline – WT PaoABC

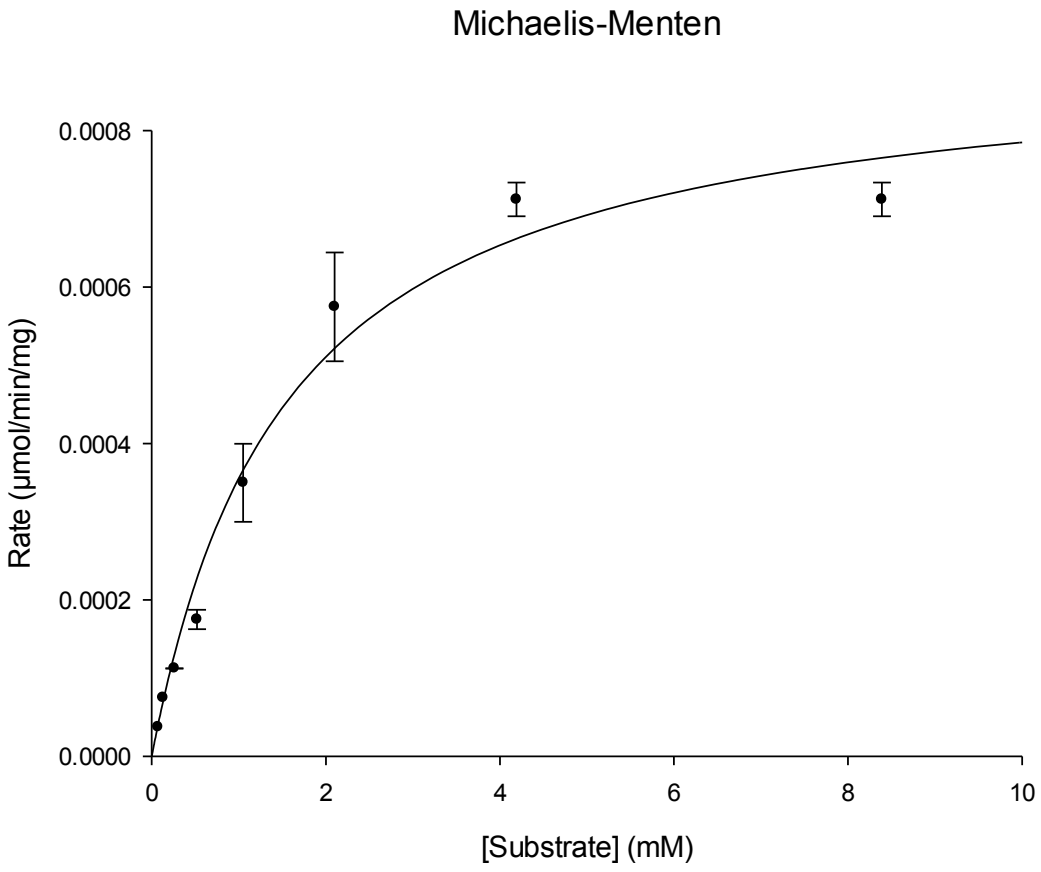

Vmax = 0.0009067
Km = 1.5

Calculation

Pao MW = 136357.7 g mol^{-1} (mg $mmol^{-1}$) = **136.36 mg $umol^{-1}$**

Vmax unit = **umol min^{-1} mg^{-1}** Km unit = **mM**

kcat = 0.0009067 x 136.36 = **0.12 min^{-1} (± 7.31x10^{-3})**

kcat/Km = **0.08 (± 0.01) min^{-1} mM^{-1}**

Parameters

	Value	±Std. Error	95% Conf. Interval
Vmax	**9.07x10^{-4}**	**5.36x10^{-5}**	7.96x10^{-4} to 1.02x10^{-3}
Km	**1.55**	**0.26**	1.02 to 2.08

Dihydroisoquinoline – PaoABC L246G

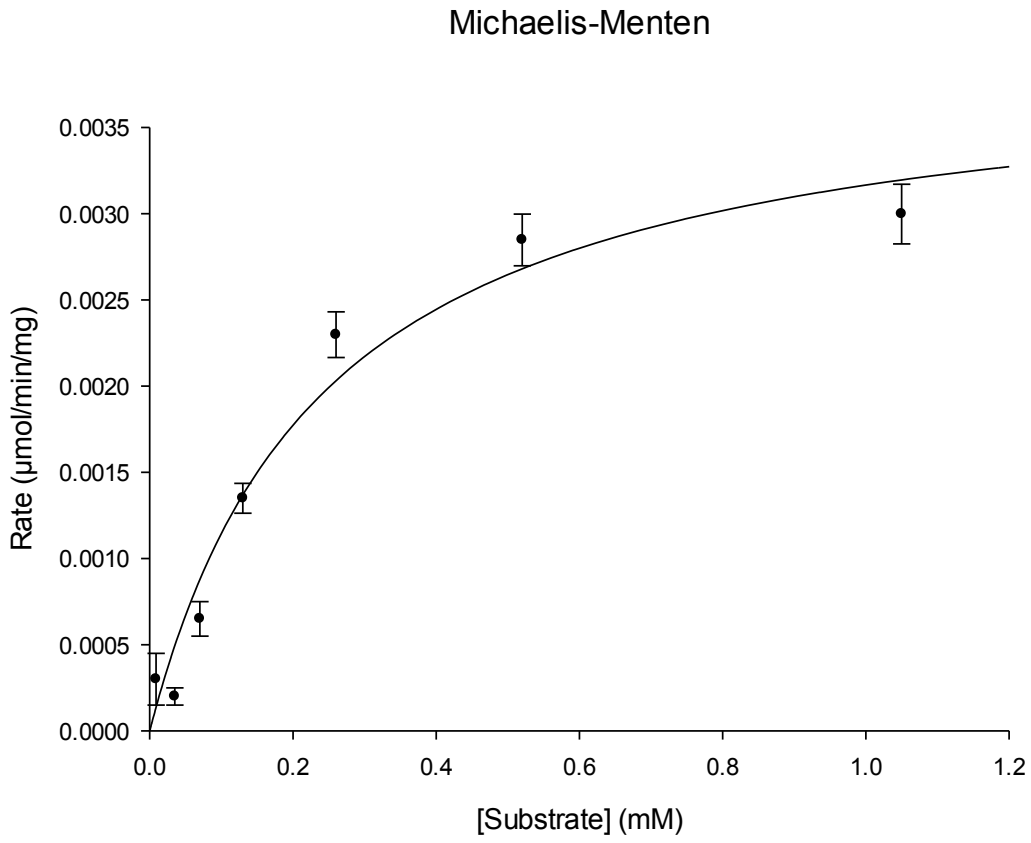

Vmax = 0.003939
Km = 0.244

Calculation

Pao MW = 136357.7 g mol^{-1} (mg $mmol^{-1}$) = **136.36 mg $umol^{-1}$**

Vmax unit = **umol min^{-1} mg^{-1}** Km unit = **mM**

kcat = 0.003939 x 136.36 = **0.54 min^{-1} (± 3.94x10^{-2})**

kcat/Km = **2.24 (± 0.47) min^{-1} mM^{-1}**

Parameters

	Value	±Std. Error	95% Conf. Interval
Vmax	**3.90x10^{-3}**	**2.89x10^{-4}**	3.33x10^{-3} to 4.55x10^{-3}
Km	**0.24**	**4.72x10^{-2}**	0.14 to 0.34

Dihydroisoquinoline – PaoABC L246S

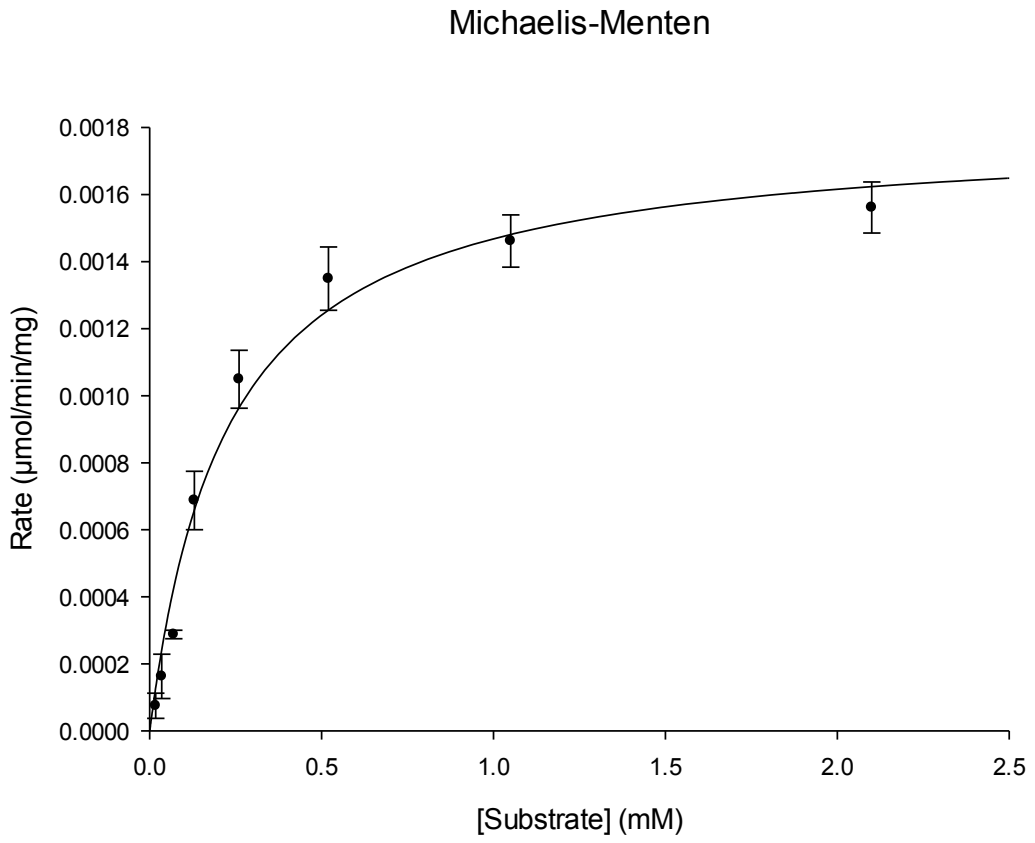

Calculation

Pao MW = 136357.7 g mol^{-1} (mg $mmol^{-1}$) = **136.36 mg $umol^{-1}$**

Vmax unit = **umol min^{-1} mg^{-1}** Km unit = **mM**

kcat = 0.001797 x 136.36 = **0.25 min^{-1} (± 1.16x10^{-2})**

kcat/Km = **1.11 (± 0.18) min^{-1} mM^{-1}**

Parameters

	Value	±Std. Error	95% Conf. Interval
Vmax	**1.80x10^{-3}**	**8.49x10^{-5}**	1.62x10^{-3} to 1.97x10^{-3}
Km	**0.22**	**3.41x10^{-2}**	0.15 to 0.29

Dihydroisoquinoline – PaoABC T318G

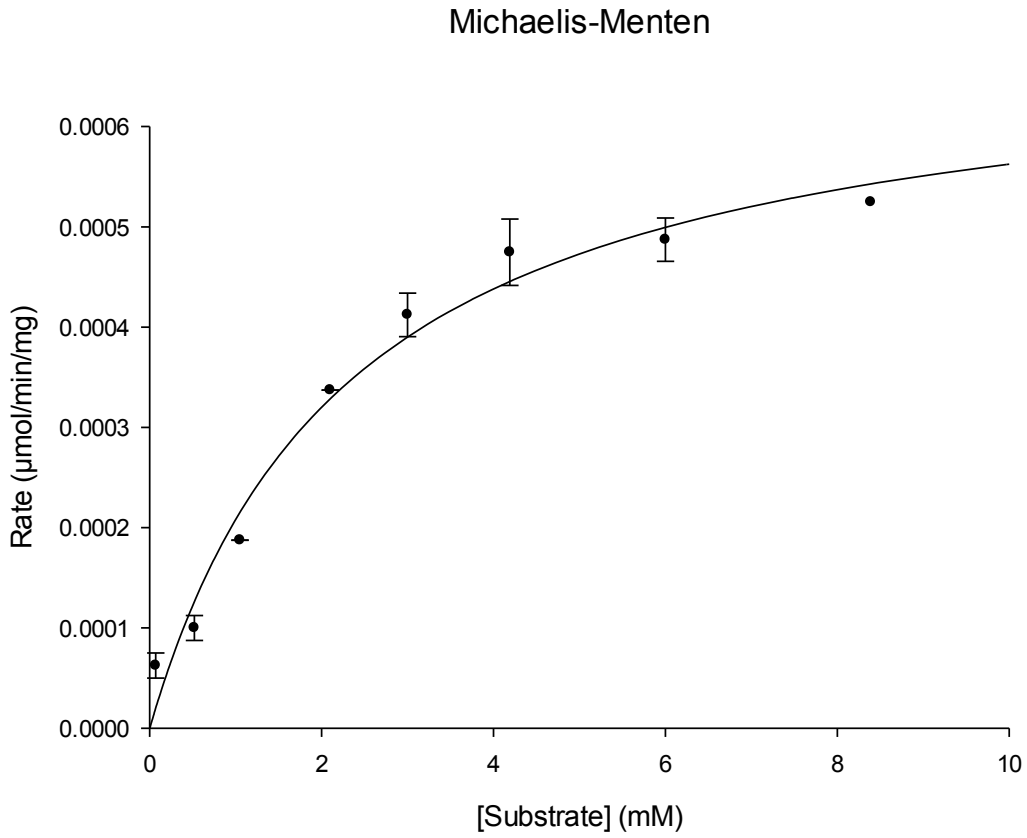

Vmax = 0.0006937
Km = 2.3

Calculation

Pao MW = 136357.7 g mol^{-1} (mg $mmol^{-1}$) = **136.36 mg $umol^{-1}$**

Vmax unit = **umol min^{-1} mg^{-1}** Km unit = **mM**

kcat = 0.0006937 x 136.36 = **0.09 min^{-1} (± 5.33x10^{-3})**

kcat/Km = **0.04 (± 6.51x10^{-3}) min^{-1} mM^{-1}**

Parameters

	Value	±Std. Error	95% Conf. Interval
Vmax	**6.94x10^{-4}**	**3.91x10^{-5}**	6.13x10^{-4} to 7.75x10^{-4}
Km	**2.33**	**0.35**	1.61 to 3.06

Dihydroisoquinoline – PaoABC T318P

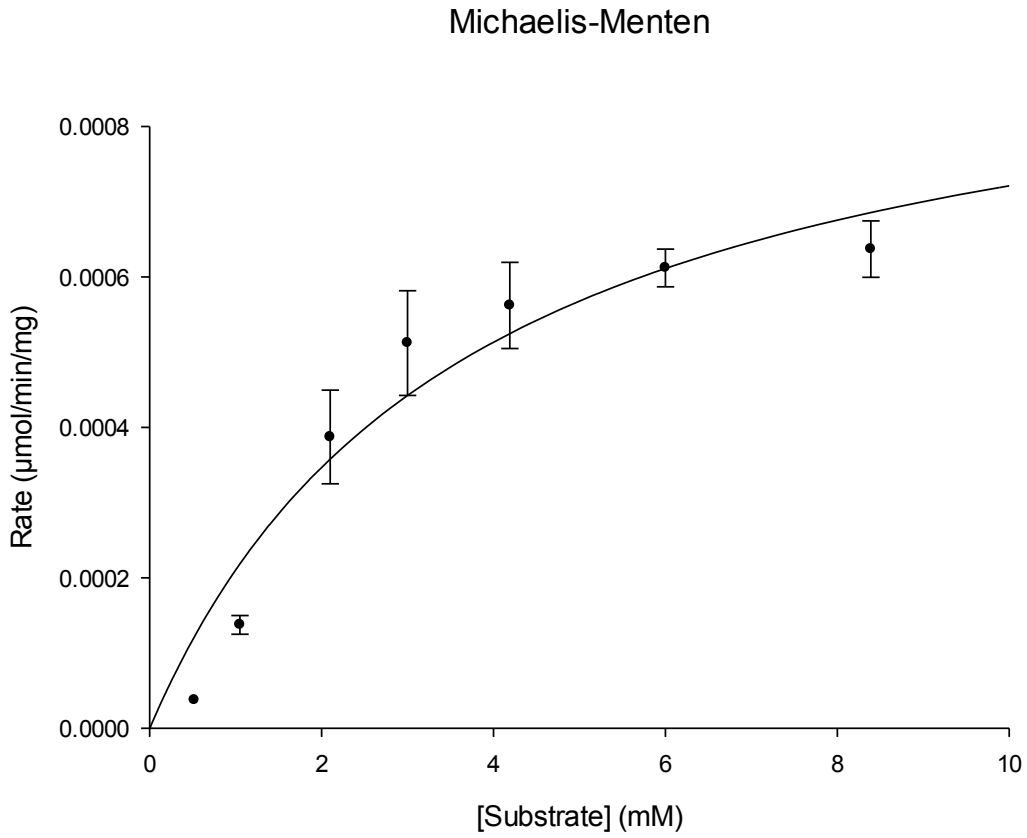

Vmax = 0.0009875
Km = 3.7

Calculation

Pao MW = 136357.7 g mol^{-1} (mg $mmol^{-1}$) = **136.36 mg $umol^{-1}$**

Vmax unit = **umol min^{-1} mg^{-1}** Km unit = **mM**

kcat = 0.0009875 x 136.36 = **0.13 min^{-1} (± 2.00x10^{-2})**

kcat/Km = **0.04 (± 0.01) min^{-1} mM^{-1}**

Parameters

	Value	±Std. Error	95% Conf. Interval
Vmax	**9.88x10^{-4}**	**1.46x10^{-4}**	6.83x10^{-4} to 1.29x10^{-3}
Km	**3.69**	**1.20**	1.18 to 6.20

Dihydroisoquinoline – PaoABC T318E

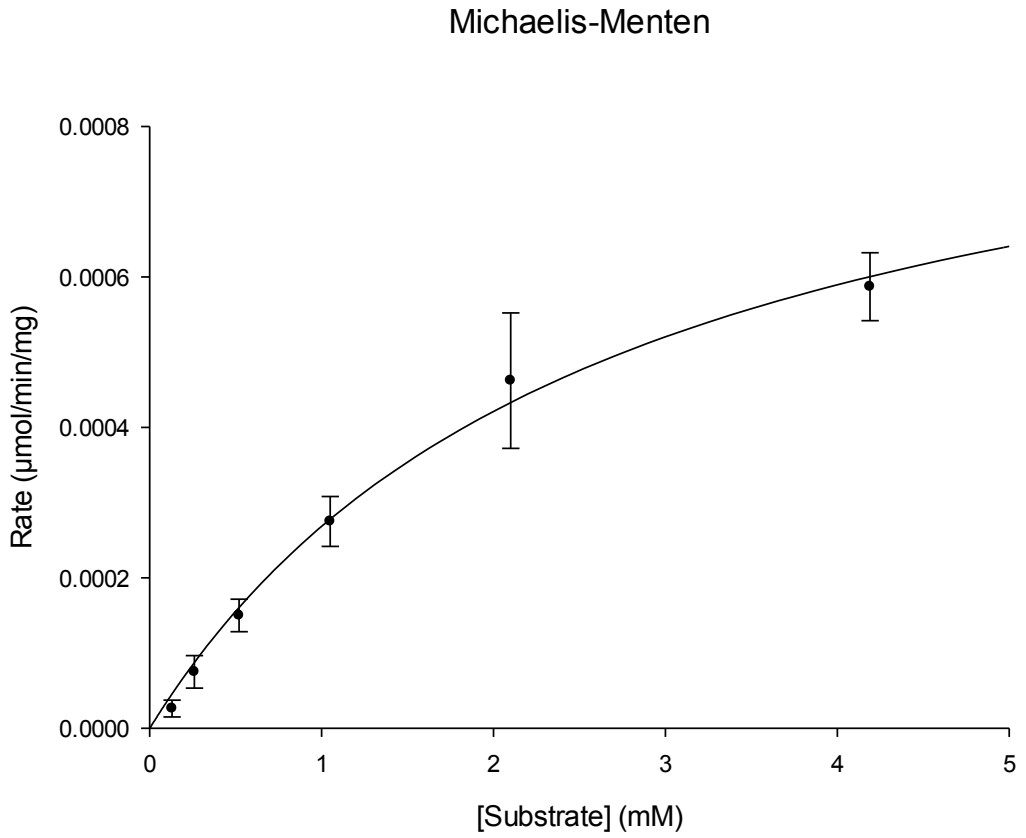

Vmax = 0.0009809
Km = 2.7

Calculation

Pao MW = 136357.7 g mol^{-1} (mg $mmol^{-1}$) = **136.36 mg $umol^{-1}$**

Vmax unit = **umol min^{-1} mg^{-1}** Km unit = **mM**

kcat = 0.0009809 x 136.36 = **0.13 min^{-1} (± 2.43x10^{-2})**

kcat/Km = **0.05 (± 0.01) min^{-1} mM^{-1}**

Parameters

	Value	±Std. Error	95% Conf. Interval
Vmax	**9.81x10^{-4}**	**1.78x10^{-4}**	6.03x10^{-4} to 1.36x10^{-3}
Km	**2.65**	**0.93**	0.69 to 4.62

Dihydroisoquinoline – PaoABC T318S

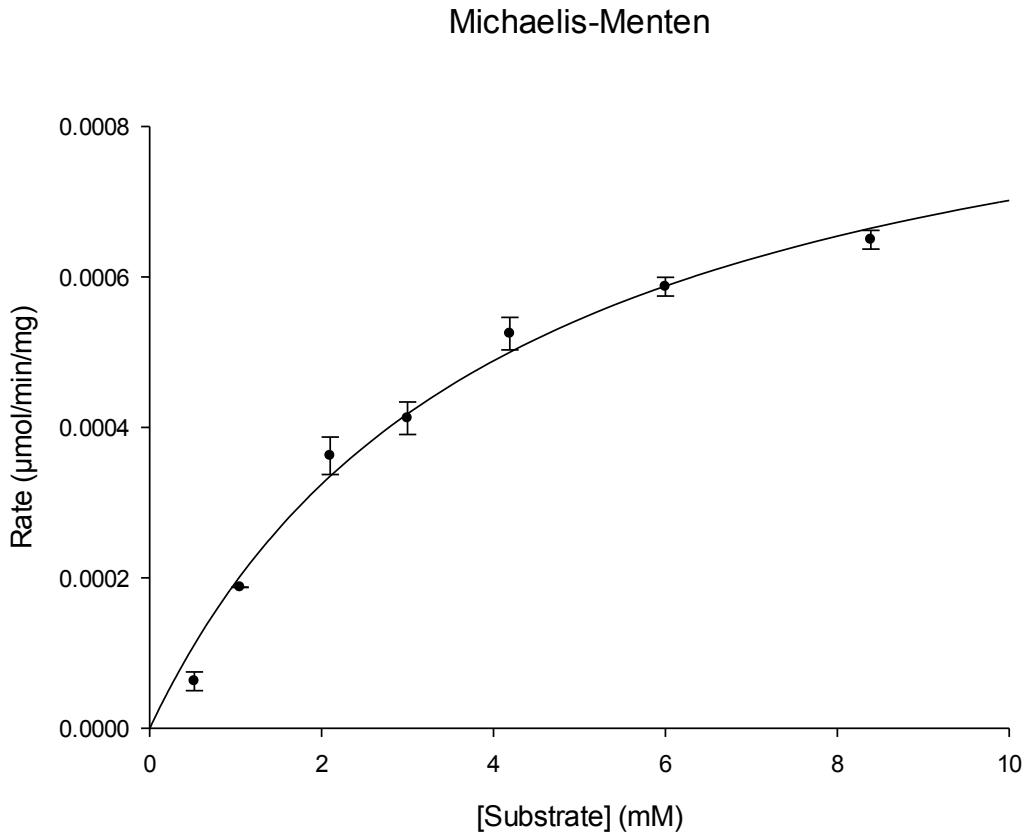

Vmax = 0.0009895
Km = 4.1

Calculation

Pao MW = 136357.7 g mol^{-1} (mg $mmol^{-1}$) = **136.36 mg $umol^{-1}$**

Vmax unit = **umol min^{-1} mg^{-1}** Km unit = **mM**

kcat = 0.0009895 x 136.36 = **0.13 min^{-1} (± $8.82x10^{-2}$)**

kcat/Km = **0.03 (± $5.00x10^{-3}$) min^{-1} mM^{-1}**

Parameters

	Value	±Std. Error	95% Conf. Interval
Vmax	**$9.90x10^{-4}$**	**$6.47x10^{-4}$**	$8.54x10^{-4}$ to $1.13x10^{-3}$
Km	**4.10**	**0.57**	2.91 to 5.28

Publication